

# Clinical pharmacology of genotype-directed anticancer therapy

*Towards rational combination strategies*

Robin M.J.M. van Geel

ISBN/EAN: 978-90-393-6640-0

© 2016 Robin van Geel

Cover design & artwork: isontwerp.nl ~ Ilse Schrauwers

Book design & layout: Robin van Geel

Printing: Gildeprint Drukkerijen

# Clinical pharmacology of genotype-directed anticancer therapy

*Towards rational combination strategies*

**Klinische farmacologie van genotypegerichte anti-kanker behandeling**

*Ontwikkeling van rationele combinatiestrategieën*

(met een samenvatting in het Nederlands)

## **Proefschrift**

ter verkrijging van de graad van doctor aan de Universiteit Utrecht  
op gezag van de rector magnificus, prof. dr. G.J. van der Zwaan,  
ingevolge het besluit van het college voor promoties  
in het openbaar te verdedigen op woensdag  
5 oktober 2016 des middags te 4.15 uur

door

**Robin Mattheus Johannes Maria van Geel**

geboren op 2 september 1987  
te Roosendaal

**Promotoren:** Prof. dr. J.H.M. Schellens  
Prof. dr. J.H. Beijnen

The research described in this thesis was performed at the Department of Clinical Pharmacology and the Department of Pharmacy & Pharmacology of the Netherlands Cancer Institute, Amsterdam, the Netherlands.

**Publication of this thesis was financially supported by:**

Utrecht Institute of Pharmaceutical Sciences (UIPS)  
The Netherlands Cancer Institute  
Boehringer Ingelheim BV  
Amgen BV  
Pfizer BV



"Your assumptions are your windows on the world.  
Scrub them off every once in a while, or the light won't come in."

– *Isaac Asimov*

Voor alle patiënten en hun dierbaren

## CONTENTS

Chapter 1	General introduction	11
Chapter 2	Clinical pharmacology of targeted anti-cancer drugs	
2.1	Concise drug review: pazopanib and axitinib <i>The Oncologist 2012;17(8):1081-9</i>	17
2.2	Crizotinib-induced fatal fulminant liver failure <i>Lung Cancer 2016; 93: 17-19</i>	33
Chapter 3	Drug-drug interactions in oncology: bogey or godsend? <i>Submitted for publication</i>	41
Chapter 4	Treatment individualization in colorectal cancer <i>Current Colorectal Cancer Reports 2015;11(6):335-344</i>	71
Chapter 5	Clinical pharmacology of combined targeted therapy targeting mutated <i>BRAF</i>	
5.1	Phase Ib dose-escalation study of encorafenib (LGX818) and cetuximab with or without alpelisib in patients with metastatic <i>BRAF</i> -mutated colorectal cancer <i>Submitted for publication</i>	87
5.2	Randomized phase II study comparing encorafenib combined with cetuximab versus encorafenib with cetuximab plus alpelisib in patients with advanced <i>BRAF</i> mutant colorectal cancer	107
5.3	Phase I study of dabrafenib, panitumumab and trametinib in patients with <i>BRAF</i> V600E-mutation positive colorectal cancer	123



<b>Chapter 6</b>	<b>Clinical pharmacology of combined targeted therapy targeting mutated <i>KRAS</i></b>	
6.1	Phase I study of dacomitinib plus PD-0325901 in patients with advanced <i>KRAS</i> mutation positive colorectal, non-small cell lung and pancreatic cancer	141
6.2	Phase I study of lapatinib plus trametinib in patients with <i>KRAS</i> mutant colorectal, non-small cell lung and pancreatic cancer	161
<b>Chapter 7</b>	<b>Clinical pharmacology of targeted therapy combined with chemotherapy</b>	
7.1	Phase I study evaluating WEE 1 inhibitor AZD1775 (MK-1775) as monotherapy and in combination with Gemcitabine, Cisplatin or Carboplatin in adult patients with advanced solid tumors <i>Journal of Clinical Oncology 2016, in press</i>	179
7.2	Phase II study of WEE1 inhibitor AZD1775 plus carboplatin in patients with <i>TP53</i> mutated ovarian cancer refractory or resistant (< 3 Months) to first-line therapy <i>Journal of Clinical Oncology 2016, in press</i>	205
<b>Chapter 8</b>	<b>Conclusions and perspectives</b>	227
<b>Appendix</b>	Summary	235
	Summary in Dutch	241
	Acknowledgements	248
	Curriculum Vitae	251
	List of publications	252



# Chapter 1

## General introduction and outline of this thesis



### INTRODUCTION

Historically, anticancer therapy is selected based on the histology of a tumor. However, improved understanding of the molecular characteristics of cancer initiated a dramatic change in this mindset. Genetic analysis of histologically similar cancer cells, revealed a high degree of heterogeneity at the molecular level. Although the number of somatic mutations found in tumors is often enormous, only a subset is actually driving tumorigenic processes.<sup>1</sup> A large proportion of these mutations affects genes that encode tyrosine kinase proteins, which are involved in multiple cellular mechanisms. Perturbation of tyrosine kinase activity by genetic mutations results in deregulated kinase signaling and contributes to tumor development and progression.<sup>2,3</sup> Therefore, targeting of specific driver mutations by inhibiting their related tyrosine kinase proteins has emerged as an attractive treatment strategy.

Already in 1960, researchers reported the first consistent genetic abnormality associated with human cancer by the discovery of the Philadelphia chromosome, a fusion of the *BCR* and *ABL* genes, in chronic myeloid leukemia (CML).<sup>4</sup> As the resulting BCR-ABL tyrosine kinase is constitutively active, it promotes cell division and neoplastic expansion. By occupying the adenosine triphosphate (ATP) binding pocket of BCR-ABL, imatinib prevents further tumorigenic signaling, which translated into extraordinary clinical activity in patients with *BCR-ABL*-positive CML.<sup>5</sup> Consequently, imatinib was the first tyrosine kinase inhibitor (TKI) obtaining proof of concept in the clinic and received FDA and EMA approval in 2001.

Fueled by this success of targeted therapy, a plethora of novel TKIs were developed against specific tyrosine kinase proteins that have been associated with cancer. Proteins involved in the mitogen-activated protein kinase (MAPK) or phosphoinositide 3-kinase (PI3K) pathways received significant attention in this respect as these signal transduction cascades are amongst the most commonly activated in human cancer.<sup>6,7</sup> Initial studies focused on the development of drugs that target receptor tyrosine kinases, situated at the cell membrane, to avoid receptor-mediated pathway activation upon ligand-receptor binding. The small-molecule inhibitor gefitinib and the monoclonal antibody trastuzumab, targeting the epidermal growth factor receptor (EGFR) and the human epidermal growth factor receptor 2 (HER2), respectively, were among the first receptor-targeted drugs providing clinical benefit for patients with solid tumors.<sup>8</sup> In **chapter 2.1**, we provide a concise drug review on two more novel compounds, pazopanib and axitinib, that were approved for the treatment of metastatic renal cell carcinoma by virtue of their antitumor activity through targeting primarily the vascular endothelial growth factor receptor.

Upon the recognition that clinical responses of multiple targeted agents were restricted to patients with tumors containing genetic alterations within the targeted protein, drug development evolved by implementing a more genotype-directed strategy. The majority of first-in-human phase I studies with novel targeted agents are now selecting patients on the basis of specific molecular aberrations rather than on histological tumor type. This biomarker-driven approach is based on the principle of oncogene addiction; cancer cells become dependent on the effect of oncogenic driver mutations, making inhibition of this signal harmful to the cancer cell.<sup>9</sup> Globally coordinated genotyping projects provided insight into which mutations most commonly occur in cancer, and drugs targeting these aberrations are increasingly investigated in clinical studies. Besides high frequency mutations, a large number of genetic anomalies have been reported that occur in only a small percentage of patients with a specific tumor type. One example is the discovery of the *EML4-ALK* fusion oncogene, occurring in approximately 4-7% of patients with non-small cell lung cancer (NSCLC).<sup>10,11</sup> Targeting of the resulting constitutive active ALK tyrosine kinase using small molecule inhibitors such as crizotinib resulted in a significant progression-free survival benefit compared to chemotherapy and became standard of care for this subset of patients.<sup>12</sup> Although crizotinib's toxicity profile is generally manageable, some patients experience intolerable adverse events. An exceptionally severe case of crizotinib-induced toxicity is described in **chapter 2.2**, emphasizing the rare, but considerable dangers that off-target effects of targeted agents hold.

The expanse of novel anticancer agents also bears a risk of new drug-drug interactions (DDIs) with concurrently used medications. Especially in oncology, DDIs with potential detrimental effects are looming, as patients with cancer are often older, have multiple comorbidities and use multiple concomitant medications. In **chapter 3**, we discuss this aspect, together with the potential beneficial effects for which DDIs may be deployed.

Although promising results have been obtained, the concept of a single driver mutation that is responsible for cancer survival and progression has a number of limitations. Most tumors harbor multiple oncogenic mutations, making them less dependent on a single driver, acquired resistance

may emerge through new mutations, and as many molecular signaling pathways are interconnected, inhibiting one may activate the other.<sup>13</sup> Therefore, patients with tumors harboring the same genetic driver mutation may still respond differently to therapy due to distinct genetic and phenotypic differences. For colorectal cancer (CRC), one of the most common human cancers worldwide, we discuss this extensive heterogeneity together with our view on further improving the treatment individualization in **chapter 4**. The impact of inter-pathway cross talk became particularly evident when BRAF inhibitors were investigated in patients with *BRAF* mutated (*BRAF*m) CRC. Whereas in patients with *BRAF*m melanoma, pharmacological inhibition of BRAF resulted in dramatic responses and a significant survival benefit compared to standard chemotherapy, the antitumor activity of BRAF inhibitors in patients with *BRAF*m CRC was disappointing.<sup>14,15</sup> Using a synthetic lethality screen, researchers of our institute elucidated the underlying molecular mechanism of this unresponsiveness by discovering the presence of a negative feedback loop that, upon BRAF inhibition, causes EGFR-mediated reactivation of downstream tumorigenic pathways.<sup>16</sup> Based on these preclinical findings, we developed multiple clinical phase I studies and a randomized phase II study, to evaluate combination strategies using targeted agents against BRAF and EGFR in patients with *BRAF*m CRC. These studies are described in **chapters 5.1, 5.2 and 5.3**. Analogously, a feedback mechanism was detected in *KRAS* mutated tumor cells, explaining their unresponsiveness to inhibition of MEK, a tyrosine kinase protein downstream of *KRAS*.<sup>17</sup> **Chapter 6.1 and 6.2** focus on the clinical evaluation of MEK inhibitors combined with agents that target multiple members of the human epidermal growth factor receptor family, in patients with *KRAS* mutated tumors.

In addition to combining multiple targeted agents in our effort to further improve patient outcome, targeted therapy is increasingly combined with chemotherapy. In particular, compounds that interfere with DNA damage repair mechanisms hold great promise to combine synergistically with DNA damaging chemotherapy, especially in patients whose tumors harbor genetic DNA repair deficiencies.<sup>18-20</sup> DNA damage-induced checkpoint control is critical for the maintenance of genomic stability and is governed in part by the p53 tumor suppressor protein. Mutations in *TP53* occur commonly in cancer, compromising G1 arrest as well as tight G2 arrest in response to DNA damage. This leaves cells highly dependent on components of the G2 checkpoint that converge on the inhibition of CDK1 in order to achieve cell cycle arrest and time for DNA repair.<sup>21,22</sup> Inhibition of the tyrosine kinase WEE1, one of the key proteins regulating the G2 checkpoint, results in G2 checkpoint abrogation.<sup>23,24</sup> Based on their increased G2 checkpoint dependency for DNA repair, p53-deficient tumor cells are especially sensitive to WEE1 inhibition in combination with DNA damaging chemotherapy.<sup>25-28</sup> In this regard, we conducted a phase I study, investigating the safety of AZD1775, a WEE1 inhibitor, in combination with different chemotherapeutic agents (**chapter 7.1**), followed by a proof-of-concept phase II study evaluating the clinical antitumor activity of AZD1775 combined with carboplatin in patients with *TP53* mutated ovarian cancer (**chapter 7.2**).

Taken together, the research described in this thesis was aimed to provide insight in the pharmacology of novel targeted agents and to improve their antitumor activity using rational combination strategies directed against specific genetic aberrations.

## References

1. Torkamani A, Verkhivker G, Schork NJ. Cancer driver mutations in protein kinase genes. *Cancer Lett* 2009;281:117–27.
2. Blume-Jensen P, Hunter T. Oncogenic kinase signalling. *Nature* 2001;411:355–65.
3. Baselga J. Targeting tyrosine kinases in cancer: the second wave. *Science* 2006;26;312:1175–8.
4. Nowell P, Hungerford D. Chromosome studies on normal and leukemic human leukocytes. *J Natl Cancer Inst* 1960;25:85–109.
5. Wood AJJ, Savage DG, Antman KH. Imatinib Mesylate – A New Oral Targeted Therapy. *N Engl J Med* 2002;346:683–93.
6. Liu P, Cheng H, Roberts TM, Zhao JJ. Targeting the phosphoinositide 3-kinase pathway in cancer. *Nat Rev Drug Discov* 2009;8:627–44.
7. Sebolt-Leopold JS, Herrera R. Targeting the mitogen-activated protein kinase cascade to treat cancer. *Nat Rev Cancer* 2004;4:937–47.
8. Schilsky RL. Personalized medicine in oncology: the future is now. *Nat Rev Drug Discov* 2010;9:363–6.
9. Weinstein IB. Addiction to oncogenes—the Achilles heel of cancer. *Science* 2002;297:63–4.
10. Soda M, Choi YL, Enomoto M, et al. Identification of the transforming EML4-ALK fusion gene in non-small-cell lung cancer. *Nature* 2007;448:561–6.
11. Inamura K, Takeuchi K, Togashi Y, et al. EML4-ALK fusion is linked to histological characteristics in a subset of lung cancers. *J Thorac Oncol* 2008;3:13–7.
12. Shaw AT, Kim DW, Nakagawa K, et al. Crizotinib versus chemotherapy in advanced ALK-positive lung cancer. *N Engl J Med* 2013;368:2385–94.
13. Bernards R. A missing link in genotype-directed cancer therapy. *Cell* 2012;151:465–8.
14. Chapman PB, Hauschild A, Robert C, et al. Improved survival with vemurafenib in melanoma with BRAF V600E mutation. *N Engl J Med* 2011;364:2507–16.
15. Kopetz S, Desai J, Chan E, et al. Phase II pilot study of vemurafenib in patients with metastatic BRAF-mutated colorectal cancer. *J Clin Oncol* 2015;33:4032–8.
16. Prahallad A, Sun C, Huang S, et al. Unresponsiveness of colon cancer to BRAF(V600E) inhibition through feedback activation of EGFR. *Nature* 2012;483:100–3.
17. Sun C, Hobor S, Bertotti A, et al. Intrinsic resistance to MEK inhibition in kras mutant lung and colon cancer through transcriptional induction of ERBB3. *Cell Rep* 2014;7:86–93.
18. Banerjee S, Kaye SB, Ashworth A. Making the best of PARP inhibitors in ovarian cancer. *Nat Rev Clin Oncol* 2010;7:508–19.
19. Oza AM, Cibula D, Benzaquen AO, et al. Olaparib combined with chemotherapy for recurrent platinum-sensitive ovarian cancer: a randomised phase 2 trial. *Lancet Oncol* 2015;16:87–97.
20. Hirai H, Iwasawa Y, Okada M, et al. Small-molecule inhibition of Wee1 kinase by MK-1775 selectively sensitizes p53-deficient tumor cells to DNA-damaging agents. *Mol Cancer Ther* 2009;8:2992–3000.
21. Macleod KF, Sherry N, Hannon G, et al. p53-Dependent and independent expression of p21 during cell growth, differentiation, and DNA damage. *Genes Dev* 1995;9:935–944.
22. Kuerbitz SJ, Plunkett BS, Walsh BS, Kastan MB. Wild-type p53 is a cell cycle checkpoint determinant following irradiation. *Proc Natl Acad Sci USA* 1992;89:7491–95.
23. Parker LL, Piwnicka-Worms H. Inactivation of the p43cds2-cyclin B complex by the human WEE1 tyrosine kinase. *Science* 1992;257:1955–7.
24. McGowan CH, Russell P. Cell cycle regulation of human WEE1. *EMBO J* 1995;14:2166–75.

25. Bridges KA, Hirai H, Buser CA, et al. MK-1775, a novel Wee1 kinase inhibitor, radiosensitizes p53-defective human tumor cells. *Clin Cancer Res* 2011;17:5638–48.
26. Kawabe T. G2 checkpoint abrogators as anticancer drugs. *Mol Cancer Ther* 2004;3:513–9.
27. Levine AJ, Oren M. The first 30 years of p53: growing even more complex. *Nat Rev Cancer* 2009;9:749–58.
28. Bucher N, Britten CD. G2 checkpoint abrogation and checkpoint kinase-1 targeting in the treatment of cancer. *Br J Cancer* 2008;98:523–8.





# Chapter 2

## Clinical pharmacology of targeted anticancer drugs



### 2.1

#### Concise drug review: pazopanib and axitinib

*The Oncologist* 2012;17(8):1081–9

Robin M.J.M. van Geel, Jos H. Beijnen, Jan H.M. Schellens

## ABSTRACT

Pazopanib and axitinib are both FDA approved ATP-competitive inhibitors of the vascular endothelial growth factor receptor (VEGFR). Pazopanib and axitinib have shown to be effective and tolerable treatment options for metastatic renal cell cancer and therefore have enlarged the armamentarium for this disease. This concise drug review discusses clinical benefits, clinical use, mechanism of action, bioanalysis, pharmacokinetics, pharmacogenetics, pharmacodynamics, drug resistance, toxicity and patient instructions and recommendations for supportive care for these two drugs.

## Introduction

Pazopanib (Votrient<sup>®</sup>, GlaxoSmithKline, Brentford, United Kingdom) (Fig. 1A) is currently approved by the U.S. Food and Drug Administration (FDA) and the European Medicines Agency (EMA) for metastatic renal cell carcinoma (mRCC).<sup>1</sup> In the pivotal phase III study in patients with mRCC, pazopanib showed a clinically relevant and statistically significant prolongation of progression free survival (PFS) of five months versus placebo, and it has shown clinical benefit in various other tumor types, including soft tissue sarcoma, non-small cell lung-, ovarian-, and thyroid cancer.<sup>2-6</sup> Axitinib (Inlyta<sup>®</sup>, Pfizer Inc., New York City, NY) (Fig. 1B) has recently been approved by the FDA for the treatment of mRCC after failure of one prior systemic therapy. This approval followed the FDA advisory committees, which described the favourable benefit/risk profile of axitinib in previously treated advanced RCC, based on a comparative phase III trial of axitinib versus sorafenib.<sup>7,8</sup> Pazopanib and axitinib are both small molecule angiogenesis inhibitors with similar drug profiles. Pazopanib is being studied in additional indications in adults, including adjuvant treatment of renal cell cancer, advanced soft tissue sarcoma and ovarian cancer, whereas axitinib is being studied as single agent as well as in combination with chemotherapy across several tumor types, such as hepatocellular carcinoma, pancreatic-, thyroid- and advanced refractory non-small cell lung cancer.<sup>9</sup> Furthermore, a phase I pediatric dose finding study of pazopanib is currently ongoing and phase II and III pediatric trials have been planned.<sup>10</sup>

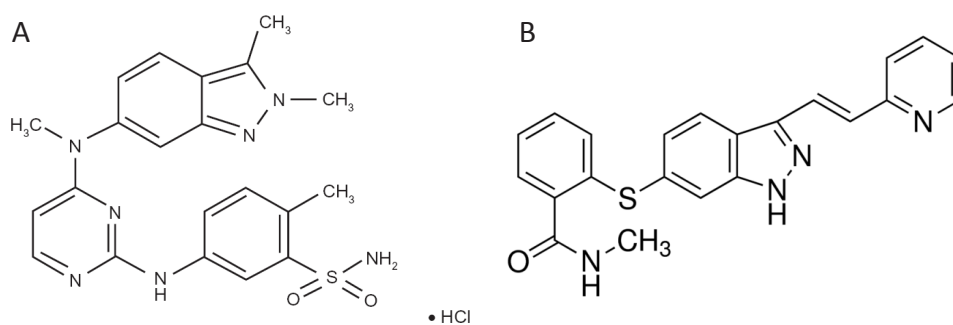


Figure 1. Chemical structures of pazopanib (A) and axitinib (B)

## Clinical benefits

In a phase II study with pazopanib 800 mg QD in 225 patients with metastatic or locally recurrent RCC an overall response rate of 34.7% (95% CI, 28% to 41%) and a median PFS of 51.7 weeks was demonstrated. In a randomized placebo comparison ( $n = 55$ ) the PFS was 11.9 months for pazopanib versus 6.2 months for placebo.<sup>11</sup> In the pivotal randomised phase III placebo-controlled clinical trial, pazopanib demonstrated a highly significant improvement in PFS in either treatment-naïve or cytokine pre-treated patients with mRCC. Median PFS for patients receiving pazopanib was 9.2 months versus 4.2 months for patients in the placebo group, with a more pronounced difference in the treatment-naïve group (11.1 months vs 2.8 months) than in the cytokine refractory group (7.4 months vs 4.2 months). These benefits, together with pazopanib's relatively low incidence of severe myelosuppression, hand-foot syndrome, stomatitis and fatigue compared with the safety profile of other agents of this class such as sunitinib, positions pazopanib as a therapeutic option for mRCC. However, studies directly

comparing activity and safety of pazopanib and other registered TKIs in mRCC are lacking. Results from the ongoing clinical trial comparing the efficacy and safety profiles of pazopanib and sunitinib are expected to further determine the position of pazopanib in the treatment of mRCC.<sup>2,12</sup>

In a randomised phase III clinical trial, axitinib has been shown to benefit patients with mRCC after failure of one previous systemic therapy. Compared to sorafenib, axitinib led to a statistically significant and clinically meaningful increase in PFS (6.7 versus 4.7 months; HR = 0.665, one-sided  $P < 0.0001$ ) in this study group. Median PFS was 12.1 months for axitinib versus 6.5 months for sorafenib (HR = 0.464,  $P < 0.0001$ ) in patients previously treated with cytokines, and 4.8 versus 3.4 months (HR = 0.741,  $P = 0.0107$ ), respectively, in patients who were previously treated with sunitinib. The objective response rate was 19% for axitinib and 9% for sorafenib ( $P = 0.001$ ), with a median duration of response of 11 months for axitinib versus 10.6 months for sorafenib. Overall survival (OS) was not significantly different between both groups.<sup>8</sup> Furthermore, in phase II studies, axitinib demonstrated antitumor activity in patients with cytokine-refractory and sorafenib-refractory mRCC, with an objective response rate of 44% and 22.6%, a median PFS of 15.7 and 7.4 months, and a median OS of 29.9 and 13.6 months, respectively.<sup>13,14</sup> The five-year overall survival data from the phase II study with axitinib in patients with cytokine-refractory mRCC were presented recently. The median follow-up for OS was 5.9 years and the five-year survival was 20.6% (95% CI, 10.9–32.4%). Axitinib treatment can result in greater than five-year overall survival in a subgroup of patients with mRCC and could therefore be considered as a treatment option for second-line therapy of mRCC.<sup>15</sup>

## Clinical Use

Pazopanib is available as film coated tablets of 200 mg and 400 mg. The recommended dose is 800 mg once daily (QD), administered at least 1 hour before or 2 hours after food intake. The dose of pazopanib should be reduced to 400 mg QD in patients who also use strong CYP3A4 inhibitors and a dose reduction of 75% is advised for patients with moderate hepatic impairment. Individual dose adaptations based on tolerability should be taken in steps of 200 mg.<sup>2,16</sup> In a phase I study in children (aged 4–21 years) with relapsed or refractory solid tumors, the maximum tolerated dose of pazopanib was 450 mg/m<sup>2</sup>.<sup>10</sup>

Axitinib is available as 1 and 5 mg oral tablets, and the recommended starting dose is 5 mg twice daily (BID) on a continuous dosing schedule. The axitinib dose could be increased to 7 mg BID in patients who experienced no adverse events above grade 2, according to Common Terminology Criteria for Adverse Events (CTCAE) for at least 2 weeks, unless the patient's blood pressure is higher than 150/90 mm Hg or the patient receives antihypertensive medication. Subsequently, the treatment dose could be further increased to 10 mg BID according to the same criteria. However, the clinical benefit of increasing the dose of axitinib in the treatment of mRCC is yet to be defined in an ongoing phase II trial. If needed, the dose of axitinib could be decreased to 3 mg BID. If further dose reduction is necessary, the recommended dose is 2 mg BID.<sup>8,17</sup>

## Mechanism of Action

Pazopanib and axitinib are second-generation potent inhibitors of multiple protein targets involved in tumor cell proliferation and angiogenesis. Angiogenesis plays a critical role in the progression of solid tumors as small as 1–2 mm in diameter. In this process, several proangiogenic factors are involved

<b>Table 1. Summary table</b>		
	<b>Pazopanib</b>	<b>Axitinib</b>
<b>Commercial name</b>	Votrient®	Inlyta®
<b>Molecular weight</b>	437.52 g/mol	386.47 g/mol
<b>Mechanism of action</b>	ATP-competitive inhibition of VEGFR-1, VEGFR-2, VEGF-3, PDGFR- $\alpha$ , PDGFR- $\beta$ , c-kit, FGFR-1, FGFR-3, Itk, Lek, c-fms	ATP-competitive inhibition of VEGFR-1, VEGFR-2, VEGFR-3
<b>Route of administration</b>	Oral	Oral
<b>Bioavailability</b>	Variable, 14–39%	Variable, approximately 58%
<b>Protein binding (%)</b>	> 99%	> 99%
<b>Metabolism</b>	Mainly via CYP3A4 with minor contribution from CYP1A2 and CYP2C8	Primarily via CYP3A4/5, and to a lesser extent via CYP1A2 and CYP2C19, and by glucuronidation via UGT1A1
<b>Elimination</b>	Primarily via feces, and <4% via renal elimination	Fecal elimination (via hepatobiliary secretion) 30-60%, renal elimination 23%
<b>Terminal half-life</b>	31 hours	2–6 hours
<b>Main toxicities</b>	Diarrhea, hypertension, hair color changes, nausea, anorexia, vomiting Laboratory abnormalities: elevated ALT/AST, increased glucose, increased total bilirubin, leukopenia, proteinuria	Diarrhea, hypertension, fatigue, nausea, decreased appetite, dyspnea, dysphonia Laboratory abnormalities: elevated creatinine, anaemia, hypocalcaemia lymphopenia, proteinuria
<b>Pharmacogenetics</b>	<i>UGT1A1</i> polymorphism is associated with pazopanib induced hyperbilirubinaemia; polymorphisms in <i>IL8</i> , <i>HIF1A</i> , <i>NR1/2</i> and <i>VEGFA</i> may predict treatment response	Polymorphisms analyzed in CYP isozymes, UGT1A1, ABCB1 and OATP1B1 were of no significant relevance in predicting pharmacokinetic variability
<b>Resistance</b>	Will develop as a result of amplification of pro-angiogenic genes, secretion of multiple pro-angiogenic factors, recruitment of pro-angiogenic bone marrow-derived cells and escape mechanisms via different modes of vascularization	
<b>Unique features</b>		Selective inhibition of VEGF receptors
<b>Main drug interactions</b>	Strong CYP3A4, P-gp and BCRP inhibitors; CYP3A4, P-gp and BCRP inducers and substrates; OATP1B1 substrates (e.g. statins)	CYP3A4 inhibitors, inducers and substrates; e.g. ketoconazole, rifampicin, carbamazepin, cyclosporine and simvastatin
<b>Dose adaptations</b>	Reduce dosage to 200 mg QD in patients with moderate hepatic impairment; Reduce dosage to 400 mg QD if concomitant use of a strong CYP3A4 inhibitor is warranted. Strong CYP3A4 inducers should not be used	Dose reduction of 50-75% may be necessary in patients with moderate (or worse) hepatic impairment or with concomitant use of strong CYP3A4 inhibitors
<b>Recommendations for supportive care</b>	Monitor blood pressure frequently. Treat mild to moderate hypertension with standard antihypertensive therapy; consider omitting pazopanib in patients experiencing severe or persistent hypertension. Monitor liver biochemistry, thyroid function and urine protein periodically throughout treatment.	

Abbreviations: ABC, ATP-binding cassette; BCRP, breast cancer resistant protein (ABCG2); CYP, cytochrome P450; FGFR, fibroblast growth factor receptor; Itk, interleukin-2 receptor inducible T-cell kinase; Lek, leucocyte-specific protein tyrosine kinase; OATP, Organic anion transporting polypeptide; PDGFR platelet-derived growth factor receptor; P-gp, permeability glycoprotein; UGT, uridine diphosphate glucuronosyltransferase; VEGFR, vascular endothelial growth factor receptor

with a central role for the vascular endothelial growth factor (VEGF) family. VEGF binds to the cell surface receptors VEGFR-1, -2 and -3 which subsequently leads to the recruitment of ATP. ATP in turn binds to the so-called ATP-binding pocket of VEGFR, causing activation of the VEGF signalling pathway which ultimately results in cellular effects that are pivotal for angiogenesis. Inhibition of this pathway demonstrated antitumor activity in several tumor types, including RCC, colorectal-, breast-, and non-small cell lung cancer.<sup>18</sup> Pazopanib inhibits this signalling pathway via ATP-competitive inhibition of VEGFR-1, VEGFR-2 and VEGFR-3, with *in vitro* inhibitory concentrations (IC)<sub>50</sub> of 10, 30, and 47 nm for VEGFR-1, -2, and -3, respectively. Similar activity was demonstrated against platelet-derived growth factor receptors (PDGFR) PDGFR $\alpha$ , PDGFR $\beta$ , fibroblast growth factor receptor (FGFR)-1, FGFR-3 and c-Kit. The transmembrane glycoprotein receptor tyrosine kinase (c-fms) is inhibited as well, but with modest potency.<sup>19,20</sup> Axitinib is a more selective tyrosine kinase inhibitor, as it only shows activity against VEGFR-1, VEGFR-2 and VEGFR-3. Furthermore, its potency *in vitro* is higher compared to pazopanib and first-generation VEGFR inhibitors, such as sunitinib and sorafenib.<sup>8,21,22</sup> Additionally, in contrast to first-generation inhibitors, axitinib has no substantial inhibitory effect on PDGFR, B-RAF, c-kit and FLT-3, which might contribute to less off-target adverse effects and an improved therapeutic window.<sup>8</sup>

## Bioanalysis

Bioanalysis of pazopanib and axitinib can be exerted by high performance liquid chromatography with tandem mass spectrometry.<sup>23,24</sup>

## Pharmacokinetics

### Absorption

At the recommended dose of 800 mg pazopanib QD, the maximum plasma concentration ( $C_{max}$ ) after the first dose of approximately  $19 \pm 13$   $\mu\text{g/mL}$  is reached after 2–4 hours, and a geometric mean area under the plasma concentration time curve (AUC) from time zero extrapolated to infinity ( $AUC_{0-\infty}$ ) of approximately  $650 \pm 500$   $\mu\text{g}\cdot\text{h/mL}$  is obtained. Continuous dosing at 800 mg QD results in a mean AUC of  $1,037$   $\mu\text{g}\cdot\text{h/mL}$  and a  $C_{max}$  of  $58.1$   $\mu\text{g/mL}$ . The mean steady state concentration ( $C_{trough}$ ) was  $\geq 15$   $\mu\text{g/mL}$ , which appeared to correlate with clinical activity in patients with mRCC. Pazopanib doses above 800 mg QD are not likely to produce higher plasma concentrations.<sup>16,19,24</sup> Systemic exposure to pazopanib did not increase in a dose-proportional manner in a phase I dose-escalation study in patients with hepatocellular carcinoma, and ranged from  $151$   $\mu\text{g}\cdot\text{h/mL}$  at 200 mg pazopanib QD to  $214$   $\mu\text{g}\cdot\text{h/mL}$  at 800 mg pazopanib QD. The mean  $C_{max}$  values for the pazopanib doses used in this study also did not show linear PK and was  $29.8$   $\mu\text{g/mL}$  at 200 mg QD,  $31.6$   $\mu\text{g/mL}$  at 400 mg,  $28.8$   $\mu\text{g/mL}$  at 600 mg QD and  $39.5$   $\mu\text{g/mL}$  at 800 mg QD.  $C_{trough}$  levels were above  $15$   $\mu\text{g/mL}$  for all doses and was highest at 800 mg pazopanib QD;  $28.1$   $\mu\text{g/mL}$ .<sup>25</sup> Administration of pazopanib with both low- and high-fat meals resulted in an approximate twofold higher systemic exposure, as indicated by a twofold increase in AUC and  $C_{max}$ . Pazopanib should therefore be administered to patients in the fasted state, at least 2 hours after or at least 1 hour before food intake.<sup>26</sup> Administration of a single pazopanib 400 mg crushed tablet resulted in an approximate 2-fold increased  $C_{max}$  and a decreased  $t_{max}$  by approximately 2 hours compared to administration of the whole tablet.<sup>27</sup>

After oral administration in the fed state, axitinib is rapidly absorbed from the gut, with peak plasma levels occurring within 2 to 6 hours after intake.<sup>28</sup> The rate and extent of drug absorption is higher in an

overnight fasted state with peak plasma concentrations occurring 0.5 to 4 hours post-dose.<sup>28-30</sup> At the recommended dose of 5 mg BID, mean C<sub>max</sub> and AUC<sub>0-24</sub> after the first dose, are 37 ng/mL and 188 ng·h/mL, respectively, in the overnight fasted state versus 22 ng/mL and 194 ng·h/mL, respectively, in the fed state. These data are indicating a food effect on the pharmacokinetics of axitinib. Further studies however, have confirmed that overnight fasting is not required and administration of axitinib with food is recommended.<sup>28,31</sup> At doses of 2 to 10 mg BID, axitinib exhibits linear pharmacokinetics, and steady state is reached within 15 days, with no unexpected accumulation.<sup>28</sup>

### **Protein binding**

Both pazopanib and axitinib are highly protein bound (> 99%). *In vitro* studies demonstrated that axitinib binds mostly to albumin and, more restricted, to  $\alpha$ -1-acid glycoprotein.<sup>16,32</sup>

### **Metabolism**

Results from *in vitro* studies demonstrated that pazopanib is metabolized by cytochrome P450 (CYP) 3A4, and to a lesser degree by CYP1A2 and CYP2C8. Only 6% of the exposure in plasma represents the four principle pazopanib metabolites. One of these metabolites, GSK1268997, shows similar potency *in vitro* employing human umbilical vein endothelial cells (HUVEC) compared to pazopanib, whereas the other metabolites are 10- to 20-fold less active.<sup>19,33</sup>

*In vitro* metabolism studies show that axitinib metabolism consists primarily of oxidation via CYP3A4 and to a lesser extent via CYP2C19 and CYP1A2, with additional metabolism occurring by glucuronidation via diphosphate glucuronosyltransferase (UGT) 1A1. The main metabolites of axitinib, a sulfoxide and an N-glucuronide, are inactive.<sup>28,31</sup>

### **Elimination**

After administration of the recommended dose of 800 mg, the elimination of pazopanib occurs slowly at a mean terminal plasma half-life ( $t_{1/2}$ ) of approximately 31 hours.<sup>24</sup> Elimination of pazopanib and its metabolites occurs primarily via the feces and no more than 4% of the orally administered dose is eliminated via renal excretion.<sup>19</sup>

The  $t_{1/2}$  of axitinib is 2 to 5 hours, with hepatobiliary excretion being the major elimination pathway. Approximately 30-60% of orally administered axitinib is eliminated in feces, with renal elimination accounting for a further 23%. The predominant component of eliminated axitinib in feces is unchanged axitinib, where in urine less than 1% of the administered dose was found as unchanged drug.<sup>28,32,34</sup>

### **Drug interactions**

Since pazopanib and axitinib are largely metabolised by CYP3A4, co-administration of agents known to be potent inducers or inhibitors of the CYP3A4 isozyme should be avoided. A study examining the concomitant administration of rifampicin, a potent inducer of CYP3A4, CYP1A2 and UGT1A1, and axitinib in healthy volunteers demonstrated a decrease by 79% and 71%, respectively, in geometric mean AUC<sub>0-∞</sub> and C<sub>max</sub> of axitinib.<sup>30</sup> Furthermore, data from a single patient demonstrated that after concomitant use of phenytoin, a potent inducer of multiple CYP450 enzymes, the AUC<sub>0-24</sub> and C<sub>max</sub> of axitinib were reduced approximately 10-fold. Despite earlier clinical evidence of response to axitinib, this reduction in plasma exposure and C<sub>max</sub> subsequently resulted in disease progression, which led

to discontinuation from study treatment.<sup>28</sup> A phase I study examining the influence of ketoconazole, a potent CYP3A4 inhibitor, on the pharmacokinetics of axitinib, demonstrated that concurrent administration of ketoconazole increased the geometric mean  $AUC_{\infty}$  and  $C_{max}$  of axitinib 2- and 1.5-fold, respectively.<sup>29</sup>

Concurrent administration of 1,500 mg lapatinib, a substrate for and weak inhibitor of CYP3A4 and P-gp and a potent inhibitor of BCRP, with 800 mg pazopanib resulted in an increased systemic exposure of pazopanib, with  $AUC_{0-24}$  and  $C_{max}$  elevations of 50% to 60%, respectively.<sup>35</sup> This increased pazopanib exposure is likely the result of P-gp and/or BCRP inhibition by lapatinib. Combination with strong P-gp, and BCRP inhibitors and inducers should therefore be avoided.<sup>19</sup> Pazopanib itself is also able to inhibit several CYP enzymes, including CYP3A4, BCRP, P-gp and OATP1B1. For example, co-administration of pazopanib 800 mg QD and paclitaxel 80 mg/m<sup>2</sup>, a CYP3A4 and CYP2C8 substrate, once weekly resulted in an increased AUC and  $C_{max}$  of paclitaxel, of 45% and 40% respectively.<sup>36</sup> Care should therefore be taken when pazopanib is co-administered with other oral CYP3A4, BCRP, P-gp and OATP1B1 substrates.<sup>19</sup>

### Alterations with disease or age

Although limited data are available about the use of pazopanib in patients aged 65 years and older, no clinically significant differences in safety of pazopanib were observed in patients of different ages.<sup>19</sup> In patients with moderate hepatic impairment, as indicated by elevated bilirubin and aminotransferases, pazopanib clearance was decreased by 50% resulting in a 2-fold increased AUC and  $C_{max}$  compared to subjects with normal hepatic function.<sup>37</sup> It is therefore recommended that patients with hepatic abnormalities are treated initially according to the pazopanib doses mentioned in table 2. Starting dose of pazopanib should therefore be reduced to 200 mg QD in patients with moderate hepatic impairment and in patients with severe hepatic impairment pazopanib is contraindicated.<sup>19</sup>

Currently, no age-related influences on the pharmacokinetics of axitinib have been reported, and information about the potential effect of diseases on its pharmacokinetics and –dynamics is limited. In a phase I study evaluating the effects of hepatic impairment, as indicated by the Child-Pugh classification, on the pharmacokinetics and safety of a single oral dose of axitinib, subjects with mild hepatic dysfunction had similar pharmacokinetics compared to those with normal hepatic function. Subjects with moderate hepatic impairment however, had increased axitinib exposure compared to subjects with normal hepatic function, as indicated by an approximate two-fold higher  $AUC_{0-\infty}$ . The effect of severe hepatic impairment was not evaluated in this study. However, it can be reasonably

**Table 2. Pazopanib and axitinib starting dose in patients with hepatic impairment**

	Pazopanib		Axitinib		
	Bilirubine	ALT	Starting dose	Child-Pugh Class	Starting dose
Mild	≤ ULN	> ULN	800 mg	A	5 mg
	> 1 to 1.5 x ULN	regardless	800 mg		
Moderate	> 1.5 to 3 x ULN	regardless	200 mg	B	2 mg
Severe	> 3 x ULN	regardless	contraindicated	C	Not investigated

Abbreviations: ALT, alanine aminotransferase; ULN, upper limit of normal



expected to exceed or equal the effect of moderate hepatic dysfunction.<sup>32</sup> The recommended initial doses of axitinib are listed in table 2. After the initial dose, subsequent doses can be increased or decreased based on individual safety and tolerability.

To date, no dedicated renal impairment trials for pazopanib and axitinib have been conducted. However, renal impairment is unlikely to significantly affect the pharmacokinetic properties of both drugs since less than 4% of orally administered pazopanib is eliminated via renal excretion and after oral administration of axitinib no renal elimination of unchanged drug could be found.<sup>17,19</sup> Furthermore, based on pharmacokinetic analysis no significant difference in clearance of both compounds was observed in patients with mild to severe renal impairment.<sup>16,17</sup>

### Pharmacogenetics

Since metabolism of pazopanib and axitinib occurs principally via CYP isozymes, polymorphisms in genes encoding these enzymes might contribute to the pharmacokinetic variability of these compounds. Next to CYP isozymes, axitinib is also a substrate for UGT1A1 and the drug transporters P-glycoprotein, encoded by the *ABCB1* gene, and OATP1B1, encoded by *SLC01B1*, which are also potential contributors to the interpatient variability in the pharmacokinetics of axitinib. However, in a meta-analysis using data pooled from 11 clinical pharmacological trials in healthy volunteers, none of the 15 polymorphisms analysed were of significant relevance in explaining axitinib pharmacokinetic variability. Genotype-based dose adjustment is therefore not warranted after patients have been started on the initial dose of 5 mg BID.<sup>38</sup>

Also for pazopanib, *CYP3A4* polymorphisms have no known effect on the pharmacokinetics of this compound. However, in a study examining 27 single nucleotide polymorphisms in 13 genes in 397 mRCC patients receiving pazopanib, polymorphisms in *IL-8*, *HIF1A*, *NR1I2* and *VEGFA* showed significant association with PFS when compared to wild-type genotypes.<sup>39</sup> Validation of these results is now ongoing to evaluate if these germline genetic markers can be used as predictive markers of the likelihood of response. In a preclinical *in vivo* study examining the effects of different *BRAF* genotypes on the anti-tumor activity of pazopanib, significant differences were found between several xenograft tumor models. Only cell lines exhibiting either exon 11 mutations of *BRAF*, HER2 overexpression, or multiple pazopanib targets demonstrated a significant anti-angiogenic response to pazopanib treatment. This result indicates a significant role of *BRAF* in angiogenesis and suggests that *BRAF* status might be a predictive marker for pazopanib efficacy.<sup>40</sup>

### Drug Resistance

Mechanisms of resistance to anti-angiogenic therapy include amplification of pro-angiogenic genes, secretion of multiple pro-angiogenic factors (e.g. angiopoietin, VEGF(R) and ephrins), recruitment of pro-angiogenic bone marrow-derived cells and escape mechanisms via different modes of vascularization.<sup>41</sup> The first three mechanisms will ultimately result in increased levels of VEGF. Increased levels of VEGF and VEGFR might lead to specific angiogenic inhibitor-related toxicities and a faster regrowth of tumor vasculature when the anti-VEGF drug is discontinued.<sup>42,43</sup>

## Pharmacodynamics

The relationship between the dose of axitinib and response has not been extensively explored. In one study the pharmacodynamic response to treatment with axitinib was measured by dynamic contrast-enhanced magnetic resonance imaging (DCE-MRI). Indicators of vascular response, such as the volume transfer constant ( $K^{trans}$ ), which correlates with tumor vascular permeability and perfusion, and initial area under the curve (IAUC), were calculated to examine the effect of axitinib treatment on tumor vascular function. By day 2 of therapy, a 50% decrease in  $K^{trans}$  and IAUC was demonstrated, which persisted through week 4 of treatment and corresponded to a plasma  $AUC_{0-24}$  of  $> 200 \text{ ng} \cdot \text{h/mL}$ . Furthermore, both  $K^{trans}$  and IAUC percentage changes correlated in a linear manner with the  $AUC_{0-24}$  and  $C_{max}$  of axitinib plasma.<sup>44</sup> Another study retrospectively examined the correlation between the diastolic blood pressure (dBp) and the antitumor response to axitinib. This study demonstrated that patients with at least 1 dBp  $\geq 90 \text{ mm Hg}$  during therapy had a significantly lower relative risk of death compared to those with dBp  $< 90 \text{ mm Hg}$  throughout therapy (HR = 0.55,  $P < 0.001$ ). The relative risk of progression was lower in patients with dBp  $\geq 90 \text{ mm Hg}$ , and the objective response rate was significantly higher (43.9% vs. 12%,  $P < 0.001$ ). Furthermore, median PFS (10.2 vs. 7.1 months) and median OS (25.8 vs. 14.9 months) were greater for patients with dBp  $\geq 90 \text{ mm Hg}$ .<sup>45</sup> Additional studies to examine the pharmacodynamics of axitinib are currently ongoing.

The pharmacokinetic-pharmacodynamic relationships of pazopanib have not been extensively studied either. In a phase II trial the relationship between plasma concentrations of pazopanib and drug exposure was investigated in 205 patients after 4 and 12 weeks of treatment. Patients with a plasma concentration of pazopanib  $\geq 20.6 \text{ } \mu\text{g/mL}$  ( $n = 143$ ) at week 4 had a median PFS of 49.4 weeks and patients with plasma concentrations  $< 20.6 \text{ } \mu\text{g/mL}$  20.3 weeks ( $n = 62$ ,  $P = 0.0041$ ). The overall response rate in these patients was 45% versus 18% ( $P = 0.000017$ ). Plasma levels of pazopanib  $\geq 20.6 \text{ } \mu\text{g/mL}$  may therefore be associated with improved efficacy.<sup>46</sup> However, this needs to be proven in prospective studies. Furthermore, results of a phase I study of pazopanib in patients with advanced tumors suggested that hypertension may represent a general pharmacodynamic marker of the activity of pazopanib. Further research however is necessary to examine the clinical relevance of this finding.<sup>24</sup> In a phase II study with pazopanib in patients with RCC, no significant correlation was observed between 12-week treatment response and the von Hippel-Lindau (VHL) status or other soluble markers including sVEGFR1, VEGF and CEC.<sup>47</sup>

## Toxicity

Chronic administration of axitinib and pazopanib is associated with manageable toxicities and a low rate of treatment discontinuation. The most common adverse events (all grades) reported in clinical trials with axitinib were diarrhea, hypertension, fatigue, nausea, decreased appetite, dyspnea, dysphonia, hand-foot syndrome and decreased weight.<sup>8,14,28</sup> In the pivotal phase III trial of pazopanib, diarrhea, hypertension, hair color changes, nausea, anorexia and vomiting were the most common adverse reactions (all grades). The most frequent adverse events of grade 3 or higher were hypertension (16%), diarrhea (11%) and fatigue (11%) during treatment with axitinib, and hypertension (4%), diarrhea (3%) and asthenia (3%) during treatment with pazopanib. Creatinine elevation (55%), hypocalcaemia (39%), anaemia (33%), lymphocytopenia (33%) and lipase elevation (27%) were the most frequently reported laboratory abnormalities (all grades) in the pivotal phase III trial of axitinib, whereas ALT/AST increase

(53%) hyperglycemia (41%), leukopenia (37%), total bilirubin increase (36%) and neutropenia (34%) accounted for the most common laboratory abnormalities during pazopanib treatment (see table 3).<sup>2,8</sup>

2.1

**Table 3. Common treatment-emergent all causality adverse events in the pivotal phase III trials**

<b>Pazopanib (n = 290)</b>					
Adverse event	All grades (%)	≥ grade 3 (%)	Laboratory abnormalities	All grades (%)	≥ grade 3 (%)
Diarrhea	52	4	ALT increase	53	12
Hypertension	40	4	AST increase	53	8
Hair color changes	38	<1	Hyperglycemia	41	<1
Nausea	26	<1	Leukopenia	37	0
Anorexia	22	2	Bilirubine increase	36	4
Vomiting	21	2	Hypophosphatemia	34	4
Fatigue	19	2	Neutropenia	34	1
Asthenia	14	3	Hypocalcemia	33	3
Abdominal pain	11	2	Thrombocytopenia	32	1
Headache	10	0	Lymphopenia	31	4
			Hyponatremia	31	5
			Hypoglycaemia	17	<1
			Hypomagnesemia	11	4
<b>Axitinib (n = 359)</b>					
Adverse event	All grades (%)	≥ grade 3 (%)	Laboratory abnormalities	All grades (%)	≥ grade 3 (%)
Diarrhea	55	11	Creatinine elevation	55	0
Hypertension	40	16	Hypocalcemia	39	1
Fatigue	39	11	Anemia	35	<1
Decreased appetite	34	5	Lymphopenia	33	3
Nausea	32	3	Lipase elevation	27	5
Dysphonia	31	0	Thrombocytopenia	15	<1
Hand-foot syndrome	27	5	Hypophosphatemia	13	2
Weight decreased	25	2	Haemoglobin elevation	10	0
Vomiting	24	3	Neutropenia	6	1
Asthenia	21	5	Hypercalcemia	6	0
Constipation	20	1			
Hypothyroidism	19	<1			
Mucosal inflammation	15	1			

Abbreviations: ALT, alanine aminotransferase; AST, aspartate aminotransferase.

## Patient Instructions and Recommendations for Supportive Care

Pazopanib should be administered without food and the tablet must not be crushed. Axitinib may be taken with or without food. Since hypertension is a frequently occurring adverse reaction associated with both drugs, blood pressure should be monitored frequently. Mild to moderate hypertension should be treated with standard antihypertensive therapy and axitinib/pazopanib treatment may be continued. In patients who experience severe or persistent hypertension, while using antihypertensive therapy, discontinuation of axitinib/pazopanib should be considered.<sup>13,14,16,17</sup> Both compounds should not be used in pregnancy, as this may cause fetal harm, and men and women should use effective birth control during treatment with pazopanib or axitinib, because both drugs are teratogenic. As pazopanib and axitinib may increase serum levels of transaminases and bilirubin, liver biochemistry should be measured before treatment initiation and regularly during treatment. Additionally, monitoring of thyroid function and urine protein is recommended during treatment with both pazopanib and axitinib.<sup>16,17</sup>

## Conclusions

Pazopanib and axitinib are both FDA approved ATP-competitive VEGFR inhibitors and represent treatment options for patients with mRCC. The efficacy of pazopanib appears to be comparable to sunitinib, one of the main treatment options in the mRCC, and it may have a better tolerability profile. Therefore, pazopanib appears to be a valuable addition to the treatment of mRCC. However, results from head-to-head comparative studies, such as the COMPARZ clinical trial, are to be awaited to make a definitive statement about the position of pazopanib in relation to other medications for mRCC. Compared with sorafenib, axitinib demonstrated improved progression free survival, objective response rate and overall survival in previously treated patients with mRCC. This makes axitinib a treatment option for second-line therapy of mRCC and ongoing clinical trials have to determine the suitability of axitinib in the first-line setting. To conclude, pazopanib and axitinib, together with other recently approved drugs, including sorafenib, sunitinib, tamsirolimus, everolimus and bevacizumab altered the treatment paradigm of metastatic renal cell cancer and offer patients multiple treatment options.

## References

1. Bukowski RM, Yasothan U, Kirkpatrick P. Pazopanib. *Nat Rev Drug Disc* 2010;9:17-18.
2. Sternberg CN, Davis ID, Mardiak J et al. Pazopanib in locally advanced or metastatic renal cell carcinoma: results of a randomized phase III trial. *J Clin Oncol* 2010;28:1061-1068.
3. Sleijfer S, Ray-Coquard I, Papai Z et al. Pazopanib, a multikinase angiogenesis inhibitor, in patients with relapsed or refractory advanced soft tissue sarcoma: a phase II study from the European organisation for research and treatment of cancer-soft tissue and bone sarcoma group (EORTC study 62043). *J Clin Oncol* 2009;27:3126-3132.
4. Friedlander M, Hancock KC, Rischin D et al. A Phase II, open-label study evaluating pazopanib in patients with recurrent ovarian cancer. *Gynecol Oncol* 2010;119(1):32-37.
5. Altorki N, Lane ME, Bauer T et al. Phase II proof-of-concept study of pazopanib monotherapy in treatment-naive patients with stage I/II resectable non-small-cell lung cancer. *J Clin Oncol* 2010;28:3131-3137.
6. Bible KC, Suman VJ, Molina JR et al. Efficacy of pazopanib in progressive, radioiodine-refractory, metastatic differentiated thyroid cancers: results of a phase 2 consortium study. *Lancet Oncol* 2010;11:962-972.
7. Food and Drug Administration. FDA Briefing Document Oncologic Drugs Advisory Committee Meeting NDA 202324 Axitinib (Inlyta®). 2011.
8. Rini BI, Escudier B, Tomczak P et al. Comparative effectiveness of axitinib versus sorafenib in advanced renal cell carcinoma (AXIS): a randomised phase 3 trial. *Lancet* 2011;378:1931-1939.
9. U.S. National Institutes of Health. <http://www.clinicaltrials.gov>. Accessed on 24 april, 2012.
10. Glade Bender JL, Lee A, Adamson PC et al. Phase I study of pazopanib in children with relapsed or refractory solid tumors (ADVL0815): A Children's Oncology Group Phase I Consortium. *J Clin Oncol* 2011;29 (suppl; abstr 9501).
11. Hutson TE, Davis ID, Machiels JPH et al. Efficacy and safety of pazopanib in patients with metastatic renal cell carcinoma. *J Clin Oncol* 2010;28:475-480.
12. Bukowski RM. Critical appraisal of pazopanib as treatment for patients with advanced metastatic renal cell carcinoma. *Cancer Manag Res* 2011;3:273-285.
13. Rini BI, Wilding G, Hudes G et al. Phase II study of axitinib in sorafenib-refractory metastatic renal cell carcinoma. *J Clin Oncol* 2009;27:4462-4468.
14. Rixe O, Bukowski RM, Michaelson MD et al. Axitinib treatment in patients with cytokine-refractory metastatic renal-cell cancer: a phase II study. *Lancet Oncol* 2007;8:975-984.
15. Motzer RJ, de La Motte Rouge T, Harzstark AL et al. Axitinib second-line therapy for metastatic renal cell carcinoma (mRCC): Five-year (yr) overall survival (OS) data from a phase II trial. *J Clin Oncol* 2011;29 (suppl; abstr 4547).
16. Full Prescribing Information, Votrient (pazopanib) tablets. Brentford, United Kingdom: GlaxoSmithKline, 2009.
17. Full Prescribing Information, Inlyta (axitinib) tablets. New York city, NY, USA: Pfizer, 2012.
18. Hamberg P, Verweij J, Sleijfer S. (Pre-)clinical pharmacology and activity of pazopanib, a novel multikinase angiogenesis inhibitor. *The Oncologist* 2010;15:539-547.

19. European Medicines Agency. Votrient (Pazopanib): Summary of Product Characteristics. Available at [http://www.ema.europa.eu/docs/en\\_GB/document\\_library/EPAR\\_-\\_Product\\_Information/human/001141/WC500094272.pdf](http://www.ema.europa.eu/docs/en_GB/document_library/EPAR_-_Product_Information/human/001141/WC500094272.pdf). Accessed April 29, 2012.
20. Sonpavde G, Hutson TE. Pazopanib: a novel multitargeted tyrosine kinase inhibitor. *Curr Oncol Rep* 2007;9:115-119.
21. Scagliotti G, Govindan R. Targeting angiogenesis with multitargeted tyrosine kinase inhibitors in the treatment of non-small cell lung cancer. *The Oncologist* 2010;15:436-446.
22. Bhargava P, Robinson MO. Development of second-generation VEGFR tyrosine kinase inhibitors: current status. *Curr Oncol Rep* 2011;13:103-111.
23. Sparidans RW, Lusuf D, Schinkel AH. Liquid chromatography-tandem mass spectrometric assay for the light sensitive tyrosine kinase inhibitor axitinib in human plasma. *J Chromatogr B Analyt Technol Biomed Life Sci* 2009;877(32):4090-4096.
24. Hurwitz HI, Dowlati A, Saini S et al. Phase I trial of pazopanib in patients with advanced cancer. *Clin Cancer Res* 2009;15:4220-4227.
25. Yau T, Chen PJ, Chan P et al. Phase I dose-finding study of pazopanib in hepatocellular carcinoma: evaluation of early efficacy, pharmacokinetics, and pharmacodynamics. *Clin Cancer Res* 2011;17:6914-6923.
26. Heath EI, Chiorean EG, Sweeney CJ et al. A phase I study of the pharmacokinetic and safety profiles of oral pazopanib with a high-fat or low-fat meal in patients with advanced solid tumors. *Clin Pharmacol Ther* 2010;88(6):818-823.
27. Heath EI, Forman K, Malburg L et al. A phase I pharmacokinetic and safety evaluation of oral pazopanib dosing administered as crushed tablet or oral suspension in patients with advanced solid tumors. *Invest New Drugs* 2011.
28. Rugo HS, Herbst RS, Liu G et al. Phase I Trial of the Oral Antiangiogenesis Agent AG-013736 in Patients With Advanced Solid Tumors: Pharmacokinetic and Clinical Results. *J Clin Oncol* 2005;23:5474-5483.
29. Pithavala YK, Tong W, Mount J et al. Effect of ketoconazole on the pharmacokinetics of axitinib in healthy volunteers. *Invest New Drugs* 2012;30(1):273-281.
30. Pithavala YK, Tortorici M, Toh M et al. Effect of rifampin on the pharmacokinetics of Axitinib (AG-013736) in Japanese and Caucasian healthy volunteers. *Cancer Chemother Pharmacol* 2010;65:563-570.
31. Kelly RJ, Rixe O. Axitinib (AG-013736). In Martens UM. *Small Molecules in Oncology*. Springer; 2010. p33-44.
32. Tortorici M, Toh M, Rahavanedran SV et al. Influence of mild and moderate hepatic impairment on axitinib pharmacokinetics. *Invest New Drugs* 2011;29:1370-1380.
33. Australian Government Department of Health and Ageing, T.G.A. Australian Public Assessment Report for Pazopanib hydrochloride. Available at: <http://www.tga.gov.au/pdf/auspar/auspar-votrient.pdf>. Accessed at April 29, 2012.
34. Spano JP, Moore MJ, Pithavala YK et al. Phase I study of axitinib (AG-013736) in combination with gemcitabine in patients with advanced pancreatic cancer. *Invest New Drugs* 2011.
35. Monk BJ, Lopez LM, Zarba JJ et al. Phase II, open-label study of pazopanib or lapatinib monotherapy compared with pazopanib plus lapatinib combination therapy in patients with advanced and recurrent cervical cancer. *J Clin Oncol*;28:3562-3569.

36. Tan AR, Dowlati A, Jones SF et al. Phase I study of pazopanib in combination with weekly paclitaxel in patients with advanced solid tumors. *The Oncologist* 2010;15:1253-1261.
37. Shibata S, Longmate J, Chung VM et al. A phase I and pharmacokinetic single agent study of pazopanib (P) in patients (Pts) with advanced malignancies and varying degrees of liver dysfunction (LD). *J Clin Oncol* 2010;28:15s (suppl; abstr 2571).
38. Brennan M, Williams JA, Chen Y et al. Meta-analysis of contribution of genetic polymorphisms in drug-metabolizing enzymes or transporters to axitinib pharmacokinetics. *Eur J Clin Pharmacol* 2012;68(5):645-655.
39. Xu CF, Bing NX, Ball HA et al. Pazopanib efficacy in renal cell carcinoma: evidence for predictive genetic markers in angiogenesis-related and exposure-related genes. *J Clin Oncol* 2011;29:2557-2564.
40. Gril B, Palmieri D, Qian Y et al. The B-Raf status of tumor cells may be a significant determinant of both antitumor and anti-angiogenic effects of pazopanib in xenograft tumor models. *PLoS One* 2011;6(10):e25625.
41. Loges S, Schmidt T, Carmeliet P. Mechanisms of resistance to anti-angiogenic therapy and development of third-generation anti-angiogenic drug candidates. *Genes Cancer* 2010;1(1):12-25.
42. Tran J, Master Z, Yu JL et al. A role for survivin in chemoresistance of endothelial cells mediated by VEGF. *Proc Natl Acad Sci U S A* 2002;99(7):4349-4354.
43. Mancuso MR, Davis R, Norberg SM et al. Rapid vascular regrowth in tumors after reversal of VEGF inhibition. *J Clin Invest* 2006;116:2610-2621.
44. Liu G, Rugo HS, Wilding G et al. Dynamic contrast-enhanced magnetic resonance imaging as a pharmacodynamic measure of response after acute dosing of AG-013736, an oral angiogenesis inhibitor, in patients with advanced solid tumors: results from a phase I study. *J Clin Oncol* 2005;23:5464-5473.
45. Rini BI, Schiller JH, Fruehauf JP et al. Diastolic blood pressure as a biomarker of axitinib efficacy in solid tumors. *Clin Cancer Res*;17(11):3841-3849.
46. Suttle B, Ball HA, Molimard M et al. Relationship between exposure to pazopanib (P) and efficacy in patients (pts) with advanced renal cell carcinoma (mRCC). *J Clin Oncol* 2010;28:15s (suppl; abstr 3048).
47. Hutson TE, Davis ID, Machiels JH et al. Biomarker analysis and final efficacy and safety results of a phase II renal cell carcinoma trial with pazopanib (GW786034), a multi-kinase angiogenesis inhibitor. *J Clin Oncol* 2008;26 (suppl; abstr 5046).





# Chapter 2

## Clinical pharmacology of targeted anticancer drugs



### 2.2

#### Crizotinib-induced fatal fulminant liver failure

**Lung Cancer** 2016;93:17-9

Robin M.J.M. van Geel, Jeroen J.M.A. Hendriks, Jelmer E. Vahl, Monique E. van Leerdam, Daan van den Broek, Alwin D.R. Huitema, Jos H. Beijnen, Jan H.M. Schellens, Sjaak A. Burgers

## ABSTRACT

Herein we describe a case of a 62-year-old female in good clinical condition with non-small-cell lung cancer who was treated with crizotinib. After 24 days of crizotinib therapy she presented with acute liver failure. Serum aspartate aminotransferase and alanine aminotransferase levels had increased from normal prior to crizotinib start to 2053 IU/L and 6194 IU/L, respectively. Total bilirubin and prothrombin time (PT-INR) increased up to 443 IU/L and 5.33, respectively, and symptoms of hepatic encephalopathy and hepatorenal syndrome emerged. Despite crizotinib discontinuation and intensive supportive therapy, the patient died 40 days after treatment with crizotinib was initiated due to acute liver failure with massive liver cell necrosis.

## Introduction

Non-small cell lung cancer (NSCLC), accounting for about 85% of all lung cancer cases, is diagnosed in approximately 1.3 million new patients worldwide each year.<sup>1</sup> Activating rearrangements of the anaplastic lymphoma kinase (ALK), causing constitutive kinase activity, are found in 5–7% of patients with NSCLC.<sup>2,3</sup> Targeting ALK using the small-molecule inhibitor crizotinib significantly improved clinical outcome of patients with ALK-positive advanced NSCLC as compared to standard chemotherapy and has become the preferred first-line therapy for this patient group.<sup>4</sup> In the present report we describe a case of fatal acute hepatic toxicity induced by crizotinib in a patient with ALK-positive NSCLC.

## Case-report

A 62-year-old female with stage IV ALK-positive NSCLC started crizotinib treatment (250 mg twice daily) after she progressed upon first-line chemotherapy with cisplatin/pemetrexed. Besides the primary tumor in the left lower lobe of the lung, radiological examination revealed lymphangitis carcinomatosa and metastases in the left breast, liver and right lobe of the lung. At baseline (day 1), Eastern Cooperative Oncology Group performance status was 1, no comorbidity other than yellow nail syndrome was present and clinical examination was normal except for diminished pulmonary sounds over the left lobe and deformed left mamma due to metastases. The patient was not known with any contra-indications for crizotinib, nor with any medication-related hypersensitivity and laboratory data revealed that serum liver enzymes were within normal limits (total bilirubin 5 µmol/L [normal reference < 16 µmol/L], AST 26 IU/L [< 31 IU/L], ALT 19 IU/L [< 34 IU/L]) (Figure 1). Lactate dehydrogenase (LDH) (246 IU/L [< 247 U/L]) was just under the upper limit of normal (ULN) and alkaline phosphatase (ALP) (184 IU/L [< 98 U/L]) and gamma-glutamyltransferase (64 IU/L [< 38 IU/L]) were slightly increased. The patient was using dexamethasone for her lymphangitis carcinomatosa, but this was discontinued at day 14 according to a planned tapering regimen. On day 7 serum ALT (44 IU/L) was slightly elevated compared to baseline while total bilirubin (3 µmol/L) remained below ULN, which was within limits to continue treatment with crizotinib.<sup>5</sup> On day 17 she showed clinical signs of tumor regression as indicated by decreased stiffness of the left mamma. Adverse drug reactions were absent and laboratory blood samples were taken and evaluated at her next visit (day 24). Retrospectively, laboratory data revealed elevated ALT (2062 IU/L), but normal total bilirubin (5 µmol/L) at day 17. Although she showed no clinical abnormalities at day 24, liver function had further decreased (total bilirubin 25 µmol/L, ALT 6194 IU/L, AST 2053 IU/L, LDH 1073 IU/L, albumin 33 g/L) and crizotinib was discontinued. She did not use alcohol nor hepatotoxic co-medication in the past weeks. On day 31, the patient suffered from diarrhea and physical examination showed icteric sclera. Total bilirubin had further increased to 286 µmol/L and infection with hepatitis A, B or C virus was excluded. Her serum tested positive for Epstein-Barr virus IgG and hepatitis E virus IgG antibodies, but not for IgM antibodies. Coagulation factor V concentration was 11% [normal reference: 70–130%], serum ferritin level (10756 µg/L) was strongly elevated and prothrombin time (PT-INR 5.33) was prolonged, matching with the King's College criteria for acute liver failure with poor prognosis, together with age (> 40 years), etiology (idiosyncratic drug-induced), icterus and bilirubin level (> 300 µmol/L).<sup>6</sup> Nevertheless, given her poor lung cancer related prognosis she was not a candidate for liver transplantation. Abdominal ultrasound showed no evidence of biliary obstruction, portal hypertension, portal vein thrombosis or ascites. At this point her model for end-stage liver disease (MELD) score was 36, indicating an estimated 3-month mortality

of 53%. As crizotinib metabolism largely depends on CYP3A, genetic variability in the gene encoding CYP3A may cause increased plasma concentrations of crizotinib. Plasma crizotinib levels in blood samples taken on days 31–36 were within the normal range of what can be expected after crizotinib discontinuation. The plasma elimination half-life ( $t_{1/2}$ ) was estimated to be ~50 h, slightly longer than average (42 h).<sup>5</sup> However, this effect may as well be a result of crizotinib-induced liver failure instead of genetic polymorphisms in CYP3A. On day 33 she was admitted to the Hospital because of acute liver failure with initial clinical signs of hepatic encephalopathy, although serum ammonia level (32  $\mu\text{mol/L}$  [normal reference < 50  $\mu\text{mol/L}$ ]) was not elevated. She was intensively treated according to the Dutch guidelines for acute hepatic failure including lactulose against encephalopathy, prophylactic antibiotics (cefotaxim, vancomycine), proton pump inhibitor and vitamin K suppletion. CT scan of the brain showed diffuse supratentorial edema and no evidence of cerebral metastases. On day 35 her consciousness deterioration persisted and she suffered from progressive edema of the lower legs, upper legs and hands. Serum creatinine had increased to 152  $\mu\text{mol/L}$  despite intravascular volume expansion, with decreased micturition and < 20 mmol/L urinary sodium. This indicated symptoms of hepatorenal syndrome for which terlipressine and albumin were initiated. She became progressively more dyspnoeic due to increasing pleural fluid and ascites. Although renal function seemed to improve on day 39 (serum creatinine 118  $\mu\text{mol/L}$ ), her liver function did not (total bilirubin 419  $\mu\text{mol/L}$ ) and her consciousness was rapidly deteriorating. On day 40 the patient died. Autopsy or liver biopsy could not be performed.

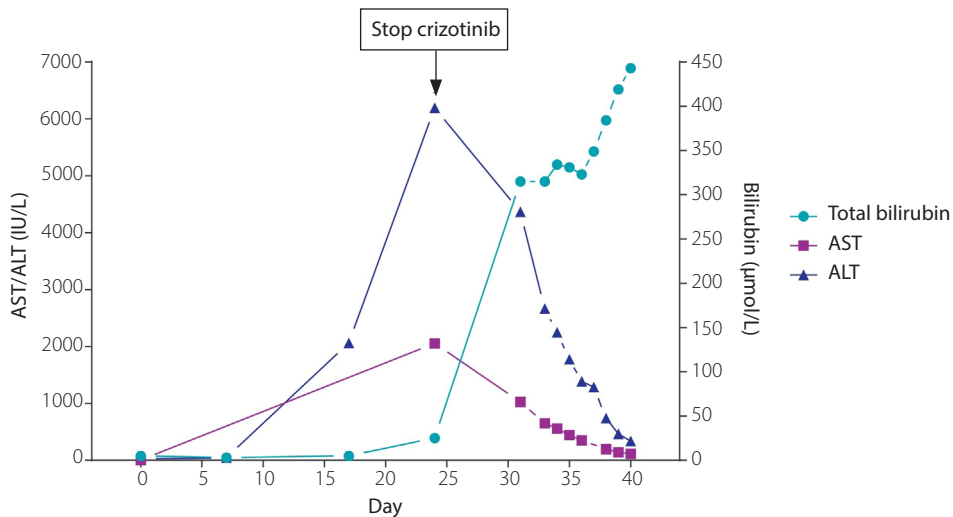


**Figure 1.** Detailed overview of liver enzymes (total bilirubin, AST and ALT) during crizotinib treatment (day 0–23) and after crizotinib discontinuation (day 24–40).

## Discussion

This report describes the first case of crizotinib-induced fatal fulminant acute liver failure due to liver cell necrosis in a Caucasian patient. Other causes of acute liver failure were excluded including biliary obstruction, viral hepatitis infection, alcoholic liver disease and concomitant medication. Moreover, liver toxicity is a common adverse event in patients using crizotinib; grade 3–4 ALT elevations occurred within the first two months of crizotinib treatment in approximately 15% of patients in pivotal phase III studies.<sup>4,7</sup> In the majority of patients ALT elevations were reversible upon dosing interruption, but in rare cases permanent discontinuation was necessary.<sup>8,9</sup> Crizotinib-induced hepatotoxicity with fatal outcome occurred in 0.2% of patients.<sup>5</sup> Therefore, monitoring of liver function including ALT and total bilirubin is recommended every week during the first 2 months of treatment and once a month thereafter according to prescribing information.<sup>5</sup> Although the mechanism of crizotinib-induced hepatotoxicity is unknown, there seems to be a pathophysiologic difference between the common gradually increasing liver enzymes and the fulminant idiosyncratic liver failure in our patient. Sato and colleagues described a similar course of disease with mildly elevated liver enzymes on day 16 of crizotinib treatment and severe liver impairment two weeks later, which ultimately caused this patient to die on day 36 despite immediate crizotinib discontinuation and supportive therapy at the intensive care unit.<sup>10</sup> Therefore, weekly liver enzyme evaluation is not sufficient to prevent these sporadic crizotinib-induced hepatotoxic events with potential fatal outcome. The dose-independent and abrupt hepatic impairment argues for an immune-related mechanism, possibly similar to lapatinib-induced hepatotoxicity which has been associated with specific HLA polymorphisms within the major histocompatibility complex (MHC).<sup>11</sup> Future research should therefore focus on elucidating the underlying mechanism of these severe cases and on identifying risk factors that may predict severe crizotinib-induced hepatitis. In the meantime, physicians should be aware of this potential fatal adverse reaction and evaluate liver function at least once a week during the first 2 months of treatment and more frequently in case of increasing liver enzymes.

## References

1. Bray F, Ren JS, Masuyer E, Ferlay. Global estimates of cancer prevalence for 27 sites in the adult population in 2008. *Int J Cancer* 2013;132:1133–45.
2. Soda M, Choi YL, Enomoto M, et al. Identification of the transforming EML4-ALK fusion gene in non-small-cell lung cancer. *Nature* 2007;448:561–6.
3. Camidge DR, Doebele RC. Treating ALK-positive lung cancer—early successes and future challenges. *Nat Rev Clin Oncol* 2012;9:268–277.
4. Shaw AT, Kim D-W, Nakagawa K, et al. Crizotinib versus chemotherapy in advanced ALK-positive lung cancer. *N Engl J Med* 2013;368:2385–94.
5. FDA. Prescribing information Xalkori® (crizotinib), (2013).
6. O'Grady JG, Alexander GJ, Hayllar KM, Williams R. Early indicators of prognosis in fulminant hepatic failure. *Gastroenterology* 1989;97:439–45.
7. Solomon BJ, Mok T, Kim D-W, et al. First-line crizotinib versus chemotherapy in ALK-positive lung cancer. *N Engl J Med* 2014;371:2167–77.
8. Camidge DR, Bang Y, Kwak EL, et al. Activity and safety of crizotinib in patients with ALK-positive non-small-cell lung cancer: updated results from a phase 1 study. *Lancet Oncol* 2012;13:1011–9.
9. Ripault M-P, Pinzani V, Fayolle V, et al. Crizotinib-induced acute hepatitis: First case with relapse after reintroduction with reduced dose. *Clin Res Hepatol Gastroenterol* 2013;37:e21–e23.
10. Sato Y, Fujimoto D, Shibata Y, et al. Fulminant Hepatitis Following Crizotinib Administration for ALK-positive Non-small-cell Lung Carcinoma. *Jpn J Clin Oncol* 2014;44:872–5.
11. Spraggs CF, Budde LR, Briley LP, et al. HLA-DQA1\*02:01 is a major risk factor for lapatinib-induced hepatotoxicity in women with advanced breast cancer. *J Clin Oncol* 2011;29:667–73.

2.2





# Chapter 3

## Drug-drug interactions in oncology: *bogey or godsend?*



Submitted for publication

Robin M.J.M. van Geel, Jos H. Beijnen, Jan H.M. Schellens

### ABSTRACT

Drug-drug interactions (DDIs) are amongst the major causes of adverse drug reactions, with fatal outcome in some cases. In oncology in particular, patients are at increased risk for detrimental effects of DDIs as anti-cancer treatment often consists of multiple, strong-acting and high-dosed medication. With the emergence of numerous targeted anticancer agents in recent years, the risk of new drug interactions continues to increase. On the other hand, DDIs also provide a unique opportunity to further improve the anti-tumour activity of anti-cancer drugs and/or overcome resistance mechanisms using synergistically acting combinations. With the rapid expansion of precision medicine aiming to paralyse malignant driver signals in cancer cells and their escape mechanisms simultaneously, the application of drug combinations will irrefutable rise further. Meticulous basic-molecular and pharmacologic research remains imperative to predict the potential harmful and favourable effects of DDIs in patients. In this review, we discuss both detrimental and beneficial DDIs with novel anticancer drugs. In addition, we highlight emerging technologies to predict potential DDIs and tools to handle DDIs in the clinic.

## Introduction

A drug-drug interaction (DDI) can be defined as an alteration of the (clinical) effect of a given drug caused by interference of another drug. DDIs pose an increasing problem in daily medical practice and comprise a significant portion of hospital visits and admissions caused by adverse drug reactions.<sup>1-3</sup> As approximately 20-30% of all adverse drug reactions are caused by DDIs,<sup>4</sup> which in some cases may have fatal outcome (Table 1), the impact should not be underestimated. Adverse drug reactions increase morbidity and mortality, diminish quality of life, promote non-adherence and ultimately lead to higher healthcare costs. The risk of DDIs is associated with the number of drugs taken by patients<sup>4</sup> and oncology in particular is a medical discipline in which patients receive multiple drugs concomitantly. Elderly cancer patients are usually exposed to even more drugs due to comorbidities and a higher incidence of disease- and treatment-related complications.<sup>5-8</sup> Moreover, the clinical impact of DDIs in oncology may be more pronounced, as the majority of anticancer drugs is strong acting, has a steep dose-response relationship, a narrow therapeutic window and is often dosed near or at the maximum tolerated dose. Therefore, minor changes in drug exposure, *e.g.* due to DDIs, can have a major effect on the clinical outcome with potentially adverse consequences.

Since our review on DDIs in oncology a decade ago, there have been many developments.<sup>9</sup> Molecular biologic insights into how cancer cells arise and survive have increased enormously and the completion of the Human Genome Project contributed to identifying the involved driver genes. In the past years this research has provided novel drug targets and a plethora of new anticancer agents that specifically interact with signalling pathways crucial for cancer survival and progression. Typically, treatment with these new agents also comprises concomitant use with other medicines, raising concern of DDIs with adverse effects. On the other hand however, there is also a trend towards the intentional use of rational combinations of anticancer agents to take advantage of their mutual, additive or synergistic interaction.

Herein, we give an update on pharmacokinetic and pharmacodynamic DDIs in oncology with selected examples, subdivided into DDIs with detrimental and advantageous effects. Additionally, we touch on novel strategies to predict DDIs and emerging tools to handle DDIs in clinical practice. Previously, multiple reviews discussed DDIs in oncology<sup>10-13</sup> and other types of drug interactions, which we leave aside here, including DDIs involving food components and herbs.<sup>14-17</sup>

## Epidemiology and relevance

Epidemiological figures on DDIs in oncology are scarce.<sup>18</sup> In a recent prospective study, Stoll and Kopittke<sup>19</sup> investigated the frequency of potential DDIs in a cohort of 113 cancer patients admitted in a public hospital in Brazil for systemic chemotherapy. All patients had at least one potential DDI, half of which were classified as major *i.e.* leading to death, hospitalization, permanent injury, or therapeutic failure. Up to 14% of all interactions involved anticancer agents.<sup>19</sup> Other studies, although with other designs, also point to high numbers.<sup>8,20-22</sup> Prevalence data of DDIs concerning novel targeted agents is growing and initial studies reported potentially interacting combinations in approximately 5–10% of patients taking oral anticancer agents.<sup>23-26</sup> Of course it makes a big difference whether there is only a theoretical indication for a DDI or whether it has convincing clinical consequences.

**Table 1. Drug-drug interactions in oncology with fatal outcome, by 'ADME classification' (selection)**

ADME	Anticancer agent	Interacting agent	Reference
<b>Absorption</b>	6-mercaptopurine	allopurinol	33
<b>Distribution</b>	methotrexate	NSAIDs	56, 167
<b>Metabolism</b>	5-FU, capecitabine	sorivudine, brivudine	57, 58, 62, 63
<b>Excretion</b>	methotrexate	trimethoprim, sulphamethoxazole	152

Abbreviations: ADME, absorption, distribution, metabolism, excretion; NSAIDs, nonsteroidal anti-inflammatory drugs; 5-FU, 5-fluorouracil

Nevertheless, despite the fact that methodologies, definitions and interpretations of DDIs and patient groups are far from uniform and not comparable between studies,<sup>27</sup> the general picture dominates that the prevalence of DDIs in oncology is high. On the other hand, unplanned hospital admissions of cancer patients due to any DDI seems rather sporadic, 0.2% of all admissions and 1.8% of all admissions due to drug-related problems<sup>28</sup>, and not much different from general medicine.<sup>1,2</sup> However, hospital admissions due to DDI-induced adverse events only provide insight into a part of the problem, as it often concerns DDIs that increase drug-exposure. DDIs that cause a reduction in bioavailability may cause less toxicity, but results in less clinical activity as well. Especially in the oncological setting, such DDIs have major clinical consequences but are often overlooked and epidemiological data thereof is lacking.

### Pharmacokinetic interactions with detrimental effects

Pharmacokinetic DDIs occur when a given compound alters the absorption, distribution, metabolism or excretion (or ADME) of another compound. Metabolising phase I-oxidative and phase II-conjugative enzymes and drug transporters are the major sites at which these interactions take place. Whereas enzyme inhibition mostly involves direct-acting reversible inhibitors with a rapid onset after administration and a rapid decay of inhibition when exposure decreases, enzyme induction usually concerns transcriptional activation leading to increased synthesis of the enzyme. Therefore, the timecourse of enzyme induction is a reflection of the enzyme turnover in addition to the half-life of the inducing agent, and is characterized by a delayed onset and a longer recovery time after discontinuation of the interacting drug.<sup>29,30</sup>

#### Absorption

In recent years a drastic paradigm shift took place in medical cancer care from intravenous towards oral therapy. It has become widely accepted that oral chemotherapy has obvious benefits such as patient convenience and reduced hospital costs, without loss of anticancer action.<sup>31,32</sup> However, combined administration of oral drugs holds potential risks for inadequate absorption (e.g. dasatinib when combined with acid suppressive drugs), but also for deleterious increased absorption (e.g. 6-mercaptopurine when combined with allopurinol).<sup>33</sup>

Because all novel small molecule signal transduction inhibitors (smSTIs) are administered orally and concurrent use of medicines and/or over-the-counter products is common, potential DDIs are looming. In particular, interactions with acid-reducing agents such as proton pump inhibitors (PPIs), H<sub>2</sub>-antagonists and antacids, require meticulous attention, as these agents are used by up to 50% of all

cancer patients.<sup>23,24,34–37</sup> Due to an increase in stomach pH, solubility of weak basic (relevant pKa-values  $\approx 2–6$ ) smSTIs decreases, leading to precipitation and thereby reduced absorption and exposure.<sup>24,36</sup> For dasatinib (pKa 3.1, 6.8 and 10.8), the solubility at pH 2.6 is 18 mg/mL and more than 18,000 times lower ( $< 0.001$  mg/mL) at pH 7.0.<sup>36</sup> When co-administered with the antacid Maalox (containing aluminium oxide and magnesium hydroxide) dasatinib area under the plasma concentration-time curve (AUC) was reduced by 55%. Combined with the H<sub>2</sub>-antagonist famotidine, dasatinib AUC decreased 61%<sup>38</sup> and with the proton pump inhibitor omeprazole 43%<sup>36</sup> compared to the exposures in the absence of gastric pH-modifying agents. These effects are considered clinically relevant and concomitant use is therefore discouraged. Other smSTIs of which the oral absorption is affected by acid suppressive agents to a clinically relevant extent are bosutinib<sup>39</sup>, crizotinib, dasatinib, erlotinib, gefitinib, lapatinib, and pazopanib.<sup>24</sup> Moreover, Chu and colleagues highlighted the clinical relevance of such DDIs reporting a significant detrimental effect of PPIs on erlotinib efficacy in terms of progression-free and overall survival in patients with non-small cell lung cancer.<sup>40</sup> Subsidiary risks lie within the fact that PPIs, antacids and H<sub>2</sub>-receptor antagonists are also over-the-counter products in many countries and, when not reported by the patient, can hide from the prescribers' review and checks by DDI software packages.

No effects of gastric acid suppression were reported for axitinib, cabozantinib<sup>41</sup>, cobimetinib<sup>42</sup>, ibrutinib<sup>43</sup>, imatinib, nilotinib, regorafenib, ruxolitinib, sorafenib, sunitinib, vandetanib, vemurafenib.<sup>24</sup> Conclusive studies on the combined use of antacids and afatinib, trametinib, dabrafenib, ceritinib, lenvatinib, olaparib, palbociclib or trametinib could not be traced in the literature, hitherto.

In addition to gastric pH and solubility properties of orally administered drugs, drug transporters play a vital role in drug absorption from the gastrointestinal tract. The interplay between intestinal transporters and metabolizing cytochrome P450 (CYP) enzymes, in which transporters regulate intracellular access to the metabolizing enzymes, enables highly efficient pre-systemic metabolism with a substantial effect on bioavailability. In this respect, ATP-binding cassette (ABC) transporters ABCB1 (or P-gp), ABCG2 (or BCRP) and ABCC2 (or MRP2) are the most investigated subtypes and act as efflux transporters in the apical membranes of epithelial cells in the small intestine. As many of the novel smSTIs are substrates of these transporters, their bioavailability is hampered (Table 2).<sup>35</sup> Vemurafenib for example, is a substrate for both ABCB1 and ABCG2. Upon oral administration of vemurafenib in *Abcb1a/1b<sup>-/-</sup>;Abcg2<sup>-/-</sup>* mice a 6.6 fold increased plasma AUC was found compared to in wild-type mice. Co-administration of the powerful dual ABCB1 and ABCG2 inhibitor elacridar, however, almost completely eliminated the action of *Abcb1* and *Abcg2* in restricting the oral availability of vemurafenib.<sup>44</sup> Similarly, elacridar boosted the oral uptake and bioavailability of the high affinity BCRP substrate topotecan from 40% to 97% and its variability almost halved in patients with solid tumors.<sup>45</sup> These examples highlight the impact of transporters on the bioavailability of substrate drugs, the potential inter-patient variability of substrate drugs due to transporter expression or activity differences, and the effect of concurrent administration of transporter inhibitors on drug exposure. Therefore, prescribing information of many novel oral anticancer drugs appeals to caution or dissuade to use a combination with known transporter substrates (e.g. digoxin, dabigatran, colchicine, pravastatin), or inducers (e.g. rifampicin, dexamethasone) or inhibitors (e.g. atorvastatin, ketoconazole).

**Table 2. Approved small molecule signal transduction inhibitors (smSTIs; “nibs”) for cancer treatment with targets, metabolising cytochrome P450 and UGT enzymes and transporters potentially involved in any process such as substrate metabolism-transport, induction or inhibition**

Agent	Target	Enzymes	Transporters
Afatinib	EGFR, HER2, HER4	-	P-gp, BCRP
Axitinib	VEGFR	3A4/5, 1A2, 2C19, UGT	P-gp
Bosutinib	Bcr-Abl	3A4	P-gp
Cabozantinib	RET, VEGFR, MET, TRKB, TIE2	3A4, 2C8	P-gp, MRP2
Ceritinib	ALK, ROS	3A, 2C9, 2A6, 2E1	P-gp, BCRP
Cobimetinib	MEK1, MEK2	-	-
Crizotinib	EML4-ALK, ROS1, MET	3A4/5, 2B6, UGT	P-gp, OCT1, OCT2
Dabrafenib	BRAFV600E	3A4, 2C8, 2B6	P-gp, BCRP, MRP2, OATP
Dasatinib	Bcr-abl, SRC, cKIT, PDGFR	3A4	P-gp, OATP, BCRP
Erlotinib	EGFR	3A4/5, 1A2, 2C8, UGT	P-gp, BCRP
Gefitinib	EGFR	3A4/5, 2D6	P-gp, OATP, BCRP
Ibrutinib	BTK	3A4, 2D6	P-gp
Imatinib	Bcr-Abl, cKIT	3A4	P-gp, OATP, BCRP
Lapatinib	EGFR, HER2	3A4/5, 2C19, 2C8	P-gp, OATP, BCRP
Lenvatinib	VEGFR, FGR, RET, KIT, PDGFR	3A4	-
Nilotinib	Bcr-abl	3A4, 2C8, 2C9, 2D6, UGT	P-gp, OATP, BCRP
Pazopanib	VEGFR, PDGFR, FGFR, KIT	3A4, 1A2, 2C8, UGT	P-gp, OATP, BCRP
Ponatinib	Bcr-Abl	3A4	P-gp, BCRP
Regorafenib	VEGFR, TIE2, PDGFR, RET, cKIT	3A4, UGT	P-gp, BCRP
Ruxolitinib	JAK1, JAK2	3A4, 2C9	P-gp, BCRP
Sorafenib	BRAF, KIT, FLT-3, RET, VEGFR, PDGFR	3A4, UGT	P-gp, OATP, BCRP, MRP2
Sunitinib	PDGFR, VEGFR, KIT, FLT-3, RET	3A4, 1A2	P-gp, OATP, BCRP
Trametinib	MEK1, MEK2	-	BCRP
Vandetanib	RET, EGFR, VEGFR, TIE2	3A4	OCT2
Vemurafenib	BRAFV600E	3A4, 1A2	P-gp, BCRP

*This table is not exhaustive. Data originate from SPCs (EMA Summary of Products Characteristics, Annex 1) and references cited in this manuscript. Abbreviations: ALK, anaplastic lymphoma kinase; BCRP, breast cancer resistance protein; BTK, Bruton's tyrosine kinase; Bcr-Abl, breakpoint cluster region-Abelson; EGFR, epidermal growth factor receptor; EML4, Echinoderm Microtubule Associated Protein Like 4; FGR, fibroblast growth factor receptor; FLT3, Fms-like tyrosine kinase-3; HER, Human Epidermal Growth Factor Receptor; JAK, Janus Associated Kinases; KIT, mast/stem cell growth factor receptor; MEK1, mitogen-activated extracellular signal regulated kinase 1; MET, hepatocyte growth factor receptor protein; MRP2, multi drug resistance associated protein 2; OATP, organic anion transporting protein; OCT1/2, organic cation transporter 1/2; PDGFR, platelet-derived growth factor receptor; P-gp, P-glycoprotein; VEGFR, vascular endothelial growth factor receptor; RET, Rearranged during Transfection; ROS1, c-ros oncogene-1; SRC, sarcoma proto oncogene; TRKB, Tropomyosin receptor kinase B; UGT, UDP-glucuronosyltransferase.*

Another group of transporters expressed in the apical membrane of the small intestinal epithelium are the organic anion-transporting polypeptides (OATPs). More specifically, OATP2B1, OATP1B1 and OATP1A2 with low expression, transporting both endogenous (*e.g.* bile acids) and exogenous substrates *e.g.* methotrexate, paclitaxel, docetaxel, pravastatin, imatinib, fexofenadine.<sup>46,47</sup> In contrast to ABCB1, ABCG2 and ABCC2, OATP transporters contribute to intestinal absorption and uptake of substrate drugs, whereas the others export their substrates back into the intestinal lumen.<sup>48</sup> Axitinib, pazopanib, nilotinib and sorafenib inhibit the OATP1B1 activity by more than 90% *in vitro*,<sup>47</sup> causing up to 80% increased exposure to OATP1B1 substrate docetaxel in patients.<sup>49-51</sup>

Organic cation transporters type 1 (OCT1) and OCT2 are expressed at the basolateral membrane of enterocytes and operate in the reverse direction as ABCB1, ABCG2 and ABCC2. OCT1 and OCT2 facilitate secretion of substrate cations from the blood compartment towards the intestinal lumen.<sup>52</sup> Crizotinib, serving as an example, inhibits OCT1 and OCT2 *in vitro*. Therefore, crizotinib may have the potential to increase plasma concentrations of co-administered drugs that are substrates of OCT1 or OCT2 (*e.g.*, metformin, procainamide).<sup>53</sup> Other intestinal (and hepatic) transporters are not considered here.<sup>54</sup>

### **Distribution**

Many anticancer drugs bind to plasma proteins. As only the unbound fraction of a drug is thought to be capable of diffusing into tissues, theoretically, protein-binding replacement by another drug could increase pharmacologically active concentrations to a toxic level. However, this type of DDIs usually rarely cause clinically relevant effects as protein-binding replacement has little effect on steady state concentration and AUC of the unbound fraction, due to rapid metabolism and excretion of the free fraction.<sup>55</sup> Nevertheless, a pharmacokinetic DDI of relevance is assumed for methotrexate when its highly protein-bound extracellular toxic metabolite 7-hydroxy-methotrexate is displaced from binding sites by other protein-bound drugs *e.g.* nonsteroidal anti-inflammatory drugs.<sup>56</sup>

### **Metabolism**

Metabolism or biotransformation in the liver, comprising oxidation, reduction, hydrolysis and conjugation reactions of substrate drugs, constitutes an important site for DDIs. The CYP enzyme family is mostly involved in drug metabolism of which CYP3A4, CYP2D6 and CYP2C9 are involved for the majority of drugs. Many drugs, including anticancer agents, can be inducers (*e.g.* corticosteroids, anticonvulsants, rifampicin, cyclophosphamide, paclitaxel, nilotinib, vandetanib) or inhibitors (*e.g.* azole antifungals, HIV protease inhibitors; vinca alkaloids, irinotecan, pazopanib, erlotinib) of these enzymes or their nuclear receptors. Drugs that share the same metabolic pathways or affect, in any way, the functioning of the involved enzymes are by definition candidates for DDIs. Competitive, reversible inhibition is the most common mechanism. In enzyme saturated conditions, competitive inhibition will theoretically lead to increased exposure, in which the extent of the alteration depends on the binding affinity or Michaelis constant (Km) of the enzyme for the interacting compounds. Other mechanisms include non-competitive inhibition (when a ligand binds to an allosteric site leading to conformational changes of the enzyme whereby its substrate's binding capacity decreases) and irreversible inhibition (when *e.g.* a reactive intermediate generated by a metabolizing enzyme binds covalently to the enzyme yielding permanent inhibition). Irreversible inhibition in particular can

have far-reaching clinical consequences. In this respect, the fatal interaction between 5-fluorouracil (5-FU) and sorivudine cannot remain undiscussed. In 1993, 18 patients died upon concurrent use of a 5-fluorouracil prodrug (oral tegafur) and the oral antiviral drug sorivudine, as a result of severe fluoropyrimidine-induced toxicity (mucositis, diarrhoea, bone marrow suppression).<sup>57,58</sup> In the gut flora, sorivudine is converted into (E)-5-(2-bromovinyl)uracil (BVU) which is reduced in the liver by dehydropyrimidine dehydrogenase (DPD) to the reactive intermediate H<sub>2</sub>-BVU. As a suicide inhibitor, H<sub>2</sub>-BVU instantly inactivates hepatic DPD through covalent binding at a cysteinyl residue in the pyrimidine binding pocket of DPD.<sup>57-60</sup> Since in human, over 85% of administered 5-FU is catabolized by DPD, treatment with sorivudine converts patients into completely DPD deficient and extremely poor fluoropyrimidine metabolizers, resulting in dramatically increased 5-FU levels and severe toxicity. Incomprehensible, this type of drug-drug interaction has not been completely eradicated yet.<sup>61-63</sup>

When a drug that is metabolized by a CYP isoenzyme is combined with an inhibitor or inducer of the same CYP enzyme, the effects of this potential metabolic DDI is worth investigating. Dasatinib for example, is primarily metabolized by CYP3A4 and may cause QT prolongation. When co-administered with the strong CYP3A4 inhibitor ketoconazole, the dasatinib AUC is markedly increased (4.8 fold), which was associated with a clinically relevant increase in corrected QT (QTc) values.<sup>64</sup> Similarly, lapatinib AUC increased 3.6 fold when combined with ketoconazole.<sup>65</sup> Abiraterone, a recently approved oral agent for metastatic, castration resistant prostate cancer, inhibits CYP2D6, CYP2C8, is a CYP3A4 substrate and has the potential to affect the exposure of other drugs metabolized by these enzymes.<sup>66</sup> Enzalutamide is metabolized by CYP2C8 and CYP3A4, both playing a role in the formation of the active metabolite N-desmethyl enzalutamide. Co-administration of the strong CYP2C8 inhibitor, gemfibrozil, increased the composite AUC of enzalutamide and its active metabolite by 2.2 fold and co-administration of the strong CYP3A4 inhibitor, itraconazole, by 1.3 fold. Conversely, enzalutamide as a moderate inducer of CYP2C9 and CYP2C19 but strong inducer of CYP3A4 reduced the AUC<sub>∞</sub> of oral S-warfarin, omeprazole, and midazolam by 56%, 70% and 86%, respectively.<sup>67</sup> CYP3A4 induction by rifampicin resulted in an approximate 64% and 80% decrease in nilotinib C<sub>max</sub> and AUC<sub>0-∞</sub>, respectively, and the elimination half-life was shortened by 4.2 hours from 18.8 to 14.6 hours.<sup>68</sup> Repeated rifampicin administration resulted in 21% increase in cabazitaxel clearance, associated with 17% decrease in AUC.<sup>69</sup>

The ligand-activated transcription factors, known as nuclear receptors, like the pregnane X receptor (PXR) and the constitutive androstane receptor (CAR), are key regulators of CYP enzymes and transporters like ABCB1 and provide a mechanism for enzyme induction.<sup>70</sup> Prototypical PXR activators such as rifampicin and hyperforin, the active constituent of St. John's wort bind and activate PXR resulting in an increase in mRNA expression of CYP3A4. The AUC and C<sub>max</sub> of imatinib was significantly reduced by 32% and 29%, respectively when the drug was given for 2 weeks in combination with this herbal product.<sup>71</sup> Furthermore, CAR activators such as the anti-epileptics phenobarbital and phenytoin are known to interact with many anticancer drugs with sometimes clinically relevant outcome.<sup>72</sup> Interestingly, anticancer drugs can also affect the nuclear receptors. For instance paclitaxel acts as PXR agonist, activates nuclear receptors and thereby induces CYP3A4 activity. In contrast, the marine derived anticancer drug trabectedin inhibits the transcriptional up-regulation of CYP3A4 and P-gp by directly antagonizing PXR.<sup>70</sup> Although PXR-specific antagonists have the potential to reduce the detrimental effects of PXR agonists,<sup>73</sup> the clinical usefulness of this approach seems limited as PXR agonists can often be omitted or replaced by non-PXR affecting alternatives.

### **Excretion**

Biliary-, direct intestinal- and renal-excretion constitute other excretory pathways of importance for some anticancer drugs *e.g.* platinum and antifolate agents. Drug transporters (*e.g.* P-gp, BCRP, MRPs, OATPs, OCTs) facilitate and are sometimes key in these processes.<sup>52</sup> When two combined drugs share the same transporters or affect their activities in any other ways then there may be an interaction. In general, any drug affecting renal functioning introduces a potential for DDIs with agents that rely on renal elimination *e.g.* cisplatin but also novel targeted agents such as imatinib and temsirolimus.<sup>74</sup>

### **Therapeutic antibodies**

Given the chemical and pharmacological properties of therapeutic antibodies, pharmacokinetic DDIs with therapeutic antibodies are not commonly expected. Few studies have investigated the DDI potential of antibodies used in oncology and mostly reported no clinical effects. Trastuzumab has no significant effect on the pharmacokinetics of concomitantly administered epirubicin<sup>75</sup>, doxorubicin<sup>76</sup>, vinflunine<sup>77</sup>, capecitabine<sup>78</sup>, cisplatin<sup>79</sup>, gemcitabine<sup>79</sup> and high dose chemotherapy (cyclophosphamide, cisplatin, carmustine).<sup>80</sup> Ado-trastuzumab emtansine (T-DM1, Kadcyla<sup>®</sup>) in which trastuzumab is conjugated through a stable thioether bond to the maytansanoid derivative emtansine has not been subject to DDI studies yet.<sup>81</sup> There is, however, a risk here.<sup>82</sup> The cytotoxic agent and CYP substrate emtansine is released, although in small quantities, in the systemic circulation<sup>83</sup> with a potential for interactions with strong CYP3A4 inhibitors. These combinations should preferably be avoided or be given with a long pause (*i.e.* several weeks, given the long terminal half-life of T-DM1).<sup>81</sup> Population pharmacokinetic analysis and other early clinical studies have demonstrated that there are no drug-drug pharmacokinetic interactions between the EGF-receptor tyrosine kinase inhibitors erlotinib and onartuzumab<sup>84</sup>, mapatumumab and carboplatin/paclitaxel<sup>85</sup>, erlotinib and bevacizumab<sup>86</sup>, rituximab with fludarabine/cyclophosphamide or bendamustine<sup>87,88</sup>, gefitinib and cetuximab<sup>89</sup>, irinotecan and cetuximab<sup>90,91</sup>, the peptibody trebananib and different chemotherapies<sup>92</sup> and ipilimumab and dacarbazine or carboplatin/paclitaxel.<sup>93</sup>

Nevertheless, DDIs that occur along other mechanisms than ADME processes cannot be ruled out as seen *e.g.* with tocilizumab (approved for the treatment of rheumatoid arthritis), which reversed IL-6 induced suppression of CYP3A4 activity, resulting in a 50% reduction of simvastatin AUC when given in combination.<sup>94</sup> Furthermore, cardiotoxicity of anthracyclines is exacerbated by contemporaneous administration of trastuzumab. Symptomatic or asymptomatic cardiotoxicity was reported in 27% of the patients treated with anthracycline plus trastuzumab versus 8% and 5% of patients treated with anthracycline and trastuzumab monotherapy, respectively.<sup>95</sup> The underlying mechanism has not been elucidated but a pharmacodynamic interaction in cardiomyocytes may occur with mitochondria as the critical target.<sup>96</sup> A pharmacokinetic DDI, however, cannot be ruled out completely as exposure to cardiotoxic doxorubicin metabolites was significantly higher in the presence of trastuzumab<sup>76</sup> and a 22% reduction of epirubicin glucuronide AUC was found with co-administered trastuzumab.<sup>89</sup>



## Drug interactions with (potential) beneficial effects

### *Pharmacodynamic interactions*

In an effort to improve anti-cancer therapy, researchers are continuously seeking for opportunities to increase treatment efficacy, decrease toxicity or enhance patient-convenience. In this respect, both pharmacodynamic and pharmacokinetic DDIs are increasingly explored.

Pharmacodynamic interactions relate to the pharmacologic drug effect(s), occur at the site(s) of action and may lead to synergistic, additive or antagonistic effects (antitumor activity and/or toxicity) despite unaltered plasma levels of the involved drugs. In oncology, pharmacodynamically interacting drug combinations are applied already from the commencement of cancer treatment with chemical agents shortly after the end of World War II. The introduction of combination chemotherapy for the treatment of lymphomas (mustargen, oncovin (vincristine), procarbazine, prednisone (MOPP) for Hodgkin and cyclophosphamide, hydroxydaunorubicin (doxorubicin), oncovin, prednisone (CHOP) for non-Hodgkin lymphomas) in the 1950s was a big leap forwards in the treatment of these haematological malignancies. Nowadays, these drug combinations still form the backbone of the treatment of lymphomas. A typical pharmacodynamic DDI is the combination of fluoropyrimidines with leucovorin. High intracellular concentrations of reduced folate stabilise the complex between the 5-FU anabolite, 5-fluoro-2'-deoxyuridine monophosphate and thymidylate synthase and thereby potentiates inhibition of thymidylate synthase and its cytotoxic action.<sup>9</sup> Another appealing beneficial pharmacodynamic DDI was investigated after it was recognized that *BRAF* mutated (*BRAFm*) colorectal cancer (CRC) is unresponsive to treatment with a BRAF inhibitor.<sup>97</sup> This in sharp contrast to the efficacy of such agents in *BRAFm* melanoma, which has been well established.<sup>98</sup> Prahallad and co-workers revealed, using an RNA-interference based genetic screen, that inhibition of the epidermal growth factor receptor (EGFR) synergizes with BRAF inhibition in *BRAFm* CRC. Mechanistically, this was explained by a negative feedback activation of EGFR signalling upon BRAF inhibition (Figure 1).<sup>99</sup> Although BRAF or EGFR inhibitors as single agent are ineffective in patients with *BRAFm* CRC, a phase I study combining the BRAF inhibitor encorafenib and the anti-EGFR antibody cetuximab revealed a promising preliminary objective response rate and disease control rate of 30% and 80%, respectively.<sup>100</sup>

Toxicity has often been regarded as a limiting factor to combine anti-cancer drugs. However, combinations of selected targeted agents are generally feasible with manageable toxicity. Interestingly, specific adverse events may even be less in some combinations. The combination of BRAF inhibitor dabrafenib combined with the MEK inhibitor trametinib not only showed a significantly improved overall survival compared with single agents, skin toxicity, including hyperkeratosis, cutaneous squamous cell carcinoma and new primary melanomas were less common in the combination group than in the dabrafenib only group.<sup>101</sup> Comparable results with less skin toxicity were reported for the encorafenib plus cetuximab combination. Whereas approximately 80% and 67% of patients treated with cetuximab or encorafenib monotherapy, respectively, develop some form of skin rash, only 20-30% of patients suffered from such events when cetuximab was combined with encorafenib.<sup>98,100,102</sup> Although the underlying mechanism of this apparent protective effect has not been fully elucidated, an explanation may lie in the paradoxical activation of the MAPK pathway by selective BRAF inhibitors in normal, *BRAF* wildtype, cells receiving upstream activating signals.<sup>103</sup> As cetuximab inhibits MAPK signalling in both tumour and normal tissue, these compounds counteract their effects in normal tissue but synergize in *BRAF* mutant tumour tissue. Other combinations of smSTIs or smSTIs with other treatment modalities

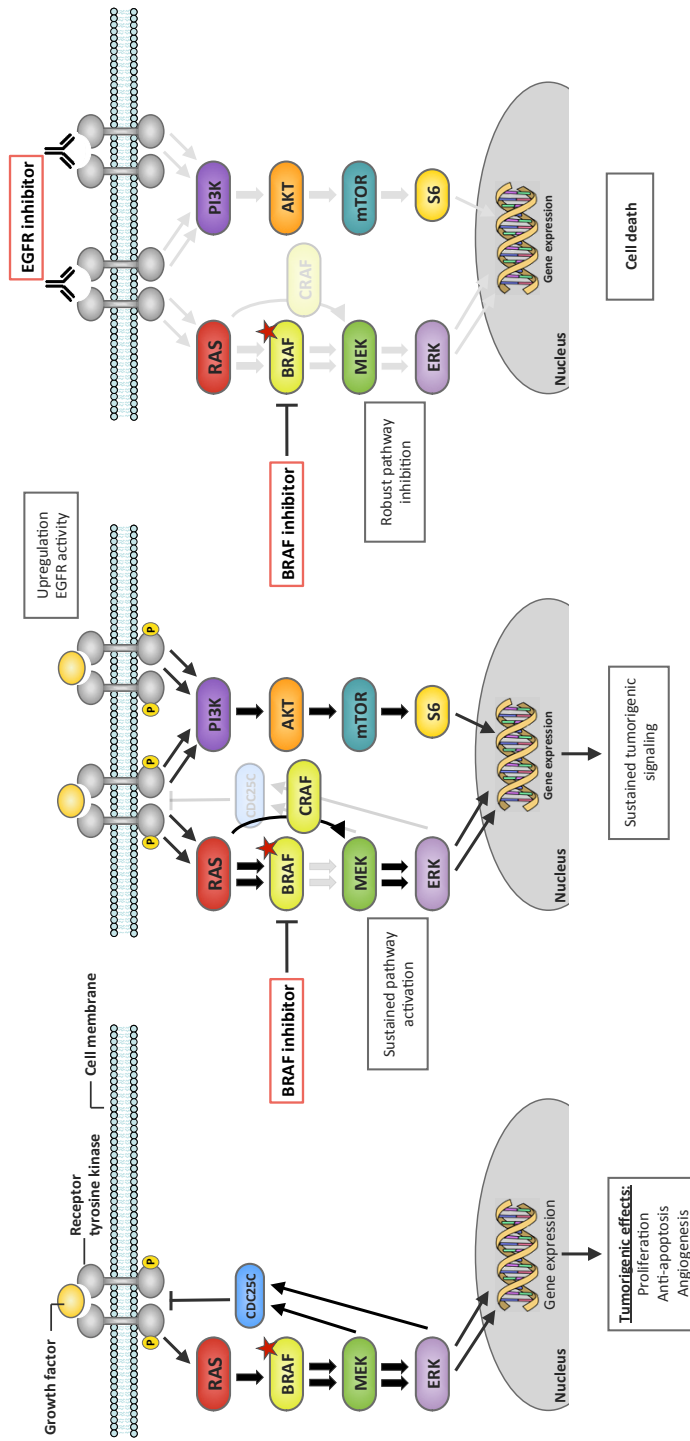


**Figure 1. Feedback regulation of BRAFm colorectal cancer cells and synergistic activity of BRAF inhibition combined with EGFR inhibition.** Oncogenic BRAF mutations cause hyperactivation of the BRAF protein and subsequently result in continuous activation of tumorigenic processes (A). Upon BRAF inhibition, the negative feedback loop from MEK/ERK, through CDC25C, towards upstream EGFR disappears, leading to upregulation of EGFR activity, EGFR-mediated reactivation of downstream pathways, and sustained tumorigenic signaling (B). The addition of an EGFR inhibitor completely blocks this EGFR-mediated resistance mechanism against inhibition of BRAF, resulting in robust pathway inhibition and tumour cell death (C).<sup>99</sup>

are increasingly investigated to find pharmacodynamic DDIs that cause synergistic anti-tumour activity or delay the development or resistance. Recent examples are combinations of chemotherapeutic agents or radiotherapy with poly (ADP-ribose) polymerase inhibitors (olaparib, veliparib, rucaparib, niraparib) in BRCA1/2 mutated tumours,<sup>104</sup> carboplatin combined with Wee1 inhibition (AZD-1775) in TP53 mutated ovarian cancer<sup>105</sup> and combined inhibition of the PD-1 and CTLA-4 checkpoints.<sup>106</sup> In addition, preclinical research has provided a wealth of combination strategies, some of which are currently investigated in the clinic or already incorporated in clinical practice (Table 3). Of note, not all drug combinations that arise from preclinical research may be feasible in patients due to overlapping toxicity profiles. Nevertheless, rational combinations may not need full monotherapy doses to acquire synergy and improved anti-tumor activity, as was shown in the encorafenib plus cetuximab clinical trial with clinical responses already at 25% of the maximum monotherapy dose of encorafenib.<sup>100</sup>

#### *Therapeutic antibodies*

Multiple target inhibition, limited overlapping toxicity and no expected pharmacokinetic interactions make combinations of antibodies an attractive new treatment modality in oncology. Combinations of monoclonal antibodies are therefore increasingly investigated; with trastuzumab plus pertuzumab in HER2-positive metastatic breast cancer being the first with FDA and EMA regulatory approval. The CLEOPATRA-trial demonstrated a significant improvement in median overall survival of 56.5 months for the combination (pertuzumab-trastuzumab-docetaxel) versus 40.8 months for the comparator cohort (placebo-trastuzumab-docetaxel), while the safety profile, including cardiac toxicity, was comparable between the groups.<sup>107</sup> As a pharmacokinetic evaluation revealed no apparent effects of trastuzumab and pertuzumab on each other's pharmacokinetic parameters,<sup>108</sup> the added benefit is likely to come from their pharmacodynamically differing mechanism of action.<sup>109</sup> Although the exact underlying molecular mechanism remains enigmatic the combination has a conclusive, clinically meaningful added value by improving efficacy without adding toxicity.

Immune-modulating antibodies in particular have achieved considerable success in recent years. Although single agents provide clinical anti-tumour activity, patient outcome may further improve using rational combinations. In a double-blind, randomized phase III trial the combination of the checkpoint inhibitors nivolumab and ipilimumab, targeting programmed death 1 (PD-1) and cytotoxic T-lymphocyte-associated antigen 4 (CTLA-4), respectively, increased the progression-free survival in patients with advanced melanoma compared with the antibodies given as monotherapies; 11.5 months for the combination vs. 6.9 (nivolumab) and 2.9 months (ipilimumab).<sup>106</sup>

#### *Pharmacokinetic interactions*

Many anticancer drugs do not penetrate into brain tissue because they are substrates for ABCB1 and ABCG2. These efflux transporters are highly expressed in the apical membranes of endothelial cells of blood capillaries in the brain and restrict drug distribution into brain tissue. This has nicely been proven in both in vitro and in vivo mouse models.<sup>110-112</sup> For example, brain accumulation of sunitinib was markedly (23-fold) increased in *Abcb1a/b/b/Abcg2*<sup>-/-</sup> mice compared with their wild-type littermates with functional transporters. Besides, when sunitinib was given to wild-type mice in combination with the ABCB1 /ABCG2 inhibitor elacridar, brain levels of sunitinib were equal to those in knockout mice, without a substantial effect on sunitinib plasma levels.<sup>113</sup> This demonstrates complete inhibition of

**Table 3. Selected novel strategies to deploy drug-drug interactions to increase bioavailability or efficacy of anticancer drugs.**

Mechanism	Effect	Ref.
<i>Pharmacokinetic DDIs</i>		
Oral taxanes + ritonavir	Inhibition of CYP3A by ritonavir prevents pre-systemic metabolism of taxanes in liver and intestine.	115–118
ABCB1/ABCG2 substrates + elacridar	Inhibition of ABCB1/ABCG1 by elacridar prevents these efflux transporters to block blood-brain-barrier passage of ABCB1/ABCG1 substrates.	113,114
<i>Pharmacodynamic DDIs with clinical evidence</i>		
Cisplatin + cimetidine	Cisplatin-uptake into proximal tubular cells is mediated by OCT2. Cimetidine, as an OCT2 antagonist inhibits this mechanism.	120,121
Trastuzumab + pertuzumab in HER2-positive breast cancer	Pertuzumab prevents HER2 from dimerizing with other HER receptor family members, thereby attacking the potential escape mechanism form the HER2 inhibitory effects of trastuzumab.	107,109
BRAF inhibitor + MEK inhibitor in BRAF mutant melanoma	BRAF mutated melanomas develop resistance against BRAF inhibitor monotherapy through MAPK reactivation. MEK inhibitors inhibit the MAPK signalling pathway downstream of BRAF.	101,159
Nivolumab + ipilimumab in melanoma	CTLA-4 and PD-1 checkpoints inhibit antitumor immunity through complementary and non-redundant mechanisms.	106,160
BRAF + EGFR inhibition in BRAF mutant colorectal cancer	BRAF mutated colorectal cancer is intrinsically resistant against BRAF inhibitors due to feedback activation of EGFR signalling upon BRAF inhibition and thereby sustained MAPK signalling.	
Palbociclib + letrozole in ER-positive, HER2-negative, breast cancer	Palbociclib as a reversible CDK4/6 inhibitor. Letrozole is a non-steroidal aromatase inhibitor.	161

**Table 3. Continued**

Mechanism	Effect	Ref.
<b>Wee1 inhibitor + chemotherapy in TP53 mutant (ovarian) cancers</b>	TP53 mutations compromise G1 arrest in response to DNA damage, leaving TP53 mutated cells highly dependent on the G2 checkpoint. Inhibition of Wee1, a key protein in G2 checkpoint regulation, results in G2 checkpoint abrogation.	105
<b>Pharmacodynamic DDIs with preclinical evidence</b>		
<b>MEK inhibitor + BCL-XL inhibitor in KRAS mutant tumors</b>	MEK inhibition primes KRAS mutated cancer cells for death through induction of the pro-apoptotic protein BIM. However, anti-apoptotic proteins such as BCL-XL bind and inhibit the increased levels of BIM.	162
<b>MEK inhibitor + Dual EGFR/HER2 inhibitor in KRAS mutant tumors</b>	KRAS mutated cancer cells are resistant to MEK inhibition due to feedback activation of HER2 and HER3, which subsequently reactivates the MAPK pathway.	163
<b>Chk1 + MK2 inhibitors in KRAS mutated cancer</b>	Chk1 and MK2 proteins control checkpoint initiation and maintenance in the DNA damage response network. KRAS mutant cancer displays intrinsic genotoxic stress, leading to tonic Chk1 and MK2 activity.	164
<b>Chk1 + Wee1 in AML</b>	G1 checkpoint is impaired AML cells and at the time of relapse, p53 function is lost as well, leaving them highly dependent on S- and G2-checkpoints, in which Chk1 and Wee1 are essential proteins in response to DNA damage.	165
<b>EGFR + HER2 inhibition in HER2 amplified (EGFR-resistant) quadruple negative CRC</b>	KRAS wild type colorectal cancer can become resistant to anti-EGFR therapy through increased HER2 amplification.	166

Abbreviations: CYP3A, cytochrome P450 family 3 subfamily A; ABCB1, ATP-binding cassette sub-family B member 1; OCT2, organic cation transporter 2; HER, human epidermal growth factor receptor; CTLA-4, cytotoxic T-lymphocyte antigen 4; PD-1, programmed cell death protein 1; EGFR, epidermal growth factor receptor; ER, estrogen receptor; CDK4/6, cyclin-dependent kinases 4/6; PFS, progression-free survival; BCL-XL, B-cell lymphoma-extra large; Chk1, checkpoint kinase-1; MK2, MAPK-activated protein kinase-2; AML, acute myeloid leukemia

these blood-brain transporters by elacridar and argues for exploiting this DDI to deliver a cytotoxic agent into the sanctuary brain tissue reaching tumour cells behind a functionally intact blood-brain barrier. However, as far as we know, this tantalizing strategy, although with a questioned feasibility in clinical practice,<sup>114</sup> has not been successfully applied in a formal trial in cancer patients so far.

In view of the cytostatic mechanism of action of docetaxel, its anti-tumour activity may be enhanced by continuous instead of intermittent dosing. However, docetaxel can only be administered intravenously due to its low oral bioavailability (< 10%). This is mainly caused by pre-systemic drug metabolism in the intestines and liver.<sup>115-117</sup> In our quest for a clinically applicable oral formulation of taxanes we demonstrated that the oral bioavailability was strongly enhanced by inhibition of CYP3A4 by ritonavir.<sup>118</sup> Docetaxel AUC was ~50 times greater after oral administration in combination with ritonavir in mice,<sup>117</sup> and comparable in patients.<sup>119</sup> This desired, interacting, boosting effect of ritonavir on oral drug bioavailability is well known from the HIV field where it is deployed to improve the oral uptake of CYP3A4 substrates and protease inhibitors such as saquinavir and lopinavir.

Cisplatin is known for its dose-limiting renal tubular dysfunction in up to 40% of patients, due to cisplatin-uptake into proximal tubular cells via organic cation transport proteins. Concurrent inhibition of OCT2 using cimetidine resulted in a protective effect against nephrotoxicity without affecting pharmacokinetic properties, cytotoxicity or tumoural uptake of cisplatin.<sup>120,121</sup> The combined use of cisplatin and cimetidine therefore forms another example of a DDI with beneficial effects.

## Prediction of DDIs

### *Pharmacokinetic interactions*

Early recognition of DDIs is pivotal as it reduces risks for adverse drug reactions, morbidity and mortality. Ideally, all relevant DDIs are known before a new agent reaches patients and enters the market. However, the number of possible drug combinations, along with the number of potential DDIs with all approved medicines (including over-the-counter and complementary-alternative herb medicines) makes investigating all of the potential DDIs unfeasible. Regulatory agencies (European Medicines Agency, EMA; Food and Drug Administration, FDA) have provided useful guidance documents and tools for DDI studies.<sup>122,123</sup> These highlight that DDIs should be addressed as early as possible during drug development and should include the identification of metabolic-elimination routes, enzymes and transporters involved, drug action as substrate-inhibitor-inducer and selection of interacting drugs.<sup>124</sup> Importance is noted to *in vitro*, *in vivo* and modelling studies with emphasis on transporter-based DDIs. Furthermore, guidance on how to translate *in vitro* results to clinical studies, application of model-based approaches, evaluation of metabolites and the impact of enzyme/transporter genotypes are given.<sup>122-125</sup> Jaiswal and colleagues critically reviewed pre-clinical methodologies for DDI studies including liver slices, microsomes, hepatocytes, isolated- purified- or cDNA expressed-CYPs, S9 fractions, and humanized, transgenic and knockout animal models.<sup>126</sup> Although novel models nearly simulate human-like drug metabolism, time-dependent inhibition, mixed inhibition and induction, and enzyme-transporter interplay can make DDIs fairly complex. *In vitro* studies can serve here as a screening mechanism to guide further *in vivo* and clinical studies. The inhibition of CYPs, as one of the most common mechanisms for DDIs, receives most attention. Mano and co-workers reported a physiologically based pharmacokinetic model to estimate the extent of hepatic CYP3A4 inhibition and the increase of intestinal bioavailability due to enzyme inhibition. Their model provided

acceptable quantitative predictions of clinical DDIs for a panel of randomly selected CYP3A substrates including dasatinib and everolimus.<sup>127</sup> In addition, Vilar et al demonstrated the usefulness of a large scale DDI predictor, based on 3D pharmacophoric similarity, to systemically identify pharmacokinetic and pharmacodynamic interactions.<sup>128</sup>

Time-dependent inhibition defines an interaction causing enhanced inhibition if the test compound is pre-incubated with the metabolizing system prior to the addition of substrate. If an irreversible interaction with time-dependent inhibition occurs the consequences are considered to be more serious because the inactivated enzyme must be re-synthesized before activity is restored. Research evaluating the *in vitro* time-dependent CYP inhibiting potential of 26 marketed oncology drugs revealed that out of 12 kinase inhibitors tested, only sorafenib had no time-dependent CYP inhibition.<sup>129</sup> In addition, the majority of the investigated drugs, including dasatinib, erlotinib, lapatinib and nilotinib, were found to form reactive intermediates capable of covalently modifying proteins, which may explain the time-dependent inhibition of CYP.<sup>129</sup> *In silico* modelling, if employed using comprehensive and high-quality data, is a useful tool to provide insight into the potential for clinically relevant DDIs and may aid in prioritizing which substrates/inhibitors are of interest to investigate further in well-designed clinical DDI studies.<sup>130</sup>

Because many cytotoxic drugs are prodrugs or are converted in metabolites, *in vitro* evaluation of the drug alone is not accurate enough to reflect DDI risks from either a competitive or time-dependent CYP inhibition standpoint. One approach that may aid herein is the concept of micro-dosed probe drugs. Microdosing may be used to obtain information on an individual's metabolic capacity, for clinical phenotyping of patients on polypharmacy and to evaluate the DDI potential of investigational drugs in first-in-man studies.<sup>131</sup>

In general, preclinical *in vitro* and *in vivo* research can be valuable to trace DDIs. Predictions of CYP-based DDIs appear plausible in qualitative terms but the quantitative prediction falls short.<sup>132</sup> Translation of preclinical data to the clinic thus remains cumbersome and cursed with risks. In this respect, microdosing may fulfil an intermediate translating role. Ultimately, a well-designed, prospective clinical DDI study in the target population is the most informative and best way to provide safe guidance on how to use drug combinations. But even then, unexpected events may occur *e.g.* when additional drugs not taken into account, are concomitantly used.<sup>133</sup>

### ***Pharmacodynamic interactions***

Originally, genotype-directed precision medicine was based on the hypothesis that a single driver mutation is responsible for cancer cell survival and progression. Inhibition of this driver mutation cuts the cancer's lifeline and results in tumour cell death. However, a number of complicating factors have been discovered in recent years. Most cancers contain multiple oncogenic mutations, making them less dependent on a single driver, and many molecular signalling pathways are interconnected, so that inhibiting one activates another.<sup>134</sup> Therefore, finding a tumour's escape mechanisms against the inhibition of its oncogenic driver is essential to predict pharmacodynamic interactions between targeted agents like smSTIs and therapeutic antibodies that yield synergistic effects. A promising approach to identify and predict such interactions is the use of high throughput synthetic lethality screens, including RNA interference screens, chemical genetic screens that already provided valuable treatment options in the clinic.<sup>135,136</sup> These techniques already provided combination treatment

strategies with preclinical and clinical evidence of pharmacodynamic synergy (Table 2). For chemotherapeutic agents as well, prediction of favourable cytotoxic combinations may aid in choosing the best treatment regimen for each patient. Komatsu et al described a set of marker genes to predict progression-free survival of ovarian cancer patients upon treatment with platinum plus paclitaxel.<sup>137</sup> In addition, researchers recently demonstrated that a large-scale genetic synthetic lethality screen in fission yeast could predict the synergistic effect of multiple drug combinations when targeting human cancers. HDAC inhibitor vorinostat was discovered as a synergy partner for the combination of doxorubicin and cisplatin in gastric adenocarcinoma as well as cervical cancer cells.<sup>138</sup> Clinical evaluation of this approach is necessary to determine its clinical value. The colorectal cancer subtyping consortium defined four different colorectal cancer subtypes based on genome-wide gene expression data, each with distinct prognostic characteristics and sensitivity to therapy. Subtype CMS4, for example was characterized by a mesenchymal phenotype, poor clinical outcome, resistance to chemotherapy and elevated transforming growth factor- $\beta$  (TGF- $\beta$ ) signalling. Inhibition of the TGF- $\beta$  pathway in CMS4 subtypes may sensitize these tumours for chemotherapy, providing rationale for such a combination.<sup>139,140</sup> Furthermore, Sadanandam and colleagues reported two CRC subtypes, identified using consensus-based unsupervised clustering of gene expression profiles, with improved response to FOLFIRI.<sup>141</sup> Ultimately, comprehensive analysis of a patient's tumour characteristics, including genetic mutations and gene expression profiles together with innovative strategies directed against these characteristics may help in selecting the most effective (combination) therapy for each patient.

### How to handle DDIs

Prevention is the best way to handle detrimental DDIs. Careful consideration of the benefit/risk profile for patients is required when multiple drugs are used. As DDIs are frequently noticed between oral anticoagulants and chemotherapy,<sup>9,142</sup> close monitoring of coagulation variables is imperative for all patients receiving concomitant anticoagulant and chemotherapy with anticoagulant dose modifications when indicated.<sup>9,143</sup> When concurrent use smSTIs and acid suppressive agents is indicated, treatment recommendations are compound-specific; *e.g.* with dasatinib, PPIs may be replaced by H2-antagonists taken at least 2 hours after dasatinib, whereas with gefitinib both PPIs and H2-antagonists are contraindicated and should be replaced by antacids taken 2 hours before or after gefitinib.<sup>24</sup> Given the shorter duration of activity of H2-antagonists (<12 hours) compared to PPIs (up to 3-5 days), their effect on oral absorption of some smSTIs may be less clinically relevant, if used in an appropriate staggered fashion, but this has not been formally investigated.

Additionally, accumulating evidence argues for the use of therapeutic drug monitoring (TDM) with smSTI treatment. Key requirements that make drugs suitable for TDM include a narrow therapeutic range, a consistent exposure-response relationship, a validated and sensitive bioanalytical method, long-term treatment, a feasible dose modification strategy and lack of reliable biomarkers to measure drug effects. For several smSTIs, including imatinib, sunitinib and pazopanib, clear exposure/response or exposure/toxicity correlations have been established in recent studies, making these compounds excellent candidates for TDM.<sup>144-147</sup> TDM is also advised for tamoxifen treatment whereby its active metabolite, endoxifen, is quantified in plasma of treated patients. It aids treatment optimization not only in case of DDIs but also with polymorphisms in metabolizing enzymes and to monitor



compliance.<sup>148,149</sup> More research is needed to define target values for other novel anti-cancer drugs and to evaluate the feasibility and efficacy of routine TDM. Nevertheless, TDM holds promise to improve efficacy and limit toxicity in general, and in the case of anticipated DDIs.

In the past years, many software tools have become available to alert prescribers and dispensing pharmacists to alert for detrimental DDIs. Warnings, however, do not always get the appropriate follow up and are sometimes even ignored.<sup>150</sup> The persistence of cases<sup>151,152</sup> of serious toxicity despite earlier warnings highlights the need for continued education, cognizance and alertness for DDIs by everyone involved. Continuous, centralized medication surveillance would be optimal but appears hard to bring about. One complicating factor is that drugs and other self-medication are prescribed and dispensed through different systems (hospital with different specialists, community pharmacy, general practitioner, druggist shop, internet). Patients should therefore be more involved in the risks of drug combinations including any other alternative products. Patient safety should never be jeopardized by combined drug use. Both medical and pharmacy staff should continue to reduce risks and to strive for safe and effective anti-cancer therapy for our patients.

Besides monitoring drug plasma concentration, ideally, the anti-cancer activity of a given treatment is monitored as well. In chronic myeloid leukemia (CML), molecular response monitoring upon smSTI therapy has become a valuable technology in patient management, as molecular responses at specific time points predict improved progression-free survival and overall survival. Moreover, using such a dynamic pharmacodynamic biomarker increases the chance for early detection of disease progression and could aid in evaluating the clinical value of pharmacodynamic DDIs.<sup>153</sup> In solid tumours as well, the interest in pharmacodynamic biomarkers to monitor the biologic activity of anti-cancer therapy is rapidly growing. Paired tumour biopsies are increasingly incorporated in phase I studies to detect target engagement and preliminary evidence for synergistic activity of combination strategies.<sup>154,155</sup> Also, novel techniques using circulating tumour cells or circulating tumour DNA improve rapidly<sup>156</sup> and are investigated for their applicability in screening for early-stage cancers, to monitor response to therapy, to predict tumour relapse and to help explain why cancer cells are, or become resistant to a given treatment.<sup>157</sup> Although a number of challenges remain to be overcome,<sup>158</sup> proper development and use of pharmacodynamic biomarkers may provide a valuable tool in the future to select the most active pharmacodynamic DDIs and to monitor their effect.

## Conclusions

DDIs are a major safety concern in oncology and account for a large portion of adverse drug reactions. Detrimental DDIs can occur at all levels of pharmacokinetics and pharmacodynamics, but mainly concern pharmacokinetic mechanisms at metabolizing enzymes and drug transporters. As preclinical data on potential DDIs are useful but translation of these data to the clinic remains cumbersome, the potential role for concepts such as micro-dosing and therapeutic drug monitoring in the clinic should be further investigated. Nevertheless, alertness for DDIs in daily clinical practice by everyone who is involved in the prescription, dispensing and administration of drugs, including patients themselves, remains imperative. Paradoxically, DDIs are increasingly deployed to enhance the efficacy of anti-cancer therapy; pharmacokinetic DDIs to improve the bioavailability of cytotoxic drugs, and pharmacodynamic DDIs to exploit their synergistic effect on anti-tumour activity. Emerging technologies like 3D pharmacophoric similarity screens and synthetic lethality screens together with novel tools such as circulating tumour cells and circulating tumour DNA foster our knowledge on handling DDIs as effectively as possible and help gaining control over this double-edged-sword.

## References

1. Dechanont S, Maphanta S, Butthum B, Kongkaew C. Hospital admissions/visits associated with drug-drug interactions: a systematic review and meta-analysis. *Pharmacoepidemiol Drug Saf* 2014;23:489–97.
2. Becker ML, Kallewaard M, Caspers PW, et al. Hospitalisations and emergency department visits due to drug-drug interactions: a literature review. *Pharmacoepidemiol Drug Saf* 2007;16:641–51.
3. Feinstein J, Dai D, Zhong W, Freedman J, Feudtner C. Potential Drug-Drug Interactions in Infant, Child, and Adolescent Patients in Children's Hospitals. *Pediatrics* 2014;135:e99–e108.
4. Leone R, Magro L, Moretti U, et al. Identifying Adverse Drug Reactions Associated with Drug-Drug Interactions. *Drug Saf* 2010;33:667–75.
5. Lees J, Chan A. Polypharmacy in elderly patients with cancer: Clinical implications and management. *Lancet Oncol* 2011;12:1249–57.
6. Hines LE, Murphy JE. Potentially Harmful Drug-Drug Interactions in the Elderly: A Review. *Am. J Geriatr Pharmacother* 2011;9:364–77.
7. Ranchon F, Vial T, Rioufol C, et al. Concomitant drugs with low risks of drug-drug interactions for use in oncology clinical trials. *Crit Rev Oncol Hematol* 2015;94:189–200.
8. Riechelmann RP, Moreira F, Smaletz O, Saad ED. Potential for drug interactions in hospitalized cancer patients. *Cancer Chemother Pharmacol* 2005;56:286–90.
9. Beijnen JH, Schellens JHM. Drug interactions in oncology. *Lancet Oncology* 2004;5:489–96.
10. McLeod HL. Clinically relevant drug-drug interactions in oncology. *Br J Clin Pharmacol* 1998;45:539–44.
11. Scripture CD, Figg WD. Drug interactions in cancer therapy. *Nat Rev Cancer* 2006;6:546–58.
12. Jansman FGA, Reyners AK, van Roon EN, et al. Consensus-Based Evaluation of Clinical Significance and Management of Anticancer Drug Interactions. *Clin Ther* 2011;33:305–14.
13. van Meerten E, Verweij J, Schellens JH. Antineoplastic agents. Drug interactions of clinical significance. *Drug Saf* 1995;12:168–82.
14. Sparreboom A, Cox MC, Acharya MR, Figg WD. Herbal remedies in the United States: Potential adverse interactions with anticancer agents. *J Clin Oncol* 2004;22:2489–503.
15. Haefeli WE, Carls A. Drug interactions with phytotherapeutics in oncology. *Expert Opin. Drug Metab. Toxicol* 2014;10:359–77.
16. Segal EM, Flood MR, Mancini RS, et al. Oral chemotherapy food and drug interactions: A comprehensive review of the literature. *J Oncol Pract* 2014;10:e255–e268.
17. An G, Mukker JK, Derendorf H, Frye RF. Enzyme- and transporter-mediated beverage-drug interactions: An update on fruit juices and green tea. *J Clin Pharmacol* 2015;55:1313–31.
18. Riechelmann RP, Saad ED. A systematic review on drug interactions in oncology. *Cancer Invest* 2006;24:704–12.
19. Stoll P, Kopittke L. Potential drug-drug interactions in hospitalized patients undergoing systemic chemotherapy: a prospective cohort study. *Int J Clin Pharm* 2015;37:475–84.
20. Riechelmann RP, Tannock IF, Wang L, et al. Potential drug interactions and duplicate prescriptions among cancer patients. *J Natl Cancer Inst* 2007;99:592–600.

21. Voll ML, Yap KD, Terpstra WE, Crul M. Potential drug-drug interactions between anti-cancer agents and community pharmacy dispensed drugs. *Pharm World Sci* 2010;32:575–80.
22. van Leeuwen RWF, Jansman FG, van den Bemt PM, et al. Drug-drug interactions in patients treated for cancer: a prospective study on clinical interventions. *Ann Oncol* 2015;26:992–7.
23. Peters S, Zimmermann S, Adjei AA. Oral epidermal growth factor receptor tyrosine kinase inhibitors for the treatment of non-small cell lung cancer: Comparative pharmacokinetics and drug-drug interactions. *Cancer Treat Rev* 2014;40:917–26.
24. van Leeuwen RWF, van Gelder T, Mathijssen RHJ, Jansman FGA. Drug-drug interactions with tyrosine-kinase inhibitors: A clinical perspective. *Lancet Oncol* 2014;15:e315–e326.
25. Chan A, Tan SH, Wong CM, Yap KYL, Ko Y. Clinically significant drug-drug interactions between oral anticancer agents and nonanticancer agents: A delphi survey of oncology pharmacists. *Clin Ther* 2009;31:2379–86.
26. Ko Y, Tan SL, Chan A, Wong YP, et al. Prevalence of the Coprescription of Clinically Important Interacting Drug Combinations Involving Oral Anticancer Agents in Singapore: A Retrospective Database Study. *Clin Ther* 2012;34:1696–1704.
27. Conde-Estévez D, Echeverría-Esnaola D, Tusquets I, Albanell J. Potential clinical relevant drug-drug interactions: comparison between different compendia, do we have a validated method? *Ann Oncol* 2015;26:1272.
28. Chan A, Soh D, Ko Y, et al. Characteristics of unplanned hospital admissions due to drug-related problems in cancer patients. *Support Care Cancer* 2014;22:1875–81.
29. Barry M, Feely J. Enzyme induction and inhibition. *Pharmacol Ther* 1990;48:71–94.
30. Burton M, Shaw L, Schentag J, Evans, W. *Applied Pharmacokinetics & Pharmacodynamics: Principles of Therapeutic Drug Monitoring* 2006.
31. Mazzaferro S, Bouchemal K, Ponchel G. Oral delivery of anticancer drugs I: General considerations. *Drug Discov Today* 2013;18:25–34.
32. Thanki K, Gangwal RP, Sangamwar AT, Jain S. Oral delivery of anticancer drugs: Challenges and opportunities. *J Control Release* 2013;170:15–40.
33. Gearry RB, Day AS, Barclay ML, et al. Azathioprine and allopurinol: A two-edged interaction. *J Gastroenterol Hepatol* 2010;25:653–5.
34. Herbrink M, Nuijen B, Schellens JHM, Beijnen JH. Variability in bioavailability of small molecular tyrosine kinase inhibitors. *Cancer Treat Rev* 2015;41:412–22.
35. Mandery K, Glaeser H, Fromm MF. Interaction of innovative small molecule drugs used for cancer therapy with drug transporters. *Br J Pharmacol* 2012;165:345–62.
36. Budha NR, Frymoyer A, Smelick GS, et al. Drug absorption interactions between oral targeted anticancer agents and PPIs: is pH-dependent solubility the Achilles heel of targeted therapy? *Clin Pharmacol Ther* 2012;92:203–213.
37. Ogawa R, Echizen H. Drug-drug interaction profiles of proton pump inhibitors. *Clin Pharmacokinet* 2010;49:509–33.
38. Eley T, Luo FR, Agrawal S, et al. Phase I study of the effect of gastric acid pH modulators on the bioavailability of oral dasatinib in healthy subjects. *J Clin Pharmacol* 2009;49:700–9.

39. Abbas R, Leister C, Sonnichsen DA. clinical study to examine the potential effect of lansoprazole on the pharmacokinetics of bosutinib when administered concomitantly to healthy subjects. *Clin Drug Investig* 2013;33:589–95.
40. Chu MP, Ghosh S, Chambers CR, et al. Gastric acid suppression is associated with decreased erlotinib efficacy in non-small-cell lung cancer. *Clin Lung Cancer* 2015;16:33–9.
41. Nguyen L, Holland J, Mamelok R, et al. Evaluation of the effect of food and gastric pH on the single-dose pharmacokinetics of cabozantinib in healthy adult subjects. *J Clin Pharmacol* 2013;55:1293–302.
42. Musib L, Choo E, Deng Y, et al. Absolute bioavailability and effect of formulation change, food, or elevated pH with rabeprazole on cobimetinib absorption in healthy subjects. *Mol Pharm* 2013;10:4046–54.
43. Marostica E, Sukbuntherng J, Louny D, et al. Population pharmacokinetic model of ibrutinib, a Bruton tyrosine kinase inhibitor, in patients with B cell malignancies. *Cancer Chemother Pharmacol* 2015;75:111–21.
44. Durmus S, Sparidans RW, Wagenaar E, et al. Oral availability and brain penetration of the B-RAFV600E inhibitor vemurafenib can be enhanced by the p-glycoprotein (ABCB1) and breast cancer resistance protein (ABCG2) inhibitor elacridar. *Mol Pharm* 2012;9:3236–45.
45. Kruijtzter CM, Beijnen JH, Rosing H, et al. Increased oral bioavailability of topotecan in combination with the breast cancer resistance protein and P-glycoprotein inhibitor GF120918. *J Clin Oncol* 2002;20:2943–50.
46. Shitara Y, Maeda K, Ikejiri K, et al. Clinical significance of organic anion transporting polypeptides (OATPs) in drug disposition: their roles in hepatic clearance and intestinal absorption. *Biopharm Drug Dispos* 2013;34:45–78.
47. Hu S, Mathijssen RHJ, de Bruijn P, et al. Inhibition of OATP1B1 by tyrosine kinase inhibitors: in vitro-in vivo correlations. *Br J Cancer* 2014;110:894–8.
48. Kalliokoski A, Niemi M. Impact of OATP transporters on pharmacokinetics. *Br J Pharmacol* 2009;158:693–705.
49. Martin LP, Kozloff MF, Herbst RS, et al. Phase I study of axitinib combined with paclitaxel, docetaxel or capecitabine in patients with advanced solid tumours. *Br J Cancer* 2012;107:1268–76.
50. Awada A, Hendlisz A, Shristensen O, et al. Phase I trial to investigate the safety, pharmacokinetics and efficacy of sorafenib combined with docetaxel in patients with advanced refractory solid tumours. *Eur J Cancer* 2012;48:465–74.
51. Hamberg P, Matthijssen RH, de Bruijn P, et al. Impact of pazopanib on docetaxel exposure: Results of a phase I combination study with two different docetaxel schedules. *Cancer Chemother Pharmacol* 2015;75:365–71.
52. Sprowl JA, Sparreboom A. Uptake carriers and oncology drug safety. *Drug Metab Dispos* 2014;42:611–22.
53. Summary of Product Characteristics - Xalkori. at <[http://www.ema.europa.eu/docs/en\\_GB/document\\_library/EPAR\\_-\\_Product\\_Information/human/002489/WC500134759.pdf](http://www.ema.europa.eu/docs/en_GB/document_library/EPAR_-_Product_Information/human/002489/WC500134759.pdf)>
54. Terada T, Hira D. Intestinal and hepatic drug transporters: pharmacokinetic, pathophysiological, and pharmacogenetic roles. *J Gastroenterol* 2015;50:508–19.
55. Ito K, Iwatsubo T, Kanamitsu S, et al. Prediction of Pharmacokinetic Alterations Caused by Drug-Drug Interactions: Metabolic Interaction in the liver. *Pharmacol Rev* 1998;50:387–410.
56. Slørdal L, Sager G, Aarbakke J. Pharmacokinetic interactions with methotrexate: is 7-hydroxy-methotrexate the culprit? *Lancet* 1988;1:591–2.

57. Okuda H, Ogura K, Kato A, et al. A possible mechanism of eighteen patient deaths caused by interactions of sorivudine, a new antiviral drug, with oral 5-fluorouracil prodrugs. *J Pharmacol Exp Ther* 1998;287:791–9.
58. Okuda, H. et al. Lethal drug interactions of sorivudine, a new antiviral drug, with oral 5-fluorouracil prodrugs. *J Pharmacol* 1997;25:270–3.
59. Kanamitsu SI, Ito K, Okuda H, et al. Prediction of in vivo drug-drug interactions based on mechanism-based inhibition from in vitro data: Inhibition of 5-fluorouracil metabolism by (E)-5-(2-bromovinyl)uracil. *Drug Metab Dispos* 2000;28:467–74.
60. Nishiyama T, Ogura K, Okuda H, et al. Mechanism-based inactivation of human dihydropyrimidine dehydrogenase by (E)-5-(2-bromovinyl)uracil in the presence of NADPH. *Mol Pharmacol* 2000;57:899–905.
61. Baena-Cañada JM, Martínez MJ, García-Olmedo O, et al. Interaction between capecitabine and brivudine in a patient with breast cancer. *Nat Rev Clin Oncol* 2010;7:55–8.
62. García Fernández V, Garrido Arévalo M, Labrada González E, Hidalgo Correas FJ. [Fatal drug-drug interaction between 5-fluorouracil and brivudine]. *Farm Hosp órgano Of expresión científica la Soc Española Farm Hosp*. 2013;37:72–3.
63. Rätz Bravo AE, Hofer S, Krähenbühl S, Ludwig C. Fatal drug-drug interaction of brivudine and capecitabine. *Acta Oncol* 2009;48:631–3.
64. Johnson FM, Agrawal S, Burris H, et al. Phase 1 pharmacokinetic and drug-interaction study of dasatinib in patients with advanced solid tumors. *Cancer* 2010;116:1582–91.
65. Smith DA, Koch KM, Arya N, et al. Effects of ketoconazole and carbamazepine on lapatinib pharmacokinetics in healthy subjects. *Br J Clin Pharmacol* 2009;67:421–6.
66. Graff JN, Beer TM. Pharmacotherapeutic management of metastatic, castration-resistant prostate cancer in the elderly: focus on non-chemotherapy agents. *Drugs Aging* 2014;31:873–82.
67. Gibbons JA, de Vries M, Krauwinkel W, et al. Pharmacokinetic Drug Interaction Studies with Enzalutamide. *Clin Pharmacokinet* 2015;54:1057–69.
68. Tanaka C, Yin OQ, Smith T, et al. Clinical Effects of Rifampin and Ketoconazole on the. *J Clin Pharmacol* 2011;51:75–83.
69. Sarantopoulos J, Mita AC, Wade JL, et al. Phase I study of cabazitaxel plus cisplatin in patients with advanced solid tumors: Study to evaluate the impact of cytochrome P450 3A inhibitors (aprepitant, ketoconazole) or inducers (rifampin) on the pharmacokinetics of cabazitaxel. *Cancer Chemother Pharmacol* 2014;74:1113–24.
70. Harmsen S, Meijerman I, Beijnen JH, Schellens JHM. The role of nuclear receptors in pharmacokinetic drug-drug interactions in oncology. *Cancer Treat Rev* 2007;33:369–80.
71. Smith P, Bullock JM, Booker BM, et al. The influence of St. John's wort on the pharmacokinetics and protein binding of imatinib mesylate. *Pharmacotherapy* 2004;24:1508–14.
72. Yap KYL, Chui WK, Chan A. Drug interactions between chemotherapeutic regimens and antiepileptics. *Clin Ther* 2008;30:1385–1407.
73. Mani S, Dou W, Redinbo MR. PXR antagonists and implication in drug metabolism. *Drug Metab Rev*. 2013;45:60–72.
74. Abbas A, Mirza MM, Ganti AK, Tendulkar K. Renal Toxicities of Targeted Therapies. *Target Oncol* 2015;10:487–99.

75. Lunardi G, Vannozi MO, Bighin C, et al. Influence of trastuzumab on epirubicin pharmacokinetics in metastatic breast cancer patients. *Ann Oncol* 2003;14:1222–6.
76. Bianchi G, Albanell J, Eiermann W, et al. Pilot Trial of Trastuzumab Starting with or after the Doxorubicin Component of a Doxorubicin plus Paclitaxel Regimen for Women with HER2-Positive Advanced Breast Cancer. *Clin Cancer Res* 2003;9:5944–51.
77. Paridaens R, Rixe O, Pinel MC, et al. A phase 1 study of vinflunine in combination with trastuzumab for the treatment for HER2-positive metastatic breast cancer. *Cancer Chemother Pharmacol* 2012;70:503–11.
78. Satoh T, Omuro Y, Sasaki Y, et al. Pharmacokinetic analysis of capecitabine and cisplatin in combination with trastuzumab in Japanese patients with advanced HER2-positive gastric cancer. *Cancer Chemother Pharmacol* 2012;69:949–55.
79. Zinner RG, Glisson BS, Fossella FV, et al. Trastuzumab in combination with cisplatin and gemcitabine in patients with Her2-overexpressing, untreated, advanced non-small cell lung cancer: report of a phase II trial and findings regarding optimal identification of patients with Her2-overexpressing disease. *Lung Cancer* 2004;44:99–110.
80. Nieto Y, Vredenburgh JJ, Shpall EJ, et al. Phase II feasibility and pharmacokinetic study of concurrent administration of trastuzumab and high-dose chemotherapy in advanced HER2+ breast cancer. *Clin Cancer Res* 2004;10:7136–43.
81. Corrigan PA, Cicci TA, Auten JJ, Lowe DK. Ado-trastuzumab Emtansine: A HER2-Positive Targeted Antibody-Drug Conjugate. *Ann Pharmacother* 2014;48:1484–93.
82. Davis JA, Rock DA, Wienkers LC, Pearson JT. In vitro characterization of the drug-drug interaction potential of catabolites of antibody-maytansinoid conjugates. *Drug Metab Dispos* 2012;40:1927–34.
83. Krop IE, Beeram M, Modi S, et al. Phase I study of trastuzumab-DM1, an HER2 antibody-drug conjugate, given every 3 weeks to patients with HER2-positive metastatic breast cancer. *J Clin Oncol* 2010;28:2698–2704.
84. Xin Y, Jin D, Eppler S, et al. Population pharmacokinetic analysis from phase I and phase II studies of the humanized monovalent antibody, onartuzumab (metmab), in patients with advanced solid tumors. *J Clin Pharmacol* 2013;53:1103–11.
85. Leong S, Cohen RB, Gustafson DL, et al. Mapatumumab, an antibody targeting TRAIL-R1, in combination with paclitaxel and carboplatin in patients with advanced solid malignancies: results of a phase I and pharmacokinetic study. *J Clin Oncol* 2009;27:4413–21.
86. Herbst RS, Johnson DH, Mininberg E, et al. Phase I/II Trial Evaluating the Anti-Vascular Endothelial Growth Factor Monoclonal Antibody Bevacizumab in Combination with the HER-1/Epidermal Growth Factor Receptor Tyrosine Kinase Inhibitor Erlotinib for Patients with Recurrent Non-Small-Cell Lung Cancer. *J Clin Oncol* 2005;23:2544–55.
87. Li J, Zhi J, Wenger M, et al. Population pharmacokinetics of rituximab in patients with chronic lymphocytic leukemia. *J Clin Pharmacol* 2012;52:1918–26.
88. Darwish M, Burke JM, Hellriegel E, et al. An evaluation of the potential for drug-drug interactions between bendamustine and rituximab in indolent non-Hodgkin lymphoma and mantle cell lymphoma. *Cancer Chemother Pharmacol* 2014;73:1119–27.
89. Seitz K, Zhou H. Pharmacokinetic drug-drug interaction potentials for therapeutic monoclonal antibodies: Reality check. *J Clin Pharmacol* 2007;47:1104–18.

90. Ettliger DE, Mitterhauser M, Wadsak W, et al. In vivo disposition of irinotecan (CPT-11) and its metabolites in combination with the monoclonal antibody cetuximab. *Anticancer Res* 2006;26:1337–41.
91. Delbaldo C, Pierga JY, Dieras V, et al. Pharmacokinetic profile of cetuximab (Erbix) alone and in combination with irinotecan in patients with advanced EGFR-positive adenocarcinoma. *Eur J Cancer* 2005;41:1739–45.
92. Wu B, Melara R, Rasmussen E, et al. Pharmacokinetic drug-drug interaction assessment of peptibody trebananib in combination with chemotherapies. *Cancer Chemother. Pharmacol* 2015;76:243–50.
93. Weber J, Hamid O, Amin A, et al. Randomized phase I pharmacokinetic study of ipilimumab with or without one of two different chemotherapy regimens in patients with untreated advanced melanoma. *Cancer Immunol* 2013;13:7.
94. Schmitt C, Kuhn B, Zhang X, et al. Disease-drug-drug interaction involving tocilizumab and simvastatin in patients with rheumatoid arthritis: Commentary. *Int J Adv Rheumatol* 2011;89:735–40.
95. Popat S, Smith IE. Therapy Insight: anthracyclines and trastuzumab—the optimal management of cardiotoxic side effects. *Nat Clin Pract Oncol* 2008;5:324–35.
96. Montaigne D, Hurt C, Neviere R. Mitochondria death/survival signaling pathways in cardiotoxicity induced by anthracyclines and anticancer-targeted therapies. *Biochem Res Int* 2012;2012:951539.
97. Kopetz S, Desai J, Chan E, et al. Phase II Pilot Study of Vemurafenib in Patients With Metastatic BRAF-Mutated Colorectal Cancer. *J Clin Oncol* 2015;33:4032–8.
98. Chapman PB, Hauschild A, Robert C, et al. Improved survival with vemurafenib in melanoma with BRAF V600E mutation. *N Engl J Med* 2011;364:2507–16.
99. Prahallad A, Sun C, Huang S, et al. Unresponsiveness of colon cancer to BRAF(V600E) inhibition through feedback activation of EGFR. *Nature* 2012;483:100–3.
100. van Geel RMJM, Elez E, Bendell JC, et al. Phase I study of the selective BRAF V600 inhibitor encorafenib (LGX818) combined with cetuximab and with or without the  $\alpha$ -specific PI3K inhibitor BYL719 in patients with advanced BRAF -mutant colorectal cancer. *J Clin Oncol* 2014;32:5s (suppl; abstr 3514).
101. Long GV, Stroyakovskiy D, Gogas H, et al. Dabrafenib and trametinib versus dabrafenib and placebo for Val600 BRAF-mutant melanoma: A multicentre, double-blind, phase 3 randomised controlled trial. *Lancet* 2015;386:444–51.
102. Cunningham D, Humblet Y, Siena S, et al. Cetuximab monotherapy and cetuximab plus irinotecan in irinotecan-refractory metastatic colorectal cancer. *N Engl J Med* 2004;351:337–45.
103. Holderfield M, Nagel TE, Stuart DD. Mechanism and consequences of RAF kinase activation by small-molecule inhibitors. *Br J Cancer* 2014;111:640–5.
104. Scott CL, Swisher EM, Kaufmann SH. Poly (ADP-Ribose) Polymerase Inhibitors: Recent Advances and Future Development. *J Clin Oncol* 2015;33:1397–1406.
105. Leijen S, van Geel RMJM, Sonke GS, et al. Phase II study with Wee1 inhibitor AZD1775 plus carboplatin in patients with p53 mutated ovarian cancer refractory or resistant (<3 months) to standard first line therapy. *J Clin Oncol* 2015;33 (suppl; abstr 2507).
106. Larkin J, Chiarion-Sileni V, Gonzalez R, et al. Combined Nivolumab and Ipilimumab or Monotherapy in Untreated Melanoma. *N Engl J Med* 2015;373:23–34.
107. Swain SM, Baselga J, Kim SB, et al. Pertuzumab, Trastuzumab, and Docetaxel in HER2-Positive Metastatic Breast Cancer. *N Engl J Med* 2015;372:724–34.



108. Cortés J, Swain SM, Kudaba I, et al. Absence of pharmacokinetic drug–drug interaction of pertuzumab with trastuzumab and docetaxel. *Anticancer Drugs* 2013;24:1084–92.
109. Scheuer W, Friess T, Burtscher H, et al. Strongly enhanced antitumor activity of trastuzumab and pertuzumab combination treatment on HER2-positive human xenograft tumor models. *Cancer Res* 2009;69:9330–6.
110. Durmus S, Hendriks JJMA, Schinkel AH. Apical ABC Transporters and Cancer Chemotherapeutic Drug Disposition. *Adv Cancer Res* 2015;125:1–41.
111. Tang SC, de Vries N, Sparidans RW, et al. Impact of P-glycoprotein (ABCB1) and breast cancer resistance protein (ABCG2) gene dosage on plasma pharmacokinetics and brain accumulation of dasatinib, sorafenib, and sunitinib. *J Pharmacol Exp Ther* 2013;346:486–94.
112. Lagas JS, van waterschoot RA, van Tilburg VA, et al. Brain accumulation of dasatinib is restricted by P-glycoprotein (ABCB1) and breast cancer resistance protein (ABCG2) and can be enhanced by elacridar treatment. *Clin Cancer Res* 2009;15:2344–51.
113. Tang SC, Lagas JS, Lankheet NA, et al. Brain accumulation of sunitinib is restricted by P-glycoprotein (ABCB1) and breast cancer resistance protein (ABCG2) and can be enhanced by oral elacridar and sunitinib coadministration. *Int J Cancer* 2012;130:223–33.
114. Kalvass JC, Polli JW, Bourdet DL, et al. Why clinical modulation of efflux transport at the human blood-brain barrier is unlikely: the ITC evidence-based position. *Clin Pharmacol Ther* 2013;94:80–94.
115. van Herwaarden AE, van Waterschoot RAB, Schinkel AH. How important is intestinal cytochrome P450 3A metabolism? *Trends Pharmacol Sci* 2009;30:223–7.
116. Hendriks JJMA, Lagas JS, Song JY, et al. Ritonavir inhibits intratumoral docetaxel metabolism and enhances docetaxel antitumor activity in an immunocompetent mouse breast cancer model. *Int J Cancer* 2015;138:758–69.
117. Bardelmeijer HA, Ouwehand M, Buckle T, et al. Low systemic exposure of oral docetaxel in mice resulting from extensive first-pass metabolism is boosted by ritonavir. *Cancer Res* 2002;62:6158–64.
118. Oostendorp RL, Huitema A, Rosing H, et al. Coadministration of ritonavir strongly enhances the apparent oral bioavailability of docetaxel in patients with solid tumors. *Clin Cancer Res* 2009;15:4228–33.
119. Koolen SLW, van Waterschoot RA, van Tellingen O, et al. From mouse to man: predictions of human pharmacokinetics of orally administered docetaxel from preclinical studies. *J Clin Pharmacol* 2012;52:370–80.
120. Sprowl JA, van Doorn L, Hu S, et al. Conjunctive Therapy of Cisplatin With the OCT2 Inhibitor Cimetidine: Influence on Antitumor Efficacy and Systemic Clearance. *Clin Pharmacol Ther* 2013;94:585–92.
121. Ciarimboli G, Deuster D, Knief A, et al. Organic cation transporter 2 mediates cisplatin-induced oto- and nephrotoxicity and is a target for protective interventions. *Am J Pathol* 2010;176:1169–80.
122. European Medicines Agency. Guideline on the Investigation of Drug Interactions Guideline on the Investigation of Drug Interactions. (2010). at <[http://www.ema.europa.eu/docs/en\\_GB/document\\_library/Scientific\\_guideline/2012/07/WC500129606.pdf](http://www.ema.europa.eu/docs/en_GB/document_library/Scientific_guideline/2012/07/WC500129606.pdf)>
123. FDA. Guidance for industry. Drug interaction studies study design, data analysis, implications for dosing, and labeling recommendations. (2012). at <<http://www.fda.gov/downloads/drugs/guidancecomplianceregulatoryinformation/guidances/ucm292362.pdf>>

124. Venkatakrishnan K, Pickard MD, Von Moltke LL. A quantitative framework and strategies for management and evaluation of metabolic drug-drug interactions in oncology drug development: New molecular entities as object drugs. *Clin Pharmacokinet* 2010;49:703–27.
125. Prueksaritanont T, Chu X, Gibson C, et al. Drug-drug interaction studies: regulatory guidance and an industry perspective. *AAPS J* 2013;15:629–45.
126. Jaiswal S, Sharma A, Shukla M, et al. Novel pre-clinical methodologies for pharmacokinetic drug-drug interaction studies: spotlight on ‘humanized’ animal models. *Drug Metab Rev* 2014;46:475–93.
127. Mano Y, Sugiyama Y, Ito K. Use of a Physiologically Based Pharmacokinetic Model for Quantitative Prediction of Drug-Drug Interactions via CYP3A4 and Estimation of the Intestinal Availability of CYP3A4 Substrates. *J Pharm Sci* 2015;104:3183–93.
128. Vilar S, Uriarte E, Santana L, et al. State of the art and development of a drug-drug interaction large scale predictor based on 3D pharmacophoric similarity. *Curr Drug Metab* 2014;15:490–501.
129. Kenny JR, Mukadam S, Zhang C, et al. Drug-drug interaction potential of marketed oncology drugs: In vitro assessment of time-dependent cytochrome P450 inhibition, reactive metabolite formation and drug-drug interaction prediction. *Pharm Res* 2012;29:1960–76.
130. Ai N, Fan X, Ekins S. In silico methods for predicting drug-drug interactions with cytochrome P-450s, transporters and beyond. *Adv Drug Deliv Rev* 2015;86:46–60.
131. Hohmann N, Haefeli WE, Mikus G. Use of Microdose Phenotyping to Individualise Dosing of Patients. *Clin Pharmacokinet* 2015;54:893–900.
132. Wienkers LC, Heath TG. Predicting in vivo drug interactions from in vitro drug discovery data. *Nat Rev Drug Discov* 2005;4:825–33.
133. Kang MH, Villablanca JG, Glade Bender JL, et al. Probable fatal drug interaction between intravenous fenretinide, ceftriaxone, and acetaminophen: a case report from a New Approaches to Neuroblastoma (NANT) Phase I study. *BMC Res Notes* 2014;7:256.
134. Bernards R. A missing link in genotype-directed cancer therapy. *Cell* 2012;151:465–8.
135. Fece de la Cruz F, Gapp BV, Nijman SMB. Synthetic lethal vulnerabilities of cancer. *Annu Rev Pharmacol Toxicol* 2015;55:513–31.
136. Diehl P, Tedesco D, Chenchik A. Use of RNAi screens to uncover resistance mechanisms in cancer cells and identify synthetic lethal interactions. *Drug Discov Today Technol* 2014;11:11–8.
137. Komatsu M, Hiyama K, Tanimoto K, et al. Prediction of individual response to platinum/paclitaxel combination using novel marker genes in ovarian cancers. *Mol Cancer Ther* 2006;5:767–75.
138. Nguyen TT, Chua JK, Seah KS, et al. Predicting chemotherapeutic drug combinations through gene network profiling. *Sci Rep* 2016;6:18658.
139. Guinney J, Dienstmann R, Wang X, et al. The consensus molecular subtypes of colorectal cancer. *Nat Med* 2015;21:1350–6.
140. Brunen D, Willem SM, Kellner U, et al. TGF- $\beta$  An emerging player in drug resistance. *Cell Cycle* 2013;12:2960–8.
141. Sadanandam A, Lyssiotis CA, Homicsko K, et al. A colorectal cancer classification system that associates cellular phenotype and responses to therapy. *Nat Med* 2013;19:619–25.
142. Ussai S, Petellin R, Giordano A, et al. A pilot study on the impact of known drug-drug interactions in cancer patients. *J Exp Clin Cancer Res* 2015;34:89.

143. Ribed A, Escudero-Vilaplana V, Gonzalez-Haba E, Sanjurjo M. Increased INR after gefitinib and acenocoumarol co-administration. *Eur Rev Med Pharmacol Sci* 2014;18:1720–2.
144. Yu H, Steeghs N, Nijenhuis CM, et al. Practical guidelines for therapeutic drug monitoring of anticancer tyrosine kinase inhibitors: Focus on the pharmacokinetic targets. *Clin Pharmacokinet* 2014;53:305–25.
145. Widmer N, Bardin C, Chatelut E, et al. Review of therapeutic drug monitoring of anticancer drugs part two - Targeted therapies. *Eur J Cancer* 2014;50:2020–36.
146. Josephs DH, Fisher DS, Spicer J, Flanagan RJ. Clinical Pharmacokinetics of Tyrosine Kinase Inhibitors. *Ther Drug Monit* 2013;35:562–8.
147. Gao B, Yeap S, Clements A, et al. Evidence for therapeutic drug monitoring of targeted anticancer therapies. *J Clin Oncol* 2012;30:4017–25.
148. Kelly CM, Juurlink DN, Gomes T, et al. Selective serotonin reuptake inhibitors and breast cancer mortality in women receiving tamoxifen: a population based cohort study. *BMJ* 2010;340:c693–c693.
149. Jager NGL, Linn SC, Schellens JHM, Beijnen JH. Tailored tamoxifen treatment for breast cancer patients: A perspective. *Clin Breast Cancer* 2015;15:241–4.
150. Mille F, Schwartz C, Brion F, et al. Analysis of overridden alerts in a drug-drug interaction detection system. *Int J Qual Heal Care* 2008;20:400–5.
151. Cudmore J, Seftel M, Sisler J, Zarychanski R. Methotrexate and trimethoprim-sulfamethoxazole: Toxicity from this combination continues to occur. *Can Fam Physician* 2014;60:53–6.
152. Bartha P, Bron R, Levy Y. Fatal pancytopenia and methotrexate-trimethoprim-sulfamethoxazole interaction. *Harefuah* 2004;143:398–400, 464.
153. Erba HP. Molecular monitoring to improve outcomes in patients with chronic myeloid leukemia in chronic phase: Importance of achieving treatment-free remission. *Am J Hematol* 2015;90:242–9.
154. Do K, Wilsker D, Ji J, et al. Phase I study of single-agent AZD1775 (MK-1775), a wee1 kinase inhibitor, in patients with refractory solid tumors. *J Clin Oncol* 2015;33:3409–15.
155. Atreya CE, van Cutsem E, Bendell JC, et al. Updated efficacy of the MEK inhibitor trametinib, BRAF inhibitor dabrafenib, and anti-EGFR antibody panitumumab in patients with BRAF V600E mutated metastatic colorectal cancer. *J Clin Oncol* 2015;33 (suppl;abstr 103).
156. Newman AM, Bratman SV, To J, et al. An ultrasensitive method for quantitating circulating tumor DNA with broad patient coverage. *Nat Med* 2014;20:548–54.
157. Karachaliou N, Mayo-de-las-casas C, Molina-vila MA, Rosell R. Real-time liquid biopsies become a reality in cancer treatment. *Ann Transl Med* 2015;3:2–4.
158. de Gramont A, Watson S, Ellis LM, et al. Pragmatic issues in biomarker evaluation for targeted therapies in cancer. *Nat Rev Clin Oncol* 2014;12:197–212.
159. Flaherty KT, Infante JR, Daud A, et al. Combined BRAF and MEK inhibition in melanoma with BRAF V600 mutations. *N Engl J Med* 2012;367:1694–703.
160. Postow MA, Chesney J, Pavlick AC, et al. Nivolumab and Ipilimumab versus Ipilimumab in Untreated Melanoma. *N Engl J Med*;372:2006–17.
161. Finn RS, Crown JP, Lang I, et al. The cyclin-dependent kinase 4/6 inhibitor palbociclib in combination with letrozole versus letrozole alone as first-line treatment of oestrogen receptor-positive, HER2-negative, advanced breast cancer (PALOMA-1/TRIO-18): A randomised phase 2 study. *Lancet Oncol* 2015;16:25–35.

162. Corcoran RB, Cheng KA, Hata AN, et al. Synthetic Lethal Interaction of Combined BCL-XL and MEK Inhibition Promotes Tumor Regressions in KRAS Mutant Cancer Models. *Cancer Cell* 2013;23:121–128.
163. Sun C, Hobor S, Bertotti A, et al. Intrinsic resistance to MEK inhibition in kras mutant lung and colon cancer through transcriptional induction of ERBB3. *Cell Rep* 2014;7:86–93.
164. Dietlein F, Kalb B, Jokic M, et al. A Synergistic Interaction between Chk1- and MK2 Inhibitors in KRAS-Mutant Cancer. *Cell* 2015;162:146–59.
165. Chaudhuri L, Vincelette ND, Koh BD, et al. CHK1 and WEE1 inhibition combine synergistically to enhance therapeutic efficacy in acute myeloid leukemia ex vivo. *Haematologica* 2014;99:688–96.
166. Bertotti A, Migliardi G, Galimi F, et al. A molecularly annotated platform of patient- derived xenografts ('xenopatients') identifies HER2 as an effective therapeutic target in cetuximab-resistant colorectal cancer. *Cancer Discov* 2011;1:508–23.
167. Jariwala P, Kumar V, Kothari K, et al. Acute methotrexate toxicity: a fatal condition in two cases of psoriasis. *Case Rep Dermatol Med* 2014;946716.





# Chapter 4

## Treatment individualization in colorectal cancer



**Current Colorectal Cancer Reports 2015;11(6):335-344**

Robin M.J.M. van Geel, Jos H. Beijnen, René Bernards, Jan H.M. Schellens

### ABSTRACT

Colorectal cancer has been characterized as a genetically heterogeneous disease, with a large diversity in molecular pathogenesis resulting in differential responses to therapy. However, the currently available validated biomarkers *KRAS*, *BRAF* and microsatellite instability do not sufficiently cover this extensive heterogeneity and are therefore not suitable to successfully guide personalized treatment. Recent studies have focused on novel targets and rationally designed combination strategies. Furthermore, a more comprehensive analysis of the underlying biology of the disease revealed distinct phenotypic differences within subgroups of patients harboring the same genetic driver mutation with both prognostic and predictive relevance. Accordingly, patient stratification based on molecular intrinsic subtypes rather than on single gene aberrations holds promise to improve the clinical outcome of patients with colorectal cancer.

## Introduction

Colorectal cancer (CRC) is one of the most prevalent cancers and a leading cause of cancer mortality worldwide.<sup>1</sup> In an effort to better understand the biologic hallmarks of the disease, CRC has undergone extensive molecular characterization in recent years, which revealed important oncogenes (e.g., *KRAS*, *BRAF*, *PIK3CA*), tumor suppressor genes (e.g., *APC*, *TP53*, *PTEN*) and signaling pathways that are critical for the development, survival and progression of CRC cells. These genes are involved in major signaling pathways that have been linked to cancer, including the WNT/ $\beta$ -catenin, mitogen-activated protein kinase (MAPK), transforming growth factor beta (TGF- $\beta$ ) and phosphoinositide 3-kinase (PI3K) pathways (figure 1).<sup>2</sup> Consequently targeted agents against a number of druggable genomic aberrations were developed. However, patients who are characterized based on these molecular markers still show remarkable variability in terms of prognosis and response to therapy.<sup>3</sup> Therefore, many studies have addressed further sub classification of CRC, focusing on epigenetic factors and gene expression profiles. Herein we outline recent advances in our understanding of the underlying biology of CRC and we address the potential clinical implications of this knowledge in order to optimize treatment individualization for patients with CRC.

## Single genetic aberration driven treatment

In the past decade, in search of better biomarkers in the metastatic setting of CRC (mCRC), a wide range of genetic alterations was found to be associated with cancer. Only a small percentage of these mutations actually drive the development and progression of malignant cells and may therefore have clinical implications.<sup>4,5</sup> Mutations in the *RAS* genes (*KRAS*, *HRAS* and *NRAS*), present in approximately 50% of all patients with CRC, result in hyper activation of *RAS* proteins and their corresponding downstream pathways such as the MAPK pathway, thereby stimulating the development and progression of malignant tumors.<sup>6</sup> As *RAS* mutations predict resistance to anti-EGFR monoclonal antibodies (mAbs) cetuximab and panitumumab, patients with *RAS* mutant disease should be excluded from treatment with these drugs.<sup>7-11</sup> However, a large part of the *RAS* wild-type patients still do not respond to cetuximab or panitumumab. Further refinement in the molecular analysis of patients who are considered for treatment with anti-EGFR mAbs is therefore needed. Others, including Saridaki et al. in this issue, describe potential additional biomarkers and the uncertainties that remain to be solved. In short, mounting evidence in the literature supports the notion that resistance to anti-EGFR mAbs can be explained by genetic alterations in the MAPK and PI3K pathways.<sup>10,12-14</sup> Although this evidence is largely based on retrospective analyses, which are often underpowered to address the impact of less common gene mutations (e.g. *HRAS*, non-codon 12 *KRAS*, *BRAF*, *PIK3CA*), there were trends of unresponsiveness upon cetuximab and panitumumab treatment. On the other hand, based on a meta-analysis of seven randomized controlled trials, Rowland et al. concluded that there is insufficient data to justify the exclusion of EGFR inhibitor therapy for patients with *BRAF* mCRC.<sup>15</sup> Nevertheless, only 15% of all patients with mCRC, who represent the quadruple wild type (*KRAS/HRAS/BRAF/PIK3CA*) group, is thought to respond to anti-EGFR therapy.<sup>13,16</sup> Therefore, effective alternatives for patients that do harbor mutations in these genes are needed.



### MAPK-pathway

Since the paradigm shift, changing from a histology-directed treatment approach to a genome-driven strategy, a large number of clinical trials investigated targeted agents against specific molecular anomalies. Patients were stratified according to their tumors' *KRAS*, *BRAF*, *HRAS*, *PIK3CA* or *PTEN* status to receive a matched targeted agent. However, none of these strategies has obtained proof of principle in patients with CRC.<sup>17-19</sup> Clearly, targeting a single mutated gene or activated protein in CRC does not yield the desired clinical benefit. In the meantime preclinical research provided more insight into the dynamic interactions between different signaling pathways and emphasized that single kinase protein inhibition is way too simplistic as it ignores the complexity of cross-talk between pathways and feedback escape mechanisms. An impressive example is the contradictory efficacy of BRAF inhibitors in patients with melanoma versus patients with activating *BRAF* mutations. Selective BRAF inhibitors such as vemurafenib and dabrafenib have shown high objective response rates of about 50% in patients with *BRAF*(V600E) mutated (*BRAF*m) melanoma.<sup>20,21</sup> Combinations of these small molecules with MEK inhibitors like cobimetinib or trametinib further improved the rate of response to over 65% and yielded a significant improvement in both progression-free survival and overall survival.<sup>22,23</sup> In contrast, CRC patients with the identical causative *BRAF* mutation appeared unresponsive to BRAF inhibitors either as single agent or in combination with a MEK inhibitor as indicated by response rates of less than 5%.<sup>24,25</sup>

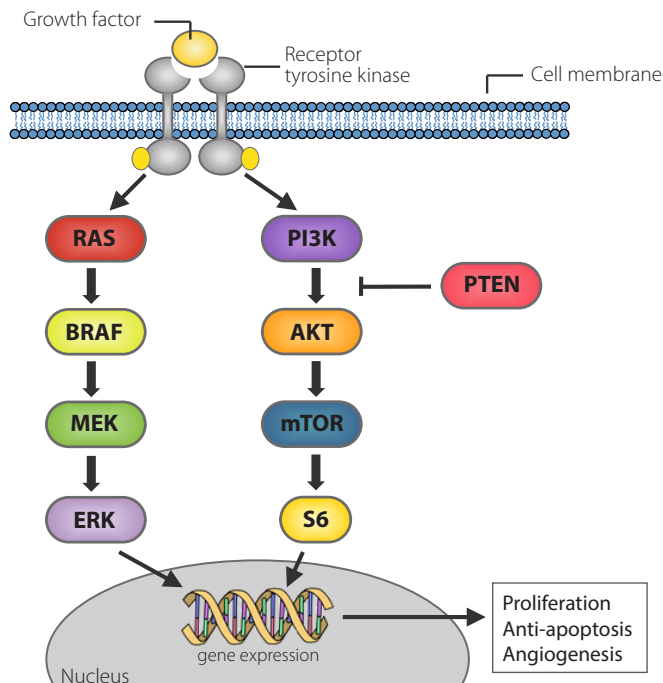


Figure 1. Simplified schematic overview of the MAPK and PI3K signaling pathway.

Prahallad and colleagues elucidated the mechanism underlying this intrinsic unresponsiveness. Using an RNA interference-based genetic screen they searched for kinase proteins, which upon suppression synergize with BRAF inhibition in *BRAFm* CRC cells. EGFR came out as the most potent synergy partner. Mechanistically, a feedback activation of EGFR was identified upon BRAF inhibition in *BRAFm* CRC supporting persistent tumor cell proliferation through reactivation of the MAPK and PI3K pathways. Combined BRAF and EGFR inhibition caused a strong synergistic effect *in vitro* and in xenograft models and resulted in complete inhibition of tumor growth.<sup>26</sup> An independent research group reported similar results, BRAF inhibition in *BRAFm* CRC triggered an EGFR-mediated rebound activation of the MAPK pathway, which can be blocked by concomitant administration of an anti-EGFR targeted agent.<sup>27</sup> This research supports clinical evaluation of combined BRAF and EGFR inhibition in patients with *BRAFm* CRC, and a number of ongoing clinical studies already have obtained clinical proof of principle. A phase I study investigating BRAF inhibitor encorafenib (LGX818) combined with cetuximab, either with or without PI3K inhibitor alpelisib (BYL719), demonstrated favorable toxicity profiles of both the dual and triple combination with objective response rates of 30% and disease control rates of 80% and 90%, respectively, in patients with pretreated advanced *BRAFm* CRC.<sup>28</sup> Comparable clinical activity was obtained in a second phase I study in which the combination of BRAF inhibitor dabrafenib, EGFR inhibitor panitumumab and MEK inhibitor trametinib resulted in an objective response rate of 26%.<sup>29</sup> Interestingly, vemurafenib plus cetuximab can also be safely combined with irinotecan and preliminary results of the first 16 patients with *BRAFm* mCRC revealed a 35% response rate.<sup>30</sup> Given the particularly poor prognosis of patients with metastatic *BRAFm* CRC and the limited anti-tumor activity of standard treatment regimens in this subset of patients, new treatment options are needed.<sup>31</sup> Although larger phase II/III trials are necessary to confirm the promising initial results, combined BRAF and EGFR inhibition is likely to improve standard of care for *BRAFm* mCRC.

A second example of the dynamic biology of CRC concerns *KRAS* mutant (*KRASm*) disease. Despite extensive investigation direct pharmacological inhibition of the KRAS protein remains difficult.<sup>32</sup> As an alternative, kinase proteins downstream of KRAS such as MEK were investigated but the anti-tumor activity was disappointing.<sup>33</sup> Upon the recognition that PI3K pathway activation due to coexisting genetic alterations or feedback up regulation may cause resistance against MEK inhibition, clinical studies focused on combining MEK inhibitors with PI3K, AKT or mTOR inhibitors, but these did not yield satisfactory results either.<sup>34</sup> Recently, investigators applied the previously described genetic screen to *KRASm* cells and found that HER3 knockdown sensitizes these cells for MEK inhibition. HER3 receptors are able to activate both the MAPK and PI3K pathway after dimerization with other members of the HER receptor family of which EGFR and HER2 are the most potent dimerization partners. Interestingly, combining a MEK inhibitor with an inhibitor of EGFR or HER2 did not result in synergy. Only MEK inhibition combined with dual EGFR/HER2 inhibitors or pan-HER inhibitors such as dacomitinib and afatinib, overcomes unresponsiveness of *KRASm* tumors *in vitro* as well as *in vivo*.<sup>35</sup> Based on a similar genetic drug screen, Corcoran et al. suggested another approach. They found that knockdown of the anti-apoptotic BH3 family gene *BCL-XL* was synergistic with MEK inhibition and targeting *BCL-XL* with ABT-263 (navitoclax) combined with a MEK inhibitor resulted in dramatic apoptosis *in vitro* and remarkable *in vivo* tumor responses in *KRASm* xenografts.<sup>36</sup> Clinical studies investigating these combinations are underway (NCT02039336, NCT02230553, NCT02450656, NCT02079740). Additionally,

recent research provided new hope for the development of drugs that directly bind and inhibit the mutated RAS protein, by exploiting a mutation-specific approach.<sup>37,38</sup> However, given the existing cross-talk between signaling pathways via feedback mechanisms these novel therapeutic agents may urge for combination strategies as well. Furthermore, even if these investigational therapies provide benefit in the clinic it seems likely, given the heterogeneity of CRC that only a subset of *KRAS* and *BRAF* patients will respond.

### ***PI3K pathway***

Similar to the MAPK-pathway, the PI3K-pathway can be activated by receptor tyrosine kinases, including EGFR-family members, platelet-derived growth-factor receptors (PDGFR) and the insulin growth-factor-1 receptors. Mutations in *PIK3CA*, the gene that codes for the p110 $\alpha$  isoform of the PI3K protein, are present in approximately 15% of CRC and are concentrated in two hot spots of the gene at exon 9 (60–65%) and exon 20 (20–25%).<sup>10,39</sup> Exon 9 mutations affect the helical domain and cause gain of function independent of dimerization with the p85 subunit of PI3K, but require interaction with activated RAS. Exon 20 mutations on the other hand result in gain of PI3K function independent of activated RAS but highly rely on the interaction with p85.<sup>40</sup> Therefore, these mutations might reflect two distinct subtypes of PI3K that behave differently upon a given treatment. Indeed *PIK3CA* exon 9 mutations have been associated with activating *KRAS* mutations in codons 12 and 13, supporting the functional link between RAS signaling and activation of the helical domain of PI3K.<sup>10,39,41</sup> In contrast, others describe an association between *KRAS* mutations and *PIK3CA* mutations regardless of the exonic site.<sup>42</sup> These mechanistic differences may explain the discordant findings regarding the detrimental effect of *PIK3CA* mutations on the efficacy of anti-EGFR treatment. Initial reports showed an association between *PIK3CA* mutations and lack of response to anti-EGFR mAbs, but these results were not confirmed by others, possibly due to the lower number of exon 20 mutations in the latter studies.<sup>13,43–45</sup> Inhibition of the PI3K pathway using small molecules targeting PI3K, mTOR or AKT was recently investigated, but has not yielded satisfactory results in CRC patients with PI3K alterations.<sup>46</sup> In addition to *PIK3CA* mutations, loss of PTEN expression is a second PI3K pathway component that has been associated with resistance to EGFR inhibition.<sup>47–50</sup> However, the effect of *PIK3CA* mutations and loss of PTEN on anti-EGFR therapy seems relatively weak and alterations in the PI3K pathway often co-occur with other important driver mutations like *KRAS* and *BRAF*, indicating that the PI3K pathway plays a less critical role compared to the MAPK pathway in unresponsiveness to EGFR inhibition in CRC and maybe even in CRC in general.<sup>13,51</sup>

Taken together, so-called quadruple-negative (no mutations in *KRAS*, *HRAS*, *BRAF*, *PIK3CA*) CRC is more likely to respond to EGFR inhibitors treatment and for those patients that do possess specific genetic mutations (*BRAF* and *KRAS*) clinical studies with new combination strategies are ongoing. However, presence of oncogenic mutations still do not fully explain the extent of non-response to EGFR inhibition and success stories with single gene mutation-directed therapy in patients with CRC are limited.<sup>52</sup>

In contrast to CRC, targeting single mutated genes in hematological malignancies yielded a number of breakthrough therapies, such as BCR-ABL kinase inhibitor imatinib, and later dasatinib and nilotinib for patients with Philadelphia chromosome positive chronic myelogenous leukemia.<sup>53–55</sup> A number of

reasons may explain this remarkable difference in success rate of targeting oncogenic drivers. First, unlike hematological malignancies, most solid tumors, and especially CRC, contain many genetic aberrations, which could make these tumors less dependent on a single oncogenic mutation. Moreover, this heterogeneity of CRC, in that it contains not only a mixture of relatively indolent and aggressive cells but also a mixture of molecularly different cell populations, makes it difficult to attack all these distinctive cells with the same targeted agents. Killing the sensitive cells might offer resistant cell populations the opportunity to expand and progress. Secondly, the affected signaling pathways often 'communicate' with each other, resulting in primary resistance against a given targeted agent as described previously for *BRAF* and *KRAS* CRC. Thirdly, CRC behavior appears largely dependent on the surrounding stromal context in which the tumor exists.<sup>56,57</sup> Therefore, treatment individualization for patients with CRC needs to take these features into account and move forward beyond the single gene paradigm.

### Towards comprehensive molecular characterization guided treatment

Traditionally, early-stage CRC is classified based on tumor stage in order to estimate prognosis and predict benefit of adjuvant treatment. All patients with stage III or high-risk stage II disease are offered adjuvant chemotherapy. However, in a significant percentage of patients adjuvant chemotherapy is ineffective. Better prognostic and predictive markers are therefore needed to identify patients who are more likely to benefit from adjuvant treatment.<sup>58</sup> Initial studies described three molecularly distinct features in CRC, namely microsatellite instability (MSI), chromosomal instability (CIN) and the CpG island methylator phenotype (CIMP). CIN is present in the vast majority (~85%) of CRCs and is characterized by alterations in the adenomatous polyposis coli (*APC*) gene, a key component of the WNT pathway. MSI on the other hand is detected in approximately 15% of all early-stage CRCs and displays a hypermutable phenotype caused by a defective mismatch repair system (dMMR). In the clinical setting, MSI may be used to genetically diagnose Lynch syndrome, to estimate the prognosis of patients with CRC and to predict the efficacy of chemotherapeutic agent 5-fluorouracil (5-FU). Together with other studies, a large meta-analysis with over 7,000 patients demonstrated that stage II or III colorectal tumors have a survival advantage if they exhibit MSI rather than a stable microsatellite status (MSS) as shown by the lower rates of tumor recurrence in MSI tumors.<sup>59</sup> The predictive role of MSI or dMMR for treatment with 5-FU and other chemotherapeutic agents has been controversial as several studies reported conflicting results. However, large recent retrospective analyses of randomized clinical trials confirmed that patients with dMMR should not be recommended for adjuvant treatment with 5-FU due to lack of benefit, but that this effect is limited to stage II patients.<sup>60-65</sup> In addition to MSI status as identified by PCR amplification of specific microsatellite repeats, Tian et al described a robust gene expression signature that identifies patients with MSI tumors and also a group of MSI-like patients who are not recognized by traditional methods but have a phenotype similar to MSI patients, including high mutation frequency, frequent *BRAF* mutations, high tumoral thymidylate synthase (TS) expression and better prognosis.<sup>66</sup> As the unresponsiveness of MSI patients to adjuvant 5-FU therapy might be related to higher TS expression, MSI-like patients might therefore present an additional population that have a lower likelihood to benefit from 5-FU treatment.<sup>66,67</sup> Furthermore, Choueiri et al. described a potential role of TS and excision repair cross-complementation group 1 (ERCC1) expression as prognostic and predictive biomarkers in mCRC. Low TS expression was associated with significant

longer overall survival and combined low expression of ERCC1 and TS was predictive of response in patients treated with FOLFOX.<sup>68</sup>

To gain more insight into the heterogeneity of CRC, the Cancer Genome Atlas Network (TCGA) conducted a comprehensive molecular characterization of CRC, including exome sequencing, DNA copy number, promoter methylation, and mRNA and miRNA expression analysis. Based on the mutational rate, an arbitrary cutoff was used to distinguish two separate groups, namely hypermutated (16%) and non-hypermutated (84%) tumor samples. The hypermutated group consisted of tumors with MSI and CpG island methylator phenotype (CIMP), whereas the non-hypermutated tumors had significantly more gene copy number alterations and *TP53* and *KRAS* mutations, indicating CIN. Analysis of the specific genes that were mutated revealed significant differences between the hypermutated and the non-hypermutated tumors, highlighting the marked differences in the biology and development of these CRC subtypes. *ACVR2A* (63%), *APC* (51%), *TGFBR2* (51%), *BRAF* (40%), *MSH3* (40%) and *MSH6* were the most frequently mutated genes in the hypermutated tumors, whereas *APC* (81%), *TP53* (60%), *KRAS* (43%), *TTN* (31%) and *PIK3CA* (18%) were the most frequent targets of mutations in non-hypermutated tumors. The RAS-MAPK, PI3K and TGF- $\beta$  signaling pathways were altered in 80% vs. 59% (hypermutated vs. non-hypermutated), 53% vs. 50% and 87% vs. 27%, respectively, but little is still known about which of these alterations are indeed necessary for continued disease progression. Despite these differences, 95% of all tumors had a deregulated WNT signaling pathway, predominantly due to mutations in *APC*, and nearly all tumors had changes in MYC transcriptional targets, emphasizing the critical role of these features in CRC.<sup>69</sup> Recent work demonstrated that *APC* inactivation is strictly required for CRC maintenance, even in the presence of additional CRC-associated oncogenic mutations in *KRAS* and *TP53*. In an shRNA-based transgenic mouse model, restoration of endogenous *Apc* protein induced a rapid and sustained tumor regression and re-established tissue homeostasis. These results suggest that small molecules that modulate the WNT pathway could be clinically active for patients with *APC*-mutated CRC.<sup>70</sup> Furthermore, Wiegering et al. described that inhibition of MYC mRNA translation using silvestrol, a compound that directly inhibits eIF4A in the translation complex of MYC, suppresses tumor growth in a mouse model of colorectal tumorigenesis.<sup>71</sup> Small molecules that modulate the WNT pathway or target MYC-translation initiation could therefore have clinical potential for patients with CRC.

Besides genetic changes, epigenetic alterations play a major role in the development of CRC. Hinoue and colleagues identified four DNA-methylation-based subgroups using a genome-scale DNA methylation profiling. A CIMP-high (CIMP-H) subgroup with an exceptionally high frequency of cancer-specific hypermethylation. A CIMP-low (CIMP-L) subgroup characterized by hypermethylation of a subset of CIMP-H associated markers. And two non-CIMP subgroups, one with a significantly higher frequency of *TP53* mutations and one with a marked low frequency of both cancer-specific DNA hypermethylation and gene mutations. Moreover, *KRAS* mutations occurred within each of these subgroups, indicating that not every *KRAS* mutant colorectal tumor has the same DNA methylation profile and that *KRAS* CRC is probably not a homogeneous group of patients who will respond similarly to therapy.<sup>72</sup>

Moreover, Popovici et al. demonstrated that a subgroup of patients with *BRAF* wild type stage II/III colon cancer have a similar phenotype as patients with *BRAF* mutant colon cancer, based on a high-sensitivity gene expression signature. Over 20% of patients that were *BRAF* wild type could be classified as being *BRAF*m-like according to this signature, showing clinicopathologic features similar to *BRAF*m patients, including higher frequencies of mucinous histology, MSI and poor overall survival and survival after relapse. As the majority of these *BRAF*m-like patients harbored *KRAS* mutations this suggests a joint underlying biology between these *KRAS*m tumors, but it also indicates histologic and prognostic heterogeneity within the *KRAS*m subpopulation.<sup>73</sup> In addition, Tian and colleagues developed gene expression profiles that characterized *KRAS*-, *BRAF*-, and *PIK3CA*-activated stage II/III tumors and they showed that tumors without mutations in either of these genes could have a similar gene expression profile.<sup>74</sup> This research indicates that mechanisms other than oncogenic mutations can cause a similar pathway activation that can be identified by a similar transcriptional pattern. More specifically, 79 of the 206 investigated tumors that had no oncogenic mutation in either *KRAS*, *BRAF* or *PIK3CA* were classified as oncogenic based on their gene expression profiles. This indicates that a significant part of the *KRAS*, *BRAF* and *PIK3CA* wild type tumors share the same phenotype of an activated MAPK or PI3K pathway as those tumors with at least one activating mutation. Indeed, the combined oncogenic pathway signature was highly predictive for response to EGFR-inhibitor therapy with better performance than each of the three single mutation signatures and using *KRAS* mutation status alone.<sup>74</sup> Furthermore, as this signature detects patients whose tumors have an activated MAPK or PI3K pathway in the absence of genetic mutations, it may also be useful to select patients for treatment with small molecule inhibitors directed against non-mutated BRAF, MEK, PI3K, mTOR or combinations of these agents.<sup>74</sup> However, paradoxical effects, such as seen with BRAF-inhibitors in non-*BRAF*m cells may be a concern of such strategy.<sup>75</sup>

Subsequently, several research groups applied unsupervised clustering methods to genome-wide expression data in order to discover intrinsic molecular subtypes of CRC. De Sousa et al. for instance described three molecularly distinct CRC subtypes, the two well-known CIN and MSI tumors, called colon cancer subtype (CCS) 1 and 2, and a third subtype (CCS3) that is largely microsatellite-stable containing relatively more CpG-island methylator phenotype-positive tumors but cannot be identified on the basis of genetic mutations. *KRAS* mutations occurred in all the subgroups and *BRAF* mutations occurred in both CCS2 and CCS3, again indicating that *KRAS* and *BRAF* mutant CRC is not a homogeneous group and can be further differentiated into multiple biological groups with potential clinical differences in both prognosis and response to therapy. In fact, there was a marked difference in response between the three subtypes to cetuximab therapy *in vitro*, in xenografts and in a clinical setting where patients with CCS3-classified tumors were resistant to cetuximab independently of *KRAS* mutation status.<sup>76</sup> Others identified similar or slightly different subtypes which ranged in number from three to six, but there was a clear overlap in key clinical and molecular features between the subtypes from different research groups. Particularly, all groups concurred on the identification of a highly aggressive CRC subtype characterized by the expression of stem-cell genes, epithelial-to-mesenchymal transition (EMT), and poor prognosis.<sup>76-81</sup> Therefore, the Colorectal Cancer Subtyping Consortium (CRCSC) was formed to reconcile data from six different research groups who subsequently established four consensus subtypes called CMS1-4. Although CMS1 was enriched for mutant *BRAF*

status, *BRAF* mutations did also occur in CMS3, CMS4 and the unclassified subgroup. *KRAS* mutations were found in the largest proportion of CMS-3 tumors, but frequently in all other subtypes as well.<sup>82</sup> Taken together, all subtyping studies illustrate heterogeneity within the most common driver mutations, *KRAS* and *BRAF*, indicating important differences in prognosis and response to therapy with anti-EGFR agents and to a lesser extent to FOLFIRI treatment. Clearly, gene mutation status alone is not enough to define the complexity of the underlying biology of colorectal tumors. Therefore, to improve personalized treatment of CRC patients, a more comprehensive analysis is needed, which is less likely to be influenced by inter- and intra-tumor heterogeneity. CRC subtypes based on gene expression profiles may represent the initial step towards a better definition of CRC at the molecular level, but their prognostic and predictive value remains to be elucidated and prospectively validated.

### Clinical implications

The major challenge now is to translate this emerging knowledge into a robust and reproducible classification system for CRC that integrates tumor biology, pathology and clinical characteristics, and connect these subtypes to prognosis and response to therapy. Genome-wide expression data already provided initial evidence that particular drugs are more likely to be effective in specific colorectal cancer subtypes. As mentioned previously, tumors belonging to the CCS3 subtype as described by De Sousa et al., or the combined oncogenic activated pathway signature as described by Tian et al., are unlikely to respond to anti-EGFR directed treatment. In addition, Sadanandam and colleagues described a further subdivision of one CRC subtype representing patients with strong anti-EGFR response.<sup>80</sup> Other favorable outcomes were reported in the metastatic setting for c-MET inhibitors in the cetuximab-resistant transit amplifying (CR-TA) subtype and FOLFIRI in the stem-like subtype.<sup>80</sup>

One subgroup of CRC that was identified in each subtyping study was the mesenchymal phenotype, characterized by worst clinical outcome, resistance to adjuvant chemotherapy and elevated transforming growth factor- $\beta$  (TGF- $\beta$ ) signaling, a well-established feature in the induction of epithelial-to-mesenchymal transition (EMT). Inhibition of the TGF- $\beta$  pathway may revert the mesenchymal tumors into a more epithelial-like phenotype, making these tumors more susceptible to chemotherapy.<sup>79,83</sup> This provides rationale to combine chemotherapy with TGF- $\beta$  receptor inhibitors in patients with CRC harboring a mesenchymal phenotype as identified by the CMS4 subtype according to the CRCSC. In addition, Calon et al found that all mesenchymal poor prognosis subtypes identified by the above-described studies rely on genes expressed by stromal components, cancer-associated fibroblasts (CAFs), rather than by epithelial cancer cells. TGF- $\beta$  signaling induces this CAF gene program, which boosts the metastatic potential and the ability to regenerate the malignant disease after therapy.<sup>56,57,84</sup> Pharmacological inhibition of TGF- $\beta$  receptor 1 in the tumor microenvironment using TGF- $\beta$ R1-specific inhibitor LY2157299 prevented metastasis formation and disease progression in patient-derived tumor organoids, which further warrants investigating TGF- $\beta$  inhibition in patients with poor-prognosis CRC.<sup>57</sup>

As previously mentioned, the genomic complexity of CRC limits the efficacy of targeted therapies. However, high mutational load may as well serve as a positive feature given the fact that somatic mutations found in tumors can be recognized by the patient's own immune system due to their potential to encode non-self immunogenic antigens.<sup>85</sup> Nonetheless, in many tumors the cytotoxic immune response is repressed by negative feedback systems, such as the programmed death 1 (PD-1)

pathway. Inhibition of PD-1 or its ligand has demonstrated impressive clinical benefit in different types of cancer. Since colorectal cancers with deficient MMR are characterized by a hypermutated phenotype and contain lymphocyte infiltrates, it was hypothesized that especially dMMR tumors are responsive to inhibition of the programmed death 1 (PD-1) pathway.<sup>86,87</sup> A recently published phase II study indeed demonstrated that patients with dMMR CRC are much more responsive to anti-PD-1 immune checkpoint inhibitor pembrolizumab, than are MMR proficient CRC patients, indicated by objective response rates of 40% versus 0%, respectively, and significantly prolonged progression-free survival and overall survival times.<sup>87</sup> These impressive results strongly argue for clinical studies investigating anti-PD-1 antibodies in patients with MSI-like CRC as this gene expression classifier identifies an additional 10% of CRC patients that harbor hypermutated tumors, adding up to an approximate 25% of all patients with CRC who could potentially benefit from this novel treatment strategy.

### Conclusions and future perspectives

We begin to understand the heterogeneous character of CRC and its impact on prognosis and response to therapy. To optimize personalized therapy for patients with CRC we should focus on new patient selection strategies based on this increased understanding of the underlying biology of the disease. In the metastatic setting, clinicians should already expand their mutational analysis beyond *KRAS* (exon 2), as patients harboring other *KRAS* or *HRAS* mutations are unlikely to respond to EGFR inhibitors as well. The predictive role of *BRAF* mutations for response to anti-EGFR treatment remains inconclusive. Nevertheless, genomically driven clinical trials provide promising treatment strategies for patients who may not be eligible for anti-EGFR therapy (e.g., *BRAF*m and *KRAS*m patients). Emerging molecularly defined CRC subtypes based on gene expression patterns highlight the heterogeneity beyond genetic mutations and the lack of unique driver mutations in each of these subtypes indicates distinct differences within the *KRAS*m and *BRAF*m populations. Clearly, genetic aberrations are often not accurately defining a colorectal tumor's phenotype and are highly insufficient to guide treatment decisions in most cases. In fact, thus far only one single-gene guided approach has obtained proof of principle in the clinic, namely combined *BRAF* and EGFR inhibition in *BRAF*m patients. Even in these successful initial studies, patients respond very differently. Therefore, validation of gene expression signatures, or equivalent simpler marker systems, and implementing these in the stratification of patients receiving pharmacological therapy may help defining the patient population most likely to benefit from a given (experimental) therapy. Furthermore, novel therapeutic strategies should be investigated beyond the currently used targets and drugs for CRC. Given the distinct differences between molecular CRC subtypes vulnerability screens on representative cell lines for each subtype, rather than on cell line panels that contain multiple subtypes chosen on the basis of single genetic mutations may be useful to this purpose.<sup>88,89</sup> Ultimately, this updated and improved treatment individualization based on comprehensive analysis of a patient's tumor should enable physicians to make rational treatment decisions for each individual CRC patient.



## References

• Of importance

•• Of major importance

1. DeSantis CE, Lin CC, Mariotto AB, et al. Cancer treatment and survivorship statistics, 2014. *CA. Cancer J Clin* 2014.
2. Fearon ER. Molecular genetics of colorectal cancer. *Annu Rev Pathol* 2011;6:479–507.
3. Martini M, Vecchione L, Siena S, et al. Targeted therapies: how personal should we go? *Nat Rev Clin Oncol* 2012;9:87–97.
4. Torkamani A, Verkhivker G, Schork N. Cancer Driver Mutations in Protein Kinase Genes. *Cancer* 2010;281:117–27.
5. Stratton MR, Campbell PJ, Futreal PA. The cancer genome. *Nature* 2009;458:719–24.
6. Sorich MJ, Wiese MD, Rowland A, et al. Extended RAS mutations and anti-EGFR monoclonal antibody survival benefit in metastatic colorectal cancer: a meta-analysis of randomized controlled trials. *Ann Oncol* 2014;1–27.
7. Douillard J, Siena S, Cassidy J, Tabernero J. Final results from PRIME: randomized phase III study of panitumumab with FOLFOX4 for first-line treatment of metastatic colorectal cancer. *Ann Oncol* 2014;25:1346–55.
8. Karapetis CS, Khambata-Ford S, Jonker D, et al. K-ras Mutations and Benefit from Cetuximab in Advanced Colorectal Cancer. *N Engl J Med* 2008;609–19.
9. Amado RG, Wolf M, Peeters M, et al. Wild-type KRAS is required for panitumumab efficacy in patients with metastatic colorectal cancer. *J Clin Oncol* 2008;26:1626–34.
10. De Roock W, De Vriendt V, Normanno N, et al. KRAS, BRAF, PIK3CA, and PTEN mutations: implications for targeted therapies in metastatic colorectal cancer. *Lancet Oncol* 2011;12:594–603.
11. Douillard J-Y, Oliner KS, Siena S, et al. Panitumumab-FOLFOX4 treatment and RAS mutations in colorectal cancer. *N Engl J Med* 2013;369:1023–34.
12. Saridaki Z, Asimakopoulou N, Boukovinas I, Souglakos J. How to Identify the Right Patients for the Right Treatment in Metastatic Colorectal Cancer (mCRC). *Curr Colorectal Cancer Rep* 2015;11:151–9.
13. De Roock W, Claes B, Bernasconi D, et al. Effects of KRAS, BRAF, NRAS, and PIK3CA mutations on the efficacy of cetuximab plus chemotherapy in chemotherapy-refractory metastatic colorectal cancer: a retrospective consortium analysis. *Lancet Oncol* 2010;11:753–62.
14. Pentheroudakis G, Kotoula V, De Roock W, et al. Biomarkers of benefit from cetuximab-based therapy in metastatic colorectal cancer: interaction of EGFR ligand expression with RAS/RAF, PIK3CA genotypes. *BMC Cancer* 2013;13:49.
15. Rowland a, Dias MM, Wiese MD, et al. Meta-analysis of BRAF mutation as a predictive biomarker of benefit from anti-EGFR monoclonal antibody therapy for RAS wild-type metastatic colorectal cancer. *Br J Cancer* 2015;112:1888–94.
16. Dienstmann R, Salazar R, Tabernero J. Overcoming Resistance to Anti-EGFR Therapy in. *ASCO Educational Book* 2015.
17. Dienstmann R, Serpico D, Rodon J, et al. Molecular profiling of patients with colorectal cancer and matched targeted therapy in phase I clinical trials. *Mol Cancer Ther* 2012;11:2062–71.
18. Bendell JC, Rodon J, Burris H a, et al. Phase I, dose-escalation study of BKM120, an oral pan-Class I PI3K inhibitor, in patients with advanced solid tumors. *J Clin Oncol* 2012;30:282–90.

19. Ganesan P, Janku F, Naing A, et al. Target-Based Therapeutic Matching in Early-Phase Clinical Trials in Patients with Advanced Colorectal Cancer and PIK3CA mutations. *Mol Cancer Ther* 2012;29:997–1003.
20. Chapman PB, Hauschild A, Robert C, et al. Improved survival with vemurafenib in melanoma with BRAF V600E mutation. *N Engl J Med* 2011;364:2507–16.
21. Hauschild A, Grob J-J, Demidov L V, et al. Dabrafenib in BRAF-mutated metastatic melanoma: a multicentre, open-label, phase 3 randomised controlled trial. *Lancet* 2012;380:358–65.
22. Larkin J, Ascierto PA, Dréno B, et al. Combined Vemurafenib and Cobimetinib in BRAF -Mutated Melanoma. *N Engl J Med* 2014;371:1867–76.
23. Robert C, Karaszewska B, Schachter J, et al. Improved Overall Survival in Melanoma with Combined Dabrafenib and Trametinib. *N Engl J Med* 2015;372:30–9.
24. Kopetz S, Desai J, Hecht JR, et al. PLX4032 in metastatic colorectal cancer patients with mutant BRAF tumors. *J Clin Oncol* 2010;28:(suppl; abstract 3534).
25. Corcoran RB, Falchook GS, Infante JR, et al. BRAF V600 mutant colorectal cancer (CRC) expansion cohort from the phase I / II clinical trial of BRAF inhibitor dabrafenib (GSK2118436) plus MEK inhibitor trametinib (GSK1120212). *J Clin Oncol* 2012;30:(suppl; abstr 3528).
26. Prahallad A, Sun C, Huang S, et al. Unresponsiveness of colon cancer to BRAF(V600E) inhibition through feedback activation of EGFR. *Nature* 2012;483:100–3.  
*Provides preclinical rationale for combining BRAF inhibitors with EGFR inhibitors in BRAFm CRC.*
27. Corcoran RB, Ebi H, Turke AB, et al. EGFR-mediated re-activation of MAPK signaling contributes to insensitivity of BRAF mutant colorectal cancers to RAF inhibition with vemurafenib. *Cancer Discov* 2012;2:227–35.  
*Provides preclinical rationale for combining BRAF inhibitors with EGFR inhibitors in BRAFm CRC.*
28. Van Geel R, Elez E, Bendell JC, et al. Phase I study of the selective BRAF V600 inhibitor encorafenib (LGX818) combined with cetuximab and with or without the  $\alpha$ -specific PI3K inhibitor BYL719 in patients with advanced BRAF -mutant colorectal cancer. *J Clin Oncol* 2014;32:5s:(suppl; abstr 3514).
29. Atreya CE, Cutsem E Van, Bendell JC, et al. Updated efficacy of the MEK inhibitor trametinib (T), BRAF inhibitor dabrafenib (D), and anti-EGFR antibody panitumumab (P) in patients (pts) with BRAF V600E mutated (BRAFm) metastatic colorectal cancer (mCRC). *J Clin Oncol* 2015;(suppl;abstr 103).
30. Hong DS, Morris VK, Edmond B, et al. Phase Ib study of vemurafenib in combination with irinotecan and cetuximab in patients with BRAF -mutated metastatic colorectal cancer and advanced cancers. *J Clin Oncol* 2015;(suppl; abstr 3511).
31. Yuan Z-X, Wang X-Y, Qin Q-Y, et al. The prognostic role of BRAF mutation in metastatic colorectal cancer receiving anti-EGFR monoclonal antibodies: a meta-analysis. *PLoS One* 2013;8:e65995.
32. Cox AD, Fesik SW, Kimmelman AC, et al. Drugging the undruggable RAS: Mission Possible? *Nat Rev Drug Discov* 2014;13:828–51.
33. Migliardi G, Sassi F, Torti D, et al. Inhibition of MEK and PI3K/mTOR suppresses tumor growth but does not cause tumor regression in patient-derived xenografts of RAS-mutant colorectal carcinomas. *Clin Cancer Res* 2012;18:2515–25.
34. Shimizu T, Tolcher AW, Papadopoulos KP, et al. The clinical effect of the dual-targeting strategy involving PI3K/AKT/mTOR and RAS/MEK/ERK pathways in patients with advanced cancer. *Clin Cancer Res* 2012;18:2316–25.

35. Sun C, Hobor S, Bertotti A, et al. Intrinsic resistance to MEK inhibition in kras mutant lung and colon cancer through transcriptional induction of ERBB3. *Cell Rep* 2014;7:86–93.
36. Corcoran RB, Cheng KA, Hata AN, et al. Synthetic Lethal Interaction of Combined BCL-XL and MEK Inhibition Promotes Tumor Regressions in KRAS Mutant Cancer Models. *Cancer Cell* 2013;23:121–8.
37. Ostrem JM, Peters U, Sos ML, et al. K-Ras(G12C) inhibitors allosterically control GTP affinity and effector interactions. *Nature* 2013;503:548–51.
38. Ledford H. The ras renaissance. *Nature* 2015;520:278–80.
39. Rosty C, Young JP, Walsh MD, et al. PIK3CA Activating Mutation in Colorectal Carcinoma: Associations with Molecular Features and Survival. *PLoS One* 2013;8:1–9.
40. Zhao L, Vogt PK. Helical domain and kinase domain mutations in p110alpha of phosphatidylinositol 3-kinase induce gain of function by different mechanisms. *Proc Natl Acad Sci USA* 2008;105:2652–7.
41. Janku F, Lee JJ, Tsimberidou AM, et al. PIK3CA mutations frequently coexist with RAS and BRAF mutations in patients with advanced cancers. *PLoS One* 2011;6:e22769.
42. Whitehall VLJ, Rickman C, Bond CE, et al. Oncogenic PIK3CA mutations in colorectal cancers and polyps. *Int J Cancer* 2012;131:813–20.
43. Sartore-Bianchi A, Martini M, Molinari F, et al. PIK3CA mutations in colorectal cancer are associated with clinical resistance to EGFR-targeted monoclonal antibodies. *Cancer Res* 2009;69:1851–7.
44. Prenen H, De Schutter J, Jacobs B, et al. PIK3CA mutations are not a major determinant of resistance to the epidermal growth factor receptor inhibitor cetuximab in metastatic colorectal cancer. *Clin Cancer Res* 2009;15:3184–8.
45. Saridaki Z, Tzardi M, Papadaki C, et al. Impact of KRAS, BRAF, PIK3CA Mutations, PTEN, AREG, EREG expression and skin rash in ≥2nd line cetuximab-based therapy of colorectal cancer patients. *PLoS One* 2011;6:e15980.
46. Gonzalez-Angulo A, Juric D, Argiles G, et al. Safety, pharmacokinetics, and preliminary activity of the  $\alpha$ -specific PI3K inhibitor BYL719: Results from the first-in-human study. *J Clin Oncol* 2013;(suppl; abstr 2531).
47. Laurent-Puig P, Cayre A, Manceau G, et al. Analysis of PTEN, BRAF, and EGFR status in determining benefit from cetuximab therapy in wild-type KRAS metastatic colon cancer. *J Clin Oncol* 2009;27:5924–30.
48. Frattini M, Saletti P, Romagnani E, et al. PTEN loss of expression predicts cetuximab efficacy in metastatic colorectal cancer patients. *Br J Cancer* 2007;97:1139–45.
49. Loupakis F, Pollina L, Stasi I, et al. PTEN expression and KRAS mutations on primary tumors and metastases in the prediction of benefit from cetuximab plus irinotecan for patients with metastatic colorectal cancer. *J Clin Oncol* 2009;27:2622–9.
50. Perrone F, Lampis A, Orsenigo M, et al. PI3KCA/PTEN deregulation contributes to impaired responses to cetuximab in metastatic colorectal cancer patients. *Ann Oncol* 2009;20:84–90.
51. Peeters M, Oliner KS, Parker A, et al. Massively parallel tumor multigene sequencing to evaluate response to panitumumab in a randomized phase III study of metastatic colorectal cancer. *Clin Cancer Res* 2013;19:1902–12.
52. Argilés G, Élez E, Ortiz C, et al. Outcome evolution of matched molecular targeted agents (MTAs) in metastatic colorectal cancer (CRC) patients (pts): VHIO experience. *J Clin Oncol* 2015;2015:3602.
53. O'Brien SG, Guilhot F, Larson RA, et al. Imatinib compared with interferon and low-dose cytarabine for newly diagnosed chronic-phase chronic myeloid leukemia. *N Engl J Med* 2003;348:994–1004.

54. Saglio G, Kim D, Issaragrisil S, le Coutre P. Nilotinib versus imatinib for newly diagnosed CML. *N Engl J Med* 2010;362:2373–83.
55. Kantarjian H, Shah NP, Hochhaus A, et al. Dasatinib versus imatinib in newly diagnosed chronic-phase chronic myeloid leukemia. *N Engl J Med* 2010;362:2260–70.
56. Isella C, Terrasi A, Bellomo SE, et al. Stromal contribution to the colorectal cancer transcriptome. *Nat Genet* 2015;47:312–9.
57. Calon A, Lonardo E, Berenguer-Illergo A, et al. Stromal gene expression defines poor-prognosis subtypes in colorectal cancer. *Nat Genet* 2015;47:320–9.
58. Saridaki Z, Souglakos J, Georgoulas V. Prognostic and predictive significance of MSI in stages II/III colon cancer. *World J Gastroenterol* 2014;20:6809–14.
59. Popat S, Hubner R, Houlston RS. Systematic review of microsatellite instability and colorectal cancer prognosis. *J Clin Oncol* 2005;23:609–18.
60. Sinicrope FA, Foster NR, Thibodeau SN, et al. DNA mismatch repair status and colon cancer recurrence and survival in clinical trials of 5-fluorouracil-based adjuvant therapy. *J Natl Cancer Inst* 2011;103:863–75.
61. Tejpar S, Bosman F, Delorenzi M, et al. Microsatellite instability (MSI) in stage II and III colon cancer treated with 5FU-LV or 5FU-LV and irinotecan (PETACC 3-EORTC 40993-SAKK 60/00 trial). *J Clin Oncol* 2009;27: (suppl; abstr 4001).
62. Sargent DJ, Marsoni S, Monges G, et al. Defective mismatch repair as a predictive marker for lack of efficacy of fluorouracil-based adjuvant therapy in colon cancer. *J Clin Oncol* 2010;28:3219–26.
63. Webber EM, Kauffman TL, O'Connor E, Goddard KA. Systematic review of the predictive effect of MSI status in colorectal cancer patients undergoing 5FU-based chemotherapy. *BMC Cancer* 2015;15:1–12.
64. Des Guetz G, Schischmanoff O, Nicolas P, et al. Does microsatellite instability predict the efficacy of adjuvant chemotherapy in colorectal cancer? A systematic review with meta-analysis. *Eur J Cancer* 2009;45:1890–6.
65. Sargent DJ, Shi Q, Yothers G, et al. Prognostic impact of deficient mismatch repair (dMMR) in 7, 803 stage II / III colon cancer (CC) patients (pts): A pooled individual pt data analysis of 17 adjuvant trials in the ACCENT. *J Clin Oncol* 2014;32 (suppl; abstr 3507).
66. Tian S, Roepman P, Popovici V, et al. A robust genomic signature for the detection of colorectal cancer patients with microsatellite instability phenotype and high mutation frequency. *J Pathol* 2012;228:586–95.
67. Ricciardiello L, Ceccarelli C, Angiolini G, et al. High Thymidylate Synthase Expression in Colorectal Cancer with Microsatellite Instability: Implications for Chemotherapeutic Strategies. *Clin Cancer Res* 2005;11:4234–40.
68. Choueiri MB, Shen JP, Gross AM, et al. ERCC1 and TS Expression as Prognostic and Predictive Biomarkers in Metastatic Colon Cancer. *PLoS One* 2015;10:e0126898.
69. ••The Cancer Genome Atlas Network. Comprehensive molecular characterization of human colon and rectal cancer. *Nature* 2012;487:330–7.  
*Comprehensive genetic analysis of colorectal cancer.*
70. Dow LE, O'Rourke KP, Simon J, et al. Apc Restoration Promotes Cellular Differentiation and Reestablishes Crypt Homeostasis in Colorectal Cancer *Cell* 2015;161:1539–52.
71. Wiegering A, Uthe FW, Jamieson T, et al. Targeting translation initiation bypasses signaling crosstalk mechanisms that maintain high MYC levels in colorectal cancer. *Cancer Discov* 2015;5:768–81.
72. Hinoue T, Weisenberger DJ, Lange CPE, et al. Genome-scale analysis of aberrant DNA methylation in colorectal cancer. *Cancer Res* 2012;72:271–82.

73. Popovici V, Budinska E, Tejpar S, et al. Identification of a poor-prognosis BRAF-mutant-like population of patients with colon cancer. *J Clin Oncol* 2012;30:1288–95.
74. Tian S, Simon I, Moreno V, et al. A combined oncogenic pathway signature of BRAF, KRAS and PI3KCA mutation improves colorectal cancer classification and cetuximab treatment prediction. *Gut* 2013;62:540–9.
75. Holderfield M, Nagel TE, Stuart DD. Mechanism and consequences of RAF kinase activation by small-molecule inhibitors. *Br J Cancer* 2014;111:1–6.
76. •De Sousa E Melo F, Wang X, Jansen M, et al. Poor-prognosis colon cancer is defined by a molecularly distinct subtype and develops from serrated precursor lesions. *Nat Med* 2013;19:614–8.
77. •Budinska E, Popovici V, Tejpar S, et al. Gene expression patterns unveil a new level of molecular heterogeneity in colorectal cancer. *J Pathol* 2013;231:63–76.
78. •Marisa L, de Reyniès A, Duval A, et al. Gene expression classification of colon cancer into molecular subtypes: characterization, validation, and prognostic value. *PLoS Med* 2013;10:e1001453.
79. •Roepman P, Schlicker A, Tabernero J, et al. Colorectal cancer intrinsic subtypes predict chemotherapy benefit, deficient mismatch repair and epithelial-to-mesenchymal transition. *Int J Cancer* 2014;134:552–62.
80. •Sadanandam A, Lyssiotis CA, Homicsko K, et al. A colorectal cancer classification system that associates cellular phenotype and responses to therapy. *Nat Med* 2013;19:619–25.
81. •Schlicker A, Beran G, Chresta CM, et al. Subtypes of primary colorectal tumors correlate with response to targeted treatment in colorectal cell lines. *BMC Med Genomics* 2012;5:66.  
*Six research groups describing subtypes of colorectal cancer with prognostic and predictive implications.*
82. Dienstmann R, Guinney J, Delorenzi M, et al. Colorectal Cancer Subtyping Consortium (CRCSC) Identifies Consensus of Molecular Subtypes. Presented at ASCO Annual Meeting 2014.
83. Brunen D, Willems SM, Kellner U, et al. TGF- $\beta$ : An emerging player in drug resistance. *Cell Cycle* 2013;12:2960–8.
84. Oskarsson T, Batlle E, Massague J. Metastatic Stem Cells: Sources, Niches, and vital pathways. *Cell Stem Cell* 2012;29:997–1003.
85. Segal NH, Parsons DW, Peggs KS, et al. Epitope landscape in breast and colorectal cancer. *Cancer Res* 2008;68:889–92.
86. Smyrk TC, Watson P, Kaul K, Lynch HT. Tumor-infiltrating lymphocytes are a marker for microsatellite instability in colorectal carcinoma. *Cancer* 2001;91:2417–22.
87. •Le DT, Uram JN, Wang H, et al. PD-1 Blockade in Tumors with Mismatch-Repair Deficiency. *N Engl J Med* 2015;26:2509–20.  
*Demonstrates MMR deficiency is a predictive marker for response to PD-1 blockade in patients with CRC.*
88. Linnekamp JF, Wang X, Medema JP, Vermeulen L. Colorectal Cancer Heterogeneity and Targeted Therapy: A Case for Molecular Disease Subtypes. *Cancer Res* 2015;2:245–9.
89. Medico E, Russo M, Picco G, et al. The molecular landscape of colorectal cancer cell lines unveils clinically actionable kinase targets. *Nat Commun* 2015;6:7002.



# Chapter 5

## Clinical pharmacology of combined targeted therapy targeting mutated *BRAF*



### 5.1

#### Phase Ib dose-escalation study of encorafenib (LGX818) and cetuximab with or without alpelisib in patients with metastatic *BRAF*-mutant colorectal cancer

##### Submitted for publication

Robin M.J.M. van Geel\*, Josep Tabernero\*, Elena Elez, Johanna C. Bendell, Anna Spreafico, Martin Schuler, Takayuki Yoshino, Jean-Pierre Delord, Yasuhide Yamada, Martijn P. Lolkema, Jason E. Faris, Ferry A.L.M. Eskens, Sunil Sharma, Rona Yaeger, Heinz-Josef Lenz, Zev A. Wainberg, Emin Avsar, Arkendu Chatterjee, Savina Jaeger, Eugene Tan, Tim Demuth, Jan H.M. Schellens\*

*\* Authors contributed equally*

## ABSTRACT

Preclinical evidence suggests that concomitant *BRAF* and EGFR inhibition leads to sustained suppression of MAPK signaling and tumor growth in *BRAF* V600E colorectal cancer (CRC) models. Patients with refractory *BRAF* V600-mutant metastatic CRC (mCRC) were treated with either a selective RAF kinase inhibitor (encorafenib) plus a monoclonal antibody targeting EGFR (cetuximab) or encorafenib and cetuximab with a phosphoinositide 3-kinase alpha inhibitor (alpelisib). The primary objective was to determine the maximum tolerated dose and recommended phase 2 dose (RP2D). Patients were enrolled in either the dual- ( $n = 26$ ) or triple-combination ( $n = 28$ ) groups. Dose-limiting toxicities were reported in three patients receiving dual (grade 3 arthralgia, vomiting, and QT interval prolongation) and two patients receiving triple treatment (grade 4 increased creatinine, grade 3 bilateral interstitial pneumonitis). RP2D was established as 200 mg encorafenib (both groups) and 300 mg alpelisib. Combinations of cetuximab and encorafenib show promising clinical activity and tolerability in *BRAF*-mutant mCRC.

**SIGNIFICANCE:** Herein we demonstrate that dual- (encorafenib plus cetuximab) and triple- (encorafenib plus cetuximab and alpelisib) combination treatments are tolerable and provide promising clinical activity in the difficult-to-treat patient population with *BRAF*-mutant mCRC.



## Introduction

Colorectal cancer (CRC) is the third most commonly diagnosed cancer in men and the second in women; 693,900 patients with CRC died in 2012.<sup>1</sup> The anti-epidermal growth factor receptor (EGFR) monoclonal antibody cetuximab is indicated for wild-type *RAS* metastatic CRC (mCRC), either in combination with cytotoxic chemotherapy or as a single agent.

Investigations of the signaling pathways downstream of EGFR have shown that mutations of Kirsten rat sarcoma viral oncogene homolog (*KRAS*), Neuroblastoma RAS viral oncogene homolog (*NRAS*) and B-Raf proto-oncogene (*BRAF*) play an important role in cancer progression.<sup>2</sup> Mutations in the *BRAF* gene at valine 600 occur in approximately 7% of all cancers, including approximately 5% to 8% of CRCs.<sup>3,4</sup> *BRAF*-mutant CRC is molecularly distinct to *BRAF* wild-type CRC<sup>5</sup> and is associated with a significantly poorer prognosis and poor response to standard treatments, highlighting the unmet medical need for this group of patients.<sup>6,7</sup>

Two *BRAF* inhibitors (vemurafenib and dabrafenib) have been approved for the treatment of *BRAF*-mutant melanoma.<sup>8,9</sup> In contrast, *BRAF* inhibitors have shown limited efficacy in *BRAF*-mutant mCRC.<sup>10-15</sup> Preclinical studies of *BRAF*-mutant CRC and melanoma cell lines treated with selective *BRAF* V600 inhibitors have found that rapid EGFR-mediated reactivation of the mitogen-activated protein kinase (MAPK) pathway contributed to the unresponsiveness of *BRAF*-mutant CRC cells.<sup>10,12</sup>

Despite the limited efficacy of EGFR and *BRAF* inhibitors given as single agents in patients with *BRAF*-mutant CRC, preclinical evidence suggests that concomitant inhibition leads to sustained suppression of MAPK signaling resulting in reduced cell proliferation and increased antitumor activity.<sup>10,12,16</sup>

Activation of the phosphoinositide 3-kinase (PI3K)/AKT pathway has also been identified as a mechanism of resistance to *BRAF* inhibitors in *BRAF*-mutant CRC cell lines.<sup>11,17</sup> Combinatorial approaches with *BRAF* and PI3K inhibitors have been suggested to improve outcomes in patients with *BRAF*-mutant mCRC.<sup>11</sup> Encorafenib is a potent, selective RAF kinase inhibitor with promising activity in preclinical models, including greater potency compared with vemurafenib and dabrafenib.<sup>18</sup> Alpelisib is a class I  $\alpha$ -specific PI3K inhibitor with antitumor activity in various cancer cell lines, especially those with documented *PIK3CA* mutations, and in tumor xenograft models with mutated or amplified *PIK3CA*.<sup>19</sup>

The synergistic activity of *BRAF* + EGFR  $\pm$  PI3K inhibition reported in preclinical studies<sup>10-12,16,17</sup> led to the initiation of this phase 1b/2 study of encorafenib + cetuximab with or without alpelisib in patients with *BRAF*V600-mutant mCRC. Herein we report results of the phase 1b portion of this study, which had the primary aim of selecting a dose of encorafenib and alpelisib for phase 2 by determining the incidence of dose-limiting toxicities (DLTs).

## Patients and methods

### Study Design

This multicenter, open-label, phase 1b dose-escalation study enrolled patients with *BRAF*V600-mutant mCRC. The primary objective of phase 1b was to determine the maximum tolerated dose (MTD) and/or recommended dose for phase 2 (RP2D) of encorafenib in combination with cetuximab or with cetuximab and alpelisib. Adult patients with mCRC were enrolled on the basis of documented wild-type *KRAS* and a *BRAF* V600 mutation. Eligibility criteria included: Eastern Cooperative Oncology Group performance status (ECOG PS) of  $\leq 2$ , either progression after  $\geq 1$  prior standard-of-care regimen or intolerance to irinotecan-based regimens, and life expectancy of  $\geq 3$  months. All patients gave

written informed consent, per Declaration of Helsinki recommendations. The study is registered with ClinicalTrials.gov (NCT01719380).

### ***Study Treatment***

Patients were assigned sequentially to either encorafenib and cetuximab (dual) or encorafenib, cetuximab, and alpelisib (triple) combination therapy groups. Treatment cycles were 28 days in length. Cetuximab was dosed intravenously according to the label for mCRC: a 400 mg/m<sup>2</sup> loading dose (cycle 1 day 1) and 250 mg/m<sup>2</sup> for subsequent weekly doses. In the dual combination, the starting dose of encorafenib was chosen as 100 mg daily based on available data from the first-in-human study of encorafenib.<sup>20</sup> The triple combination was not initiated until a minimum of 12 evaluable patients had been treated with the dual combination. The starting dose of encorafenib in the triple-combination therapy group was based on the dual-combination dose, and the starting dose of alpelisib (100 mg) was selected at 25% of the single-agent MTD identified in a phase 1 clinical study of alpelisib in patients with solid tumors.<sup>21</sup> Dose-escalation decisions were based on data from all evaluable patients, including safety information, DLTs, all grade  $\geq 2$  toxicity data during cycle 1, pharmacokinetics (PK), and pharmacodynamics. The recommended dose for each level was guided by a Bayesian logistic regression model.<sup>22,23</sup> A DLT was defined as an adverse event (AE) or abnormal lab value assessed as unrelated to disease, disease progression, inter-current illness, or concomitant medications that occurred within the first 28 days of treatment, with the exceptions listed in Supplementary Table S1. In order to be evaluable, patients had to complete a minimum of one cycle of treatment with the minimum safety evaluation and drug exposure (21 of the 28 oral daily doses and the cetuximab loading dose, plus two weekly doses within the 28-day cycle). The MTD was defined as the highest combination drug dosage not causing medically unacceptable DLTs in > 35% of treated patients in the first cycle.

### ***Study Assessments***

Tumor response was evaluated locally based on RECIST v1.1 assessments, by means of CT scan with intravenous contrast of chest, abdomen, and pelvis, which were performed at screening and every 6 weeks after starting study treatment until disease progression. Safety was monitored at screening and throughout the treatment period by physical examination and collection of AEs. Blood samples for plasma PK analysis were collected from all patients during treatment. A full PK profile (pre-dose, 0.5, 1, 2, 4, 6, 8, and 24 h) was performed on day 1 of cycles 1 and 2. Samples were assayed using validated liquid chromatography-tandem mass spectrometry. When feasible, fresh tumor biopsies were collected before and during treatment for the investigation of the pharmacodynamic effects of the drugs, including comprehensive genomic analysis. Somatic mutations, loss of heterozygosity, and copy number aberrations were assessed by Foundation Medicine assay analytics. Additional annotations from the Catalog of Somatic Mutations in Cancer were used to filter functional mutations.

### ***Statistical methods***

An adaptive Bayesian logistic regression model (BLRM) guided by the escalation with overdose control principle directed the dose escalation to its MTD/RP2D.<sup>22</sup> A 10-parameter BLRM for combination treatment was fitted on the cycle 1 DLT data accumulated throughout the dose escalation to model the dose-toxicity relationship of encorafenib, cetuximab and alpelisib given in combination. Dose

recommendation was based on posterior summaries including the mean, median, standard deviation, 95% credibility interval and the probability that the true DLT rate for each dose lies in one of the following categories: under-dosing (0-16%), targeted toxicity (16-35%) or excessive toxicity (35-100%). The recommended next dose was the one with the highest posterior probability of DLT in the targeted toxicity interval and less than 25% chance of excessive toxicity. Initially, cohorts of three to six evaluable patients were enrolled. At least six evaluable patients were treated at MTD/RP2D.

## Results

### *Patient Disposition and Characteristics*

A total of 54 patients were enrolled into either the dual- ( $n = 26$ ) or triple-combination ( $n = 28$ ) therapy groups and received escalating doses of encorafenib and/or alpelisib (Table 1). By February 1, 2015, treatment had been discontinued in 24 (92.3%) of the patients in the dual-combination therapy group due to disease progression ( $n = 18$ ; 69.2%), AEs ( $n = 3$ ; 11.5%), physician decision ( $n = 1$ ; 3.8%), patient decision ( $n = 1$ ; 3.8%), or death ( $n = 1$ ; 3.8%). In the triple-combination therapy group, treatment had been discontinued in 22 (78.6%) patients due to disease progression ( $n = 19$ ; 67.9%), AEs ( $n = 2$ ; 7.1%), or death ( $n = 1$ ; 3.6%). Patient characteristics in the two groups were similar; however, more patients had a poorer ECOG PS in the dual-combination group than the triple-combination group (ECOG PS  $\geq 1$ : 69.2% vs 35.7%, respectively) (Table 2). The majority of patients had received two prior lines of therapy and a considerable proportion had been treated with 3 or more lines of therapy (23.1% in the dual- and 10.7% in the triple-combination therapy groups). Most patients had *BRAF* V600E, only two patients had mutations outside the 600 codon.

5.1

**Table 1. Dose-escalation cohorts for dual- and triple-combination therapies**

ENC + CTX ( $n = 26$ )			ENC + ALP + CTX ( $n = 28$ )			
Patient number, $n$	ENC dose, mg QD	DLT	Patient number, $n$	ENC dose, mg QD	ALP dose, mg QD	DLT
2	100	None	3	200	100	none
7	200	G3 arthralgia ( $n = 1$ )	8	200	200	none
9	400	G3 vomiting ( $n = 1$ )	7	300	200	G4 increased creatinine ( $n = 1$ )
8	450	G3 QT interval prolongation ( $n = 1$ )	10	200	300	G3 bilateral interstitial pneumonitis ( $n = 1$ )

Abbreviations: ENC, encorafenib; CTX, cetuximab; ALP, alpelisib; G3, grade 3; G4, grade 4; QD, daily.

### *Dose Determination*

In order to be evaluable, patients had to complete a minimum of one cycle of treatment with the minimum safety evaluation and drug exposure. Twenty-one patients in the dual-combination therapy group and 25 patients in the triple-combination therapy group were considered evaluable. Three DLTs were identified in the dual-combination therapy group: grade 3 arthralgia ( $n = 1$ ) with 200 mg encorafenib, grade 3 vomiting ( $n = 1$ ) with 400 mg encorafenib, and grade 3 corrected QT interval prolongation ( $n = 1$ ) with 450 mg encorafenib. Two DLTs were identified in the triple-combination therapy group: grade 4 increased creatinine ( $n = 1$ ) with 300 mg encorafenib and 200 mg alpelisib, and

<b>Table 2. Patient and disease characteristics at baseline</b>		
	<b>ENC + CTX (n = 26)</b>	<b>ENC + ALP + CTX (n = 28)</b>
<b>Sex, n (%)</b>		
Female	15 (58)	18 (64)
Male	11 (42)	10 (36)
<b>Age, median (range), years</b>		
	63 (43–80)	59 (40–76)
<b>Primary site of cancer derived, n (%)</b>		
Colon	24 (92)	25 (89)
Rectum	2 (8)	3 (11)
<b>ECOG PS, n (%)</b>		
0	8 (31)	18 (64)
1	16 (62)	10 (36)
2	2 (8)	0
<b>Visceral involvement at baseline, n (%)</b>		
Liver	15 (58)	16 (57)
Peritoneum	5 (19)	8 (29)
<b>Lactate dehydrogenase levels at baseline, n (%)</b>		
Normal	9 (35)	10 (36)
> ULN	15 (58)	14 (50)
<b>Number of prior treatment regimens, n (%)</b>		
1	7 (27)	10 (36)
2	8 (31)	14 (50)
3	5 (20)	1 (4)
≥ 3	6 (23)	3 (11)
<b>Best response to last prior therapy, n (%)</b>		
Partial response	7 (27)	2 (7)
Stable disease	8 (31)	12 (43)
Progressive disease	5 (20)	9 (32)
Unknown/not applicable	6 (23)	6 (21)

Abbreviations: ECOG PS, Eastern Cooperative Oncology Group performance status; ENC, encorafenib; CTX cetuximab; ALP, alpelisib; ULN, upper limit of normal

grade 3 bilateral interstitial pneumonitis ( $n = 1$ ) with 200 mg encorafenib and 300 mg alpelisib. Following assessment of the overall tolerability of treatment, it was decided not to complete dose escalation up to the MTD in either of the treatment combinations. Studies of single-agent alpelisib have suggested that a clinical dose of  $\geq 270$  mg is required for efficacy.<sup>24</sup> As one DLT was reported in the triple-combination therapy group at a dose level of 200 mg encorafenib and 300 mg alpelisib (+ cetuximab), it was considered unlikely that a dose of  $>300$  mg alpelisib could be achieved. The MTD for single-agent alpelisib was established as 400 mg;<sup>25</sup> however, at this dose there were more treatment interruptions due to hyperglycemia. Hence, 300 mg alpelisib was established as the RP2D in the triple-combination therapy arm. Similarly, a dose of 300 mg encorafenib plus 200 mg alpelisib (+ cetuximab) led to renal toxicity, suggesting that higher doses of encorafenib were not tolerable with higher alpelisib doses, resulting in the establishment of 200 mg encorafenib as the RP2D in the triple-combination therapy group. To allow for the assessment of safety and efficacy of additive alpelisib compared with the encorafenib + cetuximab combination, the encorafenib dose was kept consistent

in dual and triple combinations. Hence, the doses selected for the phase 2 portion of the study were 200 mg encorafenib daily + weekly cetuximab for the dual combination and 200 mg encorafenib daily + 300 mg alpelisib daily + weekly cetuximab for the triple combination. These dose levels fulfilled the protocol criteria for MTD/RP2D:  $\geq 6$  patients had been treated at this dose and either the posterior probability of targeted toxicity at this dose exceeded 50% or a minimum of 12 patients had been treated with the dual and triple combinations.

### Safety

The overall safety profiles for the two therapy groups are shown in Table 3. AEs occurred in all patients in both treatment groups, with the most common AEs being fatigue ( $n = 13$ ; 50%) in the dual-combination and nausea ( $n = 17$ ; 61%) in the triple-combination therapy group. Grade 3/4 AEs were more common in the triple- vs dual-combination therapy group (79% vs 69%), with the most common grade 3/4 AEs being hypophosphatemia ( $n = 5$ ; 19%) in the dual-combination therapy group and dyspnea and hyperglycemia ( $n = 3$ ; 11% each) in the triple-combination therapy group.

Adverse event, $n$ (%)	ENC + CTX ( $n = 26$ )		ENC + ALP + CTX ( $n = 28$ )	
	All grades	Grade 3/4	All grades	Grade 3/4
Fatigue	13 (50.0)	3 (11.5)	12 (42.9)	1 (3.6)
Vomiting	12 (46.2)	2 (7.7)	14 (50.0)	0
Dyspnea	9 (34.6)	1 (3.8)	5 (17.9)	3 (10.7)
Abdominal pain	8 (30.8)	3 (11.5)	7 (25.0)	1 (3.6)
Nausea	8 (30.8)	0	17 (60.7)	1 (3.6)
Hyperglycemia	2 (7.7)	0	11 (39.3)	3 (10.7)
Back pain	7 (26.9)	1 (3.8)	3 (10.7)	1 (3.6)
Constipation	7 (26.9)	1 (3.8)	4 (14.3)	0
Decreased appetite	7 (26.9)	0	8 (28.6)	1 (3.6)
Hypophosphatasemia	7 (26.9)	5 (19.2)	4 (14.3)	1 (3.6)
Infusion-related reaction	7 (26.9)	0	1 (3.6)	0
Weight decreased	7 (26.9)	0	10 (35.7)	1 (3.6)
Dysphonia	2 (7.7)	0	7 (25.0)	0
Melanocytic nevus	1 (3.8)	0	7 (25.0)	0
Peripheral edema	2 (7.7)	0	7 (25.0)	0
Cough	6 (23.1)	0	2 (7.1)	1 (3.6)
Headache	6 (23.1)	0	4 (14.3)	0
Myalgia	6 (23.1)	0	4 (14.3)	0
Pain in extremity	6 (23.1)	0	2 (7.1)	0
Stomatitis	6 (23.1)	0	4 (14.3)	1 (3.6)
Dysgeusia	1 (3.8)	0	6 (21.4)	0
Diarrhea	5 (19.2)	1 (3.8)	15 (53.6)	1 (3.6)
Dry skin	5 (19.2)	0	9 (32.1)	0
Rash	5 (19.2)	0	10 (35.7)	0
Hypomagnesaemia	4 (15.4)	0	8 (28.6)	1 (3.6)
Dermatitis acneiform	3 (11.5)	0	8 (28.6)	1 (3.6)
Pyrexia	3 (11.5)	0	8 (28.6)	1 (3.6)

All patients had at least 1 AE. Abbreviations: ENC, encorafenib; CTX, cetuximab; ALP, alpelisib.

Dermatologic AEs were more common in the triple- than the dual-combination therapy group (rash [ $n = 10$ , 36% vs  $n = 5$ ; 19%], dermatitis acneiform [ $n = 8$ ; 29% vs  $n = 3$ ; 12%], dry skin [ $n = 9$ ; 32% vs  $n = 5$ ; 19%] and melanocytic nevus [ $n = 7$ ; 25% vs  $n = 1$ ; 4%]). Eleven (39%) patients in the triple-combination therapy group exhibited hyperglycemia (29% grade 1/2; 11% grade 3/4) compared with two patients (8% grade 1/2) in the dual-combination therapy group.

**Efficacy**

The dual- and triple-combination therapies both demonstrated efficacy in patients with *BRAF*-mutant mCRC (Table 4), with overall response rates of 23% in the dual- and 32% in the triple-combination therapy group (Fig. 1). The median duration of response was 35 weeks in the dual- and 12 weeks in the triple-combination therapy group for patients with confirmed responses (five patients in either arm). Two of the ten patients with confirmed responses continued to respond (one in their 23<sup>rd</sup> cycle of treatment and one in their 16<sup>th</sup> cycle of treatment) at the data cutoff date of February 1, 2015 (both are in the dual-combination therapy arm). The main reason for some responses being unconfirmed was related to patients exhibiting new lesions at subsequent scans or in one case a 20% increase in the

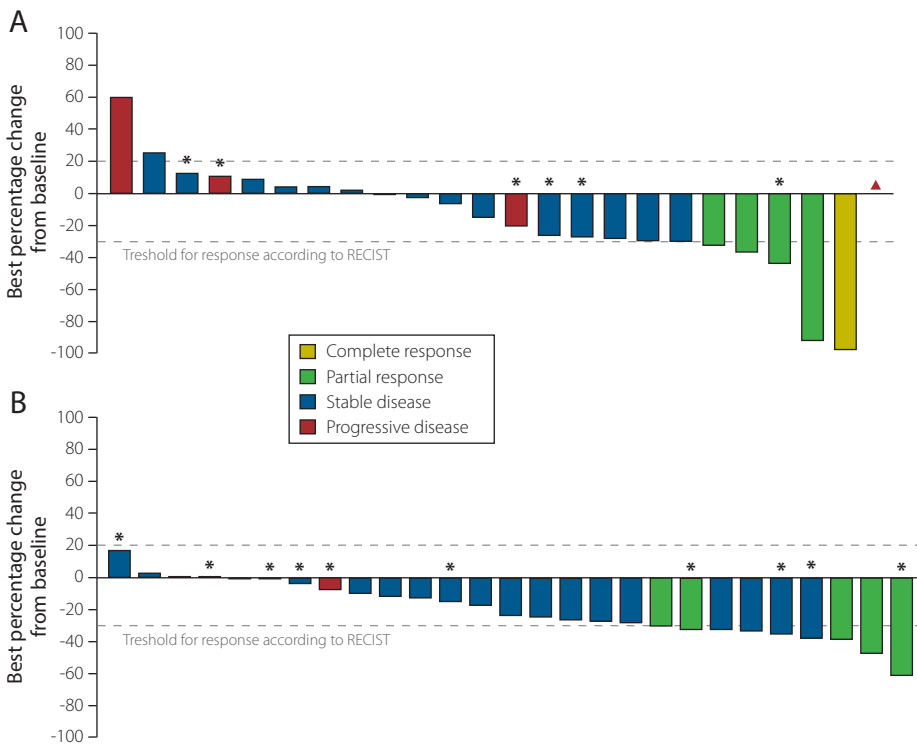


**Figure 1. Waterfall plot of best percentage change of tumor size from baseline by best response.**

(A) Dual combination, (B) triple combination. \*Patients treated at the Recommended phase 2 dose.

Abbreviations: RECIST, Response Evaluation Criteria in Solid Tumors.

Table 4. Best overall response to treatment		
Response, n (%)	ENC + CTX (n = 26)	ENC + ALP + CTX (n = 28)
Complete response (CR)	1 (3.8)	0
Partial response (PR)	4 (15.4)	5 (17.9)
Unconfirmed partial response (uPR)	1 (3.8)	4 (14.3)
Stable disease (SD)	14 (53.8)	17 (60.7)
Progressive disease (PD)	4 (15.4)	1 (3.6)
Unknown	2 (7.7)	1 (3.6)
Overall response rate (CR + PR + uPR)	6 (23.1)	9 (32.1)
Disease control rate (CR + PR + uPR + SD)	20 (76.9)	26 (92.8)

Abbreviations: ENC, encorafenib; CTX, cetuximab; ALP, alpelisib.

sum of target lesions from the nadir even though there had been a >30% target lesion reduction at the first CT scan. Duration of exposure to treatment was longer in the dual-combination therapy arm than the triple-combination therapy arm (Supplementary Figure 1). When comparing patients who were treated with doses of >200 mg encorafenib with those who were treated with ≤200 mg encorafenib, no difference in activity was observed. Median progression-free survival (PFS) for the dual- and triple-combination therapy groups was 3.7 and 4.3 months, respectively (Fig. 2). A group of patients in each treatment arm (≈20%–30%) remained on treatment for ≥32 weeks.

5.1

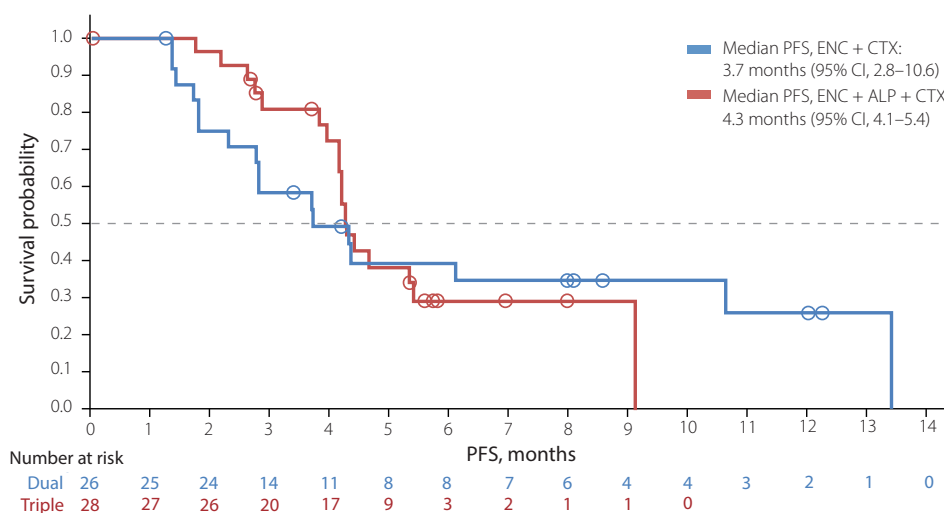


Figure 2. Progression-free survival for all patients.

Abbreviations: ENC, encorafenib; CTX, cetuximab; ALP, alpelisib; PFS, progression-free survival. Censored patients are indicated by circles.

### **Biomarker Analyses**

Fresh tumor biopsies were collected before and during treatment where feasible. Genes from key signaling pathways (MAPK, PI3K, WNT/ $\beta$ -catenin, and EGFR) were investigated over the course of treatment in both treatment combinations (Fig. 3). Significant correlations between exploratory genetic analyses and clinical outcomes were not observed in this small sample of patients. However, some interesting trends were noted. At baseline, KRAS gain of copy number was observed in 6 patients and neutral LOH was observed in two patients. KRAS gain was seen both in patients with long PFS as well as shorter PFS, suggesting that modest gains of KRAS did not preclude response to the encorafenib/cetuximab combination. Patients with *EGFR* amplification appeared to experience longer progression-free survival. Six patients treated with the dual combination showed gain of copies in the *EGFR* gene; these same patients also had MET copy number gain in most cases, most likely due to global amplification of chromosome 7. These patients had a median of 225 days on treatment (range, 67 to 437 days). One patient had a complete response (CR), four had a partial response (PR), and one had stable disease (SD), with all patients having  $\geq 28\%$  reduction in their target lesions. In contrast, five patients in the dual-combination therapy group did not show any alteration in the *EGFR* gene; these patients had a median of 50 days of treatment (range, 16 to 110 days); one patient had a PR that progressed after 110 days. A similar trend was observed in patients receiving triple treatment: four patients showed gain of copies in the *EGFR* gene and had a median of 124 days on treatment (range, 117 to 227 days); however, none of the patients had tumor regression meeting RECIST criteria for a radiological response (all SD with target tumor shrinkage of 0% to 28%). In contrast to patients in the dual-combination therapy group, the five patients who did not have any alterations in the *EGFR* gene also exhibited prolonged treatment durations, with a median of 175 days (range, 70 to 408 days), and one patient achieved a PR. However, these patients had alterations in the PI3K pathway, including phosphatase and tensin homolog (*PTEN*), *PIK3CA*, or *AKT1*; hence the addition of alpelisib may explain the differences in observation.

Initial observations for patients with PI3K pathway alterations did not reveal clear associations with treatment response. Patients who received dual treatment appeared to have similar responses to patients who received triple treatment. Seven patients in the dual-combination therapy group had *PIK3CA* alterations; this did not appear to preclude benefit because the median duration of treatment for these patients was still 119 days (range, 16–437), and two of the patients experienced PRs. Only two patients in the triple-combination therapy group had *PIK3CA* mutations. One patient remained on treatment for 175 days and the other for 274 days. Six patients had *PTEN* loss or deletions: the two patients in the dual-combination therapy group did not respond and remained on treatment for 67 and 42 days and the four patients in the triple-combination therapy group had a median of 139 days on treatment (range, 70–175).

Alterations in the WNT pathway were also observed. Fourteen patients (71%) had Adenomatous Polyposis Coli (*APC*) mutations: nine in the dual and five in the triple-combination therapy group. Patients treated with dual-combination therapy whose tumors harbored *APC* mutations had shorter treatment durations, with a median of 52 days on treatment (range, 16 to 338). Patients who received triple-combination therapy had longer treatment durations with a median of 124 days (range, 70 to 274 days). Seventeen patients (81%) had Ring Finger Protein 43 (*RNF43*) alterations, and the majority, ten patients, was treated with the dual-combination. These patients had a median of 96 days on treatment



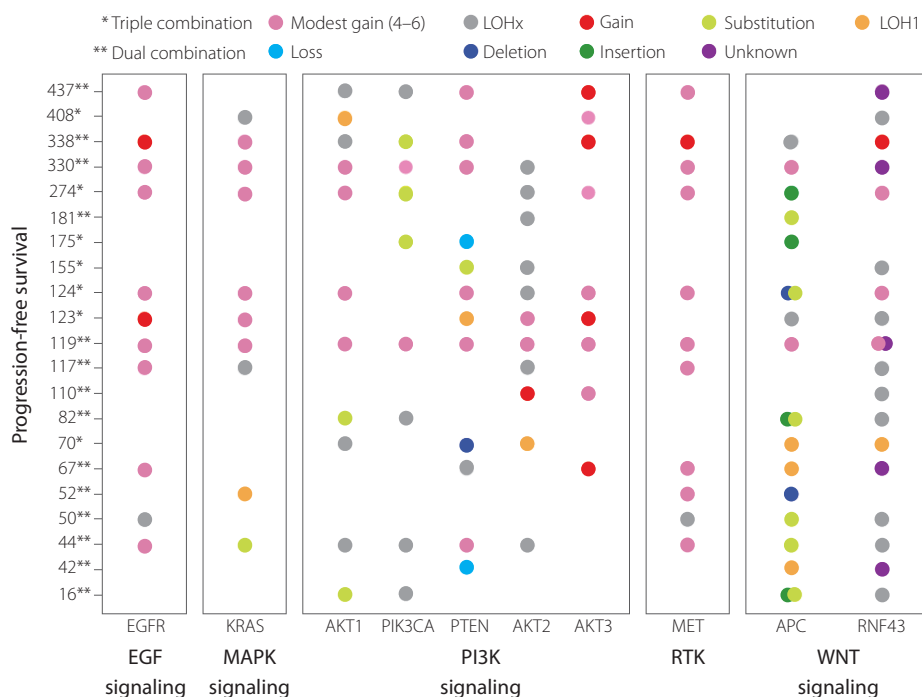


**Figure 3. Progression-free survival vs genetic alterations and allele frequency by gene pathways.**

Abbreviations: APC, adenomatous polyposis coli; EGFR, epidermal growth factor receptor; KRAS, Kirsten rat sarcoma viral oncogene homolog; LOH1, copy-loss loss of heterozygosity; LOHx, copy-neutral loss of heterozygosity; MAPK, mitogen-activated protein kinase; MET, MET proto-oncogene, receptor tyrosine kinase; PI3K, phosphoinositide 3-kinase; PTEN, phosphatase and tensin homolog; RNF43, ring finger protein 43; RTK, receptor tyrosine kinase.

(range, 16 to 437), with three patients having a PR and one a CR. Patients with *RNF43* alterations that were treated in triple treatment responded well to treatment and had a median treatment duration of 124 days (70–408). End-of-treatment biopsies were collected from six patients who had responded to study treatment. Interestingly, acquired mutations or amplifications of the *KRAS* gene were noted in four of these patients. *PTEN* loss was observed in one patient, and an *AKT1* mutation was seen in the remaining patient.

### Pharmacokinetics

Exposure of encorafenib increased with dose in the dual-combination group and had a half-life that ranged from 3 to 4 hours (Supplementary Table S2). Exposure was similar to levels observed in an unpublished monotherapy study ( $C_{max}$ :  $1427 \pm 824$  ng/mL,  $T_{max}$ : 2 (1–4) hours and  $AUC_{tau}$ :  $7172 \pm 2888$  h·ng/mL with 200 mg encorafenib at steady state in the current study). For the triple-combination therapy group, the exposure of 200 mg encorafenib in the presence of 100 mg alpelisib was similar to that in the dual-combination therapy group. However, the exposure of 200 mg encorafenib increased by about 2-fold in the presence of 300 mg alpelisib ( $C_{max}$ :  $2394 \pm 2077$  ng/mL,  $T_{max}$ : 3 (1–8) hours and  $AUC_{tau}$ :  $12,948 \pm 10,649$  h·ng/mL at steady state; Supplementary Table S2). Exposure of alpelisib increased with dose and was similar to levels observed in an unpublished monotherapy study

( $C_{max}$ : 2743 ± 520 ng/mL,  $T_{max}$ : 4 (2–6) hours and  $AUC_{tau}$ : 25,126 ± 3513 h·ng/mL with 300 mg alpelisib at steady state in the current study).

## Discussion

The primary objective of the phase 1b portion of this study was to establish a recommended dose for the dual- and triple-combination therapies for use in the phase 2 section of the study. The selected doses were 200 mg encorafenib daily plus cetuximab in the dual-combination therapy group and 200 mg encorafenib daily plus 300 mg alpelisib daily plus cetuximab in the triple-combination therapy group. Following an overall assessment of tolerability and observation of objective responses in all tested dose cohorts, it was decided not to proceed to the MTD in either the dual- or triple-combination therapy arms, and doses for the triple-combination therapy were selected on the basis of the overall tolerability profiles. The encorafenib dose was selected to be the same in both groups to allow for the assessment of safety and efficacy of additive alpelisib compared with encorafenib plus cetuximab dual-combination therapy.

Both the dual- and triple-combination treatments showed clinical efficacy and acceptable safety profiles in patients with *BRAF*-mutant mCRC. Efficacy and safety in the two groups may be compared only with caution: the ECOG PS suggests the health of patients in the dual-combination therapy group was poorer than that of patients in the triple-combination therapy group prior to the start of treatment and patients in the triple-combination therapy group also showed a better response to the last prior therapy than patients in the dual-combination therapy group. This phase 1b portion of the study was also not powered or designed for comparison purposes, and patient numbers are small.

Previous studies of single-agent *BRAF* or EGFR inhibitors have shown limited activity in patients with *BRAF*-mutant mCRC.<sup>10-12,26-30</sup> However, clinical studies of combinations of *BRAF* inhibitors with EGFR inhibitors or MEK inhibitors have shown improved efficacy in this patient population.<sup>14,15,31,32</sup> Results from our study compare favorably with combinations of *BRAF* and EGFR inhibitors in these studies. In our study ORRs of 23% in the dual- and 32% in the triple-combination therapy group were achieved. In a study of 55 patients treated with dabrafenib plus panitumumab vs dabrafenib + panitumumab + trametinib the dual combination of *BRAF* and EGFR inhibitor achieved an ORR of 10% and the triple combination of *BRAF*, EGFR and MEK inhibitors achieved an ORR of 26%.<sup>31</sup> In another study of 15 patients treated with vemurafenib plus panitumumab two (13%) achieved a PR.<sup>32</sup> Furthermore, a phase 2 study of vemurafenib in nonmelanoma cancers with *BRAF* V600 mutations that enrolled 27 patients with *BRAF*-mutant CRC showed an ORR of 4% when treated with vemurafenib + cetuximab.<sup>14</sup> Median PFS in our study (3.7 months in the dual- and 4.3 months in the triple-combination therapy arm) also compare well with results from these studies: 3.2 months (95% CI: 1.6–5.3 months) for vemurafenib + panitumumab<sup>32</sup> and 3.7 months (95% CI: 1.8–5.1) for vemurafenib + cetuximab.<sup>14</sup> It should be noted that these studies were small and further follow-up is required.

In our study, the safety profile was acceptable for both combination treatments. More dermatologic AEs were reported in the triple- than the dual-combination therapy group. It should be noted, however, that the incidence of dermatologic AEs was much lower than has been previously reported for single-agent use of *BRAF* inhibitors (67% of 18 patients had hand-foot skin reaction)<sup>33</sup> or EGFR inhibitors (82% of 116 patients had papulopustular rash),<sup>34</sup> consistent with an opposing effect of encorafenib and cetuximab on ERK signaling in skin. Paradoxical activation of ERK signaling in *BRAF* wild-type

tissues with encorafenib likely opposes cetuximab mediated inhibition of ERK signaling, decreasing skin toxicity with the combination. More cases of melanocytic nevi were seen in the triplet than in the doublet arm (25% versus 4%), possibly secondary to higher effective doses of encorafenib in the triplet arm as encorafenib exposure was increased 2-fold with the addition of 300 mg alpelisib. Hyperglycemia was more common in the triple- than the dual-combination therapy group due to the ability of PI3K inhibitors to regulate the insulin-like growth factor receptor. Compared with the incidence of hyperglycemia in patients with solid tumors treated with single-agent alpelisib (47% all grade; 24% grade 3/4),<sup>21</sup> the incidences reported for either therapy group in this trial were lower.

Alterations in genes associated with the key signaling pathways were assessed and correlated with clinical activity. Due in part to the limited availability of tumor biopsies in the phase 1 population of the study, no significant correlations could be determined, and further follow-up will be carried out in phase 2; however, some preliminary observations were noted. A subgroup of patients with *EGFR* amplifications or gain of copies, especially those patients who received dual-combination therapy, responded well to study treatment, and better than patients without *EGFR* alterations. In agreement with previous reported data<sup>38,39</sup>, these results suggest that the presence of *EGFR* alterations may identify tumors more dependent on EGFR signaling that are thus more sensitive to combined EGFR- and BRAF-targeted treatment, whereas in patients with no EGFR-mediated pathway activation, other signaling pathways may be activated and may need to be co-targeted with BRAF to lead to tumor regressions. Patients with WNT pathway alterations, especially those patients with *APC* mutations, had a tendency towards lower PFS rates. This trend was not clear for *RNF43* mutations, suggesting, in agreement with previous theories, that *RNF43* mutations do not activate the WNT pathway in the same manner as *APC* mutations.<sup>37</sup> It will be of interest to see whether trials of combination treatments targeting the WNT pathway (eg, NCT02278133) yield higher response rates.

As has been previously documented for *BRAF*-mutant mCRC, alterations in the PI3K pathway were noted in the limited patient samples.<sup>15</sup> Unfortunately, the majority of patients with *PIK3CA* mutations received the dual-combination treatment; however, these patients still responded and remained on treatment for prolonged periods of time, suggesting that such activating mutations may not be a primary source of resistance. Furthermore, some patients with *PTEN* loss responded well to both the triple- and dual-combination treatments. Due to the small sample size, however, it is impossible to draw significant correlations. Data from previous studies have reported conflicting information with either no association between response to cetuximab treatment and *PIK3CA* mutation/*PTEN* expression or a correlation with low response to cetuximab.<sup>28,38</sup>

Interestingly, the few samples collected during acquired resistance showed MAPK activation, where patients developed either *KRAS* mutations or amplifications. Similar results have been previously reported for other RAF/EGFR/MEK targeted treatments.<sup>39</sup>

No evidence of drug–drug interaction between encorafenib and cetuximab was observed in the dual-combination therapy group. In the triple-combination therapy group, a mild drug–drug interaction was observed with encorafenib (encorafenib exposure increased 2-fold) in the presence of high alpelisib dose levels, possibly due to alpelisib inhibiting the metabolic enzyme (CYP3A4) of encorafenib. Alpelisib exposure was not affected by encorafenib and cetuximab.

In conclusion, data from this phase 1b study show promising clinical activity and tolerability, warranting further evaluation.

## References

1. Torre LA, Bray F, Siegel RL, et al. Global cancer statistics, 2012. *CA: A Cancer Journal for Clinicians*. 2015;65(2):87-108.
2. Chappell WH, Steelman LS, Long JM, et al. Ras/Raf/MEK/ERK and PI3K/PTEN/Akt/mTOR inhibitors: rationale and importance to inhibiting these pathways in human health. *Oncotarget* 2011;2(3):135-64.
3. Davies H, Bignell GR, Cox C, et al. Mutations of the *BRAF* gene in human cancer. *Nature* 2002;417(6892):949-54.
4. Sorbye H, Dragomir A, Sundstrom M, et al. High *BRAF* Mutation Frequency and Marked Survival Differences in Subgroups According to *KRAS/BRAF* Mutation Status and Tumor Tissue Availability in a Prospective Population-Based Metastatic Colorectal Cancer Cohort. *PLoS One* 2015;10(6):e0131046.
5. Shen L, Toyota M, Kondo Y, et al. Integrated genetic and epigenetic analysis identifies three different subclasses of colon cancer. *Proc Natl Acad Sci U S A* 2007;104(47):18654-9.
6. Van Cutsem E, Kohne CH, Lang I, et al. Cetuximab plus irinotecan, fluorouracil, and leucovorin as first-line treatment for metastatic colorectal cancer: updated analysis of overall survival according to tumor *KRAS* and *BRAF* mutation status. *J Clin Oncol* 2011;29(15):2011-9.
7. Modest DP, Jung A, Moosmann N, et al. The influence of *KRAS* and *BRAF* mutations on the efficacy of cetuximab-based first-line therapy of metastatic colorectal cancer: an analysis of the AIO KRK-0104-trial. *Int J Cancer* 2012;131(4):980-6.
8. Zelboraf. Summary of Product Characteristics. [Internet].: F. Hoffmann-La Roche; 2012 [cited May 2015].
9. Tafinlar. Summary of Product Characteristics [Internet].: GlaxoSmithKline; 2013 [cited May 2015].
10. Corcoran RB, Ebi H, Turke AB, et al. EGFR-mediated re-activation of MAPK signaling contributes to insensitivity of *BRAF* mutant colorectal cancers to RAF inhibition with vemurafenib. *Cancer Discov* 2012;2(3):227-35.
11. Mao M, Tian F, Mariadason JM, et al. Resistance to *BRAF* inhibition in *BRAF*-mutant colon cancer can be overcome with PI3K inhibition or demethylating agents. *Clin Cancer Res* 2013;19(3):657-67.
12. Prahallad A, Sun C, Huang S, et al. Unresponsiveness of colon cancer to *BRAF*(V600E) inhibition through feedback activation of EGFR. *Nature* 2012;483(7387):100-3.
13. Kopetz S, Desai J, Chan E, et al. PLX4032 in metastatic colorectal cancer patients with mutant *BRAF* tumors. *J Clin Oncol* 2010;28(15s):3534.
14. Hyman DM, Puzanov I, Subbiah V, et al. Vemurafenib in Multiple Nonmelanoma Cancers with *BRAF* V600 Mutations. *N Engl J Med* 2015;373(8):726-36.
15. Corcoran RB, Atreya CE, Falchook GS, et al. Combined *BRAF* and MEK Inhibition With Dabrafenib and Trametinib in *BRAF* V600-Mutant Colorectal Cancer. *J Clin Oncol* 2015;33(34):4023-31.
16. Yang H, Higgins B, Kolinsky K, et al. Antitumor activity of *BRAF* inhibitor vemurafenib in preclinical models of *BRAF*-mutant colorectal cancer. *Cancer Res* 2012;72(3):779-89.
17. Caponigro G, Cao ZA, Zhang X, et al. Efficacy of the RAF/PI3Ka/anti-EGFR triple combination LGX818 + BYL719 + cetuximab in *BRAF*V600E colorectal tumor models. *Cancer Research* 2013;73(8 Supplement):2337.
18. Stuart DD, Li N, Poon DJ, et al. Preclinical profile of LGX818: A potent and selective RAF kinase inhibitor. *Cancer Res* 2012;72(8):Abstract 3790.

19. Fritsch C, Huang A, Chatenay-Rivauday C, et al. Characterization of the novel and specific PI3Kalpha inhibitor NVP-BYL719 and development of the patient stratification strategy for clinical trials. *Mol Cancer Ther* 2014;13(5):1117-29.
20. Dummer R, Robert C, Nyakas M, et al. Initial results from a Phase I, open-label, dose escalation study of the oral BRAF inhibitor LGX818 in patients with BRAF V600 mutant advanced or metastatic melanoma. *J Clin Oncol* 2013;31:9028.
21. Juric D, Burris H, Schuler M, et al. Phase I study of the PI3K $\alpha$  inhibitor BYL719, as a single agent in patients with advanced solid tumors (AST). *Annals of Oncology*. 2014 September 01;25(suppl 4):451PD.
22. Neuenschwander B, Branson M, Gsponer T. Critical aspects of the Bayesian approach to phase I cancer trials. *Stat Med* 2008;27(13):2420-39.
23. Neuenschwander B, Capkun-Niggli G, Branson M, Spiegelhalter DJ. Summarizing historical information on controls in clinical trials. *Clin Trials*. 2010;7(1):5-18.
24. Juric D, Rodon J, Gonzalez-Angulo AM, et al. BYL719, a next generation PI3K alpha specific inhibitor: Preliminary safety, PK, and efficacy results from the first-in-human study. *Cancer Research*. 2012 April 15;72(8 Supplement):CT-01.
25. De Buck SS, Jakab A, Boehm M, et al. Population pharmacokinetics and pharmacodynamics of BYL719, a phosphoinositide 3-kinase antagonist, in adult patients with advanced solid malignancies. *Br J Clin Pharmacol* 2014;78(3):543-55.
26. Pietrantonio F, Petrelli F, Coiu A, et al. Predictive role of BRAF mutations in patients with advanced colorectal cancer receiving cetuximab and panitumumab: a meta-analysis. *Eur J Cancer* 2015;51(5):587-94.
27. Rowland A, Dias MM, Wiese MD, et al. Meta-analysis of BRAF mutation as a predictive biomarker of benefit from anti-EGFR monoclonal antibody therapy for RAS wild-type metastatic colorectal cancer. *Br J Cancer* 2015;112(12):1888-94.
28. De Roock W, Claes B, Bernasconi D, et al. Effects of KRAS, BRAF, NRAS, and PIK3CA mutations on the efficacy of cetuximab plus chemotherapy in chemotherapy-refractory metastatic colorectal cancer: a retrospective consortium analysis. *Lancet Oncol* 2010;11(8):753-62.
29. Yuan ZX, Wang XY, Qin QY, et al. The prognostic role of BRAF mutation in metastatic colorectal cancer receiving anti-EGFR monoclonal antibodies: a meta-analysis. *PLoS One* 2013;8(6):e65995.
30. Seymour MT, Brown SR, Middleton G, et al. Panitumumab and irinotecan versus irinotecan alone for patients with KRAS wild-type, fluorouracil-resistant advanced colorectal cancer (PICCOLO): a prospectively stratified randomised trial. *Lancet Oncol* 2013;14(8):749-59.
31. Atreya CE, Van Cutsem E, Bendell JC, et al. Updated efficacy of the MEK inhibitor trametinib (T), BRAF inhibitor dabrafenib (D), and anti-EGFR antibody panitumumab (P) in patients (pts) with BRAF V600E mutated (BRAFM) metastatic colorectal cancer (mCRC). *J Clin Oncol* 2015;33 (suppl;abstr 103).
32. Yaeger R, Cercek A, O'Reilly EM, et al. Pilot trial of combined BRAF and EGFR inhibition in BRAF-mutant metastatic colorectal cancer patients. *Clin Cancer Res* 2015;21(6):1313-20.
33. Gomez-Roca CA, Delord J, Robert C, et al. Encorafenib (LGX818), an oral BRAF inhibitor, in patients (pts) with BRAF V600E metastatic colorectal cancer (MCR): Results of dose expansion in an open-label, Phase 1 study. *Ann Oncol* 2014;25(suppl 4):535P.

34. Jaka A, Gutierrez-Rivera A, Lopez-Pestana A, et al. Predictors of Tumor Response to Cetuximab and Panitumumab in 116 Patients and a Review of Approaches to Managing Skin Toxicity. *Actas Dermosifiliogr* 2015;106(6):483-92.
35. Moroni M, Veronese S, Benvenuti S, et al. Gene copy number for epidermal growth factor receptor (EGFR) and clinical response to antiEGFR treatment in colorectal cancer: a cohort study. *Lancet Oncol* 2005;6:279–286.
36. Sartore-Bianchi A, Moroni M, Veronese S, et al. Epidermal growth factor receptor gene copy number and clinical outcome of metastatic colorectal cancer treated with panitumumab. *J Clin Oncol* 2007;25:3238–3245.
37. Koo BK, Spit M, Jordens I, et al. Tumour suppressor RNF43 is a stem-cell E3 ligase that induces endocytosis of Wnt receptors. *Nature* 2012;488(7413):665-9.
38. Karapetis CS, Jonker D, Daneshmand M, et al. PIK3CA, BRAF, and PTEN status and benefit from cetuximab in the treatment of advanced colorectal cancer--results from NCIC CTG/AGITG CO.17. *Clin Cancer Res* 2014;20(3):744-53.
39. Ahronian LG, Sennott EM, Van Allen EM, et al. Clinical Acquired Resistance to RAF Inhibitor Combinations in BRAF-Mutant Colorectal Cancer through MAPK Pathway Alterations. *Cancer Discov* 2015;5(4):358-67.

## APPENDIX

**Table S1. Criteria for defining dose-limited toxicities**

Toxicity	Any of the following criteria
Blood and lymphatic disorders*	<ul style="list-style-type: none"> <li>• Febrile neutropenia (absolute neutrophil count <math>&lt;1.0 \times 10^9/L</math> with fever <math>\geq 38.5^\circ C</math>)<sup>†</sup></li> </ul>
Blood investigations	<ul style="list-style-type: none"> <li>• Grade 3 absolute neutrophil count for <math>&gt;7</math> consecutive days or grade 4 absolute neutrophil count</li> <li>• Grade 3 platelet count for <math>&gt;7</math> consecutive days and/or with signs of bleeding or grade 4 platelet count</li> </ul>
Skin and subcutaneous disorders	<ul style="list-style-type: none"> <li>• Grade 3 rash/photosensitivity/hand-foot skin reaction (HFSR) for <math>&gt;7</math> consecutive days despite skin toxicity treatment or grade 4 rash/photosensitivity/HFSR</li> </ul>
Metabolism and nutrition disorders <sup>‡</sup>	<ul style="list-style-type: none"> <li>• Grade 2 hyperglycemia that does not resolve to grade 0 within 14 consecutive days (after initiation of oral antidiabetic treatment)</li> <li>• Grade 3 hyperglycemia for <math>&gt;7</math> consecutive days despite oral antidiabetic treatment</li> <li>• Grade 4 hyperglycemia or hyperglycemia that leads to diabetic ketoacidosis, hospitalization for IV insulin infusion, or non-ketotic coma</li> </ul>
Gastrointestinal disorders	<ul style="list-style-type: none"> <li>• <math>\geq</math>grade 3 vomiting or nausea or diarrhea lasting more than 48 h despite optimal therapy</li> <li>• <math>\geq</math>grade 3 pancreatitis</li> </ul>
Renal investigations	<ul style="list-style-type: none"> <li>• <math>\geq</math>grade 3 serum creatinine</li> </ul>
Hepatic investigations <sup>§</sup>	<ul style="list-style-type: none"> <li>• <math>\geq</math>grade 3 blood bilirubin</li> <li>• AST or ALT <math>\geq 3 \times</math> ULN in conjunction with blood bilirubin <math>\geq 2 \times</math> ULN of any duration</li> <li>• Grade 3 AST or ALT for <math>&gt;7</math> consecutive days or grade 4 AST or ALT</li> <li>• Grade 4 serum alkaline phosphatase for <math>&gt;7</math> consecutive days</li> </ul>
Metabolic investigations	<ul style="list-style-type: none"> <li>• Grade 3 lipase and/or serum amylase for <math>&gt;7</math> consecutive days or grade 4 lipase and/or serum amylase</li> </ul>
Vascular disorders	<ul style="list-style-type: none"> <li>• <math>\geq</math>grade 3 persistent hypertension requiring more than one drug or more intensive therapy than previously</li> </ul>
Cardiac disorders	<ul style="list-style-type: none"> <li>• <math>\geq</math>grade 3</li> </ul>
Tumor lysis syndrome (TLS)	<ul style="list-style-type: none"> <li>• <math>\geq</math>grade 4 TLS (life-threatening)**</li> </ul>
General disorders	<ul style="list-style-type: none"> <li>• Grade 3 fatigue for <math>&gt;7</math> consecutive days</li> <li>• <math>\geq</math>grade 3 edema for <math>&gt;14</math> consecutive days</li> </ul>
Ophthalmologic disorders	<ul style="list-style-type: none"> <li>• Grade 3 retinopathy/uveitis for <math>&gt;21</math> days or grade 4 retinopathy/uveitis confirmed by ophthalmologic examination</li> <li>• Any grade retinal vein occlusion</li> <li>• Any other eye disorders of grade 3 for <math>&gt;14</math> days or grade 4</li> </ul>
Any other AE (excluding squamous cell carcinoma) <sup>††</sup>	<ul style="list-style-type: none"> <li>• <math>\geq</math>grade 3</li> </ul>

\* $\geq$ grade 3 anemia was not considered a DLT unless judged to be a hemolytic process secondary to study drug.  $\geq$ grade 3 lymphopenia was not considered a DLT unless clinically significant.

<sup>†</sup>Not according to CTCAEv4.0.

<sup>‡</sup>Hyperglycemia occurring during corticosteroids administration was only considered a DLT if not resolved within 2 days after the end of corticosteroid treatment.

<sup>§</sup>For any grade  $\geq 3$  hepatic toxicity that did not resolve within 7 days to  $\leq$ grade 1 (or  $\leq$ grade 2 if liver infiltration with tumor present), an abdominal CT scan was performed to assess if it was related to disease progression.

\*\*All patients diagnosed with TLS were discussed with the sponsor as soon as possible after the diagnosis.

††An AE was required to be clinically significant to be defined as a DLT: study drug-related fever, alkaline phosphatase elevation, electrolyte abnormalities (including K, NA, Cl, HCO<sub>3</sub>, Mg, Ca, PO<sub>4</sub>) were not considered a DLT unless clinically significant. Squamous cell carcinoma has been reported as an on-target side effect of BRAF inhibitors that is manageable and will not be considered a DLT. Cetuximab-induced infusion reactions will not be considered a DLT.

Abbreviations: AE, adverse event; ALT, alanine aminotransferase; AST, aspartate aminotransferase; CT, computed tomography; DLT, dose-limiting toxicity; ULN, upper limit of normal.

**Table S2. Pharmacokinetic parameters of encorafenib and alpelisib at steady state (cycle 2 day 1).**

Treatment	C <sub>max</sub> (ng/mL)*	T <sub>max</sub> (h) <sup>†</sup>	AUC <sub>tau</sub> (h·ng/mL)*
<b>Encorafenib PK in the dual-combination therapy group:</b>			
100 mg encorafenib (n = 2; 2; 2) <sup>‡</sup>	1507 ± 768	2 (1–2)	7662 ± 2611
200 mg encorafenib (n = 6; 6; 6)	1427 ± 824	2 (1–4)	7172 ± 2888
400 mg encorafenib (n = 8; 8; 7)	3803 ± 1314	2 (1–4)	15300 ± 5640
450 mg encorafenib (n = 6; 6; 5)	5153 ± 2564	2 (1–2)	16946 ± 5757
<b>Encorafenib PK in the triple-combination therapy group:</b>			
200 mg encorafenib + 100 mg alpelisib (n = 3; 3; 3)	1552 ± 534	2 (1–2)	6308 ± 1190
200 mg encorafenib + 200 mg alpelisib (n = 7; 7; 6)	2427 ± 2143	2 (1–6)	11079 ± 3822
200 mg encorafenib + 300 mg alpelisib (n = 8; 8; 7)	2394 ± 2077	3 (1–8)	12948 ± 10649
300 mg encorafenib + 200 mg alpelisib (n = 3; 3; 1)	1595 ± 876	2 (2–4)	5998
<b>Alpelisib PK in the triple-combination therapy group:</b>			
100 mg alpelisib + 200 mg encorafenib (n = 3; 3; 2)	680 ± 93	2 (1–4)	5458 ± 236
200 mg alpelisib + 200 mg encorafenib (n = 7; 7; 4)	2057 ± 717	4 (1–6)	19673 ± 2361
300 mg alpelisib + 200 mg encorafenib (n = 8; 8; 7)	2743 ± 520	4 (2–6)	25126 ± 3513
200 mg alpelisib + 300 mg encorafenib (n = 4; 4; 2)	1562 ± 816	4 (4–8)	11179 ± 3830

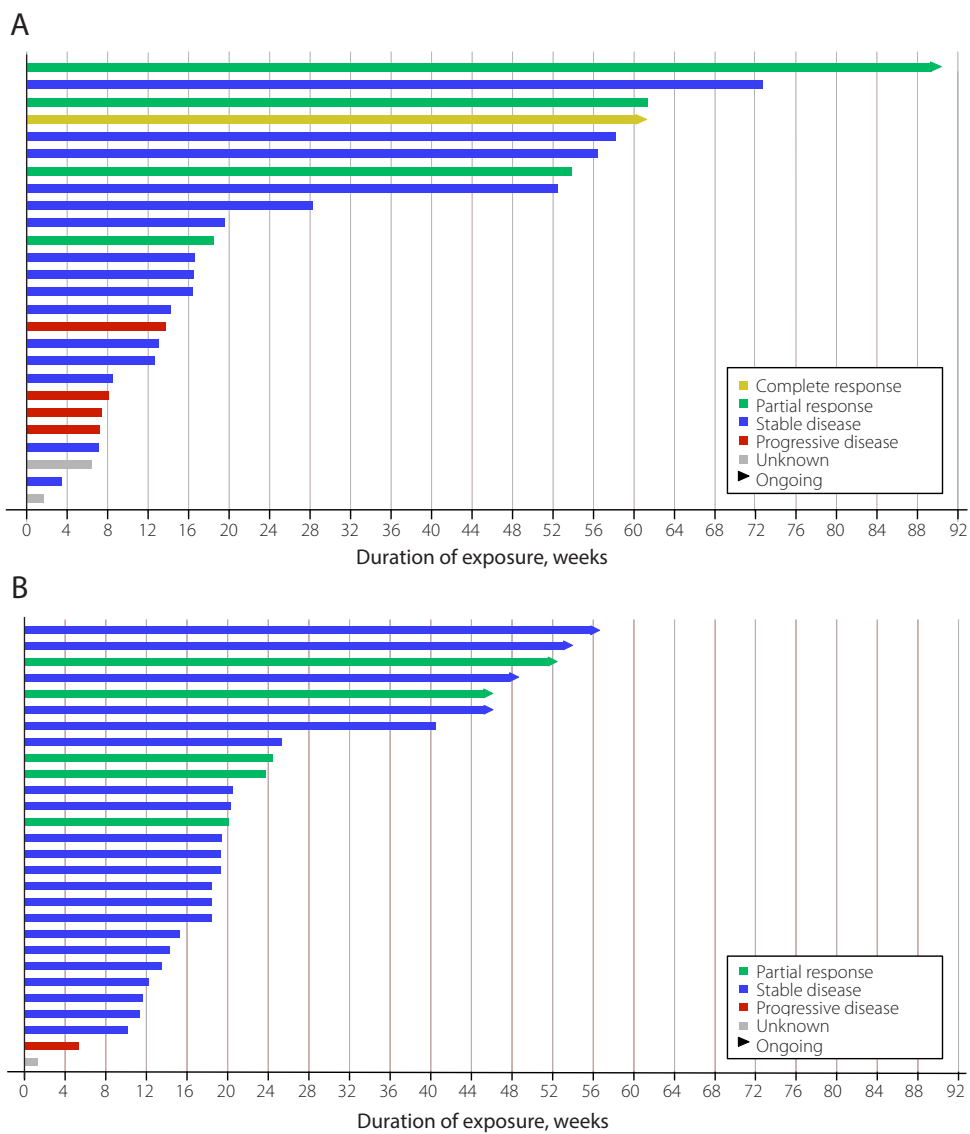
\*Arithmetic mean ± standard deviation.

<sup>†</sup>Median (minimum – maximum) value.

<sup>‡</sup>Number of patients for C<sub>max</sub>, T<sub>max</sub>, AUC<sub>tau</sub>, respectively. Some patients only had C<sub>max</sub> and T<sub>max</sub>, and AUC<sub>tau</sub> could not be calculated (Phoenix PK software; version 6.2; Pharsight, St. Louis, MO) due to a lack of sufficient PK data.

Abbreviations: AUC<sub>tau</sub>, area under the plasma concentration time curve for a dosing interval; C<sub>max</sub>, maximum serum concentration; PK, pharmacokinetics; T<sub>max</sub>, time of maximum serum concentration.





5.1

Figure S1. Time on study by response.

For patients treated with the dual-combination therapy of encorafenib and cetuximab (A) and patients treated with the triple-combination therapy of encorafenib, alpelisib, and cetuximab (B).



# Chapter 5

## Clinical pharmacology of combined targeted therapy targeting mutated *BRAF*



### 5.2

#### Randomized phase II study comparing encorafenib plus cetuximab versus encorafenib with cetuximab plus alpelisib in patients with advanced *BRAF* mutant colorectal cancer

##### Interim analysis

Robin M.J.M. van Geel, Josep Tabernero, Tormod K. Guren, Rona Yaeger, Anna Spreafico, Jason Faris, Takayuki Yoshino, Yasuhide Yamada, Tae Won Kim, Johanna C. Bendell, Martin Schuler, Heinz-Josef Lenz, Ferry A.L.M. Eskens, Jayesh Desai, Howard S. Hochster, Emin Avsar, Tim Demuth, Victor Sandor, Elena Elez, René Bernards, Jan H.M. Schellens

## ABSTRACT

### Background

Patients with advanced *BRAF* mutant (*BRAF*<sub>m</sub>) colorectal cancer (CRC) who progress following first-line treatment have a poor prognosis, with overall survival of 5-6 months. In contrast to *BRAF*<sub>m</sub> melanoma, *BRAF* inhibitor monotherapy has shown limited clinical activity in *BRAF*<sub>m</sub> CRC, presumably due to feedback activation of epidermal growth factor receptor (EGFR) signaling. Combined inhibition of *BRAF* and EGFR resulted in strong synergistic activity with complete inhibition of tumor growth in vitro and in vivo. Addition of an  $\alpha$ -specific PI3K inhibitor further strengthened this synergy. We developed a clinical study to investigate the efficacy and safety of the *BRAF* inhibitor encorafenib combined with anti-EGFR antibody cetuximab, with or without PI3K $\alpha$  inhibitor alpelisib in patients with advanced *BRAF*<sub>m</sub> CRC.

### Methods

In this open-label, randomized phase II study we randomly assigned 102 patients with advanced *BRAF*<sub>m</sub> CRC who failed at least one prior therapy to receive dual or triple combination therapy. Progression-free survival was the primary endpoint. Secondary endpoints included overall response rate (ORR), disease control rate (DCR) and overall survival (OS). Patients were treated with the recommended phase II doses as established in a previous phase I study.

### Results

Out of the 102 patients, 52 were randomized to receive the triple combination and 50 to receive the dual combination. In both groups, patients had received a median of two prior therapies. A planned progression-free survival analysis comparing the triple to the dual combination after 77 events showed a hazard ratio (HR; 95% confidence interval [CI]) of 0.8 (0.5–1.2;  $P = 0.14$ ), with median progression-free survival (95% CI) of 5.4 (4.1–7.2) and 4.2 (3.4–5.4) months, respectively. Confirmed ORR (95% CI) and DCR (95% CI) were 27% (16%–41%) and 85% (71%–93%), respectively, with the triple and 22% (12%–36%) and 84% (71%–93%), respectively, with the dual combination therapy. Grade 3/4 adverse events, regardless of causality, occurred in 79% (triple) and 58% (dual) of patients, and consisted mainly of anemia (17% vs 6%), hyperglycemia (13% vs 2%), and increased lipase (8% vs 18%) for the triple and dual arm, respectively.

### Conclusions

Combined targeted therapy with encorafenib and cetuximab with or without alpelisib was safe and tolerable. Relative to historical data, combined targeted therapy with encorafenib and cetuximab with or without alpelisib showed promising clinical activity in difficult-to-treat patients with *BRAF*<sub>m</sub> CRC.

## Introduction

Colorectal cancer (CRC) is among the most commonly diagnosed cancers worldwide and the second leading cause of cancer death in the United States and in Europe.<sup>1,2</sup> Early detection and the development of new treatments resulted in a steady decrease in CRC mortality over the past two decades. For metastatic CRC, the addition of irinotecan, oxaliplatin, bevacizumab, cetuximab and panitumumab to standard treatment with 5-fluorouracil (5-FU)/leucovorin caused a significant improvement in overall survival.<sup>3–9</sup> However, patients with metastatic *BRAF* mutated (*BRAF*m) CRC form a molecularly distinct subpopulation<sup>10</sup> and have a particularly poor response to standard treatment options. A recent study reported median progression-free survival (PFS) times of 1.8–2.5 months versus 5.5–6.9 months in *BRAF* mutant and wild type patients, respectively, upon treatment with FOLFIRI (leucovorin, 5-fluorouracil, irinotecan) or FOLFIRI plus panitumumab, respectively<sup>11</sup>. Moreover, median survival of patients with advanced *BRAF*m CRC only 9 to 14 months in the first-line setting,<sup>12–21</sup> and less than 6 months after progressing upon first-line therapy.<sup>22–24</sup>

Mutations in the *BRAF* oncogene are present in approximately 10% of patients with CRC, of which 80–90% concerns a T1799A transversion mutation in exon 15, resulting in a valine-to-glutamic acid (V600E) amino acid substitution.<sup>25,26</sup> These mutations mimic regulatory phosphorylation of the BRAF protein, causing a 10-fold increased BRAF activity and a hyperactivated mitogen activated protein kinase (MAPK) pathway.<sup>27</sup> Consequently, *BRAF* mutations have emerged as a predictive marker of resistance against upstream inhibition of the epidermal growth factor receptor (EGFR), using the anti-EGFR directed monoclonal antibodies cetuximab and panitumumab. Although several studies reported conflicting results, conferral of resistance would not be surprising as *BRAF* mutations activate the same signalling pathway as *RAS* mutations do, which are commonly known for their detrimental effect on anti-EGFR therapy.<sup>9,14,16,22,23</sup> Taken together, the poor prognosis and limited activity of currently available treatment regimens highlight the unmet medical need for novel treatment options for patients with advanced *BRAF*m CRC.

The development of selective BRAF inhibitors such as vemurafenib and dabrafenib have revolutionized the treatment of patients with *BRAF*m melanoma, providing substantially improved response rates, progression-free survival and overall survival as compared to standard chemotherapy.<sup>28,29</sup> However, in advanced *BRAF*m CRC, treatment with BRAF inhibitors has shown limited efficacy.<sup>30</sup> Preclinical work demonstrated the presence of a negative feedback activation loop that activates EGFR and thereby reactivates the MAPK- and phosphoinositide 3-kinase (PI3K) signaling pathways upon BRAF inhibition in *BRAF*m CRC cells, explaining their resistance against single-agent BRAF inhibitor.<sup>31,32</sup> These data provided a strong rationale to investigate combination regimens consisting of a BRAF inhibitor, an anti-EGFR antibody and a PI3K inhibitor in patients with *BRAF*m CRC.

In a previous phase I study, we investigated the safety, efficacy and recommended phase II doses of a dual combination consisting of encorafenib plus cetuximab and a triple combination consisting of encorafenib, cetuximab and alpelisib in patients with advanced *BRAF*m CRC.<sup>33</sup> Encorafenib is a potent and highly selective ATP-competitive small molecule BRAF inhibitor, and alpelisib is a class I  $\alpha$ -specific PI3K inhibitor.<sup>34,35</sup> In this phase 2 trial we investigated the safety and efficacy of encorafenib plus cetuximab with or without alpelisib in patients with advanced *BRAF*m CRC who failed at least one prior line of standard treatment. Herein we describe the results of a planned interim analysis after 73 events.

## Patients and methods

### *Patients*

We performed this randomized phase 2 study in 14 sites across nine countries. Patients were 18 years of age or older with histologically-confirmed diagnosis of metastatic CRC. Additional eligibility criteria included: documented *BRAF* V600 mutated and *KRAS* wild type disease, progressive disease after at least one prior standard of care treatment regimen or intolerance to irinotecan-based regimens, Eastern Cooperative Oncology Group performance status (ECOG PS) of 2 or better, evidence of measurable disease according to RECIST v1.1 criteria, and life expectancy of more than three months. Key exclusion criteria included symptomatic or untreated leptomeningeal disease, symptomatic brain metastasis, clinically manifested diabetes, acute or chronic pancreatitis, clinically significant cardiac disease, and previous treatment with EGFR inhibitors, RAF-inhibitors, PI3K inhibitors or MEK inhibitors. All patients gave written informed consent in accordance with Declaration of Helsinki recommendations.

### *Study design and assessments*

The primary objective was to directly compare the progression-free survival of encorafenib plus cetuximab and encorafenib plus cetuximab with alpelisib in patients with advanced *BRAF*<sup>m</sup> CRC. Secondary objectives included characterization of the safety and tolerability of both combinations and to assessing additional anti-tumor activity endpoints. Eligible patients were randomly assigned, in a 1:1 ratio, to receive encorafenib plus cetuximab or encorafenib plus cetuximab with alpelisib. The study protocol (ClinicalTrials.gov identifier: NCT01719380) received approval from the institutional review boards of each participating site and complied with local country regulations. Encorafenib, cetuximab and alpelisib were provided by the study sponsor (Novartis Pharmaceuticals Corporation, East Hanover, NJ, USA).

During patient screening, demographic data including medical history, ECOG performance status and concomitant medication were collected. Prior to study treatment initiation patients underwent a physical examination, laboratory investigations, ECG, dermatologic evaluation and radiographic tumor measurements. On study safety assessments, including physical examination, vital signs and laboratory investigations, were performed at least weekly during the first month and biweekly subsequently. ECGs were performed biweekly the first treatment cycle and every 4 weeks thereafter. Dermatologic evaluation was performed every 8 weeks and tumor response was evaluated locally according to RECIST v1.1 criteria every 6 weeks, and confirmed centrally by independent radiologists. Tumor biopsies were taken at baseline, and when feasible during treatment and upon progression to investigate pharmacodynamic parameters and comprehensive genomic analysis.

### *Study treatment*

Patients received the recommended phase II dose of the dual or triple combination as determined in the previous phase I study. The dual combination consisted of oral encorafenib 200 mg once daily and intravenously administered cetuximab according to the label for patients with mCRC: a loading dose of 400 mg/m<sup>2</sup> on the first day, followed by 250 mg/m<sup>2</sup> weekly. The triple combination comprised dual combination doses of encorafenib and cetuximab plus alpelisib orally at 300 mg once daily. Study treatment was administered in 28-day cycles and continued until disease progression, unacceptable toxicity, withdrawal of consent or the treatment was discontinued at the investigator's discretion. A

maximum of two dose reductions per investigational agent (encorafenib, alpelisib) were allowed for patients experiencing toxicity, according to the dose-levels investigated in the previous phase I study.

### **Outcomes**

The primary endpoint was progression-free survival. Secondary endpoints included assessments of safety and tolerability of both combinations, overall response rate and overall survival. Progression-free survival was defined as the time from start of treatment to the date of first documentation of disease progression based on RECIST v1.1 criteria, or death due to any cause. We defined overall survival as the time from start of treatment to date of death due to any cause. Patients who did not have an event at data cut-off and patients who were lost to follow-up were censored at the date of last adequate tumor assessment or at the date they were last known to be alive for progression-free survival and overall survival analysis, respectively. Overall response rate was defined as the proportion of patients with a best overall response of complete or partial response. Safety and tolerability was assessed by physical examination and clinical and laboratory investigations. Adverse events were classified using the Common Terminology Criteria of Adverse Events (version 4.0).

### **Statistical analysis**

Based on the phase I results with encorafenib plus cetuximab, we estimated the median progression-free survival of this combination to be 4 months. To claim clinically significant superiority for the triple combination compared to the dual combination, we arbitrarily chose a target median progression-free survival of 6 months. Assuming that progression-free survival functions of both groups are the same, the log of estimated hazard ratio is approximately normally distributed with mean 0 and variance of  $4/n$ , where  $n$  is the number of progression-free survival events. Based on these assumptions, at least 66 progression-free survival events are necessary to detect a median progression-free survival difference of two months with a 5% type I error rate (one-sided test).<sup>36</sup> In this planned interim progression-free survival analysis we describe the results after 73 events. A log-rank test was used to test the null hypothesis that progression-free survival distributions of the two treatment groups are equal. To determine statistical significance, a one-sided 5% level was used.

Efficacy analyses were based on all patients who were randomly allocated (*i.e.* the intention-to-treat population). Progression-free survival and overall survival were analysed using the Kaplan-Meier method and the Mantel-Haenszel stratified log-rank test. Hazard ratios and accompanying 95% confidence intervals between treatments groups were estimated with aCox proportional hazard model. Overall response rates and 95% confidence intervals were calculated using the Clopper and Pearson method.<sup>37</sup> All statistic analyses were performed in SPSS Statistics version 22.0.

## **Results**

### ***Patient disposition and characteristics***

We recruited patients between April 4, 2014, and April 15, 2015. A total of 102 patients were evaluable for safety and efficacy evaluations in either the dual ( $n = 50$ ) or triple ( $n = 52$ ) arm. Baseline patient characteristics were generally similar across both treatment groups, with the exception that the percentage of females was slightly higher in the dual treatment arm (Table 1). Patients in both arms previously received a median of 2 (range 1 to 6) standard chemotherapy regimens. Primary reason

<b>Table 1. Patient and disease characteristics at baseline</b>		
	<b>Dual combination n = 50</b>	<b>Triple combination n = 52</b>
<b>Sex, n (%)</b>		
Female	36 (72%)	27 (52%)
Male	14 (28%)	25 (48%)
<b>Age, median (range), years</b>	60 (20–79)	60 (29–76)
<b>Primary site of cancer derived, n (%)</b>		
Colon	46 (92%)	44 (85%)
Rectum	4 (8%)	8 (15%)
<b>ECOG PS, n (%)</b>		
0	21 (42%)	20 (38%)
1	28 (56%)	29 (56%)
2	1 (2%)	3 (6%)
<b>Lactate dehydrogenase levels at baseline, n (%)</b>		
Normal	26 (52%)	25 (48%)
> ULN	15 (30%)	15 (29%)
Unknown	9 (18%)	12 (23%)
<b>Number of prior treatment regimens, n (%)</b>		
1	21 (42%)	23 (44%)
2	20 (40%)	18 (35%)
3	5 (10%)	9 (17%)
≥ 4	4 (8%)	2 (4%)

Abbreviations: ECOG PS, Eastern Cooperative Oncology Group performance status; ULN, upper limit of normal.

for end of treatment was disease progression (56%), not specified (8%), adverse event (8%), physician decision (8%), death (6%), withdrawal of consent (4%), and new therapy for study indication (2%) for patients in the dual treatment arm, and disease progression (56%), not specified (8%), adverse event (6%), death (6%), physician decision (4%), and withdrawal of consent (4%) for patients in the triple treatment arm. At data cut-off, treatment was ongoing in five patients (10%) in the triple combination arm and four patients (8%) in the doublet regimen arm.

### **Anti-tumor activity**

At the time of data cut off, 77 progression-free survival events had occurred. A planned progression-free survival analysis comparing the triple to the dual combination treatment after 77 events found a hazard ratio (HR) of 0.8 (95% CI, 0.5–1.2;  $P = 0.14$ ). Median progression-free survival was 4.2 (95% confidence interval [CI], 3.4–5.4) months for the dual combination group and 5.4 (95% CI, 4.1–7.2) months (Figure 1). Median durations of response were 4.6 (95% CI, 2.0–6.7) and 9.9 (95% CI, 2.8–11.0) months for the dual and triple regimens, respectively. A confirmed objective response was achieved in 11 patients (22%) allocated to encorafenib plus cetuximab compared with 14 patients (27%) who received encorafenib plus cetuximab and alpelisib. Response evaluation by number of prior treatment regimens revealed that confirmed responses were observed in all subgroups, even among patients who were extensively pretreated (Table 2). After 44 events, interim overall survival analysis revealed an HR for the triple versus the dual combination of 1.1 (95% CI, 0.6–2.0). Median overall survival was 13.1 months with the triple combination and 12.4 months with the dual regimen (Figure 2).



**Table 2. Confirmed response rates, by number of prior treatment regimens**

	1 prior treatment regimen n = 21		2 prior treatment regimens n = 20		≥3 prior treatment regimens n = 11		All n = 52	
	Dual	Triple	Dual	Triple	Dual	Triple	Dual	Triple
<b>Best overall response, n (%)</b>								
Complete response	0	0	0	0	0	0	0	0
Partial response	6 (29%)	7 (30%)	4 (20%)	4 (22%)	1 (11%)	3 (27%)	11 (22%)	14 (27%)
Stable disease	12 (57%)	12 (52%)	14 (70%)	11 (61%)	5 (56%)	7 (64%)	31 (62%)	30 (58%)
Progressive disease	3 (14%)	2 (9%)	1 (5%)	3 (17%)	0	0	4 (8%)	5 (10%)
Unknown	0	2 (9%)	1 (5%)	0	3 (33%)	1 (9%)	4 (8%)	3 (6%)
<b>Overall response rate*</b>								
Patients with response, n	6	7	4	4	1	3	11	14
Percentage (95% CI)†	29 (11–52)	30 (13–53)	20 (6–44)	22 (6–48)	11 (0.3–48)	27 (6–61)	22 (12–36)	27 (16–41)
<b>Disease control rate‡</b>								
Patients with PR or SD, n	18	19	18	15	6	10	42	44
Percentage (95% CI)†	86 (64–97)	83 (61–95)	90 (68–99)	83 (59–96)	67 (30–93)	91 (59–100)	84 (71–93)	85 (72–93)
<b>Median (95% CI)‡ DOR, months</b>								
							4.6 (2.0–6.7)	9.9 (2.8–11.0)

Abbreviations: 95% CI, 95% confidence interval; PR, partial response; SD, stable disease.

\* Complete response plus partial response.

† The 95% CI for the frequency distribution of each variable was computed using the Clopper-Pearson method.

‡ Complete response plus partial response plus stable disease.

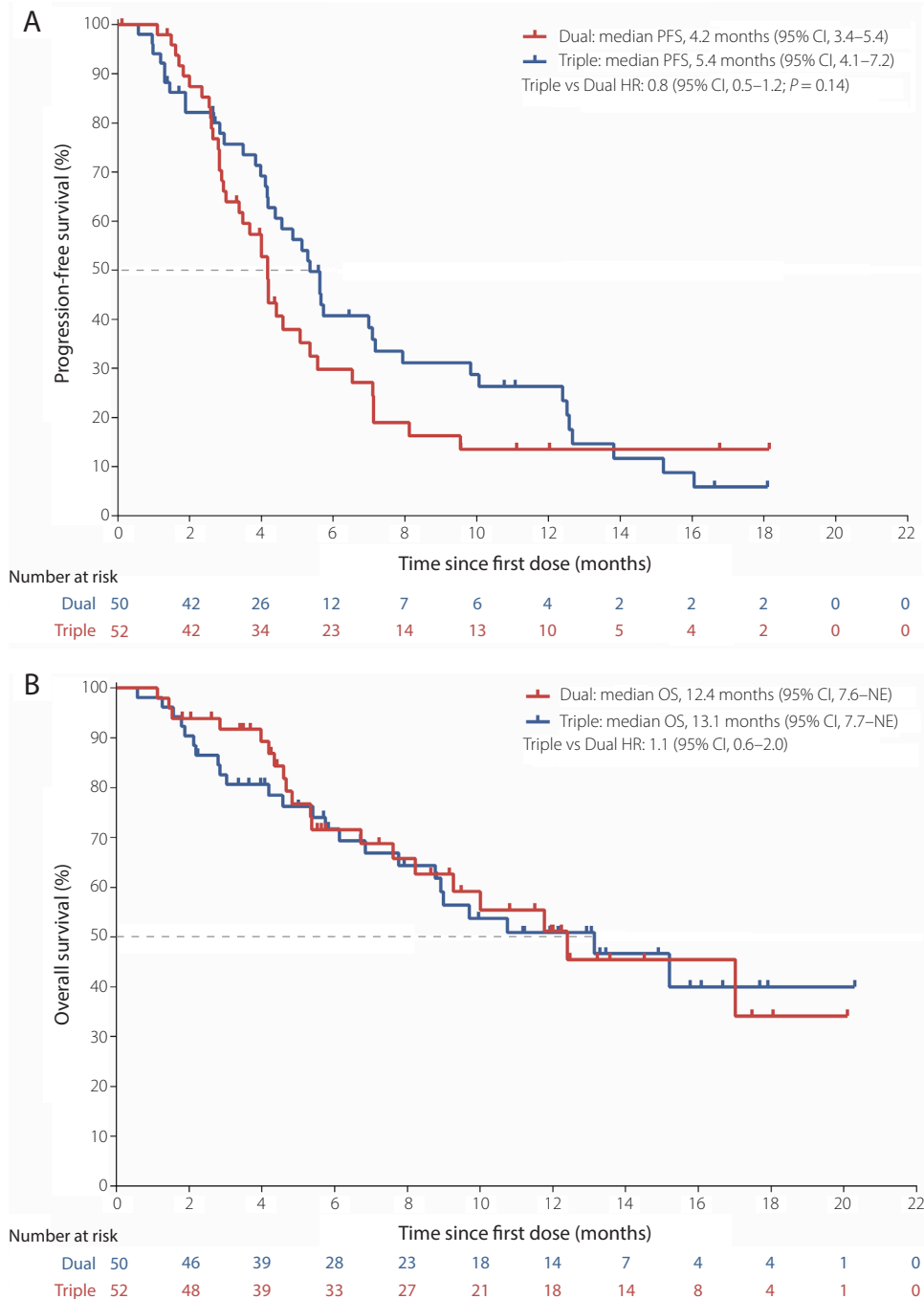


**Figure 1. Kaplan-Meier estimates of progression-free survival (A) and overall survival (B), by treatment arm**  
 Abbreviations: PFS, progression-free survival; CI, confidence interval; HR, hazard ratio; OS, overall survival; NE, not evaluable.  
 Censored patients are indicated by thick marks.

### Safety

The majority of patients experienced at least one adverse event that was at least suspected to be treatment-related; 49 (98%) patients in the dual therapy arm and 51 (98%) in the triple arm. The most common adverse events regardless of causality were fatigue (50%), nausea (46%), abdominal pain (42%), and arthralgia (34%) with the dual combination and diarrhea (54%), nausea (54%), vomiting (50%), and fatigue (46%). Grade 3/4 adverse events (AEs) were reported in 58% of patients who received the dual combination and in 79% of patients who received the triple combination treatment. Grade 3/4 AEs in >10% of patients in either arm (dual versus triple) were anemia (6% vs 17%), hyperglycemia (2% vs 13%), and increased lipase (18% vs 8%). Skin rash or dermatitis acneiform, was reported in 17 (34%) and 29 (56%) patients in the dual and triple combination group, respectively. Three patients in the triple combination group developed malignant melanoma (Table 3).

**Table 3. All-cause adverse events, occurring in > 20% of patients in either treatment group and grade 3/4 adverse events occurring in > 5% of patients in either treatment group**

Adverse event, <i>n</i> (%)	Dual combination ( <i>n</i> = 50)		Triple combination ( <i>n</i> = 52)	
	All grades	Grade 3/4	All grades	Grade 3/4
<b>Total</b>	<b>49 (98%)</b>	<b>29 (58%)</b>	<b>51 (98%)</b>	<b>41 (79%)</b>
Diarrhea	14 (28%)	1 (2%)	28 (54%)	4 (8%)
Nausea	23 (46%)	0 -	28 (54%)	3 (6%)
Vomiting	16 (32%)	0 -	26 (50%)	1 (2%)
Fatigue	25 (50%)	2 (4%)	24 (46%)	4 (8%)
Abdominal pain	2 (4%)	4 (8%)	20 (38%)	4 (8%)
Decreased appetite	17 (34%)	1 (2%)	19 (37%)	3 (6%)
Weight decreased	7 (14%)	0 -	19 (37%)	2 (4%)
Hyperglycaemia	5 (10%)	1 (2%)	19 (37%)	7 (13%)
Rash	8 (16%)	0 -	17 (33%)	0 -
Stomatitis	5 (10%)	0 -	16 (31%)	2 (4%)
Dry skin	8 (16%)	0 -	15 (29%)	0 -
Arthralgia	17 (34%)	0 -	14 (27%)	1 (2%)
Headache	16 (32%)	0 -	13 (25%)	0 -
Pyrexia	13 (26%)	0 -	12 (23%)	0 -
Dermatitis acneiform	9 (18%)	0 -	12 (23%)	0 -
Anemia	8 (16%)	3 (6%)	12 (23%)	9 (17%)
Pruritis	8 (16%)	0 -	11 (21%)	0 -
Hypomagnesemia	4 (8%)	0 -	11 (21%)	1 (2%)
Back pain	12 (24%)	1 (2%)	9 (17%)	1 (2%)
Asthenia	0 -	0 -	8 (15%)	3 (6%)
Lipase increased	14 (28%)	9 (18%)	7 (13%)	4 (8%)
Hypophosphatemia	3 (6%)	1 (2%)	7 (13%)	5 (10%)
Constipation	13 (26%)	2 (4%)	6 (12%)	0 -
Malignant melanoma	0 -	0 -	3 (6%)	3 (6%)

## Discussion

In this study, we showed that encorafenib plus cetuximab with or without alpelisib has promising clinical activity in the difficult-to-treat patient population with *BRAF*m CRC. Previous studies with single-agent BRAF inhibitors or anti-EGFR-directed agents have demonstrated unresponsiveness in patients with *BRAF*m CRC.<sup>22–24,38</sup> Upon elucidation of the underlying mechanism of this unresponsiveness, *i.e.* EGFR-mediated reactivation of downstream signaling pathways,<sup>31,32</sup> several clinical studies demonstrated efficacy with combinations of BRAF inhibitors and EGFR inhibitors.<sup>39–41</sup> Atreya et al. reported response rates of 10% and 26% with dabrafenib plus panitumumab, and dabrafenib plus panitumumab plus trametinib, respectively.<sup>41</sup> In a study of 15 patients treated with vemurafenib plus panitumumab, 13% achieved a partial response,<sup>40</sup> and in a phase II study with vemurafenib plus cetuximab, a response rate of 4% was seen.<sup>39</sup> As we achieved response rates of 22% and 27% with the dual and triple combination, respectively, our efficacy results compare favorably with other BRAF inhibitor plus EGFR inhibitor combinations. Furthermore, Peeters and colleagues previously reported median progression-free survival times of 1.8 and 2.5 months, and median overall survival times of 4.7 and 5.7 months upon second-line treatment with FOLFIRI and FOLFIRI plus panitumumab, respectively, in patients with *BRAF*m.<sup>11</sup> In other studies, overall survival medians ranged between 4.1 and 6.0 months with chemotherapy-based regimens plus cetuximab as second-line treatment in patients with advanced *BRAF*m CRC.<sup>23,42–44</sup> As we achieved median progression-free survival times of 4.2 and 5.4 months, and median overall survival times of 12.4 and 13.1 months with encorafenib plus cetuximab and encorafenib plus cetuximab plus alpelisib, respectively, progression-free and overall survival were approximately doubled with both combination regimens relative to historical data on standard chemotherapy-based regimens.

Despite the fact that overall response rate, median progression-free survival and overall survival were better with the triplet regimen compared to the doublet regimen, the primary endpoint, *i.e.* the hazard ratio for the risk of progression or death, was not statistically significant in this interim analysis. Results of our previous phase I study suggested a mild drug-drug interaction between encorafenib and alpelisib, resulting in a 2-fold increased encorafenib exposure upon concurrent administration of 300 mg alpelisib (not published). Although anti-tumor activity of the dual combination did seem to increase with higher encorafenib doses in the phase I study, a clinically relevant effect of higher encorafenib exposure on the efficacy of the triplet regimen cannot be ruled out. Therefore, it remains uncertain if the trend towards additional PFS benefit with the addition of alpelisib can be attributed to its intrinsic effect on the PI3K pathway or its effect on encorafenib exposure. The ongoing pharmacokinetic analysis may help answering this question. In addition, genetic analysis should be performed to explore potential predictive markers for anti-tumor activity in general and for efficacy with the triple regimen in particular, as molecular differences between both treatment groups may influence patient outcome as well. *PIK3CA* mutational status will be of special interest in that respect. Although the phase I study reported activity in patients with concurrent *BRAF* and *PIK3CA* mutations in the dual combination arm as well, activation of the PI3K pathway may hamper anti-tumor activity and efficacy duration of the encorafenib plus cetuximab combination.

The majority of common adverse events observed with the dual and triple combinations were of grade 1 or 2, and the safety profile was acceptable for both combinations. A number of adverse events were reported more frequently in the triple than the dual combination therapy group, including

diarrhea (62% vs 30%), hyperglycemia (50% vs 12%), weight decreased (41% vs 14%), pruritis (40% vs 22%), and skin rash (33% vs 16%). PI3K inhibitors are known for their effects on glucose homeostasis due to inhibiting the PI3K pathway-dependent activation and regulation of glycolytic enzymes and glucose transporters.<sup>45</sup> Compared with the incidence of hyperglycemia reported with single-agent alpelisib (47% all grades; 24% grade 3/4), the incidence seen in this study was lower (37% all grades; 13% grade 3/4). In addition, although more dermatologic adverse events were observed with the triple combination, the incidence of dermatologic adverse events with the dual and triple combination was much lower compared to previous reports on single-agent encorafenib (67% palmar-plantar erythrodysesthesia)<sup>46</sup> or cetuximab (82% papulopustular rash).<sup>47</sup> One plausible hypothesis to explain this apparent protective effect that *BRAF* inhibitors and anti-EGFR-directed agents have on each other's dermatologic toxicity, involves the paradoxical activation of the MAPK pathway by *BRAF* inhibitors in normal, *BRAF* wild type cells.<sup>48</sup> Whereas anti-EGFR antibodies cause cutaneous adverse events by inhibiting MAPK signaling in both tumor and normal cells, skin-related toxicity with selective *BRAF* inhibitors emerges from paradoxical MAPK pathway activation in normal skin cells, thereby counteracting the effects of EGFR inhibition.

In conclusion, our findings support further investigation of encorafenib plus cetuximab with or without alpelisib in patients with *BRAF* mutant CRC. Ongoing genetic, pharmacokinetic and pharmacodynamic analyses may obtain valuable information for further interpretation of efficacy and safety data. Results of these analyses may also shed light on which patients are most likely to benefit from combination therapy with encorafenib and cetuximab and which patients may benefit from the addition of alpelisib. A planned pivotal phase III study will evaluate encorafenib plus cetuximab versus standard second-line treatment in patients with advanced *BRAF* mutant, *RAS* wild type CRC, whose disease has progressed after 1 prior standard of care treatment regimen.

## References

1. DeSantis CE, Lin CC, Mariotto AB, et al. Cancer treatment and survivorship statistics, 2014. *CA Cancer J Clin* 2014.
2. Ferlay J, Steliarova-foucher E, Lortet-tieulent J, Rosso S. Cancer incidence and mortality patterns in Europe: Estimates for 40 countries in 2012. *Eur J Cancer* 2013;49:1374–403.
3. Saltz LB, Cox J, Blanke C, et al. Irinotecan plus fluorouracil and leucovorin for metastatic colorectal cancer. *N Engl J Med* 2000;343: 905–14.
4. Goldberg RM, Sargent DJ, Morton RF, et al. A randomized controlled trial of fluorouracil plus leucovorin, irinotecan, and oxaliplatin combinations in patients with previously untreated metastatic colorectal cancer. *J Clin Oncol* 2004;22:23–30.
5. Hurwitz HI, Tebbutt NC, Kabbinavar F, et al. Efficacy and safety of bevacizumab in metastatic colorectal cancer: pooled analysis from seven randomized controlled trials. *Oncologist* 2013;18:1004–12.
6. Van Cutsem E, Köhne C-H, Hitre E, et al. Cetuximab and chemotherapy as initial treatment for metastatic colorectal cancer. *N Engl J Med* 2009;360:1408–17.
7. Van Cutsem E, Peeters M, Siena S, et al. Open-label phase III trial of panitumumab plus best supportive care compared with best supportive care alone in patients with chemotherapy-refractory metastatic colorectal cancer. *J Clin Oncol* 2007;25:1658–64.
8. Douillard J-Y, Siena S, Cassidy J, et al. Randomized, phase III trial of panitumumab with infusional fluorouracil, leucovorin, and oxaliplatin (FOLFOX4) versus FOLFOX4 alone as first-line treatment in patients with previously untreated metastatic colorectal cancer: the PRIME study. *J Clin Oncol* 2010;28:4697–705.
9. Douillard J-Y, Oliner KS, Siena S, et al. Panitumumab-FOLFOX4 treatment and RAS mutations in colorectal cancer. *N Engl J Med* 2013;369:1023–34.
10. Popovici V, Budinska E, Tejpar S, et al. Identification of a poor-prognosis *BRAF*-mutant - Like population of patients with colon cancer. *J Clin Oncol* 2012;30:1288–95.
11. Peeters M, Oliner K, Price T, et al. Updated analysis of *KRAS*-*NRAS* and *BRAF* mutations in mCRC. 2014;32:5s (suppl; abstr 3568).
12. Van Cutsem E, Köhne C-H, Láng I, et al. Cetuximab plus irinotecan, fluorouracil, and leucovorin as first-line treatment for metastatic colorectal cancer: updated analysis of overall survival according to tumor *KRAS* and *BRAF* mutation status. *J Clin Oncol* 2011;29:2011–9.
13. Modest DP, Jung A, Moosmann N, et al. The influence of *KRAS* and *BRAF* mutations on the efficacy of cetuximab-based first-line therapy of metastatic colorectal cancer: An analysis of the AIO KRK-0104-trial. *Int J Cancer* 2012;131:980–6.
14. Maughan T, Adams R, Smith C, Meade A. Addition of cetuximab to oxaliplatin-based first-line combination chemotherapy for treatment of advanced colorectal cancer: results of the randomised phase 3 MRC COIN trial. *Lancet* 2011;377:2103–14.
15. Souglakos J, Philips J, Wang R, et al. Prognostic and predictive value of common mutations for treatment response and survival in patients with metastatic colorectal cancer. *Br J Cancer* 2009;101:465–72.
16. Bokemeyer C, Cutsem E Van, Rougier P, et al. Addition of cetuximab to chemotherapy as first-line treatment for *KRAS* wild-type metastatic colorectal cancer: Pooled analysis of the CRYSTAL and OPUS randomised clinical trials. *Eur J Cancer* 2012;48:1466–75.
17. Tveit KM, Guren T, Glimelius B, et al. Phase III trial of cetuximab with continuous or intermittent fluorouracil, leucovorin, and oxaliplatin (Nordic FLOX) versus FLOX alone in first-line treatment of metastatic colorectal cancer: The NORDIC-VII study. *J Clin Oncol* 2012;30:1755–62.

18. Richman SD, Seymour MT, Chambers P, et al. KRAS and BRAF mutations in advanced colorectal cancer are associated with poor prognosis but do not preclude benefit from oxaliplatin or irinotecan: results from the MRC FOCUS trial. *J Clin Oncol* 2009;27:5931–7.
19. Tran B, Kopetz S, Tie J, et al. Impact of BRAF mutation and microsatellite instability on the pattern of metastatic spread and prognosis in metastatic colorectal cancer. *Cancer* 2011;117:4623–32.
20. Yokota T, Ura T, Shibata N, et al. BRAF mutation is a powerful prognostic factor in advanced and recurrent colorectal cancer. *Br J Cancer* 2011;104:856–62.
21. Tie J, Gibbs P, Lipton L, et al. Optimizing targeted therapeutic development: Analysis of a colorectal cancer patient population with the BRAFV600E mutation. *Int J Cancer* 2011;128:2075–84.
22. Di Nicolantonio F, Martini M, Molinari F, et al. Wild-type BRAF is required for response to panitumumab or cetuximab in metastatic colorectal cancer. *J Clin Oncol* 2008;26:5705–12.
23. Loupakis F, Ruzzo A, Cremolini C, et al. KRAS codon 61, 146 and BRAF mutations predict resistance to cetuximab plus irinotecan in KRAS codon 12 and 13 wild-type metastatic colorectal cancer. *Br J Cancer* 2009;101:715–21.
24. Laurent-Puig P, Cayre A, Manceau G, et al. Analysis of PTEN, BRAF, and EGFR status in determining benefit from cetuximab therapy in wild-type KRAS metastatic colon cancer. *J Clin Oncol* 2009;27: 924–30.
25. Rook W De, Vriendt V De, Normanno N, et al. KRAS, BRAF, PIK3CA, and PTEN mutations: Implications for targeted therapies in metastatic colorectal cancer. *Lancet Oncol* 2011;12:594–603.
26. Wan PTC, Garnett MJ, Roe SM, et al. Mechanism of activation of the RAF-ERK signaling pathway by oncogenic mutations of B-RAF. *Cell* 2004;116:855–67.
27. Davies H, Bignell GR, Cox C, et al. Mutations of the BRAF gene in human cancer. *Nature* 2002;417:949–54.
28. Chapman PB, Hauschild A, Robert C, et al. Improved survival with vemurafenib in melanoma with BRAF V600E mutation. *N Engl J Med* 2011;364:2507–16.
29. Hauschild A, Grob J-J, Demidov L V, et al. Dabrafenib in BRAF-mutated metastatic melanoma: a multicentre, open-label, phase 3 randomised controlled trial. *Lancet* 2012;380:358–65.
30. Kopetz S, Desai J, Chan E, et al. Phase II Pilot Study of Vemurafenib in Patients With Metastatic BRAF-Mutated Colorectal Cancer. *J Clin Oncol* 2015;33:4032–8.
31. Prahallad A, Sun C, Huang S, et al. Unresponsiveness of colon cancer to BRAF(V600E) inhibition through feedback activation of EGFR. *Nature* 2012;483:100–3.
32. Corcoran RB, Ebi H, Turke AB, et al. EGFR-mediated reactivation of MAPK signaling contributes to insensitivity of BRAF-mutant colorectal cancers to RAF inhibition with vemurafenib. *Cancer Discov* 2012;2:227–35.
33. Elez E, Bendell JC, Tabernero J, et al. Results of a phase 1b study of the selective BRAF V600 inhibitor encorafenib in combination with cetuximab alone or cetuximab + alpelisib for the treatment of patients with advanced BRAF-mutant metastatic colorectal cancer. *Ann Oncol* 2015;26:117–22.
34. Stuart D, Li N, Poon D, et al. Preclinical profile of LGX818: A potent and selective RAF kinase inhibitor. *Cancer Res* 2012;72:3790–3790.
35. Fritsch C, Huang A, Chatenay-rivauday C, et al. Characterization of the Novel and Specific PI3K Inhibitor NVP-BYL719 and Development of the Patient Stratification Strategy for Clinical Trials. *Mol Cancer Ther* 2014;13:1117–30.

36. Schoenfeld D. The asymptotic properties of nonparametric tests for comparing survival distributions. *Biometrika* 1981;68:316–9.
37. Clopper CJ, Pearson ES. the Use of Confidence or Fiducial Limits. *Biometrika* 1934;26:404–13.
38. Kopetz S, Desai J, Chan E, et al. Phase II pilot study of vemurafenib in patients with metastatic BRAF-mutated colorectal cancer. *J Clin Oncol* 2015;33:4032–8.
39. Hyman DM, Puzanov I, Subbiah V, et al. Vemurafenib in Multiple Nonmelanoma Cancers with BRAF V600 Mutations. *N Engl J Med* 2015;373:726–36.
40. Yaeger R, Cercek A, O'Reilly EM, et al. Pilot trial of combined BRAF and EGFR inhibition in BRAF-mutant metastatic colorectal cancer patients. *Clin Cancer Res* 2015;21:1313–20.
41. Atreya CE, Cutsem E Van, Bendell JC, et al. Updated efficacy of the MEK inhibitor trametinib (T), BRAF inhibitor dabrafenib (D), and anti-EGFR antibody panitumumab (P) in patients (pts) with BRAF V600E mutated (BRAFM) metastatic colorectal cancer (mCRC). *J Clin Oncol* 2015;33 (suppl;abstr 103).
42. De Roock W, Claes B, Bernasconi D, et al. Effects of KRAS, BRAF, NRAS, and PIK3CA mutations on the efficacy of cetuximab plus chemotherapy in chemotherapy-refractory metastatic colorectal cancer: A retrospective consortium analysis. *Lancet Oncol* 2010;11:753–62.
43. Ulivi P, Capelli L, Valgiusti M, et al. Predictive role of multiple gene alterations in response to cetuximab in metastatic colorectal cancer: a single center study. *J Transl Med* 2012;10:87.
44. Saridaki Z, Tzardi M, Papadaki C, et al. Impact of KRAS, BRAF, PIK3CA Mutations, PTEN, AREG, EREG expression and skin rash in ≥2nd line cetuximab- based therapy of colorectal cancer patients. *PLoS One* 2011;6:e15980.
45. Rodón J, Dienstmann R, Serra V, Tabernero JM. Development of PI3K inhibitors: lessons learned from early clinical trials. *Nat Rev Clin Oncol* 2013;10:143–53.
46. Gomez-roca C, Delord J, Robert C, et al. Encorafenib (LGX818), an Oral BRAF Inhibitor, in Patients With BRAF V600E Metastatic Colorectal Cancer: Results of Dose Expansion in an Open-Label, Phase 1 Study. *Ann Oncol* 2014;25 (suppl 4):iv182–iv183
47. Jaka A, Gutierrez-Rivera A, Lopez-Pestana A, et al. Predictors of Tumor Response to Cetuximab and Panitumumab in 116 Patients and a Review of Approaches to Managing Skin Toxicity. *Actas Dermosifiliogr* 2014;106:483–92.
48. Holderfield M, Nagel TE, Stuart DD. Mechanism and consequences of RAF kinase activation by small-molecule inhibitors. *Br J Cancer* 2014;111:640–5.







# Chapter 5

## Clinical pharmacology of combined targeted therapy targeting mutated *BRAF*



### 5.3

#### Phase I study of dabrafenib, panitumumab and trametinib in patients with advanced *BRAF*V600E mutated colorectal cancer

##### Interim analysis

Robin M.J.M. van Geel, Chloe E. Atreya, Eric van Cutsem, Thierry André, Johanna C. Bendell, Michael S. Gordon, Autumn McRee, Takayuki Yoshino, Kei Muro, Peter J. O'Dwyer, Josep Taberner, Gary Middleton, Michel Ducreux, Roger Sidhu, James G. Greger, Fatima Rangwala, Yuan Liu, Bijoyesh Mookerjee, Ryan B. Corcoran, René Bernards, Jan H.M. Schellens

## ABSTRACT

### Background

*BRAF* V600E mutations are present in approximately 10% of the patients with colorectal cancer (CRC) resulting in a poor prognosis and worse response to standard treatment regimens. Whereas treatment with *BRAF* and MEK inhibitors have improved patient outcome in *BRAF* mutated (*BRAF*m) melanoma, these treatments have only minimal anti-tumor activity in patients with metastatic *BRAF*m CRC, due to feedback activation of the epidermal growth factor receptor (EGFR). In this study we investigated the safety and clinical activity of combination strategies containing the *BRAF* inhibitor dabrafenib, anti-EGFR monoclonal antibody panitumumab and MEK inhibitor trametinib in patients with advanced *BRAF*m CRC.

### Methods

We performed a multicenter, open-label, phase I dose-escalation study, followed by a cohort expansion part. Patients with advanced *BRAF*m CRC were assigned sequentially to receive dabrafenib plus panitumumab, dabrafenib plus panitumumab plus trametinib or trametinib plus panitumumab. The primary objective was to determine the safety and tolerability of these combinations. Secondary objectives included assessing the pharmacodynamic response in tumor tissue and the clinical anti-tumor activity following combination therapy.

### Results

A total of 74 patients were enrolled across the dabrafenib plus panitumumab doublet ( $n = 20$ ), the dabrafenib-panitumumab-trametinib triplet ( $n = 35$ ), and the trametinib plus panitumumab doublet ( $n = 19$ ). One patient experienced dose-limiting grade 3 acneiform rash in the trametinib plus panitumumab arm. The most common adverse events were dermatitis acneiform (60%) and fatigue (45%) for dabrafenib plus panitumumab, diarrhea (86%) and dermatitis acneiform (66%) for the triplet, and dermatitis acneiform (63%) and diarrhea (52%) for trametinib plus panitumumab. Pharmacodynamic response, as measured by pERK modulation in tumor biopsies taken at baseline and after 15 days of treatment, was seen with all regimens. Confirmed response rates were 10% and 26% for the dabrafenib plus panitumumab doublet and the triplet, respectively.

### Conclusions

Combinations of dabrafenib plus panitumumab and dabrafenib plus panitumumab plus trametinib showed manageable toxicity profiles at their full monotherapy doses. Full dose trametinib plus panitumumab was associated with intolerable dermatologic toxicity. The triplet combination demonstrated promising clinical activity, warranting further exploration in patients with *BRAF*m CRC.

## Introduction

Colorectal cancer (CRC) is the fourth most common visceral malignancy and the second most frequent cause of cancer death worldwide.<sup>1</sup> Approximately 10% of all patients with CRC harbor a *BRAF* V600E mutation, resulting in hyper activation of the BRAF protein and increased mitogen activated protein kinase (MAPK) signaling. Accumulating evidence demonstrates that the presence of a *BRAF* mutation is a poor prognostic factor in CRC, with median overall survival times in the first-line setting of 9 to 14 months, versus 20 to 34 months in *RAS/BRAF* wild-type patients.<sup>2-6</sup> Beyond the first-line setting, currently available treatment options provide very little benefit resulting in median overall survival times in the range of 4 to 7 months.<sup>7-9</sup> Addition of epidermal growth factor receptor (EGFR) directed monoclonal antibodies provides no or limited clinical activity in patients with *BRAF*m CRC as well, similar to the conferral of resistance to anti-EGFR treatment in patients with *RAS* mutated CRC.<sup>3,5,7,8,10</sup> Given the poor prognosis and lack of effective treatment options, *BRAF*m CRC holds an unmet medical need.

Direct inhibition of BRAF using selective BRAF inhibitors demonstrated encouraging anti-tumor activity in patients with *BRAF*m melanoma.<sup>11,12</sup> Combinations of BRAF inhibitors and MEK inhibitors further improved the clinical outcome of these patients.<sup>13,14</sup> In contrast, studies investigating the clinical activity of BRAF and MEK inhibitors in patients with *BRAF*m CRC were disappointing, with response rates of 5-12%.<sup>15,16</sup> Prahallad and colleagues used an RNA-interference-based genetic screen to explore kinase proteins whose inhibition synergizes with BRAF inhibition and found EGFR as one of the most potent synergy partners. Mechanistically, the unresponsiveness of *BRAF*m CRC to BRAF inhibitors was found to be caused by a feedback activation of EGFR that despite BRAF inhibition supports continued activation of the MAPK- and phosphoinositide 3-kinase signaling pathways, leading to sustained proliferation. Whereas CRC cells express high levels of EGFR, melanoma cells generally lack expression of EGFR, explaining the differential response to BRAF inhibition alone.<sup>17</sup> The addition of EGFR inhibiting agents sensitized *BRAF*m CRC cells to BRAF inhibition and resulted in a synergistic anti-tumor activity *in vitro* and *in vivo*.<sup>17,18</sup> These findings provided strong rationale to evaluate combinations of targeted agents against BRAF, EGFR and MEK in the clinic.

The current phase I study was designed to identify the recommended phase 2 regimen and assess the clinical activity of the dabrafenib plus panitumumab doublet, the dabrafenib-panitumumab-trametinib triplet, and the trametinib-panitumumab doublet. Herein we describe an interim analysis of data from 74 evaluable patients.

## Patients and Methods

### Patients

In this phase I study, we enrolled patients at twenty sites in eight different countries. Eligible patients had histologically- or cytologically-confirmed diagnosis of advanced or metastatic CRC, were 18 years or older, had an Eastern Cooperative Oncology Group performance status (ECOG PS) of 0 or 1, had measurable disease per Response Evaluation Criteria In Solid Tumors (RECIST) v1.1, had adequate organ function, and had documented *BRAF* V600E mutated disease. Key exclusion criteria were history of prior malignancy, other than CRC, brain metastases, history of retinal vein occlusion, and prior exposure to a MEK inhibitor. The institutional review boards and regulatory authorities approved the study protocol, and all patients gave written informed consent in accordance with Declaration

of Helsinki recommendations. The study (ClinicalTrials.gov identifier: NCT01750918) was conducted according to the guidelines for Good Clinical Practice as defined by the International Conference on Harmonization.

### Study design and procedures

We initiated this study with the combination therapy of dabrafenib plus panitumumab. The starting dose of dabrafenib and panitumumab consisted of their respective recommended single agent doses of 150 mg twice daily (BID) orally and 6 mg/kg biweekly (Q2W) intravenously, respectively. Upon determination of a tolerable dose of the dabrafenib plus panitumumab doublet, orally administered trametinib was added in subsequent cohorts, according to predefined dose-escalation steps. Additionally, a second doublet, containing trametinib and panitumumab was investigated to evaluate which components contribute the most in achieving synergistic anti-tumor activity, and to find a regimen with an optimal response-toxicity ratio. Dose-escalation followed a 3 + 3 design and escalation decisions were based on dose-limiting toxicity (DLT) data. A DLT was defined as an adverse event or laboratory abnormality that occurs within the first 28 days of dosing, has a possible causal relationship to the study treatment based on investigator assessment and meets at least one of the criteria mentioned in supplementary table S1. Adverse events were graded using the National Cancer Institute's Common Terminology Criteria for Adverse Events (NCI-CTCAE) v4.0. After completion of the dose-escalation phase, the established recommended phase II regimens were further evaluated in the cohort expansion phase to obtain adequate data on safety, tolerability, pharmacokinetics, pharmacodynamics and anti-tumor activity (Figure 1).

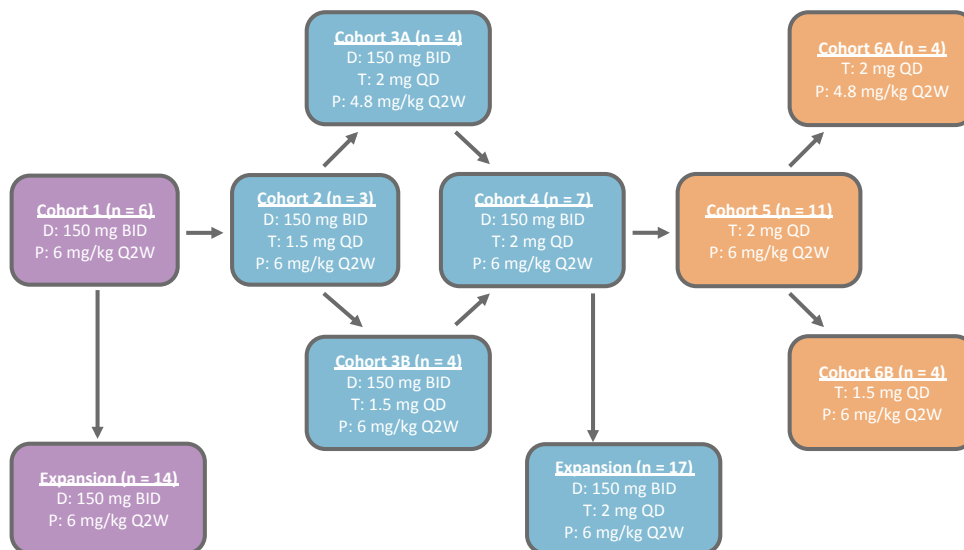


**Figure 1. Study design and dose-escalation overview.**

Colors represent the different combinations, dabrafenib-panitumumab (purple), dabrafenib-panitumumab-trametinib (blue), trametinib-panitumumab (orange). Abbreviations: D, dabrafenib; P, panitumumab; T, trametinib; BID, twice daily; Q2W, biweekly; QD, once daily

Treatment continued until disease progression, unacceptable toxicity, or withdrawal of consent. Patients were evaluable for safety if a DLT occurred or at least one treatment cycle with the minimum safety evaluation and drug exposure was completed.

Demographic data and medical history were collected during screening. At baseline, all patients underwent physical examination, electrocardiography, laboratory assessments, ophthalmic examination, left-ventricular ejection fraction evaluation, and radiographic tumor measurement, and these assessments were repeated throughout the study. Extensive blood sampling was done for plasma concentration analysis of dabrafenib, panitumumab and trametinib on day 1 and 15 of cycle 1, and through samples were collected on day 1 of each subsequent cycle. Paired tumor biopsies were obtained from all patients at baseline and after 15 days of study treatment for pharmacodynamic analysis, *i.e.* evaluation of phosphorylated ERK staining intensity as measured using immunohistochemistry by independent and adequately trained pathologists. Radiographic tumor measurements were performed every 6 weeks using computed tomography (CT), and tumor response was evaluated according RECIST v1.1 criteria.

### **Statistical analysis**

This interim report includes results based on a data cut off after results of 74 evaluable patients were obtained. Response rates and corresponding 95% confidence intervals (95% CI) were calculated with the Clopper and Pearson method.<sup>19</sup> Median progression-free survival (PFS) was estimated using the Kaplan-Meier method and estimated 95% ICs were calculated using Brookmeyer and Crowley's method.<sup>20</sup> Overall response rate was defined as the proportion of patients who had a partial or complete response as best overall response, and PFS was defined as the time from start of study treatment to the date of first documentation of disease progression, or death due to any cause. The study was not developed to test a formal hypothesis on the difference in clinical activity of the three combination regimens. We used a paired T-test to determine the statistical significance of the pharmacodynamic modulation in tumor biopsies taken before start and while on treatment. Statistical analyses were performed using SPSS Statistics version 22.0.

5.3

## **Results**

### ***Patient disposition and characteristics***

In total, 74 patients were enrolled across the three treatment regimens. Baseline patient characteristics were generally similar, except for the proportion of patients previously treated with anti-EGFR targeted therapy, which was 42% in the trametinib plus panitumumab treated patients versus 5% and 4 % in patients treated with dabrafenib plus panitumumab and the triplet, respectively (Table 1). The majority of patients (90%) were pretreated with at least 2 prior lines of therapy for metastatic disease, of which 55% received 3 or more regimens. Twenty patients were treated with dabrafenib plus panitumumab, 35 patients received dabrafenib, panitumumab and trametinib, and 19 patients were treated with the trametinib plus panitumumab doublet. All patients received at least one dose of dabrafenib, panitumumab or trametinib and were included in the safety analysis set. At data cut off, 23 patients had died, 8 were ongoing, of which 3 on the triplet therapy and 5 on the trametinib plus panitumumab doublet, and 36 patients had discontinued study treatment due to adverse events or disease progression.

<b>Table 1. Patient and disease characteristics at baseline</b>			
	<b>D + P (n = 20)</b>	<b>D + P + T (n = 52)</b>	<b>T + P (n = 19)</b>
<b>Sex, n (%)</b>			
Female	11 (55%)	22 (63%)	11 (58%)
Male	9 (45%)	13 (37%)	8 (42%)
<b>Age, median (range), years</b>	58 (42–84)	58 (28–83)	59 (39–70)
<b>Primary site of cancer derived, n (%)</b>			
Colon, right sided	14 (70%)	25 (71%)	8 (42%)
Colon, left sided	4 (20%)	5 (14%)	7 (37%)
Rectum	2 (10%)	5 (14%)	3 (16%)
<b>ECOG PS, n (%)</b>			
0	14 (70%)	20 (57%)	12 (63%)
1	6 (30%)	15 (43%)	7 (37%)
<b>Number of prior therapy regimens, n (%)</b>			
0	3 (15%)	3 (9%)	1 (5%)
1	9 (45%)	13 (37%)	8 (42%)
≥2	8 (40%)	19 (54%)	10 (53%)
<b>Prior anti-EGFR treatment, n (%)</b>			
No	19 (95%)	30 (86%)	11 (58%)
Yes	1 (5%)	5 (14%)	8 (42%)

Abbreviations: D, dabrafenib; P, panitumumab; T, trametinib ECOG PS, Eastern Cooperative Oncology Group performance status.

### **Dose determination**

DLTs were not identified with the dabrafenib-panitumumab doublet and the triplet. Therefore, both combinations were escalated up to the full monotherapy dose of each component, being 150 mg BID for dabrafenib, 6 mg/kg Q2W for panitumumab and 2 mg once daily (QD) for trametinib. One patient treated with the trametinib-panitumumab doublet at their full respective single agent doses experienced a DLT due to grade 3 acneiform rash. In addition, significantly more patients experienced grade 3 dermatologic toxicity with the trametinib-panitumumab doublet compared to the other combinations and in 58% of the patients dose modifications were necessary due to adverse events (Figure 2). Therefore, we considered 2 mg QD trametinib plus 6 mg/kg Q2W panitumumab not tolerable and initiated exploration of two lower dose levels; 1.5 mg QD trametinib plus 6 mg/kg Q2W panitumumab and 2 mg QD trametinib plus 4.8 mg/kg Q2W panitumumab. This part of the study was ongoing at the time this interim analysis was performed.

### **Safety**

All patients experienced at least 1 study treatment-related adverse event. Adverse events, regardless of treatment, occurring in more than 25% of patients are listed in Table 2. The most frequently occurring adverse events of any grade were dermatitis acneiform (60%), diarrhea (45%) and fatigue (45%) for dabrafenib plus panitumumab, diarrhea (86%), dermatitis acneiform (66%) and fatigue for dabrafenib-panitumumab-trametinib, and dermatitis acneiform (63%), diarrhea (52%) and skin rash (37%) for trametinib plus panitumumab. Treatment-related grade 4 or 5 events were not observed.

Of the patients experiencing dermatologic toxicity, dose modification, *i.e.* reduction or interruption,



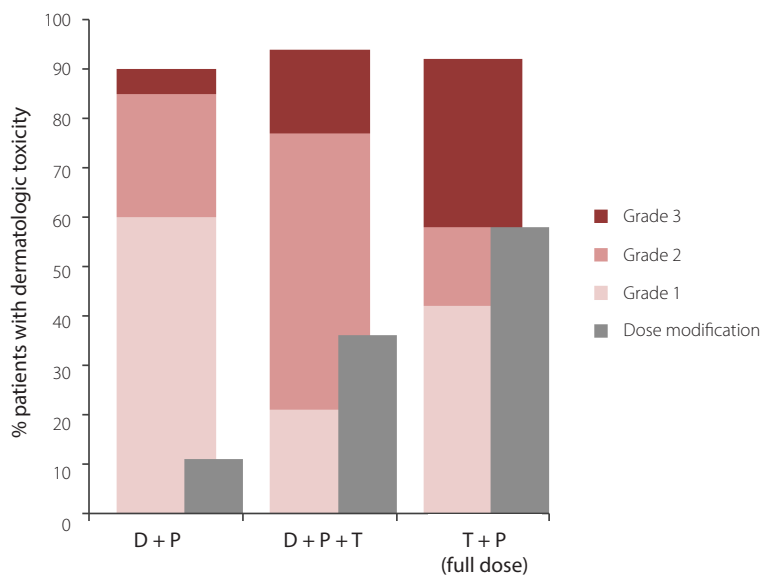


**Figure 2. Dermatologic toxicity and dermatologic toxicity-induced dose modifications.**

Abbreviations: D, dabrafenib; P, panitumumab; T, trametinib

was necessary in 2 (11%), 12 (36%) and 7 (54%) patients treated with dabrafenib-panitumumab, dabrafenib-panitumumab-trametinib and trametinib-panitumumab, respectively. For patients experiencing pyrexia, dose modifications were required for 5 (63%) patients treated with dabrafenib plus panitumumab, for 2 (13%) patients treated with the triplet, and for none of the patients on the trametinib plus panitumumab doublet. Overall mean drug compliance during the first 2 treatment cycles was 95% with dabrafenib plus panitumumab and 80% with dabrafenib-panitumumab-trametinib. During the first and second cycle, mean drug compliance was 95% and 96%, respectively, with the dabrafenib-panitumumab doublet, and 89% and 76% for the triplet (Figure S1).

5.3

Adverse event, n (%)	Table 2. Adverse events, regardless of treatment, occurring in $\geq 25\%$ of patients					
	D + P (n = 20)		D + P + T (n = 52)		T + P (n = 19)	
	Grade 1/2	Grade 3	Grade 1/2	Grade 3	Grade 1/2	Grade 3
Dermatitis acneiform	12 (60%)	-	20 (57%)	3 (9%)	9 (47%)	3 (16%)
Diarrhea	9 (45%)	-	27 (77%)	3 (9%)	9 (47%)	1 (5%)
Fatigue	9 (45%)	-	18 (51%)	2 (6%)	6 (32%)	-
Hypomagnesemia	8 (40%)	1 (5%)	13 (37%)	1 (3%)	4 (21%)	-
Nausea	8 (40%)	-	17 (49%)	1 (3%)	5 (26%)	1 (5%)
Skin rash	6 (30%)	1 (5%)	13 (37%)	1 (3%)	5 (26%)	2 (11%)
Pyrexia	8 (40%)	-	16 (46%)	-	1 (5%)	-
Xerosis	7 (35%)	1 (5%)	17 (49%)	1 (3%)	6 (32%)	1 (5%)
Decreased appetite	5 (25%)	-	16 (46%)	2 (6%)	4 (21%)	-

Abbreviations: D, dabrafenib; P, panitumumab; T, trametinib

**Anti-tumor activity**

The overall response-evaluable population consisted of 70 patients. The remaining 4 patients had inadequate baseline scans ( $n = 1$ ) or had not reached the first on-treatment response evaluation after 6 weeks of treatment ( $n = 3$ ). Out of the evaluable patients, 15 achieved an objective response and 11 of those patients achieved a confirmed objective response (16%, 95% CI 7–25%). Tumor regression was seen in 11 (55%) patients on dabrafenib plus panitumumab, in 30 (86%) patients on the triplet and in 8 (53%) patients treated with trametinib plus panitumumab.

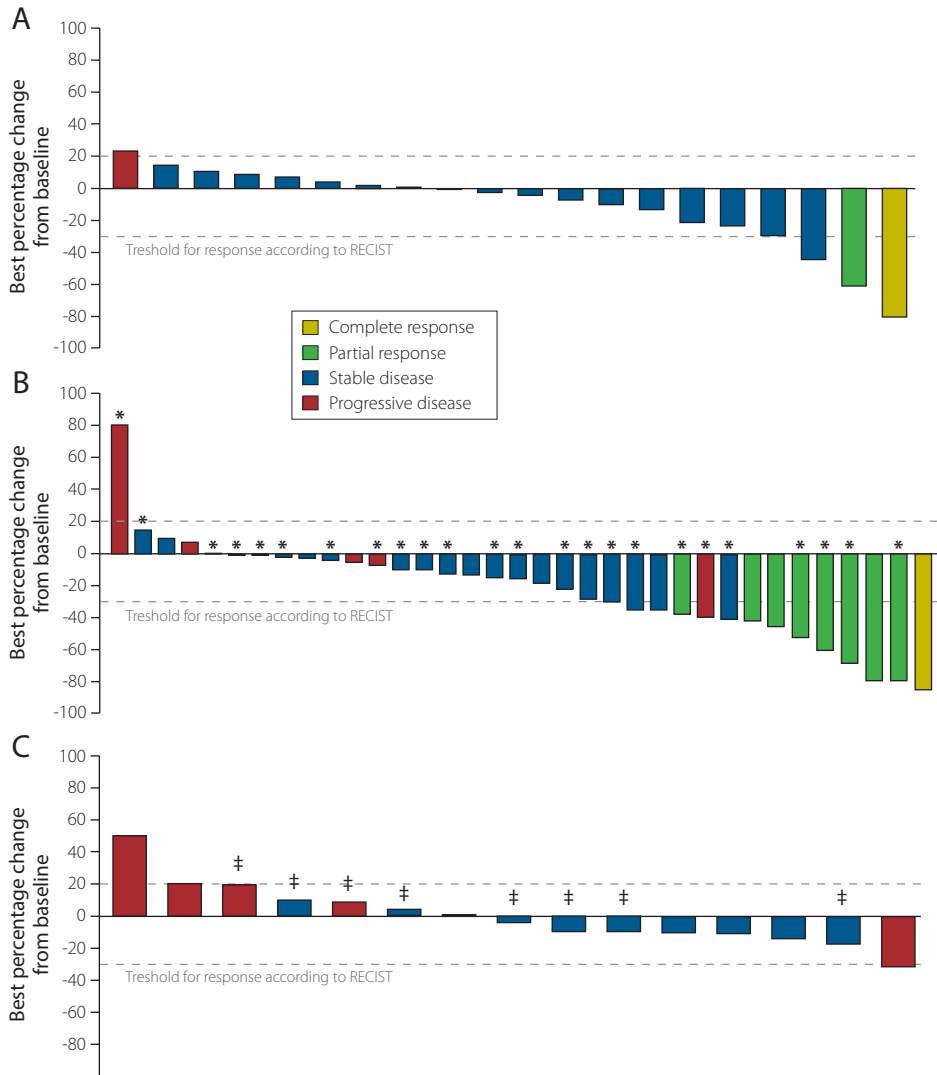


**Figure 3. Maximum percentage change in target lesion size from baseline, by treatment group.** (A) dabrafenib plus panitumumab. (B) dabrafenib plus panitumumab plus trametinib. (C) trametinib plus panitumumab. \* Recommended phase 2 regimen cohort; † Full dose cohort

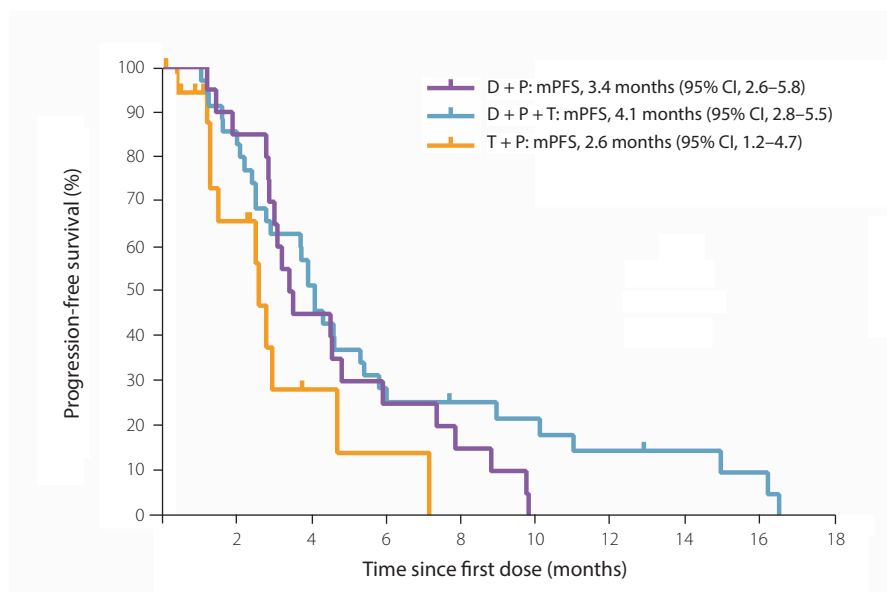


**Figure 4.** Kaplan-Meier estimates of progression-free survival, by treatment group

Abbreviations: D, dabrafenib; P, panitumumab; T, trametinib; mPFS, median progression-free survival; 95% CI, 95%-Confidence interval

The per treatment regimen confirmed response rates were 10% (95% CI 1–32%), 26% (13–43%) and 0% for dabrafenib plus panitumumab, dabrafenib plus panitumumab plus trametinib, and trametinib plus panitumumab, respectively (Figure 3). In patients treated with the triple combination, confirmed response rates were 67%, 50%, 0% and 21% in cohorts 2 ( $n = 3$ ), 3A ( $n = 4$ ), 3B ( $n = 4$ ) and 4 plus expansion ( $n = 24$ ), respectively. Median duration of response was 5.4 (95% CI 2.7–not reached) with the triplet regimens. Disease control (*i.e.* complete or partial response, or stable disease) was achieved in 58 (83%) patients. The median PFS was 3.4 months (95% CI 2.6–5.8) with dabrafenib plus panitumumab, 4.1 months (95% CI 2.8–5.5) with the triple combination, and 2.6 months (95% CI 1.2–4.7) for trametinib plus panitumumab (Figure 4 & S2). Three patients continued study treatment after 6, 7.5 and 12.8 months on the triplet therapy and 5 patients on the trametinib-panitumumab doublet were ongoing at data cut off.

#### Pharmacokinetic and pharmacodynamic analysis

Pharmacokinetic data were not yet available at the time this interim analysis was performed. Paired tumor biopsy samples taken at baseline and after 15 days of study treatment were available for 9 patients in the dabrafenib plus panitumumab arm, 7 patients in the triplet arm and 4 patients in the trametinib plus panitumumab arm. Staining intensity analysis using immunohistochemistry revealed inhibition of pERK in 5/9 (56%) patients treated with dabrafenib plus panitumumab and in all patients treated with dabrafenib-panitumumab-trametinib or the trametinib plus panitumumab doublet. The median pERK modulation was -21% with dabrafenib-panitumumab ( $n = 9$ ), -56% with the triplet ( $n = 7$ ), and -68% with trametinib-panitumumab ( $n = 4$ ), calculated as percentage change in H-score from baseline (Figure 5).

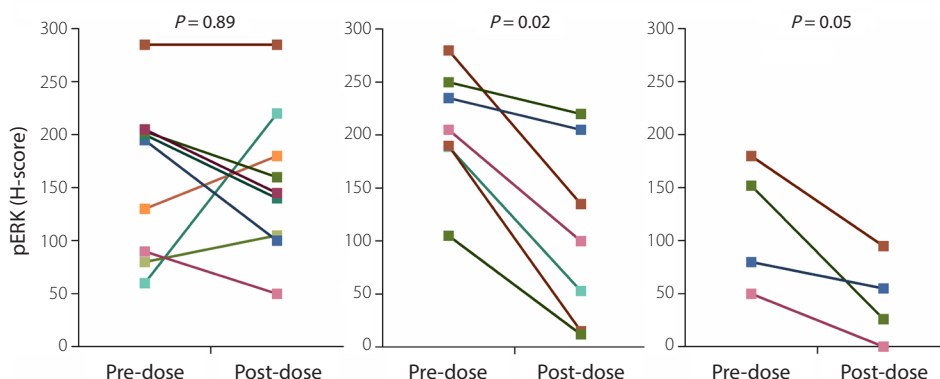


**Figure 5. Phosphorylated ERK modulation in tumor tissue, by treatment group**  
 pERK staining intensity at baseline versus on-treatment for the three combination regimens. Statistical significance of the difference in mean H-score pre-dose versus post-dose was estimated using a paired T-test.

## Discussion

In this phase I study, we demonstrated that combination regimens consisting of dabrafenib plus panitumumab with or without trametinib were overall well tolerated and could be combined safely at full single agent doses. Therefore, the established recommended phase II regimens comprises 200 mg dabrafenib BID, 6 mg/kg panitumumab Q2W, with or without 2 mg trametinib QD. Although both combinations had acceptable safety profiles, the triplet was associated with more frequent and more severe dermatologic adverse events, pyrexia and diarrhea. In addition, drug compliance was considerably less in patients treated with the triplet (80%) than patients treated with the dabrafenib plus panitumumab doublet (95%), due to toxicity-induced treatment interruptions or reductions (Figure S1). On the other hand, overall dermatologic toxicity was generally mild, given the overlap in dermatologic adverse events between BRAF inhibitors and anti-EGFR antibodies. Dabrafenib has been associated with hyperkeratosis (27%), skin papilloma (15%) and cutaneous squamous cell carcinoma (10%) due to paradoxical activation of the MAPK pathway in normal *BRAF* wild type cells, whereas panitumumab mainly causes acneiform rash (80%), alopecia (45%), xerosis (20%) and paronychia (10%) through inhibition of EGFR and downstream pathways in normal skin tissue.<sup>12,21,22</sup> With the exception of one patient who developed a squamous cell carcinoma upon treatment with dabrafenib plus panitumumab, other events of such typical dabrafenib-related dermatologic toxicity were not observed in patients treated in the present study, suggesting that EGFR inhibition reduces BRAF inhibitor-induced cutaneous toxicity, similar to the effects observed with combined BRAF and MEK inhibition.<sup>13,23,24</sup> Interestingly, in contrast to the triplet combination, panitumumab combined with trametinib at full single agent doses was not tolerable due to dermatologic toxicity, indicating that BRAF inhibition also mitigates anti-EGFR antibody/MEK inhibitor-induced toxicity. The opposing mechanisms by which BRAF and EGFR inhibitors induce their cutaneous toxicity may explain these favorable outcomes.<sup>25</sup> Although not tolerable at full monotherapy doses, the combination of trametinib and panitumumab may be a valuable treatment option for anti-EGFR-naïve or anti-EGFR-resistant patients with *KRAS* and *BRAF* wildtype CRC. Therefore, we continue to explore the trametinib-

panitumumab doublet at reduced doses in this patient population in an ongoing expansion arm. Previous clinical trials with *BRAF* inhibitors as single agent have shown limited anti-tumor activity in patients with *BRAF*m CRC<sup>15,26</sup> and the use of anti-EGFR antibodies has not significantly improved patient outcome either.<sup>7–9,27,28</sup> With this study we provide proof of concept for combined *BRAF* and EGFR inhibition in patients with *BRAF*m CRC as clinical efficacy was demonstrated for dabrafenib plus panitumumab with or without trametinib. Although our study was not designed or powered to formally compare clinical efficacy, the triplet combination showed superior anti-tumor activity in terms of response rate and progression-free survival compared to the other combinations. The larger proportion of patients who previously received anti-EGFR-containing therapy in the trametinib plus panitumumab treated patients may explain the limited antitumor activity with this combination, as anti-EGFR therapy may prime tumors to contain more *KRAS* mutant or *KRAS* amplified cells.<sup>29,30</sup> Nevertheless, two patients who received anti-EGFR-directed therapy in their prior treatment regimen did respond to the triplet suggesting that *BRAF* inhibition is a critical component for these combination strategies in *BRAF*m CRC. Moreover, downstream inhibition may not be as effective as directly targeting the mutated *BRAF* protein itself, which has been suggested by studies investigating *BRAF* and MEK inhibitors in patients with *BRAF*m melanoma.<sup>31,32</sup>

In small studies evaluating combinations of *BRAF* inhibitors and MEK or EGFR inhibitors, overall response rates and median progression-free survival times ranged from 4%–16% and 3.2–3.7 months respectively.<sup>26,33</sup> The dabrafenib-panitumumab doublet in our study provided similar results, with a confirmed response rate of 10% and a median progression-free survival of 3.4 months. However, in our study with the *BRAF* inhibitor encorafenib plus anti-EGFR antibody cetuximab, we demonstrated an overall response rate of 23% in patients with *BRAF*m CRC.<sup>34</sup> Differences in drug-specific characteristics may explain this finding, with the *BRAF* dissociation half-life being of particular interest in this respect, as encorafenib has a dissociation half-life of > 24 hours versus < 1 hour for dabrafenib.

Furthermore, in the present study, the addition of trametinib substantially improved the confirmed response rate up to 26% and also achieved more durable responses compared to historical data on other combinations,<sup>16,26,33</sup> suggesting that MAPK pathway inhibition remains suboptimal with dabrafenib plus panitumumab alone in *BRAF*m CRC. As *BRAF*m tumors are highly dependent on *BRAF* kinase activity, strong suppression of the MAPK pathway is necessary to obtain anti-tumor activity.<sup>35</sup> Indeed, our pharmacodynamic analysis of paired tumor biopsies revealed that pERK was inhibited to a larger extent in patients treated with the triplet compared to dabrafenib plus panitumumab. The degree of pERK inhibition was even more with trametinib plus panitumumab, although this did not translate into clinical responses. Importantly, our sample sizes were small and baseline pERK H-scores in patients treated with the trametinib-panitumumab doublet were significantly lower compared to those in patients treated with the triplet, which may inflate the percentage pERK modulation and overestimate the clinical importance. Therefore, comparing pERK modulation between the different treatment arms in this study is cumbersome; let alone comparison between different studies. Another complicating factor lies in the larger portion of patients pre-treated with anti-EGFR therapy in the trametinib plus panitumumab group, which may prime tumors to develop resistance against retreatment with anti-EGFR-containing combinations through activation of alternative signaling pathways, e.g. via increased expression of HER2, HER3, c-MET, TGF- $\beta$ .<sup>36</sup> Nevertheless, the importance of robust MAPK inhibition in *BRAF*m CRC is irrefutable and further supported by research from Ahronian

et al., reporting that acquired resistance against BRAF-EGFR or BRAF-MEK inhibitor combinations in patients with *BRAF*<sup>m</sup> CRC rely on reactivating alterations in the MAPK pathway, including *KRAS* amplification, *BRAF* amplification and *MEK1* mutations.<sup>37</sup>

Although we achieved improved clinical outcome with the dabrafenib-panitumumab-trametinib combination compared to historical data on standard treatment regimens and other experimental combination strategies, a substantial portion of patients still did not respond and those patients who did respond, eventually became resistant. The planned comprehensive genetic analysis should therefore focus on identifying biomarkers that better define the subpopulation of *BRAF*<sup>m</sup> CRC patients most likely to respond to this combination strategy. In addition, a significant proportion of patients on the full dose triplet combination needed dose modifications due to toxicity, especially upon receiving multiple cycles (Figure S1B-C). As this may hamper the anti-tumor efficacy and thereby shorten duration of response and progression-free survival, we will further investigate patient outcome in ongoing additional expansion cohorts with triplets containing 4.8 mg/kg or 6 mg/kg panitumumab.

In conclusion, our results demonstrate that combined dabrafenib and panitumumab with or without trametinib is safe and overall reasonably to well tolerated. Clinical efficacy has been observed with both combinations, but the most promising anti-tumor activity was achieved with the triplet. We believe these results provide an important step towards effective targeted therapy combinations for the difficult-to-treat patient population with advanced *BRAF*<sup>m</sup> CRC.

## References

1. Torre LA, Bray F, Siegel RL, Ferlay J, et al. Global Cancer Statistics, 2012. *CA a cancer J Clin* 2015; 65: 87–108.
2. Cremolini C, Loupakis F, Antoniotti C, et al. FOLFOXIRI plus bevacizumab versus FOLFIRI plus bevacizumab as first-line treatment of patients with metastatic colorectal cancer: Updated overall survival and molecular subgroup analyses of the open-label, phase 3 TRIBE study. *Lancet Oncol* 2015;16:1306–15.
3. Maughan TS, Adams RA, Smith CG, et al. Addition of cetuximab to oxaliplatin-based first-line combination chemotherapy for treatment of advanced colorectal cancer: Results of the randomised phase 3 MRC COIN trial. *Lancet* 2011;377:2103–14.
4. Souglakos J, Philips J, Wang R, et al. Prognostic and predictive value of common mutations for treatment response and survival in patients with metastatic colorectal cancer. *Br J Cancer* 2009;101:465–72.
5. Bokemeyer C, Cutsem E Van, Rougier P, et al. Addition of cetuximab to chemotherapy as first-line treatment for *KRAS* wild-type metastatic colorectal cancer: Pooled analysis of the CRYSTAL and OPUS randomised clinical trials. *Eur J Cancer* 2012;48:1466–75.
6. Tveit KM, Guren T, Glimelius B, et al. Phase III trial of cetuximab with continuous or intermittent fluorouracil, leucovorin, and oxaliplatin (Nordic FLOX) versus FLOX alone in first-line treatment of metastatic colorectal cancer: The NORDIC-VII study. *J Clin Oncol* 2012;30:1755–62.
7. Loupakis F, Ruzzo A, Cremolini C, et al. *KRAS* codon 61, 146 and *BRAF* mutations predict resistance to cetuximab plus irinotecan in *KRAS* codon 12 and 13 wild-type metastatic colorectal cancer. *Br J Cancer* 2009;101:715–21.
8. Di Nicolantonio F, Martini M, Molinari F, et al. Wild-type *BRAF* is required for response to panitumumab or cetuximab in metastatic colorectal cancer. *J Clin Oncol* 2008;26:5705–12.
9. Laurent-Puig P, Cayre A, Manceau G, et al. Analysis of *PTEN*, *BRAF*, and *EGFR* status in determining benefit from cetuximab therapy in wild-type *KRAS* metastatic colon cancer. *J Clin Oncol* 2009;27:5924–30.
10. Douillard J-Y, Oliner KS, Siena S, et al. Panitumumab-FOLFOX4 treatment and *RAS* mutations in colorectal cancer. *N Engl J Med* 2013;369:1023–34.
11. Chapman PB, Hauschild A, Robert C, et al. Improved survival with vemurafenib in melanoma with *BRAF* V600E mutation. *N Engl J Med* 2011;364:2507–16.
12. Hauschild A, Grob JJ, Demidov LV, et al. Dabrafenib in *BRAF*-mutated metastatic melanoma: A multicentre, open-label, phase 3 randomised controlled trial. *Lancet* 2012;380: 358–65.
13. Larkin J, Ascierto PA, Dréno B, et al. Combined vemurafenib and cobimetinib in *BRAF*-mutated melanoma. *N Engl J Med* 2014;371:1867–76.
14. Robert C, Karaszewska B, Schachter J, et al. Improved Overall Survival in Melanoma with Combined Dabrafenib and Trametinib. *N Engl J Med* 2014;372:30–9
15. Kopetz S, Desai J, Chan E, et al. Phase II pilot study of vemurafenib in patients with metastatic *BRAF*-mutated colorectal cancer. *J Clin Oncol* 2015;33:4032–8.
16. Corcoran RB, Atreya CE, Falchook GS, et al. Combined *BRAF* and *MEK* inhibition with dabrafenib and trametinib in *BRAF* V600-Mutant colorectal cancer. *J Clin Oncol* 2015;33:4023–31.
17. Prahallad A, Sun C, Huang S, et al. Unresponsiveness of colon cancer to *BRAF*(V600E) inhibition through feedback activation of *EGFR*. *Nature* 2012;483:100–3.
18. Corcoran RB, Ebi H, Turke AB, et al. *EGFR*-mediated reactivation of *MAPK* signaling contributes to insensitivity of *BRAF*-mutant colorectal cancers to *RAF* inhibition with vemurafenib. *Cancer Discov* 2012;2:227–35.

19. Clopper CJ, Pearson ES. the Use of Confidence or Fiducial Limits. *Biometrika* 1934;26:404–13.
20. Brookmeyer R, Crowley J. A confidence interval for the median survival time. *B iometrics* 1982;38:29–41. 1982; : 1982.
21. Ascierto PA, Minor D, Ribas A, et al. Phase II trial (BREAK-2) of the BRAF inhibitor dabrafenib (GSK2118436) in patients with metastatic melanoma. *J Clin Oncol* 2013;31:3205–11.
22. Fabbrocini G, Panariello L, Caro G, Cacciapuoti S. Acneiform Rash Induced by EGFR Inhibitors: Review of the Literature and New Insights. *Skin Appendage Disord* 2015;1:31–7.
23. Flaherty KT, Infante JR, Daud A, et al. Combined BRAF and MEK inhibition in melanoma with BRAF V600 mutations. *N Engl J Med* 2012;367:1694–703.
24. Long G V, Stroyakovskiy D, Gogas H, et al. Combined BRAF and MEK inhibition versus BRAF inhibition alone in melanoma. *N Engl J Med* 2014;371:1877–88.
25. Holderfield M, Nagel TE, Stuart DD. Mechanism and consequences of RAF kinase activation by small-molecule inhibitors. *Br J Cancer* 2014;111:640–5.
26. Hyman DM, Puzanov I, Subbiah V, et al. Vemurafenib in Multiple Nonmelanoma Cancers with BRAF V600 Mutations. *N Engl J Med* 2015;373:726–36.
27. Maughan T, Adams R, Smith C, Meade A. Addition of cetuximab to oxaliplatin-based first-line combination chemotherapy for treatment of advanced colorectal cancer: results of the randomised phase 3 MRC COIN trial. *Lancet* 2011;377:2103–14.
28. De Roock W, Claes B, Bernasconi D, et al. Effects of KRAS, BRAF, NRAS, and PIK3CA mutations on the efficacy of cetuximab plus chemotherapy in chemotherapy-refractory metastatic colorectal cancer: A retrospective consortium analysis. *Lancet Oncol* 2010;11:753–62.
29. Misale S, Yaeger R, Hobor S, et al. Emergence of KRAS mutations and acquired resistance to anti EGFR therapy in colorectal cancer. *Nature* 2012;486:532–6.
30. Misale S, Di Nicolantonio F, Sartore-Bianchi A, Siena S, Bardelli A. Resistance to Anti-EGFR therapy in colorectal cancer: From heterogeneity to convergent evolution. *Cancer Discov* 2014;4:1269–80.
31. Falchook GS, Long GV, Kurzrock R, et al. Dabrafenib in patients with melanoma, untreated brain metastases, and other solid tumours: A phase 1 dose-escalation trial. *Lancet* 2012;379:1893–901.
32. Flaherty KT, Robert C, Hersey P, et al. Improved Survival with MEK Inhibition in BRAF-Mutated Melanoma. *N Engl J Med* 2012;367:107–14.
33. Yaeger R, Cercek A, O'Reilly EM, et al. Pilot trial of combined BRAF and EGFR inhibition in BRAF-mutant metastatic colorectal cancer patients. *Clin Cancer Res* 2015;21:1313–20.
34. Elez E, Bendell JC, Tabernero J, Yamada Y, et al. Results of a phase 1b study of the selective BRAF V600 inhibitor encorafenib in combination with cetuximab alone or cetuximab + alpelisib for the treatment of patients with advanced BRAF-mutant metastatic colorectal cancer. *Ann Oncol* 2015;26:117–22.
35. Bollag G, Hirth P, Tsai J, et al. Clinical efficacy of a RAF inhibitor needs broad target blockade in BRAF-mutant melanoma. *Nature* 2010;467:596–9.
36. Bertotti A, Papp E, Jones S, et al. The genomic landscape of response to EGFR blockade in colorectal cancer. *Nature* 2015;526:263–7.
37. Ahronian LG, Sennott EM, Van Allen EM, et al. Clinical acquired resistance to RAF inhibitor combinations in BRAF-mutant colorectal cancer through MAPK pathway alterations. *Cancer Discov* 2015;5:358–67.



## APPENDIX

**Table S1. Criteria for defining dose-limiting toxicities**

Toxicity	DLT definition
Hematologic	<ul style="list-style-type: none"> <li>• Grade 4 absolute neutrophil count (ANC) for <math>\geq 5</math> days</li> <li>• Febrile neutropenia (defined as concurrent Grade 4 neutropenia and fever <math>&gt;38.5^{\circ}\text{C}</math> and lasting <math>&gt;24</math> hours)</li> <li>• Grade 4 anemia of any duration</li> <li>• Grade 4 thrombocytopenia (platelets <math>&lt;25,000/\text{mm}^3</math>) of any duration</li> </ul>
Non-hematologic	<ul style="list-style-type: none"> <li>• Alanine aminotransferase (ALT) <math>&gt;5\text{X ULN}</math> OR, ALT <math>&gt;3\text{X ULN}</math> AND bilirubin <math>&gt;2\text{X ULN}</math> (after exclusion of disease progression and/or bile duct obstruction)</li> <li>• Grade <math>\geq 4</math> rash</li> <li>• Grade 4 Squamous Cell Carcinoma, keratoacanthoma or basal cell carcinoma</li> <li>• Grade 3 or greater clinically significant non-hematologic toxicity per NCICTCAE, v 4.0, other than those listed above, with the following exceptions:               <ul style="list-style-type: none"> <li>◦ Grade 3 or greater nausea, vomiting, diarrhea, or mucositis/esophagitis that responds to maximal supportive treatment(s) within 48 hours</li> <li>◦ Electrolyte disturbances that respond to correction within 24 hours</li> <li>◦ Grade 3 hypertension that is adequately controlled by the addition of up to 2 additional antihypertensive medications</li> <li>◦ Grade 3 pyrexia that does not result in study discontinuation</li> </ul> </li> </ul>
Cardiac	<ul style="list-style-type: none"> <li>• Ejection fraction <math>&lt; \text{LLN}</math> with an absolute decrease of <math>&gt;20\%</math> from baseline</li> </ul>
Other	<ul style="list-style-type: none"> <li>• Inability to receive <math>\geq 75\%</math> of scheduled doses in treatment period due to toxicity</li> <li>• Grade 2 or higher toxicity that occurs beyond 28 days which in the judgment of the investigator and GSK Medical Monitor is considered to be a DLT</li> </ul>

Abbreviations: DLT, dose-limiting toxicity; ANC, absolute neutrophil count; ALT, alanine aminotransferase; ULN, upper limit of normal; NCI-CTCAE, National Cancer Institute - Common Terminology Criteria for Adverse Events; LLN, lower limit of normal.

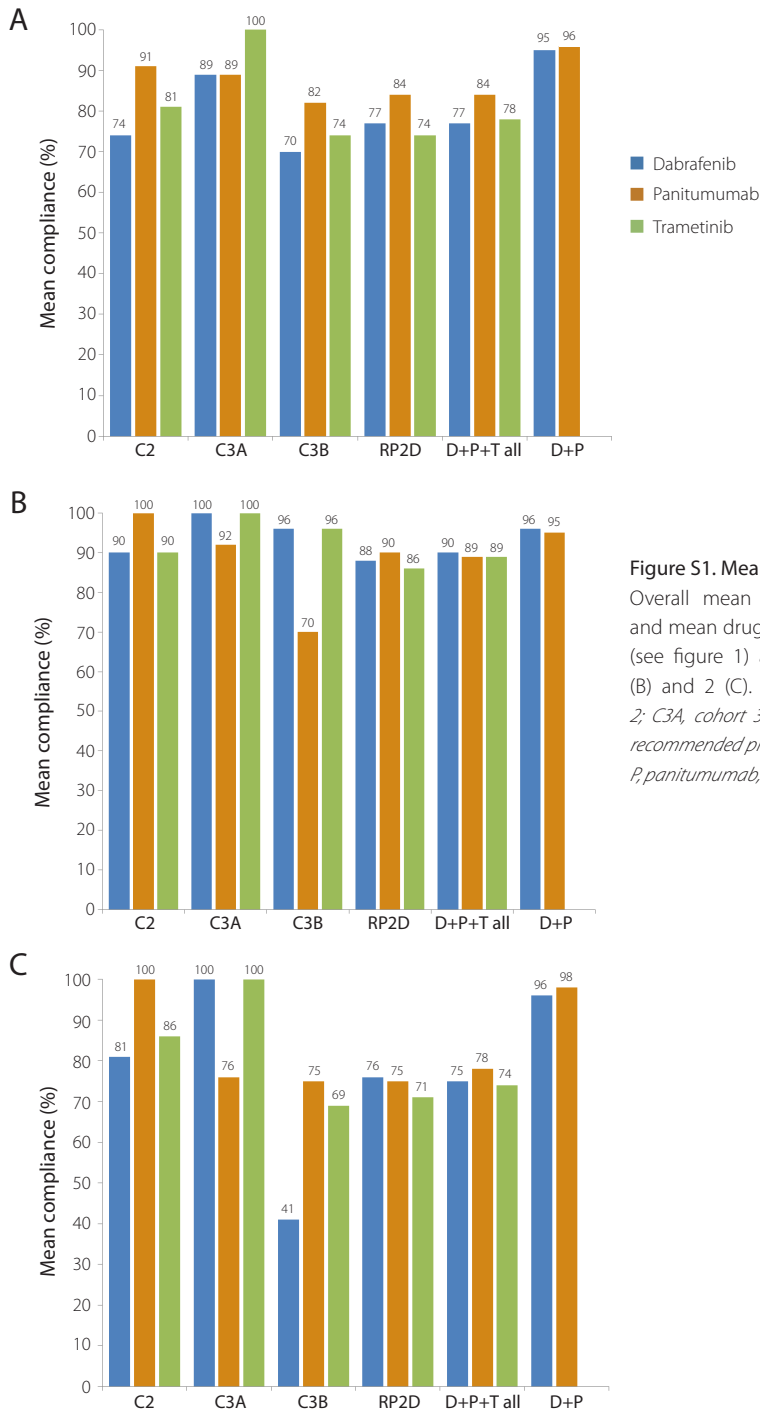
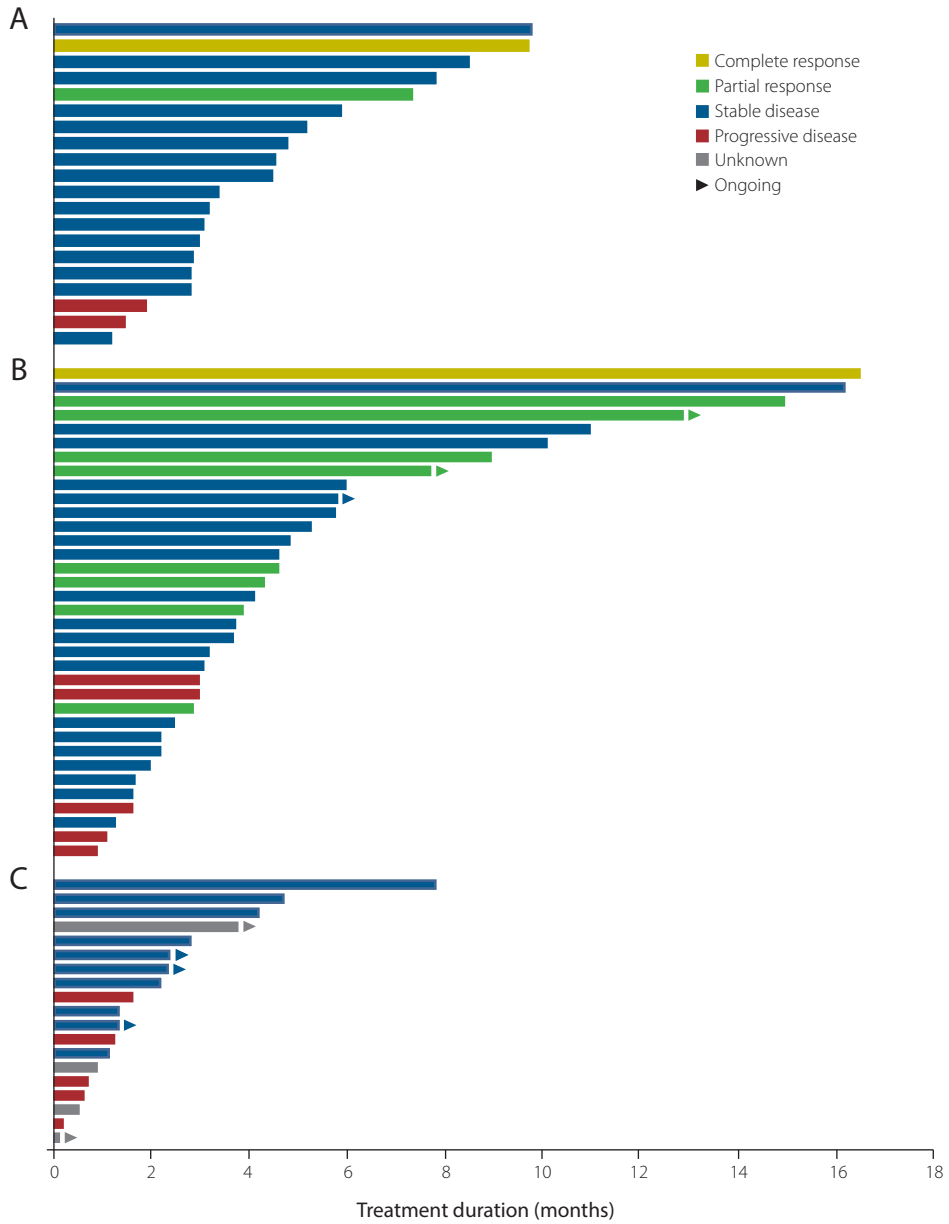


**Figure S1. Mean drug compliance**

Overall mean drug compliance (A), and mean drug compliance by cohort (see figure 1) and treatment cycle 1 (B) and 2 (C). Abbreviations: C2, cohort 2; C3A, cohort 3A; C3B, cohort 3B; RP2D, recommended phase 2 dose; D, dabrafenib; P, panitumumab; T, trametinib



5.3

Figure S2. Treatment duration, by treatment group  
 (A) dabrafenib plus panitumumab. (B) dabrafenib plus panitumumab plus trametinib. (C) trametinib plus panitumumab.



# Chapter 6

## Clinical pharmacology of combined targeted therapy targeting mutated *KRAS*



### 6.1

**Phase I study of dacomitinib plus PD-0325901 in patients with advanced *KRAS* mutation positive colorectal, non-small cell lung and pancreatic cancer**

#### Interim analysis

Robin M.J.M. van Geel, Ferry A.L.M. Eskens, Marlies H.G. Langenberg, Martijn P.J.K. Lolkema, Frans Opdam, Serena Marchetti, Neeltje Steeghs, Maja J.A. de Jonge, Diane A.J. van der Biessen, Filip Y. de Vos, Bas Thijssen, Hilde Rosing, Alejandro Pérez Pitarch, Alwin D.R. Huitema, René Bernards, Jos H. Beijnen, Jan H.M. Schellens

## ABSTRACT

### Background

Mutations in the Kirsten rat sarcoma viral oncogene homolog (*KRAS*) gene are common in several cancer types and result in a constitutively activated RAS-RAF-MEK-ERK (MAPK) pathway. As hyperactive MAPK pathway signaling leads to sustained stimulation of tumorigenic mechanisms, *KRAS* is an attractive target for anti-cancer therapy. However, until now, the development of effective agents acting directly against the *KRAS* protein has been challenging. In addition, *KRAS* mutant (*KRAS*<sup>m</sup>) tumors have been unresponsive to downstream inhibition of MEK as well. Preclinical work showed that *KRAS*<sup>m</sup> cancer cells are intrinsically resistant against MEK inhibition due to feedback activation of upstream tyrosine kinase receptors, providing rationale to investigate combined MEK and upstream receptor inhibition.

### Methods

In this multicenter, open-label, phase I, dose-escalation study we investigated a combination of a human epidermal growth factor receptor (HER) family inhibitor, dacomitinib, plus a selective MEK1/2 inhibitor, PD-0325901, in patients with *KRAS*<sup>m</sup> colorectal cancer (CRC), non-small cell lung cancer (NSCLC) and pancreatic cancer. Patients received escalating doses of once daily oral dacomitinib, administered continuously or intermittently, and twice daily (BID) oral PD-0325901 (21 days on / 7 days off) to determine the recommended phase II dose (RP2D). Starting doses were 30 mg QD dacomitinib and 2 mg BID PD-0325901 (21 days on / 7 days off). The study is registered at ClinicalTrials.gov (NCT02039336).

### Results

We enrolled 33 patients, of whom 25 had CRC, five NSCLC, and three patients had pancreatic cancer. The most common treatment-related adverse events were acneiform rash (94%), diarrhea (85%), and nausea (54%). Dose-limiting toxicities were grade 3 increased liver enzymes, fatigue, skin rash, and the inability to take  $\geq 75\%$  of the assigned dose in the first 4 weeks of treatment due to grade 2 diarrhea and fatigue (all  $n = 1$ ). The MTD with continuous dacomitinib dosing was established at 15 mg dacomitinib QD plus 6 mg PD-0325901 (21 days on / 7 days off). Intermittent dosing schedules are currently being explored. Significant pharmacokinetic drug-drug interactions were not observed. Clinical activity was seen in six patients, of whom five had NSCLC and 1 pancreatic cancer.

### Conclusions

Dacomitinib can be combined safely with PD-0325901, albeit not at full single agent doses, with manageable toxicity. Intermittent dosing schedules will be explored in our effort to enhance anti-tumor activity and to establish a RP2D with an optimal efficacy to toxicity ratio.

## Introduction

The RAS-RAF-MEK-ERK (MAPK) pathway plays a pivotal role in the regulation of cell proliferation, survival and differentiation. Persistent activation of this pathway is frequently observed in human cancers and is associated with high rates of cancer cell proliferation. Commonly, pathway activation occurs as a consequence of oncogenic gain-of-function mutations in Kirsten rat sarcoma viral oncogene homolog (*KRAS*). The *KRAS* protein stimulates multiple downstream effector pathways, which are activated in a growth factor-independent fashion in cancer cells expressing oncogenic *KRAS*.<sup>1-3</sup> The high frequency of *KRAS* mutations in human cancers (~20%)<sup>4</sup> makes targeting of these aberrations an attractive strategy for cancer therapy. However, to date, therapeutic approaches that were developed to target and block *KRAS* directly have been unsuccessful. Small molecule inhibitors against the downstream effectors of *KRAS*, such as MEK, demonstrated only limited anti-tumor activity in *KRAS* mutated (*KRAS*<sub>M</sub>) cancers as well.<sup>5-7</sup>

Preclinical work from Sun and colleagues revealed that in *KRAS*<sub>M</sub> cancer cells, inhibition of MEK leads to feedback activation of upstream tyrosine kinase receptors, human epidermal growth factor receptor 2 (HER2) and 3 (HER3) in particular, causing intrinsic resistance through reactivation of the MAPK and phosphoinositide 3-kinase (PI3K) pathways.<sup>8</sup> Concurrent treatment with a MEK inhibitor and an inhibitor of multiple HER receptor subtypes (pan-HER inhibitor) completely suppressed this feedback activation and resulted in synergistic anti-tumor activity in *KRAS*<sub>M</sub> cells *in vitro* and in xenograft models.<sup>8</sup> As preclinical proof of concept was obtained in *KRAS*<sub>M</sub> colorectal cancer (CRC) and non-small cell lung cancer (NSCLC), we hypothesized the anti-tumor activity of this therapeutic approach is independent of tumor histology. Together with the high frequency of *KRAS* mutations in patients CRC (45%), NSCLC (35%) and pancreatic cancer (90%)<sup>4</sup>, this provided rationale to investigate such a combination of targeted therapy in patients with these tumor types.

In this phase I dose-finding study, we investigated the combination of the potent irreversible ATP-competitive inhibitor (*in vitro* IC<sub>50</sub> values of 6.0 nM, 45.7 nM and 74 nM against the human catalytic domains of HER1, HER2 and HER4) of the HER kinase family dacomitinib with the highly specific non-ATP-competitive inhibitor of MEK1 and MEK2 PD-0325901, in patients with *KRAS*<sub>M</sub> CRC, NSCLC or pancreatic cancer. The primary study objective was to determine the maximum-tolerated dose (MTD) or recommended phase II dose of dacomitinib plus PD-0325901. Secondary objectives included characterizing safety and tolerability, exploring anti-tumor activity, and assessing the pharmacokinetic profiles of dacomitinib and PD-0325901 when given concurrently. Herein, we describe an interim analysis after determination of the MTD of a dosing schedule with continuous dacomitinib administration.

## Patients and Methods

### *Patient population*

This investigator-initiated, multi-center, open-label, phase I dose-escalation study enrolled patients at three sites in the Netherlands. Adult patients with histologically- or cytologically-confirmed advanced CRC, NSCLC or pancreatic cancer were enrolled on the basis of documented *KRAS* mutation in exon 2, 3 or 4, and PIK3CA wildtype status. Eligibility criteria included: Eastern Cooperative Oncology Group (ECOG) performance status of ≤ 2, life expectancy of ≥ 3 months, measurable disease according to

Response Evaluation Criteria In Solid Tumors (RECIST) version 1.1, adequate bone marrow (absolute neutrophil count  $\geq 1.5 \times 10^9/L$ , platelets  $\geq 100 \times 10^9/L$ , hemoglobin  $\geq 6.0$  mmol/L), hepatic (total bilirubin  $\leq 1.5 \times$  upper limit of normal [ULN], aspartate aminotransferase (AST) and alanine aminotransferase (ALT)  $\leq 2.5 \times$  ULN), and renal (serum creatinine  $\leq 1.5 \times$  ULN) functions. Radiotherapy, immunotherapy, chemotherapy or any treatment with investigational medication within 4 weeks prior to study treatment were not allowed, and patients with a history of other primary malignancies were excluded. Additional exclusion criteria included symptomatic or untreated leptomeningeal disease, symptomatic brain metastasis, history of interstitial lung disease or pneumonitis, history of retinal vein occlusion, and prior therapy containing targeted drug combinations known to interfere with EGFR, HER2, HER3, HER4 or MAPK- and PI3K-pathway components, including PI3K, AKT, mTOR, BRAF, MEK and ERK. The study (ClinicalTrials.gov identifier: NCT02039336) was conducted in accordance with guidelines for Good Clinical Practice as defined by the International Conference on Harmonization. Regulatory authorities and the institutional review boards approved the study protocol, and all patients gave written informed consent, per Declaration of Helsinki recommendations. Pfizer Inc. funded this study and provided the investigational drugs dacomitinib and PD-0325901.

### ***Study design and procedures***

Patients were treated at varying dose-levels of orally administered dacomitinib and PD-0325901 in cycles of 28 days. The starting doses were chosen based on previous data from single agent phase I studies with both compounds. Dose-level 1 consisted of 30 mg dacomitinib once daily (QD) continuously, which is 67% of its single agent MTD, and 2 mg PD-0325901 twice daily (BID) administered on the first 21 days of each 28-day cycle, which is 25% of its single agent MTD. Subsequently, PD-0325901 was escalated according to a classical 3 + 3 design with fixed maximum escalation increments. Dose-escalation decisions were based on safety evaluation of all evaluable patients, performed after completion of the first treatment cycle. Patients were considered evaluable for the dose-determining set if at least 1 cycle of study treatment was completed, with the minimum safety evaluation and drug exposure ( $\geq 75\%$  of the planned doses of dacomitinib and PD-0325901) or if dose-limiting toxicity (DLT) had occurred during the first cycle. If one out of three patients experienced DLT, the number of patients treated at that dose-level was expanded to a maximum of six. Dose-escalation continued until a dose-level was reached at which no more than one out of six patients experienced DLT during the first 28 days of treatment, provided that the single agent MTD of both compounds were not exceeded. Upon assessment of the MTD of the two-drug combination with continuously dosed dacomitinib, intermittent dacomitinib dosing was investigated to optimize drug exposure and to enable selection of the optimal dose and schedule. Patients were to continue study treatment until disease progression, unacceptable toxicity, or investigator/patient decision to discontinue.

Safety was monitored throughout the treatment by physical examination, laboratory assessments, electrocardiography, ophthalmic evaluation, and collection of adverse events. Adverse events were graded according to Common Terminology Criteria for Adverse Events version 4.0. DLT was defined as an adverse event or laboratory abnormality occurring within the first treatment cycle that meets at least one of the criteria described in supplementary table S1.

Radiologic tumor measurements were performed using computed tomography scans at baseline and every 6 weeks throughout the study. Tumor response was evaluated according to RECIST version



1.1.<sup>9</sup> Patients were evaluable for anti-tumor activity if at least one follow-up radiologic evaluation was performed after 6 weeks of study treatment.

When feasible, patients underwent tumor biopsies prior to study treatment initiation and upon progression. Whole genome sequencing of tumor tissue was used to explore potential determinants of response and mechanisms of resistance.

### **Pharmacokinetic analysis**

Serial blood samples for plasma concentration analysis were obtained from all patients prior to treatment administration on day 1, and 1, 2, 3, 4, 6, 8, 12, 24, 72, and 144 hours after the first dose. On day 1 of cycle 2, blood samples were drawn before and 1, 2, 3, 4, 6, 8, 12 and 24 hours after administration. Plasma samples were assayed using a validated high performance liquid chromatography method coupled with tandem mass spectrometry (LC-MS/MS). Briefly, dacomitinib and PD-0325901 were extracted from plasma by protein precipitation using acetonitrile/methanol. A Waters Xbridge BEH Phenyl column with gradient elution was used for chromatographic separation, and compound detection was performed using an API4000 tandem mass spectrometer equipped with a turbo ion spray interface, operating in the positive ion mode. Pharmacokinetic parameters were calculated using non-compartmental analysis in R using package 'PK' (version 1.3).

Population pharmacokinetic models were developed using the non-linear mixed-effects modeling approach in the NONMEM 7.3 software package (ICON Development Solutions, Hanover, MD, USA). Pharmacokinetic data for dacomitinib and for PD-0325901 were first modeled independently and then correlation between model parameters and possible PK interactions between both models were explored. The first-order conditional estimation method with interaction was used for all model runs in NONMEM. A base population pharmacokinetic model was developed that defined the structural model, as well as models for the between-subject and residual variabilities. Between-subject variability (BSV) in pharmacokinetic parameters was modeled using an exponential error model:

$$\theta_i = TV\theta \times \exp(\eta^{i})$$

where  $\theta_i$  is the parameter estimate for the  $i$ th individual,  $\theta$  is the typical value of the parameter in the population, and  $\eta^{i}$  are individual-specific random effects for the  $i$ th individual and assumed to be normally distributed with mean 0 and variance  $\omega^2$ :  $\eta \sim N(0, \omega^2)$ . Proportional, exponential and additive-proportional error models were tested to describe residual variability.

One-, two- and three-compartment models with linear absorption and elimination were fitted to the data during the initial stage of model building. Elimination was assumed to take place from the central plasma compartment. Absorption, which revealed to be highly variable for both drugs, was modeled using transit compartments to mimic the delay in absorption and the gradual increase in absorption rate. As an internal validation method, a bootstrap resampling and re-estimation technic was employed ( $n = 200$ ). Median and confidence interval for parameter estimates were calculated taking into account only those runs that finished successfully and without boundary problems.

## Results

### *Patient disposition and characteristics*

In total, 33 patients were enrolled onto this study between April 2014 and December 2015, 25 patients (76%) with CRC, five with NSCLC (15%) and three (9%) with pancreatic cancer. The majority of patients had *KRAS* exon 2 mutations and were pretreated with at least two prior lines of antineoplastic therapy for advanced disease (Table 1). Thirty patients were evaluable for dose-determination; 3 patients were considered not evaluable due to clinical deterioration, patient refusal and mistakenly administration of the wrong dose. At data cut off, two patients were ongoing (Figure 1), and 31 patients had discontinued treatment due to progressive disease ( $n = 25$ ), adverse events ( $n = 3$ ), clinical deterioration ( $n = 2$ ), or patient refusal ( $n = 1$ ).

### *Safety*

Study treatment-related adverse events were reported in all patients, with the most common being rash acneiform (94%), diarrhea (85%), nausea (54%), fatigue (45%), and vomiting (45%). The most frequent grade 3 events were diarrhea (24%), nausea (12%), and fatigue (9%) (Table 2). Asymptomatic central serous retinopathy was observed in two patients in dose-level 5 and 6, including one patient with an asymptomatic unilateral retinal pigment epithelium detachment. The latter patient continued study treatment without further progression of ocular toxicity. Rash was predominantly acneiform and maculopapular in nature, mainly on the face, and upper chest and back. Supportive care, including minocycline and cetomacrogol cream or corticosteroid cream were sufficient to manage these events, with the exception of one patient in dose-level 5. Cases of retinal vein occlusion were not seen in this study. Grade 3 diarrhea, nausea, and vomiting events were mostly manageable and improved to  $\leq$  grade 1 with supportive medication.

### *Dose determination*

Three out of six patients treated at the initial dose-level experienced DLTs, being grade 3 increased AST/ALT, grade 3 fatigue, and inability to receive at least 75% of the planned dose due to grade 2 fatigue and diarrhea. Therefore, we decided to continue with a reduced dacomitinib dose of 15 mg in a continuous dosing schedule to allow for escalation of PD-0325901. In the subsequent dose-levels, DLTs were reported in two out of 27 patients; grade 3 AST/ALT increase (dose-level 2) and grade 3 skin rash (dose-level 5), respectively (Figure 1). Although the formal MTD was not reached, we decided to stop escalation of PD-0325901 in view of the increasing number of grade 2 adverse events (e.g. diarrhea, nausea, fatigue) beyond the DLT window of 28 days, together with the emergence of ocular toxicity

**Table 2. Patient and disease characteristics at baseline**

	Patients ( $n = 33$ )	
<b>Sex, <math>n</math> (%)</b>		
Female	18	(55%)
Male	15	(45%)
<b>Age, median (range), years</b>	62	(43–81)
<b>Tumor type, <math>n</math> (%)</b>		
Colonrectal	25	(76%)
Non-small cell lung	5	(15%)
Pancreatic	3	(9%)
<b>ECOG PS, <math>n</math> (%)</b>		
0	13	(39%)
1	20	(61%)
<b>Number of prior treatment regimens, <math>n</math> (%)</b>		
0	1	(3%)
1	6	(18%)
2	11	(33%)
$\geq 3$	15	(46%)
<b><i>KRAS</i> mutation, <math>n</math> (%)</b>		
Exon 2	30	(91%)
Exon 3	2	(6%)
Exon 4	1	(3%)

Abbreviations: ECOG PS, Eastern Cooperative Oncology Group performance status.

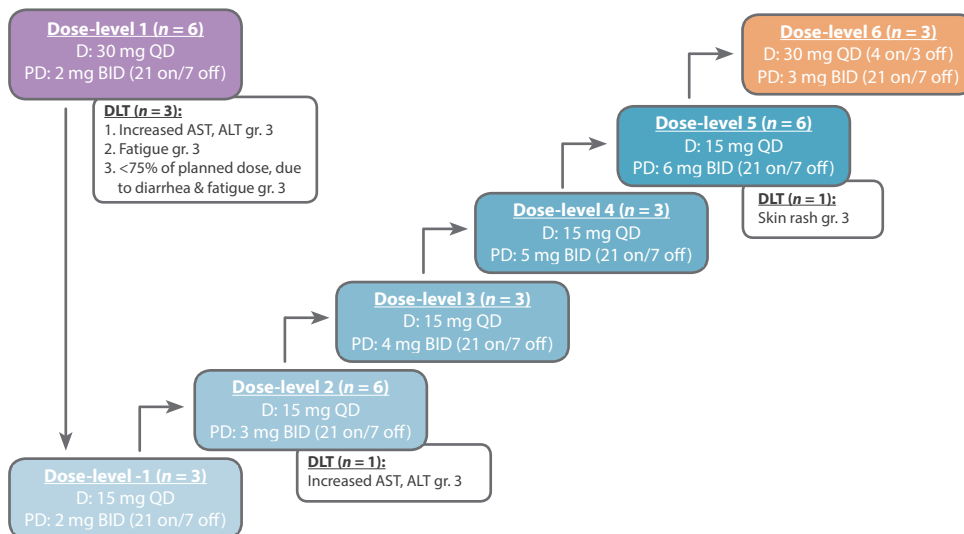


**Figure 1. Dose-escalation cohorts and dose-limiting toxicities**

Abbreviations: DLT, dose-limiting toxicity; D, dacomitinib; PD, PD-0325901; QD, once daily; BID, twice daily; AST, aspartate transaminase; ALT, alanine transaminase

at dose-level 5 and the potential for more severe ocular toxicity at higher PD-0325901 doses<sup>10,11</sup>. Consequently, the established maximum dose-level with continuous dacomitinib dosing consisted of 15 mg dacomitinib QD plus 6 mg PD-0325901 BID. In view of the available tablet strengths of dacomitinib, escalation with increments smaller than 15 mg was not possible. Therefore, as increasing dacomitinib exposure was justified according to safety, pharmacokinetic, and anti-tumor activity data, it was decided to continue with intermittent dacomitinib dosing. At the time of data cut off, this part of the study was ongoing.

6.1

**Pharmacokinetic analysis**

Pharmacokinetic parameters after the first dose and at steady-state are summarized in Table 3. PD-0325901 and dacomitinib exposure increased approximately dose-proportionally with moderate and high inter-patient variability, respectively (Figure S1). The mean dacomitinib peak plasma concentration (C<sub>max</sub>) and area under the plasma concentration-time curve from time 0 to 24 hours (AUC<sub>0-24h</sub>) increased approximately 3-fold after multiple dosing.

Population pharmacokinetic analysis for dacomitinib demonstrated that a 2-compartment model with 1 absorption transit compartment showed the best model fit. Population pharmacokinetic analysis for PD-0325901 resulted in a 3-compartment model with 3 absorption transit compartments. Final model parameters and bootstrap validation results are displayed in Table S2.

**Anti-tumor activity**

Thirty patients were evaluable for anti-tumor activity; three patients did not reach the first radiological evaluation after 8 weeks of study treatment due to clinical deterioration (n = 2) or patient refusal. Out of the evaluable patients, 16 achieved stable disease and 14 had progressive disease on their first

**Table 2. Treatment-related adverse events, occurring in ≥ 15% of patients**

Adverse event, n (%)	DL 1 (n = 6)		DL-1 (n = 4)		DL 2 (n = 6)		DL 3 (n = 3)		DL 4 (n = 3)		DL 5 (n = 8)		DL 6 (n = 3)		Total (n = 33)
	Gr. 1/2	Gr. 3	Gr. 1/2	Gr. 3	Gr. 1/2	Gr. 3	Gr. 1/2	Gr. 3	Gr. 1/2	Gr. 3	Gr. 1/2	Gr. 3	Gr. 1/2	Gr. 3	
<i>Dacomitinib QD</i>	30 mg	2 mg	15 mg	2 mg	15 mg	3 mg	15 mg	4 mg	15 mg	5 mg	15 mg	6 mg	30 mg	4/3	6 mg
<i>PD-0325901 BID</i>	30 mg	2 mg	15 mg	2 mg	15 mg	3 mg	15 mg	4 mg	15 mg	5 mg	15 mg	6 mg	30 mg	4/3	6 mg
Any skin toxicity	6 (100)	0	3 (75)	1 (25)	6 (100)	0	3 (100)	0	3 (100)	0	8 (100)	1 (13)	2 (67)	0	32 (97)
Rash acneiform	6 (100)	0	2 (50)	1 (25)	6 (100)	0	3 (100)	0	3 (100)	0	7 (88)	1 (13)	2 (67)	0	29 (88)
Hand-foot syndrome	0	0	1 (25)	0	1 (17)	0	1 (33)	0	1 (33)	0	2 (25)	0	0	0	6 (18)
Dry skin	3 (50)	0	0	0	1 (17)	0	0	0	0	0	2 (25)	0	0	0	6 (18)
Other*	5 (83)	0	0	0	0 (17)	0	1 (33)	0	0	0	3 (38)	0	0	0	9 (27)
Diarrhea	2 (33)	3 (50)	4 (100)	0	4 (67)	0	1 (33)	1 (33)	1 (33)	0	4 (50)	3 (38)	2 (67)	1 (33)	20 (61)
Nausea	2 (33)	1 (17)	3 (75)	0	1 (17)	1 (17)	2 (67)	0	1 (33)	1 (33)	3 (38)	1 (13)	2 (67)	0	14 (42)
Vomiting	2 (33)	0	3 (75)	0	1 (17)	1 (17)	2 (67)	0	1 (33)	0	4 (50)	1 (13)	0	0	13 (39)
Fatigue	3 (50)	1 (17)	1 (25)	0	1 (17)	1 (17)	1 (33)	0	0	0	3 (38)	0	0	1 (33)	12 (36)
Mucositis	1 (17)	0	2 (50)	0	1 (17)	0	1 (33)	0	0	0	3 (100)	0	1 (33)	0	9 (27)
CPK increased	1 (17)	1 (17)	0	0	2 (33)	0	1 (33)	0	1 (33)	0	2 (25)	0	2 (67)	0	9 (27)
ALT/AST increased	3 (50)	1 (17)	0	0	1 (17)	1 (17)	0	0	1 (33)	0	1 (17)	0	1 (33)	0	7 (21)
Weight loss	3 (50)	0	1 (25)	0	1 (17)	0	0	0	0	0	1 (17)	0	0	0	6 (18)
Alopecia	3 (50)	0	1 (25)	0	1 (17)	0	1 (33)	0	0	0	1 (17)	0	0	0	6 (18)

\* Includes pruritis, paronychia, skin pain, erythema and skin infection

Abbreviations: DL, dose-level; QD, once daily; BID, twice daily; ALT/AST, alanine/aspartate transaminase; 4/3, 4 days on / 3 days off; Gr, grade.

**Table 3. Pharmacokinetic parameters of dacomitinib and PD-0325901, at baseline and steady-state, per dose-level**

	DL 1	DL-1	DL 2	DL 3	DL 4	DL 5
<i>Dacomitinib QD</i>	<b>30 mg</b>	<b>15 mg</b>	<b>15 mg</b>	<b>15 mg</b>	<b>15 mg</b>	<b>15 mg</b>
<i>PD-0325901 BID</i>	<b>2 mg</b>	<b>2 mg</b>	<b>3 mg</b>	<b>4 mg</b>	<b>5 m</b>	<b>6 mg</b>
<i>Cycle 1 Day 1</i>						
<b>Dacomitinib, Mean (CV%)</b>	<i>n</i> = 6	<i>n</i> = 4	<i>n</i> = 6	<i>n</i> = 3	<i>n</i> = 3	<i>n</i> = 8
$C_{max}$ (ng/mL)	19.2 (52)	7.9 (43)	6.7 (61)	5.6 (98)	8.5 (11)	12.7 (66)
$T_{max}$ (h)	7.67	5.5	8.7	10	4.7	7.3
$AUC_{0-24h}$ (ng·h/mL)	320 (18)	127 (27)	112 (42)	92 (37)	139 (10)	146 (28)
$T_{1/2}$	41	54	41	N/C	32	28
<i>Cycle 2 Day 1*</i>						
<b>Dacomitinib, Mean (CV%)</b>	<i>n</i> = 3	<i>n</i> = 2	<i>n</i> = 5	<i>n</i> = 2	<i>n</i> = 2	<i>n</i> = 4
$C_{max}$ (ng/mL)	64.9 (51)	28.1 (78)	26.0 (44)	33.6 (42)	33.5 (47)	37.3 (33)
$T_{max}$ (h)	4	11	9.6	3	5	4.4
$AUC_{0-24h}$ (ng·h/mL)	1203 (26)	511 (41)	539 (28)	632 (17)	634 (18)	716 (22)
<i>Cycle 1 Day 1</i>						
<b>PD-0325901, Mean (CV%)</b>	<i>n</i> = 6	<i>n</i> = 4	<i>n</i> = 6	<i>n</i> = 3	<i>n</i> = 3	<i>n</i> = 8
$C_{max}$ (h)	68.7 (32)	43.7 (59)	85.0 (29)	113 (11)	179 (83)	287 (15)
$T_{max}$ (h)	1.2	1.3	1.2	1.7	1.3	1.1
$AUC_{0-12h}$ (ng·h/mL)	159 (11)	150 (16)	236 (9)	362 (25)	476 (22)	694 (18)
$T_{1/2}$	8.1	7.9	6.4	8.3	7.8	6.1
<i>Cycle 2 Day 1</i>						
<b>PD-0325901, Mean (CV%)</b>	<i>n</i> = 6	<i>n</i> = 2	<i>n</i> = 5	<i>n</i> = 2	<i>n</i> = 3	<i>n</i> = 5
$C_{max}$ (h)	69.3 (57)	55.4 (27)	62.4 (81)	125 (62)	234 (82)	243 (25)
$T_{max}$ (h)	1	1.7	1.6	1	1	1.2
$AUC_{0-12h}$ (ng·h/mL)	155 (15)	172 (20)	255 (21)	289 (17)	518 (29)	765 (21)
$T_{1/2}$	N/C	11.4	8.8	6.6	10.8	7.6

\* Data from patients with dacomitinib dose interruptions less than 7 days prior to cycle 2 day 1 were excluded in this analysis. Abbreviations: DL, dose-level; QD, once daily; BID, twice daily;  $C_{max}$ , peak plasma concentration;  $T_{max}$ , time of maximum plasma concentration observed;  $AUC_{0-24h}$ , area under the plasma concentration-time curve from time zero to 24 hours;  $AUC_{0-12h}$ , area under the plasma concentration-time curve from time zero to 12 hours;  $T_{1/2}$ , elimination half-life; N/C, could not be calculated; 4/3, 4 days on / 3 days off

radiologic evaluation scan. Tumor regression was seen in six (20%) patients treated at dose-levels 1, 3, 5 and 6. Out of the five evaluable patients with NSCLC, four achieved tumor regression within the limits of stable disease according to RECIST v1.1 criteria and one had no change in target lesion volume as best response (Figure 2). The overall median treatment duration was 53 days (range 12–469), with two CRC patients ongoing after 91 and 168 days. Patients with NSCLC achieved the longest median treatment duration, 139 days (range 84–239), versus 83 days (61–83) for patients with pancreatic cancer and 49 days (range 12–469) for patients with CRC. Across the differential dose-levels, median treatment duration was the longest with the 30 mg dacomitinib containing dose-level 1 (239 days, range 42–469), followed by dose-level 5 (89 days, range 12–182) and 6 (91 days, range 49–96), both with the highest PD-325901 dose and the latter with 30 mg dacomitinib on a 4 days on, 3 days off dosing schedule (Figure 3).

6.1

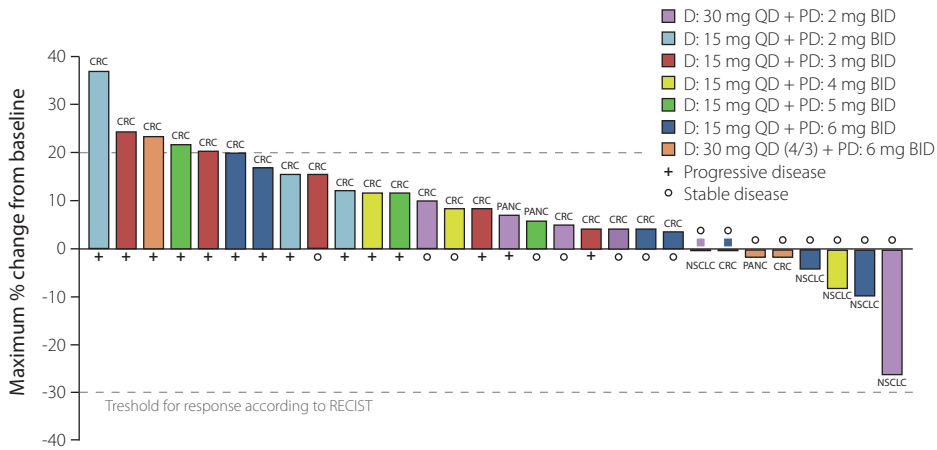


Figure 2. Maximum percentage change in sum of target lesion size from baseline, by dose-level.  
 Abbreviations: D, dacomitinib; PD, PD-0325901; QD, once daily; BID, twice daily; 4/3, 4 days on / 3 days off; CRC, colorectal cancer; NSCLC, non-small cell lung cancer; PANC, pancreatic cancer.

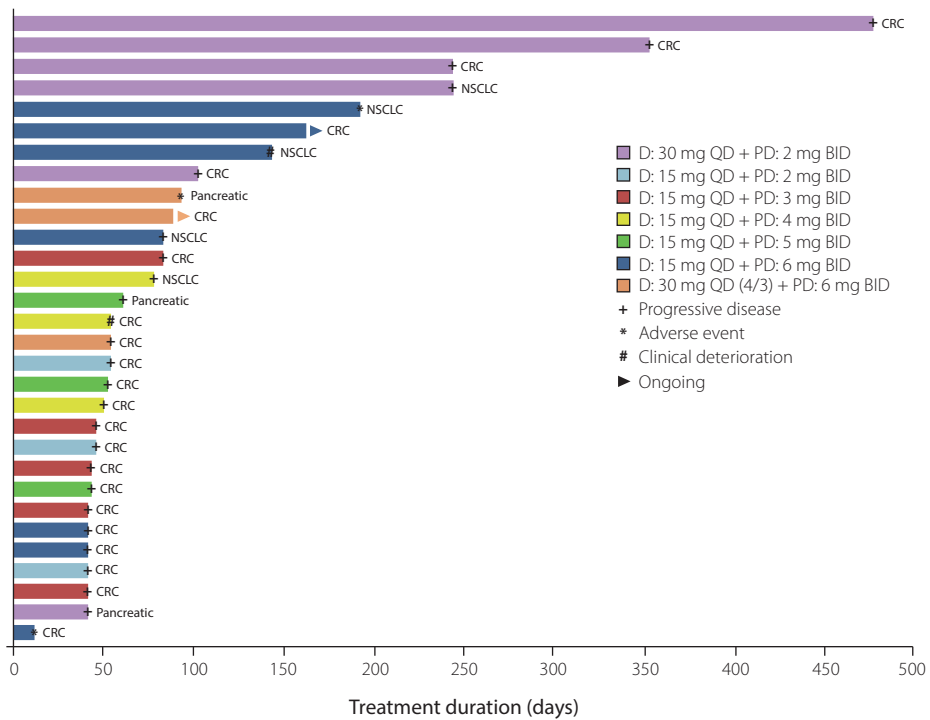


Figure 3. Swimmer plot of treatment duration, by dose-level.  
 Symbols at the end of each bar represent the reason for end of treatment for each individual patient.  
 Abbreviations: D, dacomitinib; PD, PD-0325901; QD, once daily; BID, twice daily; CRC, colorectal cancer; NSCLC, non-small cell lung cancer; 4/3, 4 days on / 3 days off.

## Discussion

In this clinical study we investigated a combination of a MEK inhibitor (PD-0325901) with a panHER inhibitor (dacomitinib). Herein, we demonstrated that dacomitinib combines safely with PD-0325901, although not at full single agent doses. In a previous phase I dose-escalation study, PD-0325901 doses up to 20 mg BID in a continuous dosing schedule, 30 mg BID in a 21 days on / 7 days off schedule, and 10 mg in a 5 days on / 2 days off schedule were investigated. Although formal MTDs were established as 15 mg BID and 10 mg BID on continuous and 5 days on / 2 days off schedules, respectively, occurrence of ocular toxicity, retinal vein occlusion in particular, prevented a clear definition of a recommended phase II dose.<sup>10</sup> As dacomitinib shows potential overlapping toxicity with PD-0325901, we decided to initiate our study with reduced doses of both agents, being 2 mg PD-0325901 BID in a 21 days on / 7 days off schedule and 30 mg dacomitinib QD. Although relatively low, these doses demonstrated target engagement and clinical activity in their respective single agent studies.<sup>10,12</sup> Nevertheless, the initial dose-level was already intolerable as indicated by DLTs in three out of six patients. Given the relatively low dose of PD-0325901 in relation to its single agent maximum-tolerated dose, toxicity was likely to be associated with dacomitinib in particular. Therefore, the dacomitinib dose was reduced to enable dose-escalation of PD-0325901, as we hypothesized that robust MEK inhibition was necessary to block the *KRAS*-activated MAPK pathway before tumor cells activate their escape mechanism through upstream tyrosine kinase receptors.<sup>8</sup> Because ocular toxicity, *i.e.* asymptomatic central serous retinopathy, started to emerge at the 5 mg and 6 mg dose-levels, we halted dose escalation at 6 mg and established the maximum tolerated dose with continuous dacomitinib dosing as 15 mg dacomitinib QD plus 6 mg PD-0325901 BID 21 days on / 7 days off. At a dose of 6 mg, the plasma concentration of PD-0325901 exceeded the minimum level (16.5 ng/mL), consistent with target inhibition based on xenograft mouse models<sup>13</sup>, during the entire dose interval.

The formal MTD was not reached, allowing us to explore other dosing schedules. Moreover, since the available clinical efficacy data demonstrated a significantly longer time to progression in patients treated on the 30 mg dacomitinib dose-level (Figure 3), and given the lack of dacomitinib tablet strengths smaller than 15 mg, exploration of intermittent dacomitinib dosing schedules in an effort to optimize anti-tumor activity without adding too much toxicity was justified. This strategy was supported by simulations of intermittent dosing schedules in our pharmacokinetic model, indicating exposure between ranges of 15 mg and 30 mg dacomitinib (Figure S2). Dacomitinib 30 mg QD 4 days on / 3 days off combined with PD-0325901 6 mg BID 21 days on / 7 days off was safe and well tolerated and further escalation to a 5 days on / 2 days off schedule is currently ongoing.

Standard pharmacokinetic parameters of both agents were largely within the previously reported ranges in their respective single agent studies.<sup>10,12</sup> The low number of patients in each dose-level, together with the high interpatient variability in dacomitinib's pharmacokinetic parameters may explain the low dacomitinib exposure in dose-level 6 relative to dose-level 1 (Table 2). No significant correlation between the parameter estimates in both described models was identified. Interestingly, a significant decrease in objective function value was evident when the inhibition of dacomitinib elimination by PD-0325901 was included in the model. However, as BSV reduction was <20%, the interaction was considered not clinically significant.

Patients with metastatic *KRAS*<sup>m</sup> tumors represent an extremely difficult-to-treat population. Multiple strategies to target *KRAS* have been explored, including farnesyltransferase inhibitors, small molecules

interfering with the prenyl-binding protein PDE $\delta$ -KRAS interaction, and small molecules targeting downstream effectors of KRAS, e.g. RAF, MEK, or PI3K. However, none of these approaches was successful.<sup>6,14,15</sup> Since all these strategies rely on targeting one protein or pathway, a complicating factor lies in the fact that many cellular signaling pathways are interconnected, providing tumor cells escape routes.<sup>16</sup> Elucidating the predominant mechanism of resistance may yield novel treatment opportunities. Previously, we demonstrated clinical proof of concept for combining BRAF and EGFR inhibition in patients with *BRAF*<sup>m</sup> CRC<sup>17</sup>, based on a synthetic lethality drug screen.<sup>18</sup> Similarly, in *KRAS*<sup>m</sup> cells, inhibition of MEK was found to synergize with HER2 and HER3 inhibition in an identical screen to identify synthetic lethal interactions.<sup>8</sup> However, in contrast to these preclinical observations, the preliminary clinical activity with dacomitinib plus PD-0325901 in *KRAS*<sup>m</sup> tumors was relatively low. Although dose-escalation is ongoing, toxicity restricted combining full single agent doses, which potentially limits clinical anti-tumor activity due to lower exposure. It remains to be established whether any of the currently explored dose levels in intermittent schedules will do better clinically. Another explanation for the limited anti-tumor activity thus far may lie in the extensive inter-pathway connections of the KRAS protein. Although we excluded patients with concurrent *KRAS* and *PIK3CA* mutations, activation of the PI3K pathway may as well be triggered by mutated *KRAS* directly, particularly in the presence of downstream MEK inhibition.<sup>19</sup> Additionally, reactivation of the MAPK pathway may occur as well, analogous to the observation with BRAF inhibition in *BRAF*<sup>m</sup> CRC cells<sup>20</sup>, especially when upstream receptors are not adequately inhibited. Indeed, although this concerns a small cohort, patients treated on the 30 mg dacomitinib dose-level had disease stabilization for a longer period of time compared to patients on dose-levels containing 15 mg dacomitinib (Figure 3). Incorporation of on-study biopsies for pharmacodynamic analyses in the ongoing study may help to shed light on this hypothesis by comparing baseline and on-treatment pERK and pS6 staining intensity as a marker for MAPK and PI3K pathway activity, respectively.

Interestingly, four out of five patients (80%) with NSCLC achieved tumor regressions, compared to one out of 22 patients (5%) with CRC (Figure 2). In addition, the median treatment duration in patients with NSCLC (139 days) was longer than that of CRC patients (49 days), suggesting a difference in sensitivity to study treatment between these histological subtypes (Figure 3). A finding that was also reflected by the results of two separate studies, showing lack of benefit of adding a MEK inhibitor to second line irinotecan therapy in patients with *KRAS*<sup>m</sup> CRC, but improved response rate and progression-free survival of patients with *KRAS*<sup>m</sup> NSCLC by the addition of the MEK inhibitor selumetinib to second line treatment with docetaxel.<sup>7,21</sup> Elucidating the underlying mechanism to explain differences in sensitivity may help to identify predictive biomarkers. As HER3 protein expression levels seemed to have predictive potential in preclinical studies<sup>8</sup>, evaluation of HER3 expression in patient samples could be considered.

In recent years, various treatment strategies for *KRAS*<sup>m</sup> tumors have emerged from synthetic lethal screens and new agents have been developed.<sup>22,23</sup> Promising combination therapies are currently under investigation in the clinic, including a MEK inhibitor plus the BCL-XL inhibitor navitoclax (NCT02079740), after showing substantial apoptosis in *KRAS*<sup>m</sup> CRC, NSCLC, and pancreatic cell lines.<sup>24</sup> In addition, researchers are working towards designing small molecules tailored to the surface of KRAS proteins, while others develop small molecules that target KRAS in a mutation-specific manner<sup>25-27</sup> or focus on deploying small interfering RNA to target KRAS.<sup>28-30</sup> Time will tell whether any of these



strategies will have clinical significance.

In conclusion, the combination of dacomitinib plus PD-0325901 was tolerable albeit only at doses lower than the recommended single agent doses. There were no signs of significant pharmacokinetic drug-drug interactions. So far, only modest clinical activity was observed, potentially due to toxicity that prevented high continuous dosing of dacomitinib. The ongoing study will focus on confirming the signs of activity in more patients and on finding a dose-level that has an optimal efficacy to toxicity ratio.

## References

1. Montagut C, Settleman J. Targeting the RAF-MEK-ERK pathway in cancer therapy. *Cancer Lett* 2009;283:125–34.
2. Roberts P, Der C. Targeting the Raf-MEK-ERK mitogen-activated protein kinase cascade for the treatment of cancer. *Oncogene* 2007;26:3291–310.
3. Dhillon, Hagan, Rath, Kolch. MAP kinase signalling pathways in cancer. *Oncogene* 2007;26:3279–90.
4. Downward J. Targeting RAS signalling pathways in cancer therapy. *Nat Rev Cancer* 2003;3:11–22.
5. Migliardi G, Sassi F, Torti D, et al. Inhibition of MEK and PI3K/mTOR suppresses tumor growth but does not cause tumor regression in patient-derived xenografts of RAS-mutant colorectal carcinomas. *Clin Cancer Res* 2012;18:2515–25.
6. Adjei AA, Cohen RB, Franklin W, et al. Phase I pharmacokinetic and pharmacodynamic study of the oral, small-molecule mitogen-activated protein kinase kinase 1/2 inhibitor AZD6244 (ARRY-142886) in patients with advanced cancers. *J Clin Oncol* 2008;26:2139–46.
7. Jänne PA, Shaw AT, Pereira JR, et al. Selumetinib plus docetaxel for *KRAS*-mutant advanced non-small-cell lung cancer: A randomised, multicentre, placebo-controlled, phase 2 study. *Lancet Oncol* 2013;14:38–47.
8. Sun C, Hobor S, Bertotti A, et al. Intrinsic resistance to MEK inhibition in *kras* mutant lung and colon cancer through transcriptional induction of ERBB3. *Cell* 2014;7:86–93.
9. Eisenhauer EA, Therasse P, Bogaerts J, et al. New response evaluation criteria in solid tumours: Revised RECIST guideline (version 1.1). *Eur J Cancer* 2009;45:228–47.
10. LoRusso PM, Krishnamurthi SS, Rinehart JJ, et al. Phase I pharmacokinetic and pharmacodynamic study of the oral MAPK/ERK kinase inhibitor PD-0325901 in patients with advanced cancers. *Clin Cancer Res* 2010;16:1924–37.
11. Haura EB, Ricart AD, Larson TG, et al. A phase II study of PD-0325901, an oral MEK inhibitor, in previously treated patients with advanced non-small cell lung cancer. *Clin Cancer Res* 2010;16:2450–7.
12. Jänne PA, Boss DS, Camidge DR, et al. Phase I dose-escalation study of the pan-HER inhibitor, PF299804, in patients with advanced malignant solid tumors. *Clin Cancer Res* 2011;17:1131–9.
13. Mansour SJ, Matten WT, Hermann AS, et al. Transformation of mammalian cells by constitutively active MAP kinase kinase. *Science* 1994;265:966–70.
14. Samatar AA, Poulidakos PI. Targeting RAS–ERK signalling in cancer: promises and challenges. *Nat Rev Drug Discov* 2014;13:928–42.
15. Baines AT, Xu D, Der CJ. Inhibition of Ras for cancer treatment: the search continues. *Future Med Chem* 2011;3:1787–808.
16. Bernards R. A missing link in genotype-directed cancer therapy. *Cell* 2012;151:465–8.
17. Van Geel R, Elez E, Bendell JC, et al. Phase I study of the selective BRAF V600 inhibitor encorafenib (LGX818) combined with cetuximab and with or without the  $\alpha$ -specific PI3K inhibitor BYL719 in patients with advanced BRAF -mutant colorectal cancer. *J Clin Oncol* 2014;32:5s: (suppl; abstr 3514).
18. Prahallad A, Sun C, Huang S, et al. Unresponsiveness of colon cancer to BRAF(V600E) inhibition through feedback activation of EGFR. *Nature* 2012;483:100–3.

19. Engelman J a, Chen L, Tan X, et al. Effective use of PI3K and MEK inhibitors to treat mutant Kras G12D and PIK3CA H1047R murine lung cancers. *Nat Med* 2008;14:1351–6.
20. Corcoran RB, Ebi H, Turke AB, et al. EGFR-mediated reactivation of MAPK signaling contributes to insensitivity of BRAF-mutant colorectal cancers to RAF inhibition with vemurafenib. *Cancer Discov* 2012;2:227–35.
21. Hochster HS, Uboha N, Messersmith W, et al. Phase II study of selumetinib (AZD6244, ARRY-142886) plus irinotecan as second-line therapy in patients with K-RAS mutated colorectal cancer. *Cancer Chemother Pharmacol* 2015;75:17–23.
22. Fece de la Cruz F, Gapp B V, Nijman SMB. Synthetic lethal vulnerabilities of cancer. *Annu Rev Pharmacol Toxicol* 2015;55:513–31.
23. Knickelbein K, Zhang L. Mutant KRAS as a critical determinant of the therapeutic response of colorectal cancer. *Genes Dis* 2015;2:4–12.
24. Corcoran RB, Cheng KA, Hata AN, et al. Synthetic Lethal Interaction of Combined BCL-XL and MEK Inhibition Promotes Tumor Regressions in KRAS Mutant Cancer Models. *Cancer Cell* 2013;23:121–8.
25. Ledford H. Cancer: The Ras renaissance. *Nature* 2015;520:278–80.
26. Ostrem JM, Peters U, Sos ML, et al. K-Ras(G12C) inhibitors allosterically control GTP affinity and effector interactions. *Nature* 2013;503:548–51.
27. McCormick F. KRAS as a therapeutic target. *Clin Cancer Res* 2015;21:1797–801.
28. Yuan TL, Fellmann C, Lee CS, et al. Development of siRNA payloads to target KRAS-Mutant cancer. *Cancer Discov* 2014;4:1182–97.
29. Xue W, Dahlman JE, Tammela T, et al. Small RNA combination therapy for lung cancer. *Proc Natl Acad Sci U S A* 2014;111:E3553–61.
30. Zorde Khvalevsky E, Gabai R, Rachmut IH, et al. Mutant KRAS is a druggable target for pancreatic cancer. *Proc Natl Acad Sci U S A* 2013;110:20723–8.

## APPENDIX

<b>Table S1. Criteria for defining dose-limiting toxicities</b>	
<b>Toxicity</b>	<b>DLT definition</b>
Hematologic	<ul style="list-style-type: none"> <li>• Grade 4 neutropenia for <math>\geq 5</math> days</li> <li>• Grade <math>\geq 3</math> febrile neutropenia</li> <li>• Grade 4 anemia</li> <li>• Grade 4 thrombocytopenia</li> </ul>
Non-hematologic	<ul style="list-style-type: none"> <li>• AST <math>&gt; 5X</math> ULN OR, ALT <math>&gt; 3X</math> ULN AND bilirubin <math>&gt; 2X</math> ULN (after exclusion of disease progression and/or bile duct obstruction)</li> <li>• Grade <math>\geq 4</math> rash, hand-foot syndrome or photosensitivity</li> <li>• Grade 3 rash, hand-foot syndrome or photosensitivity for more than 7 days despite adequate supportive treatment.</li> <li>• Grade <math>\geq 3</math> nausea, vomiting or diarrhea in the presence of maximal supportive care</li> <li>• Grade <math>\geq 2</math> peripheral sensory or motor neuropathy</li> <li>• Grade 3 or greater clinically significant non-hematologic toxicity per CTCAE<sub>v</sub> 4.0, other than those listed above, with the following exceptions:                             <ul style="list-style-type: none"> <li>o Electrolyte disturbances that respond to correction within 24 hours</li> <li>o Grade 3 hypertension that is adequately controlled by the addition of up to 2 additional antihypertensive medications</li> <li>o Grade 3 pyrexia that does not result in study discontinuation</li> </ul> </li> </ul>
Cardiac	<ul style="list-style-type: none"> <li>• Ejection fraction <math>&lt;</math> lower limit of normal (LLN) with an absolute decrease of <math>&gt;10\%</math> from baseline with confirmation within 14 days</li> </ul>
Other	<ul style="list-style-type: none"> <li>• Inability to receive <math>\geq 75\%</math> of scheduled doses in treatment period due to toxicity</li> <li>• Treatment delay of <math>&gt; 7</math> days due to study treatment-related toxicity</li> <li>• Grade 2 or higher toxicity that occurs beyond 28 days which in the judgment of the investigator is considered to be a DLT</li> </ul>

*Abbreviations: DLT, dose-limiting toxicity; AST, aspartate aminotransferase; ALT alanine aminotransferase; ULN, upper limit of normal; CTCAE, Common Terminology Criteria for Adverse Events' LLN, lower limit of normal.*

**Table S2. Pharmacokinetic model parameters and bootstrap results for dacomitinib and PD-0325901**

Parameter	Dacomitinib				PD-0325901			
	Estimate	SE (%)	Bootstrap results		Estimate	SE (%)	Bootstrap results	
			Median	95% CI			Median	95% CI
Ke (h <sup>-1</sup> )	0.0251	37	0.0414	(0.0132–0.200)	0.299	37	0.329	(0.204–1.85)
Vc (L)	1.13	36	1.70	(0.126–2.02)	12.5	67	11.62	(1.90–18.76)
Ka (h <sup>-1</sup> )	0.525	21	0.503	(0.236–0.757)	4.19	27	4.10	(2.93–5.46)
K12 (h <sup>-1</sup> )	0.211	77	0.402	(0.0299–2.17)	0.742	121	0.808	(0.463–7.37)
K21 (h <sup>-1</sup> )	0.144	31	0.126	(0.0415–0.197)	0.569	102	0.590	(0.210–0.946)
K13 (h <sup>-1</sup> )					0.748	111	0.798	(0.209–4.71)
K31 (h <sup>-1</sup> )					0.068	41	0.0670	(0.0241–0.113)
IIV Ke (CV%)	47.2	19	45.1	(22.6–60.74)	47.2	13	45.5	(33.5–58.1)
IIV Vc (CV%)	46.3	16	44.9	(28.7–59.7)	29.8	12	29.2	(21.1–37.3)
IIV Ka (CV%)	59.6	15	59.4	(39.5–83.1)	36.5	40	33.6	(7.14–50.4)
ε <sub>additive</sub>	0.118	23	0.142	(0.0175–0.532)				
ε <sub>proportional</sub>	0.0581	10	0.0546	(0.0323–0.0793)				
ε <sub>exponential</sub>					0.0875	6	0.0879	(0.0681–0.112)

Abbreviations: SE, standard error of the mean; 95% CI, 95% confidence interval; Ke, elimination rate constant; Vc, volume of distribution; Ka, absorption rate; K12, distribution rate constant from compartment 1 to compartment 2; K21, distribution rate constant from compartment 2 to compartment 1; ε<sub>additive</sub>, additive error; ε<sub>proportional</sub>, proportional error; ε<sub>exponential</sub>, exponential error

6.1

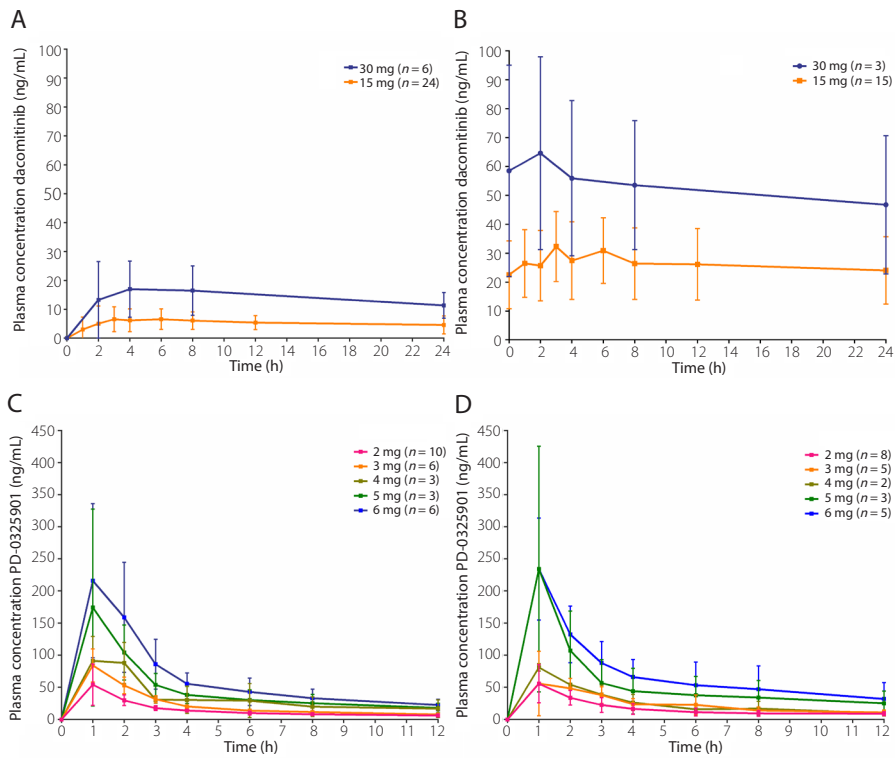
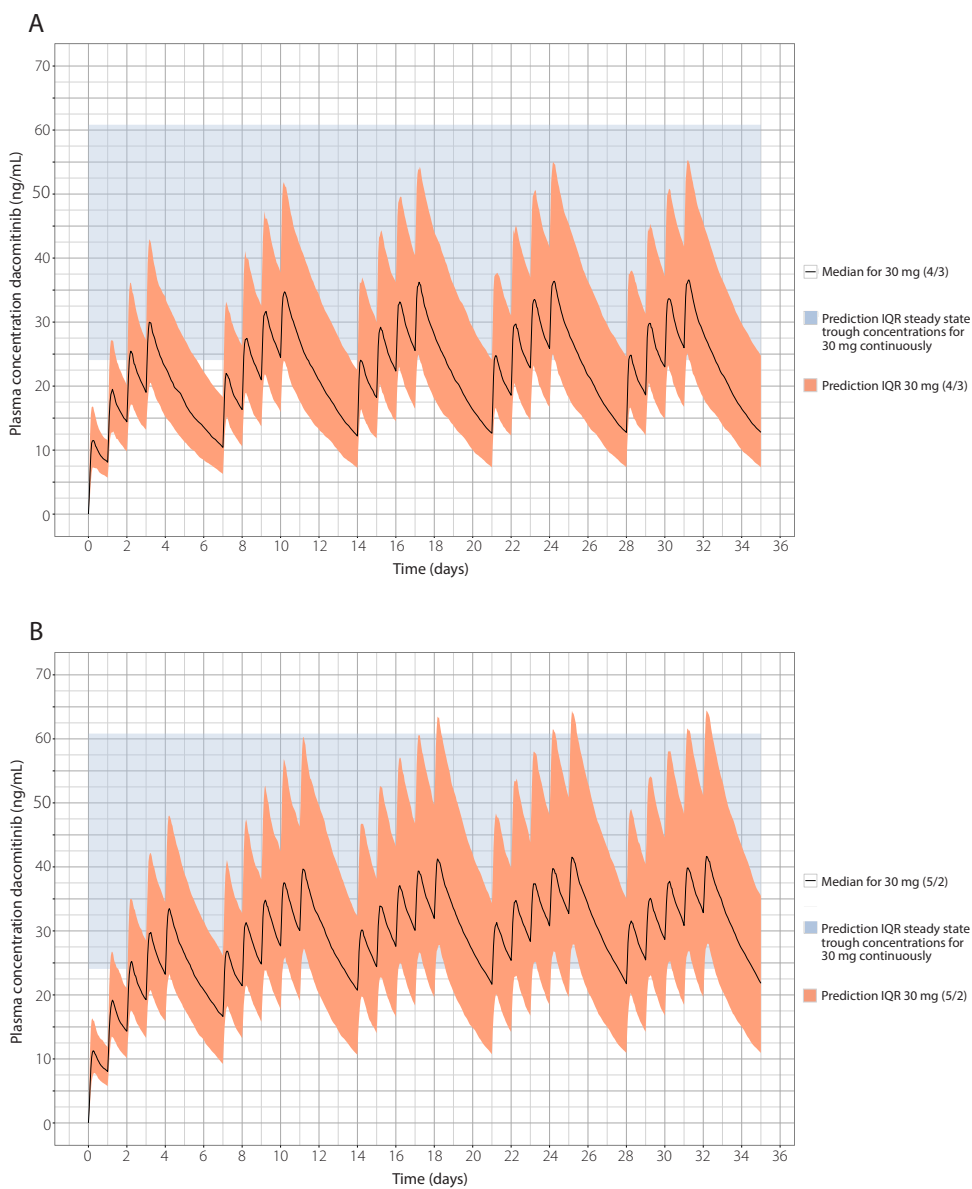


Figure S1. Pharmacokinetic profiles of dacomitinib and PD-0325901.

All figures: Plasma concentration time curves of mean with error bars representing SD. A) dacomitinib, cycle 1 day 1, B) dacomitinib, cycle 2 day 1, C) PD-0325901, cycle 1 day 1, D) PD-0325901, cycle 2 day 1.



6.1

**Figure S2. Predictive simulation of the pharmacokinetic profile of dacomitinib when administered intermittently.**

A) Dacomitinib 30 mg, 4 days on / 3 days off, B) Dacomitinib 5 days on / 2 days off.

Abbreviations: IQR, interquartile range; 4/3, 4 days on / 3 days off; 5/2, 5 days on / 2 days off.





# Chapter 6

## Clinical pharmacology of combined targeted therapy targeting mutated *KRAS*



### 6.2

#### Phase I study of lapatinib plus trametinib in patients with *KRAS* mutant colorectal, non-small cell lung and pancreatic cancer

##### Interim analysis

Robin M.J.M. van Geel, Frans Opdam, Serena Marchetti, Neeltje Steeghs, Saskia Pulleman, Bas Thijssen, Hilde Rosing, Hugo M. Horlings, Annemieke Cats, René Bernards, Jos H. Beijnen, Jan H.M. Schellens

## ABSTRACT

### Background

Mutations in the *KRAS* oncogene are amongst the most powerful cancer drivers, causing sustained signaling through the MAPK pathway to stimulate tumorigenic mechanisms. Until now, efforts to target *KRAS* directly have been unsuccessful, and pharmacological inhibition of its downstream effectors provided disappointing results in the clinic as well. Preclinical research revealed that *KRAS* mutated (*KRAS*<sub>m</sub>) cells are intrinsically resistant against MEK inhibitors due to feedback activation of upstream tyrosine kinase receptors that reactivates the MAPK and PI3K pathway. Concurrent inhibition of MEK and the human epidermal growth factor receptor family members EGFR and HER2 resulted in synergistic anti-tumor activity, with complete inhibition of tumor growth *in vitro* and *in vivo*.

### Methods

We undertook an investigator-initiated, single-center, phase I, dose-escalation study to assess the safety, tolerability and anti-tumor activity of the MEK inhibitor trametinib combined with dual EGFR/HER2 inhibitor lapatinib in patients with advanced *KRAS*<sub>m</sub> colorectal cancer (CRC), non-small cell lung cancer (NSCLC) and pancreatic cancer. Patients received escalating doses of continuous or intermittent once daily (QD) orally administered lapatinib and trametinib, starting at 750 mg and 1 mg continuously, respectively. The primary objective of this study (ClinicalTrials.gov identifier: NCT02230553) was determining the recommended phase II dose.

### Results

At the time of this interim analysis, 22 patients were enrolled across 4 different dose-levels; 16 patients with CRC, three with NSCLC, and three patients with pancreatic cancer. Dose-limiting adverse events were reported in four patients at 3 different dose-levels; grade 3 diarrhea ( $n = 2$ ), rash and aspartate aminotransferase elevation. The most frequently reported adverse events of any grade were rash acneiform (92%), fatigue (64%) and diarrhea (57%). The maximum tolerated dose-level with continuous dosing contained 750 mg lapatinib QD plus 1 mg trametinib QD. Dose-escalation with intermittent dosing is ongoing. Standard pharmacokinetic parameters were in line with previous reported data on single agent lapatinib and trametinib. Out of the 16 patients evaluable for response, regression of target lesions was seen in four patients, with one confirmed partial response in a NSCLC patient. Median time to progression was 80 days (range 38–350). Reductions in pERK and pS6 levels were demonstrated in eight out of 12 paired tumor biopsies.

### Conclusions

Combined treatment with lapatinib and trametinib was safe with manageable toxicity. Although full single agent doses could not be reached in combination, preliminary signs of anti-tumor activity have been observed at tolerable dose-levels. The ongoing study explores intermittent dosing schedules to further improve tolerability.

## Introduction

Approximately 20% of all human cancers carry mutations in the *KRAS* oncogene, including 90% of pancreatic cancers, 45% of colorectal cancers, and 35% of non-small cell lung cancers.<sup>1</sup> *KRAS* gain-of-function mutations cause continuous activation of the mitogen-activated protein kinase (MAPK) pathway, resulting in the development and progression of malignant cells. The high frequency of *KRAS* mutations in three of the most lethal tumor types makes targeting of these aberrations using small molecule tyrosine kinase inhibitors an attractive treatment strategy. However, despite extensive efforts over the past decades, an effective *KRAS* inhibitor has yet to reach the clinic.<sup>2</sup> An alternative approach to target *KRAS*-driven tumors comprises inhibition of downstream effectors of *KRAS*, such as MEK or ERK. Although MEK inhibitors were found to be among the most active agents against *KRAS* mutant (*KRASm*) cell lines, their effect was mostly cytostatic rather than cytotoxic, and the anti-tumor activity in xenograft models and patients was limited.<sup>3-5</sup>

Sun and colleagues provided insight in the underlying mechanism of this intrinsic resistance, demonstrating a MYC-dependent transcriptional upregulation of the human epidermal growth factor receptor (HER) 3 upon MEK inhibition. Subsequent reactivation of downstream signaling pathways results in sustained activation of multiple tumorigenic mechanisms. As HER3 requires formation of heterodimers with the epidermal growth factor receptor (EGFR) or HER2 in order to activate downstream signaling, inhibition of EGFR and HER2 in addition to MEK was sufficient to obtain synergistic anti-tumor activity *in vitro* and in xenograft models.<sup>6</sup> These findings provided rationale for clinical evaluation of such a combination of targeted agents.

In this phase I dose-finding study, we investigated lapatinib combined with trametinib in patients with *KRASm* colorectal cancer (CRC), non-small cell lung cancer (NSCLC) or pancreatic cancer. Lapatinib is an ATP-competitive dual tyrosine kinase inhibitor targeting EGFR and HER2, approved as standard of care for inhibiting HER2 activity in HER2-positive breast cancer.<sup>7-9</sup> Trametinib is a reversible, highly selective, allosteric MEK1 and MEK2 inhibitor, approved for the treatment of patients with metastatic *BRAF* mutant (*BRAFm*) melanoma in combination with a *BRAF* inhibitor.<sup>10,11</sup> In the present report we provide an interim analysis after enrollment of 22 patients.

## Patients and Methods

### *Patient population*

In this investigator-initiated, single-center, open label phase I study, we enrolled patients with histologically- or cytologically-confirmed advanced CRC, NSCLC or pancreatic cancer. Patients were enrolled on the basis of documented *KRAS* exon 2, 3 or 4 mutation, and *PIK3CA* wild type in view of the potential intrinsic resistance of genetically altered PI3K signaling. Eligible patients were 18 years or older, had an Eastern Cooperative Oncology performance status of 0 or 1, had a life expectancy  $\geq 3$  months, had measurable disease per Response Evaluation Criteria in Solid Tumors (RECIST) v1.1, and had adequate bone marrow (absolute neutrophil count  $\geq 1.5 \times 10^9/L$ , platelets  $\geq 100 \times 10^9/L$ , hemoglobin  $\geq 6.0$  mmol/L) and organ function (total bilirubin  $\leq 1.5 \times$  upper limit of normal [ULN], aspartate aminotransferase and alanine aminotransferase  $\leq 2.5 \times$  ULN, serum creatinine  $\leq 1.5 \times$  ULN). Any treatment within 4 weeks prior to the first dose of study treatment was not allowed. Patients with symptomatic or untreated leptomeningeal disease were excluded, as well as patients with symptomatic brain metastasis, history of interstitial lung disease, pneumonitis or retinal vein occlusion,

and patients previously treated with combinations of targeted agents known to interfere with EGFR, HER2, HER3, HER4 or MAPK- and PI3K pathway components, including BRAF, MEK, ERK, PI3K, AKT and mTOR. The study (ClinicalTrials.gov identifier: 02230553) was approved by regulatory authorities and the medical ethics committee of the Netherlands Cancer Institute. All patients gave written informed consent per Declaration of Helsinki recommendations.

GlaxoSmithKline funded this study and provided study medication. After the study was initiated, Novartis Pharma acquired lapatinib and trametinib from GlaxoSmithKline and continued the collaboration.

### ***Study design and procedures***

The primary objective was to determine the recommended phase II dose regimen, and secondary objectives included characterizing safety and tolerability, assessing preliminary anti-tumor activity, and evaluating the pharmacokinetic parameters of lapatinib and trametinib when given concomitantly. For this aim, patients were assigned to dose-levels with varying lapatinib and trametinib doses, starting at 750 mg lapatinib once daily (QD) and 1 mg trametinib QD. Dose escalation followed an alternate escalation schedule with fixed increments according to a classical 3 + 3 design. Dose escalation decisions were based on the occurrence of dose-limiting toxicity (DLT) during cycle 1. Patients were considered evaluable for the dose-determining set if at least 1 cycle of study treatment was completed, with drug exposure  $\geq 75\%$  of the assigned lapatinib and trametinib doses, or if DLT had occurred during the first treatment cycle. The maximum-tolerated dose (MTD) was defined as the dose-level at which no more than one out of six patients experienced DLT during treatment cycle 1. After assessing the MTD of lapatinib plus trametinib at continuous dosing schedules, we proceeded with investigating intermittent dosing schedules in order to find a tolerable dose and schedule with optimal anti-tumor and toxicity characteristics. Study treatment was continued until disease progression, unacceptable treatment-related toxicity, or investigator/patient decision to withdraw study consent.

Safety evaluations were performed throughout the study and included physical examination, vital signs, routine laboratory assessments, electrocardiography, ophthalmologic examination, and echocardiogram or MUGA scan to assess the left ventricular ejection fraction. Adverse events were graded according to Common Terminology Criteria for Adverse Events version 4.0. DLTs were defined as adverse events or laboratory abnormalities occurring within the first 28 days of study treatment that meet at least one of the criteria described in supplementary table S1. Tumor response was assessed radiographically every 6 weeks using RECIST version 1.1. Patients were evaluable for efficacy if at least one follow-up radiographic evaluation was performed after 6 weeks of study treatment.

All patients underwent tumor biopsies at baseline and after 15 days of treatment for investigation of pharmacodynamic parameters and genomic analysis. Additional tumor biopsies were taken upon progression, when considered relevant and feasible, to explore potential mechanisms of resistance.

### ***Pharmacokinetic and pharmacodynamic analysis***

Extensive blood sampling for plasma concentration analysis of lapatinib and trametinib was performed in all patients. Serial blood samples were taken prior to administration on the first day of cycle 1 and cycle 2, and 1, 0.5, 1, 2, 4, 6, 8, and 24 hours after dosing. Plasma was isolated and stored at  $-80^{\circ}\text{C}$  until analysis using a validated high performance liquid chromatography method coupled to tandem mass

spectrometry (LC-MS/MS). Briefly, lapatinib and trametinib were extracted from plasma by protein precipitation with acetonitrile/methanol. For chromatographic separation, we used a Waters Xbridge BEH Phenyl column (2.1 x 50 mm, 5 µm), and compound detection was performed using an API4000 tandem mass spectrometer equipped with a turbo ion spray interface, operating in the positive ion mode. The lower and upper limits of quantification were 0.5 and 50 ng/mL, respectively, for trametinib, and 50 and 5000 ng/mL, respectively, for lapatinib. Standard pharmacokinetic parameters were calculated using non-compartmental analysis in GraphPad Prism, version 6.04 (GraphPad Software, La Jolla, CA, USA).

For pharmacodynamic analysis we used immunohistochemistry to determine phosphorylated ERK (pERK) and phosphorylated S6 (pS6) ribosomal protein levels in tumor biopsy tissue taken before study enrolment and while on treatment. Tumor biopsy samples were fixed in formalin for 16–24 hours and embedded in paraffin subsequently. Immunohistochemistry of formalin-fixed paraffin-embedded tumor samples was performed on a BenchMark Ultra autostainer (Ventana Medical Systems). Briefly, paraffin sections were cut at 3 µm, heated at 75°C for 28 minutes and deparaffinised in the instrument with EZ prep solution (Ventana Medical Systems). Heat-induced antigen retrieval was carried out using Cell Conditioning 1 (CC1, Ventana Medical Systems) at 95°C for 32 and 64 minutes, for pS6 ribosomal Protein and pERK1/2, respectively. pS6 ribosomal protein was detected using clone D68F8 (1:1000 dilution, 32 minutes at room temperature, Cell Signalling) and Phospho-p44/42 MAPK (pERK1/2) (Thr202/Tyr204) using clone D13.14.4E (1:400 dilution, 1 hour at room temperature, Cell Signalling). Bound Phospho-p44/42 MAPK (pERK1/2) (Thr202/Tyr204) was detected using the UltraView Universal DAB Detection Kit (Ventana Medical Systems), while detection for Phospho-S6 Ribosomal Protein was performed using the OptiView DAB Detection Kit (Ventana Medical Systems). Slides were counterstained with Hematoxylin. Staining intensity was quantified using the H-score method; percentage of positive cells (0–100) multiplied by staining intensity (0–3).

### **Statistical analysis**

Safety data were summarized using descriptive statistics. A paired t-test was used to determine the statistical significance of the pharmacodynamic modulation (*i.e.* pERK and pS6) in tumor tissue taken before study start and while on treatment. A two sample t-test assuming unequal variances was used to assess the statistical significance of differences in drug exposure between patients with and without reduction of both pERK and pS6 H-score in paired tumor biopsies.

6.2

## **Results**

### ***Patient disposition and characteristics***

A total of 22 patients were enrolled in the study across 4 different dose-levels; 16 patients with colorectal cancer, three patients with NSCLC and three patients with pancreatic cancer. Twenty patients had a mutation in exon 2 (codon 12 or 13) of the *KRAS* gene, and two patients had an exon 4 (codon 146) *KRAS* mutation. G12C ( $n = 2$ ) and G12D ( $n = 1$ ) mutations were detected in patients with NSCLC. In CRC patients we detected G12A ( $n = 2$ ), G12C ( $n = 1$ ), G12D ( $n = 4$ ), G12R ( $n = 1$ ), G12S ( $n = 1$ ), G12V ( $n = 3$ ), G13D ( $n = 2$ ), and A146V ( $n = 2$ ) mutations. The patients with pancreatic cancer had G12R, G12D, and G12V mutations. The majority of patients were pretreated with at least 2 prior lines of therapy for metastatic disease (Table 1). Out of the 22 patients, 18 were considered evaluable

for efficacy; two patients were not evaluable due to withdrawal of consent and two patients did not reach the first radiographic evaluation, 6 weeks after study start, due to adverse events and clinical deterioration. At data cut off, all patients had discontinued study treatment, 16 patients due to progressive disease, four patients due to adverse events, and two patients due to patient refusal.

**Dose determination**

Dose-limiting toxicities were not observed in the first cohort of three patients on dose-level 1 (750 mg lapatinib QD, 1 mg trametinib QD), allowing escalation of trametinib. However, in the subsequent dose-levels 2 and 3, comprising 750 mg lapatinib QD plus 1.5 mg trametinib QD and 500 mg lapatinib QD plus 1.5 mg trametinib QD, respectively, dose-limiting toxicities were reported in two out of six and two out three patients, respectively. Therefore, we enrolled an additional three patients on the initial dose-level, in which 1 DLT was observed amongst six patients in total. Dose-limiting adverse events were grade 3 diarrhea in dose-level 1, grade 3 rash and grade 3 AST elevation in dose-level 2, and grade 3 diarrhea and inability to receive at least 75% of the planned dose due to a grade 4 creatine phosphokinase (CPK) elevation in dose-level 3 (Figure 1). Consequently, the established MTD with continuously dosed lapatinib and trametinib was 750 mg lapatinib QD plus 1 mg trametinib QD. Intermittent dosing schedules are currently being explored in the ongoing study.

**Safety**

As shown in Table 2, the most frequent adverse events regardless of treatment causality were rash acneiform (92%), diarrhea (76%), and fatigue (64%). Skin-related toxicity was the most frequent treatment-related adverse event, including acneiform rash (92%), mainly on the face chest and back, hand-foot syndrome (19%), and dry skin (10%). Diarrhea was predominantly grade 1/2 and was mostly manageable with standard supportive care. Treatment-related ocular toxicity was not observed. At the MTD, toxicities were manageable. One patient on dose-level 3 experienced a grade 4 CPK elevation, which improved to grade 1 after a 2-week study treatment interruption. Five patients experienced a decrease in left ventricular ejection fraction (LVEF), including two patients with grade 3 events. All events resolved upon study treatment interruption after which patients continued on the same or a

<b>Table 1. Patient and disease characteristics</b>	
	<b>Patients (n = 22)</b>
<b>Sex, n (%)</b>	
Female	9 (41%)
Male	13 (59%)
<b>Age, median (range), years</b>	63 (43–75)
<b>Tumor type, n (%)</b>	
Colonrectal	16 (73%)
Non-small cell lung	3 (14%)
Pancreatic	3 (14%)
<b>ECOG PS, n (%)</b>	
0	13 (59%)
1	9 (41%)
<b>Number of prior treatment regimens, n (%)</b>	
1	3 (14%)
2	12 (55%)
≥ 3	7 (32%)
<b>KRAS mutation, n (%)</b>	
Exon 2	20 (91%)
p.G12A	2 (9%)
p.G12C	3 (14%)
p.G12D	6 (27%)
p.G12R	2 (9%)
p.G12S	1 (5%)
p.G12V	4 (18%)
p.G13D	2 (9%)
Exon 3	0 -
Exon 4	2 (9%)
p.A146V	2 (9%)

Abbreviations: ECOG PS, Eastern Cooperative Oncology Group performance status.

Table 2. Adverse events, regardless of treatment, occurring in ≥ 10% of patients										
	DL 1 (n = 7)		DL 2 (n = 7)		DL 3 (n = 4)		DL 4 (n = 4)		Total (n = 22)	
	Lapatinib QD Trametinib QD		Lapatinib QD Trametinib QD		Lapatinib QD Trametinib QD		Lapatinib QD Trametinib QD			
	750 mg 1 mg		750 mg 1.5 mg		500 mg 1.5 mg		750 mg (5/2) 1.5 mg			
Adverse event, n (%)	Gr. 1/2	Gr. 3	Gr. 1/2	Gr. 3	Gr. 1/2	Gr. 3	Gr. 1/2	Gr. 3	Gr. 1/2	Gr. 3
Any skin toxicity	6 (86)	0	5 (71)	2 (29)	4 (100)	0	4 (100)	0	19 (86)	2 (10)
Rash acneiform	5 (71)	0	5 (71)	2 (29)	4 (100)	0	4 (100)	0	18 (82)	2 (10)
Hand-foot syndrome	2 (29)	0	2 (29)	0	0	0	0	0	4 (19)	0
Dry skin	0	0	2 (29)	0	0	0	0	0	2 (10)	0
Fatigue	6 (86)	0	4 (57)	0	3 (75)	0	1 (25)	0	14 (64)	0
Diarrhea	4 (57)	2 (29)	5 (71)	1 (14)	1 (25)	1 (25)	2 (50)	0	12 (57)	4 (19)
Nausea	4 (57)	0	1 (14)	0	1 (25)	1 (25)	2 (50)	0	8 (38)	1 (5)
Vomiting	0	0	4 (57)	0	1 (25)	0	2 (50)	0	7 (33)	0
CPK increased	2 (29)	0	3 (43)	1 (14)	1 (25)	1*(25)	0	1 (25)	6 (29)	2†(10)
ALT/AST increased	1 (14)	0	3 (43)	1 (14)	2 (50)	0	0	0	6 (29)	1 (5)
Mucositis	0	0	4 (57)	0	1 (25)	0	0	0	5 (24)	0
LVEF decreased	1 (14)	2 (29)	2 (29)	0	0	0	0	0	3 (14)	2 (10)
Weight loss	3 (43)	0	0	0	0	0	0	0	3 (14)	0
Hypertension	2 (29)	0	1 (14)	0	0	0	0	0	3 (14)	0

Abbreviations: CPK, creatine phosphokinase; ALT/AST, alanine aminotransferase / aspartate aminotransferase; LVEF, left ventricular ejection fraction; 5/2, 5 days on / 2 days off. \*grade 4 event; † including 1 grade 4 event

reduced dose-level. One patient discontinued study treatment permanently due to a decreased LVEF from 70% at baseline to 24% after 9 cycles that did not improve to ≥ 50% within 4 weeks of treatment interruption.

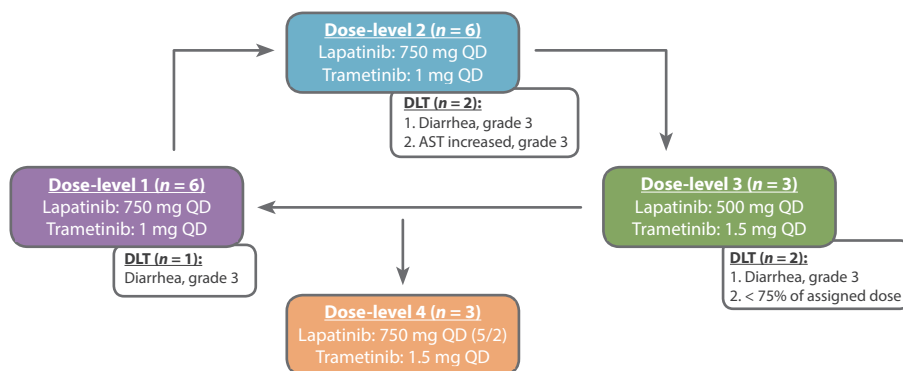


Figure 1. Dose-escalation cohorts and dose-limiting toxicities

Abbreviations: DLT, dose-limiting toxicity; QD, once daily; AST, aspartate transaminase; 5/2, 5 days on / 2 days off.

<b>Table 3. Pharmacokinetic parameters of lapatinib and trametinib at day 1 and steady-state</b>						
	DL 1	DL 2	DL 3	DL 4	Lapatinib	Trametinib
<i>Lapatinib QD</i>	750 mg	750 mg	500 mg	750 mg (5/2)	all 750 mg	All 1.5 mg
<i>Trametinib QD</i>	1 mg	1.5 mg	1.5 mg	1.5 mg	dose-levels	dose-levels
<i>Cycle 1 Day 1</i>						
<b>Lapatinib, Mean</b>	n = 7	n = 6	n = 3	n = 4	n = 17	
C <sub>max</sub> (ng/mL)	1251	1381	829	888	1173	
T <sub>max</sub> (h)	3.4	3.6	4.5	4.1	3.7	
AUC <sub>0-24h</sub> (ng·h/mL)	14,749	17,068	11,040	10,808	14,208 (62%) [9,911–18,505]	
<i>Cycle 2 Day 1</i>						
<b>Lapatinib, Mean</b>	n = 3	n = 3	n = 1	n = 2*	n = 8	
C <sub>max</sub> (ng/mL)	2070	1703	800	813	1529	
T <sub>max</sub> (h)	3.9	3.3	4.0	3.0	3.4	
AUC <sub>0-24h</sub> (ng·h/mL)	33,154	23,352	11,768	11,441	22,649 (72%) [11,977–33,321]	
<i>Cycle 1 Day 1</i>						
<b>Trametinib, Mean</b>	n = 7	n = 6	n = 3	n = 4	n = 13	
C <sub>max</sub> (h)	2.06	3.95	4.21	2.9	3.67	
T <sub>max</sub> (h)	0.8	2.3	1.7	1.5	1.9	
AUC <sub>0-24h</sub> (ng·h/mL)	15.3	34.3	37.0	23.1	31.5 (32%) [26.3–36.7]	
<i>Cycle 2 Day 1</i>						
<b>Trametinib, Mean</b>	n = 4	n = 3	n = 1	n = 2*	n = 6	
C <sub>max</sub> (h)	14.4	15.9	9.1	14.1	13.0	
T <sub>max</sub> (h)	1.2	2.5	8	1.7	4.0	
AUC <sub>0-24h</sub> (ng·h/mL)	234	273	188	233	246 (36%) [176–316]	

Data listed as geometric mean. AUC<sub>0-24</sub> data for the combined 750 mg lapatinib dose-levels and 1.5 mg trametinib dose-levels are given as mean (CV%) and [95% confidence interval]. \*Pharmacokinetic samples were taken at the last day of cycle 1 on which lapatinib and trametinib were given concurrently, i.e. cycle 1 day 26. Abbreviations: DL, dose-level; QD, once daily; 5/2, 5 days on / 2 days off.

### Pharmacokinetic analysis

Trametinib and lapatinib were absorbed rapidly, with median time to maximum plasma concentration (T<sub>max</sub>) of 4 hours for lapatinib (750 mg and 500 mg), and 1 to 2 hours for trametinib (1 mg and 1.5 mg). Median day 1 and steady-state (day 29 or day 26 [5/2 dose-level]) plasma concentration profiles at each dose are given in Figure 2. Repeated lapatinib dosing resulted in an approximate 1.5-fold increase in exposure at steady-state relative to day 1, with a mean area under the plasma concentration time curve from time zero to 24 hours (AUC<sub>0-24</sub>) of 14,208 ng·h/mL (between subject coefficient of variation [CV%], 62%) and 22,694 ng·h/mL (CV%, 72%) at day 1 and steady-state, respectively. The unique exposure profile of trametinib, including a small peak-to-trough-ratio, prolonged effective half-life and low interpatient variability was recognized in our data as well. Trametinib exposure at day 1 was significantly higher in patients who received 1.5 mg compared to patients treated with 1 mg.



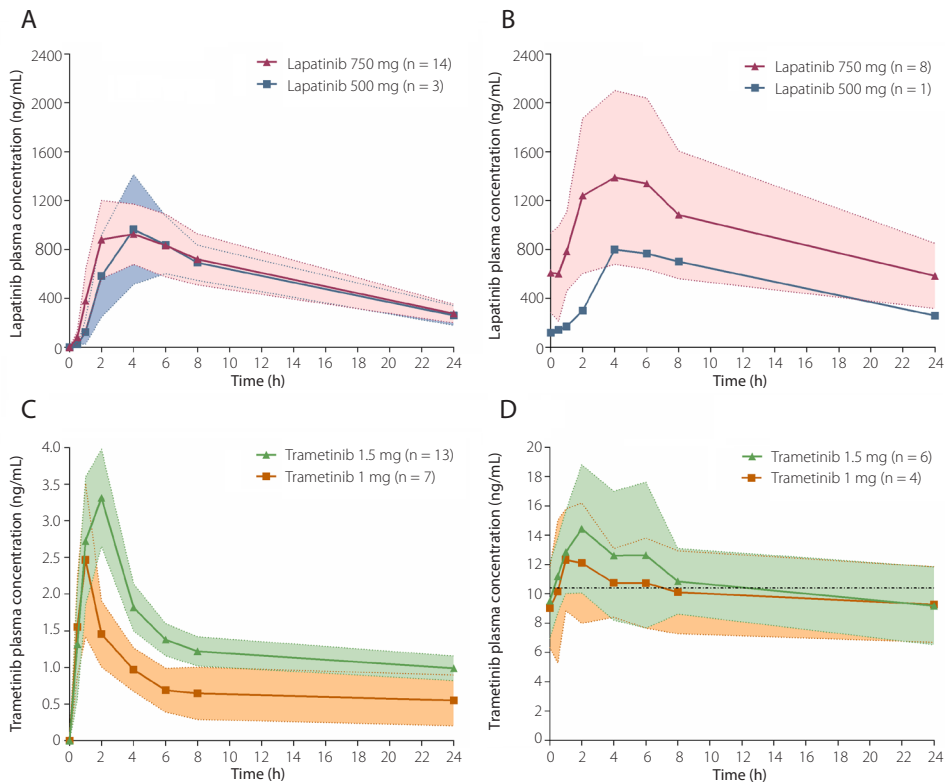


Figure 2. Pharmacokinetic profiles of lapatinib and trametinib.

Mean plasma concentration curves for lapatinib and trametinib, per dose, with 95% confidence interval bands at day 1 (A, C) and at steady-state, day 29 (B, D).

However, exposure at steady state was comparable between both groups with largely overlapping 95% confidence intervals (Figure 2, Table 3). Trametinib had an approximate accumulation ratio of 8 in the 1.5 mg dose-levels. Day 1 and steady state  $AUC_{0-24h}$ ,  $T_{max}$ , and  $C_{max}$  of lapatinib and trametinib at each dose-level are summarized in Table 3.

### Pharmacodynamic analysis

Paired tumor biopsies were obtained at baseline and on treatment from 17 patients. In total, 12 out of 17 paired tumor biopsies contained sufficient numbers of tumor cells (> 10%) and were considered evaluable for pharmacodynamic analysis. The median pERK H-score modulation was -86% ( $P = 0.02$ ), with eight out of 12 patients showing reduction in pERK intensity-score. In eight patients pS6 intensity-score was decreased upon treatment and the median pS6 modulation was -35% ( $P = 0.09$ ). In samples of six patients reduction of both pERK and pS6 were observed (figure 3, S1). Although clear correlations between different dose-levels or exposure and the extent of pERK and pS6 modulation were not detected, there was a trend towards more robust pathway inhibition in patients with higher trametinib and lapatinib plasma concentrations.

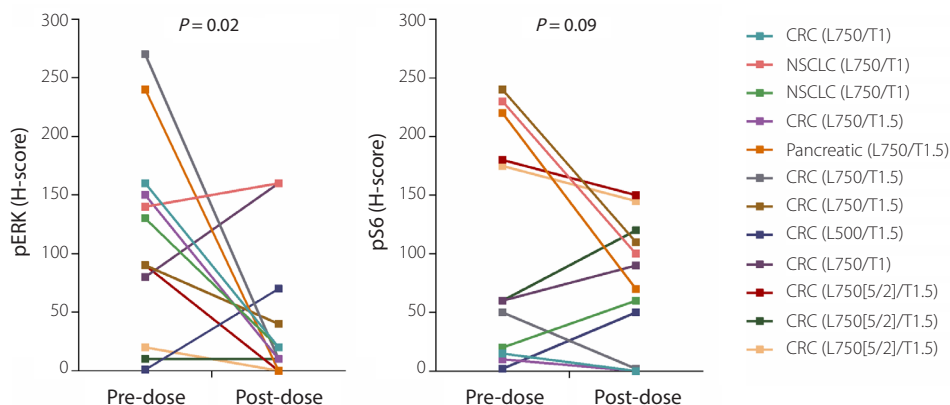


**Figure 3. Pharmacodynamic modulation in paired tumor biopsies.**

Tumor biopsies were obtained pre-dose (up to 1 week prior to treatment initiation) and post-dose (15–18 days after treatment start). Biopsy samples were analyzed for pERKThr202/Tyr204 and pS6 ribosomal protein by immunohistochemistry. Pre- and post-dose H-scores of pERK (A) and pS6 (B) are plotted for individual patients. pERK and pS6 percentage modulations (C) are plotted for individual patients. Median pERK and pS6 reduction was -86% and -35%, respectively. *Abbreviations: CRC, colorectal cancer; NSCLC, non-small cell lung cancer; L, lapatinib; T, trametinib; 5/2, 5 days on / 2 days off.*

Patients in whom pERK and pS6 were both reduced upon study treatment showed higher trametinib and lapatinib AUCs at day 1 and at steady-state, albeit not significantly with *P*-values (two-sample t-test assuming unequal variances) of 0.24 (mean AUCs, 27.7 vs 23.4 ng·h/mL) and 0.14 (mean AUCs, 257 vs 215 ng·h/mL) for trametinib at baseline and steady-state, respectively, and 0.28 (mean AUCs, 15,776 vs 12,841 ng·h/mL) and 0.09 (27,693 vs 10,251 ng·h/mL) for lapatinib at baseline and steady-state, respectively.

### **Antitumor activity**

Sixteen patients were evaluable for response evaluation; two patients were not evaluable due to withdrawal of study consent, three patients did not reach the first response evaluation after 6 weeks of treatment due to clinical deterioration, and one patient did not have measurable target lesions per RECIST v1.1 criteria. Out of these 16 evaluable patients, one patient (6%) achieved a confirmed partial response, eight (50%) had stable disease as best response, and seven (44%) had progressive disease at the first response evaluation. Tumor regression was achieved in four patients at dose-levels 1 and 2. Two out of three patients with NSCLC had tumor regression, including one confirmed partial response (Figure 4). The median time to progression was 295 days (range 168–350) for patients with NSCLC, 45 days (range 38–133) for CRC patients, and 85 days for the evaluable patient with pancreatic cancer (Figure 5).

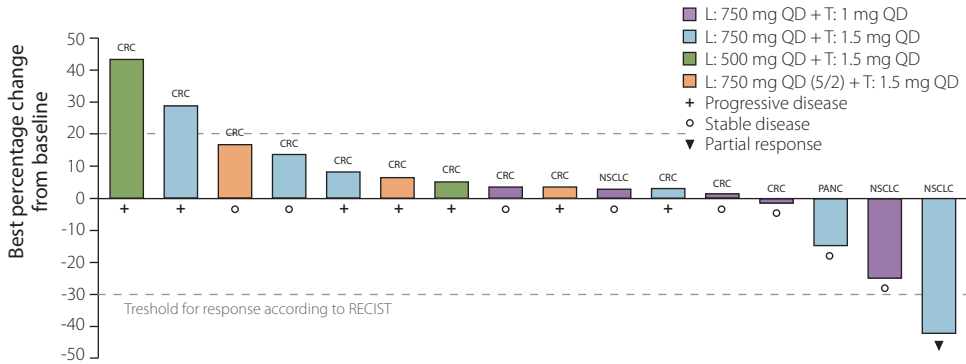


**Figure 4. Maximum percentage change in sum of target lesion size from baseline, by dose-level.**  
 Abbreviations: L, lapatinib; T, trametinib; QD, once daily; CRC, colorectal cancer; NSCLC, non-small cell lung cancer; Pancr., pancreatic cancer.

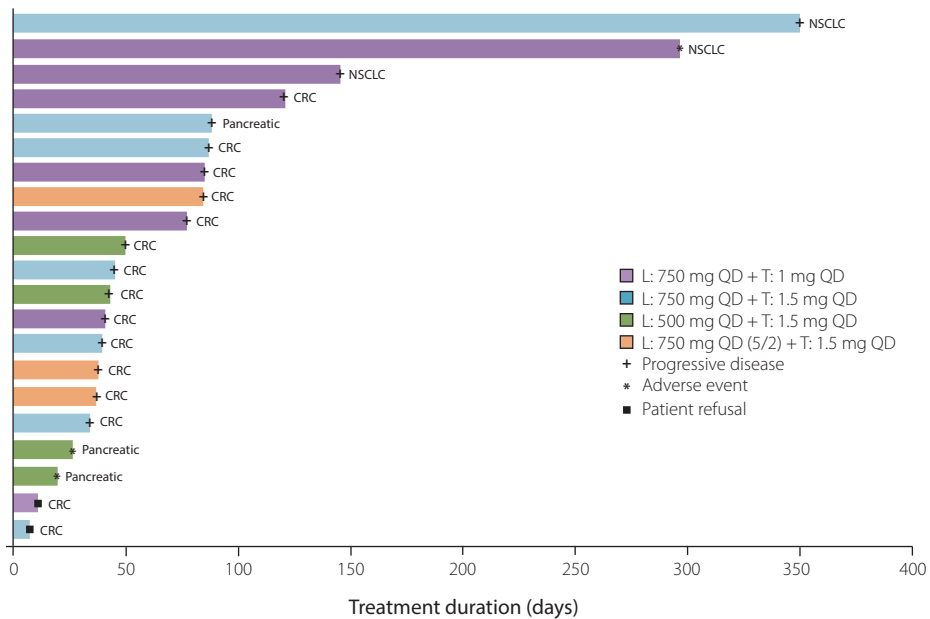


**Figure 5. Time on treatment, by dose-level.**  
 Bars represent duration on treatment by dose-level, with the reason for end of treatment displayed at the end of each bar. Abbreviations: L, lapatinib; T, trametinib; QD, once daily; CRC, colorectal cancer; NSCLC, non-small cell lung cancer.

6.2

## Discussion

Our preliminary findings show that trametinib plus lapatinib has manageable toxicity, albeit not at full single agent doses. In previous studies, lapatinib was well tolerated at doses up to 1,600 mg QD, and the recommended phase II dose of trametinib was established at 2 mg QD.<sup>12–14</sup> However, dose-limiting events, including rash, diarrhea and liver enzyme elevation prevented dose escalation beyond the 750 mg lapatinib plus 1 mg trametinib dose-level, which was declared the maximum tolerated dose with a continuous dosing schedule. Although relatively low, these doses in monotherapy achieved target engagement and clinical responses in patients with *BRAF*<sub>m</sub> melanoma and EGFR-expressing and/or HER2-overexpressing breast cancer, respectively.<sup>12–14</sup> As expected, given the overlapping toxicity profiles of lapatinib and trametinib, skin-related toxicity and diarrhea were the most common treatment-related adverse events. In the majority of patients, early recognition and adequate supportive care was sufficient to make these effects manageable. Reductions in LVEF are common with MEK inhibitors and have been reported with lapatinib as well. During our study, we recorded five occurrences of LVEF reduction. One patient experienced a LVEF reduction from 70% at baseline to 45% after five cycles of study treatment. As the LVEF recovered to > 50% within two weeks upon treatment interruption, the patient continued on the same dose-level. However, after nine cycles LVEF had decreased to 24%. Because treatment interruption did not result in improvement of LVEF to ≥ grade 1 within four weeks, the patient discontinued study treatment permanently. Three months after study discontinuation, LVEF had recovered to > 50%.

In general, pharmacokinetic data obtained in this study was in line with single agent data from previous studies, indicating the absence of an apparent pharmacokinetic drug-drug interaction between lapatinib and trametinib. Lapatinib exposure was similar between the 500 mg and 750 mg dose-levels at day 1, potentially due to the high variability and the low patient number treated at 500 mg. The unique pharmacokinetic profile of trametinib, with a prolonged effective half-life and small peak-to-trough ratio allows constant target inhibition with relatively low  $C_{max}$ .<sup>10</sup> However, at 1 and 1.5 mg, the preclinical plasma concentration target of 10.4 ng/mL (*i.e.* the estimated mean inhibitory concentration at which 50% growth occurs in *BRAF*<sub>m</sub> melanoma cell lines)<sup>14</sup>, was exceeded during only 30% and 50% of the 24-hour dosing interval, respectively. Comparable results were reported in the phase I study with single agent trametinib, showing that the preclinical target exposure concentration was exceeded during the entire dosing interval only at doses of 2 mg and higher.<sup>13</sup> As robust MEK and MAPK pathway inhibition is crucial for optimal anti-tumor activity and because higher trametinib doses yielded stronger pERK suppression and improved clinical outcome in previous studies with trametinib as single agent in patients with *BRAF* or *NRAS* mutated melanoma<sup>13,14</sup> or in combination<sup>15</sup>, this provided rationale to explore additional dosing schedules with higher trametinib doses in our patient population as well. In an effort to maintain tolerability, we chose to escalate trametinib in combination with intermittent lapatinib dosing. This strategy was supported by *in vitro* from our institute, demonstrating that sequential administration of concurrent MEK and EGFR-HER2 inhibition resulted in similar fractions of apoptotic cells in *KRAS*<sub>m</sub> cell lines as with concurrent administration (Bernards, unpublished data). The initial dose-level with intermittent dosing consisted of 750 mg lapatinib 5 days on / 2 days of combined with 1.5 mg trametinib and was well tolerated without DLTs in the first cohort of three patients. Further dose-escalation was ongoing at the time of data cut off. Previously, we demonstrated promising clinical activity with a combination strategy for patients with

*BRAF* CRC.<sup>16</sup> This combination therapy was based on a preclinical synthetic lethality drug screen showing synergistic activity between BRAF inhibition and an anti-EGFR directed antibody.<sup>17</sup> The exact same screening method identified dual EGFR-HER2 inhibitors to synergize with MEK inhibitors in *KRAS* cells.<sup>6</sup> However, whereas in the BRAF setting clinical responses were achieved already at low BRAF inhibitor doses, the anti-tumor activity obtained with trametinib plus lapatinib in patients with *KRAS* malignancies was relatively low, with only one confirmed response so far.

Interestingly, in contrast to the low radiologic response rate, a pharmacodynamic effect, *i.e.* pERK reduction, was seen in the majority of patients and in all histological tumor types, indicating suppression of the MAPK in these patients. In addition, the PI3K signaling pathway was suppressed as well, albeit to a lesser extent than pERK. Although the pharmacodynamic effects were promising, a trend towards correlation with clinical activity (*e.g.* response rate, time on treatment) could not be identified. One possible explanation for this finding may be inter-metastasis heterogeneity and sensitivity within patients. Indeed, biopsied non-target lesions in two patients that had pERK and pS6 H-score modulation between -70% and -100% upon treatment, showed radiological changes of -21% and -24%, whereas the sum of target lesion diameters had increased. Secondly, pERK suppression may be so short-lived that quickly after the on-treatment biopsy, tumor cells find escape mechanisms to reactivate ERK phosphorylation or another preferred survival pathway.

Remarkably, two out of three patients with NSCLC achieved regression of target lesions, including one confirmed partial response, suggesting a difference in sensitivity between NSCLC and CRC. This difference was even more pronounced in the time to progression data, showing prolonged benefit in all three NSCLC patients with progression-free survival times ranging between 5.5 and 11.5 months versus up to only 4.4 months in patients with CRC. Previous studies suggested a difference in sensitivity to MEK inhibition between NSCLC and CRC as well. Hochster et al. demonstrated marginal additional benefit for adding a MEK inhibitor to second-line irinotecan in patients with *KRAS* CRC<sup>18</sup>, whereas Jänne and colleagues significantly improved the median progression free survival of patients with *KRAS* NSCLC by adding the MEK inhibitor selumetinib to second-line treatment with docetaxel.<sup>5</sup> Additional work to be considered in our study therefore includes trying to elucidate the underlying biological reason of this difference in sensitivity. Evaluation of additional potential biomarkers, including HER2 and HER3 protein expression levels, may be relevant for that matter. Furthermore, given the primarily cytostatic effect of MEK inhibitors in *KRAS* tumors, it may be interesting to investigate markers for apoptosis (*e.g.* Bcl-2, caspase 3), and to explore the potential of adding anti-apoptotic protein inhibitors such as navitoclax.<sup>19</sup>

Taken together, our study established the maximum-tolerated doses for lapatinib and trametinib when given concurrently on a continuous dosing schedule. We provided evidence of pharmacodynamic effects in *KRAS* tumor tissue and we demonstrated preliminary clinical anti-tumor activity in patients with *KRAS* NSCLC. Data from additional patients is needed to confirm these signs of efficacy, and intermittent dose-levels will be explored to optimize tolerability and anti-tumor activity in this ongoing study.

## References

1. Downward J. Targeting RAS signalling pathways in cancer therapy. *Nat Rev Cancer* 2003;3:11–22.
2. Cox AD, Fesik SW, Kimmelman AC, Luo J, Der CJ. Drugging the undruggable RAS: Mission Possible? *Nat Rev Drug Discov* 2014;13:828–51.
3. Migliardi G, Sassi F, Torti D, et al. Inhibition of MEK and PI3K/mTOR suppresses tumor growth but does not cause tumor regression in patient-derived xenografts of RAS-mutant colorectal carcinomas. *Clin Cancer Res* 2012;18:2515–25.
4. Adjei AA, Cohen RB, Franklin W, et al. Phase I pharmacokinetic and pharmacodynamic study of the oral, small-molecule mitogen-activated protein kinase kinase 1/2 inhibitor AZD6244 (ARRY-142886) in patients with advanced cancers. *J Clin Oncol* 2008;26:2139–46.
5. Jänne PA, Shaw AT, Pereira JR, et al. Selumetinib plus docetaxel for *KRAS*-mutant advanced non-small-cell lung cancer: A randomised, multicentre, placebo-controlled, phase 2 study. *Lancet Oncol* 2013;14:38–47.
6. Sun C, Hobor S, Bertotti A, et al. Intrinsic resistance to MEK inhibition in *kras* mutant lung and colon cancer through transcriptional induction of ERBB3. *Cell Rep* 2014;7:86–93.
7. Xia W, Mullin RJ, Keith BR, et al. Anti-tumor activity of GW572016: a dual tyrosine kinase inhibitor blocks EGF activation of EGFR/erbB2 and downstream Erk1/2 and AKT pathways. *Oncogene* 2002;21:6255–63.
8. Guan Z, Xu B, DeSilvio ML, et al. Randomized trial of lapatinib versus placebo added to paclitaxel in the treatment of human epidermal growth factor receptor 2-overexpressing metastatic breast cancer. *J Clin Oncol* 2013;31:1947–53.
9. Untch M, Loibl S, Bischoff J, et al. Lapatinib versus trastuzumab in combination with neoadjuvant anthracycline-taxane-based chemotherapy (GeparQuinto, GBG 44): A randomised phase 3 trial. *Lancet Oncol* 2012;13:135–44.
10. Gilmartin AG, Bleam MR, Groy A, et al. GSK1120212 (JTP-74057) is an inhibitor of MEK activity and activation with favorable pharmacokinetic properties for sustained in vivo pathway inhibition. *Clin Cancer Res* 2011;17:989–1000.
11. Long GV, Stroyakovskiy D, Gogas H, et al. Dabrafenib and trametinib versus dabrafenib and placebo for Val600 BRAF-mutant melanoma: A multicentre, double-blind, phase 3 randomised controlled trial. *Lancet* 2015;386:444–51.
12. Burris HA, Hurwitz HI, Dees EC, et al. Phase I safety, pharmacokinetics, and clinical activity study of lapatinib (GW572016), a reversible dual inhibitor of epidermal growth factor receptor tyrosine kinases, in heavily pretreated patients with metastatic carcinomas. *J Clin Oncol* 2005;23:5305–13.
13. Infante JR, Fecher LA, Falchook GS, et al. Safety, pharmacokinetic, pharmacodynamic, and efficacy data for the oral MEK inhibitor trametinib: A phase 1 dose-escalation trial. *Lancet Oncol* 2012;13:773–81.
14. Falchook GS, Lewis KD, Infante JR, et al. Activity of the oral MEK inhibitor trametinib in patients with advanced melanoma: A phase 1 dose-escalation trial. *Lancet Oncol* 2012;13:782–9.
15. Flaherty KT, Infante JR, Daud A, et al. Combined BRAF and MEK inhibition in melanoma with BRAF V600 mutations. *N Engl J Med* 2012;367:1694–703.

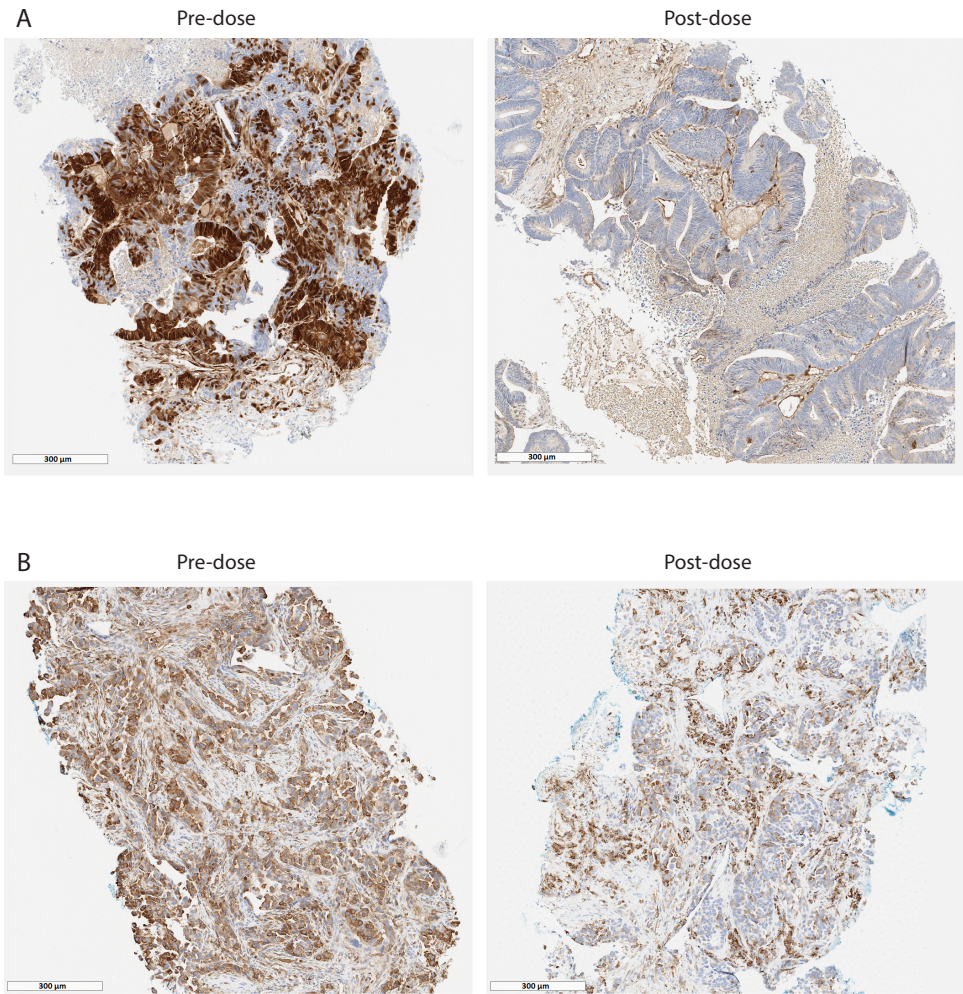
16. Van Geel R, Elez E, Bendell JC, et al. Phase I study of the selective BRAF V600 inhibitor encorafenib (LGX818) combined with cetuximab and with or without the  $\alpha$ -specific PI3K inhibitor BYL719 in patients with advanced BRAF -mutant colorectal cancer. 2014;32:5s: (suppl; abstr 3514).
17. Prahallad A, Sun C, Huang S, et al. Unresponsiveness of colon cancer to BRAF(V600E) inhibition through feedback activation of EGFR. *Nature* 2012;483:100–3.
18. Hochster HS, Uboha N, Messersmith W, et al. Phase II study of selumetinib (AZD6244, ARRY-142886) plus irinotecan as second-line therapy in patients with K-RAS mutated colorectal cancer. *Cancer Chemother Pharmacol* 2015;75:17–23.
19. Corcoran RB, Cheng KA, Hata AN, et al. Synthetic Lethal Interaction of Combined BCL-XL and MEK Inhibition Promotes Tumor Regressions in KRAS Mutant Cancer Models. *Cancer Cell* 2013;23:121–8.

## APPENDIX

<b>Table S1. Criteria for defining dose-limiting toxicities</b>	
<b>Toxicity</b>	<b>DLT definition</b>
Hematologic	<ul style="list-style-type: none"> <li>• Grade 4 neutropenia for <math>\geq 5</math> days</li> <li>• Grade <math>\geq 3</math> febrile neutropenia</li> <li>• Grade 4 anemia</li> <li>• Grade 4 thrombocytopenia</li> </ul>
Non-hematologic	<ul style="list-style-type: none"> <li>• AST <math>&gt; 5X</math> ULN OR, ALT <math>&gt; 3X</math> ULN AND bilirubin <math>&gt; 2X</math> ULN (after exclusion of disease progression and/or bile duct obstruction)</li> <li>• Grade <math>\geq 4</math> rash, hand-foot syndrome or photosensitivity</li> <li>• Grade 3 rash, hand-foot syndrome or photosensitivity for more than 7 days despite adequate supportive treatment.</li> <li>• Grade <math>\geq 3</math> nausea, vomiting or diarrhea in the presence of maximal supportive care</li> <li>• Grade <math>\geq 2</math> peripheral sensory or motor neuropathy</li> <li>• Grade 3 or greater clinically significant non-hematologic toxicity per CTCAE<sub>v</sub> 4.0, other than those listed above, with the following exceptions:                             <ul style="list-style-type: none"> <li>o Electrolyte disturbances that respond to correction within 24 hours</li> <li>o Grade 3 hypertension that is adequately controlled by the addition of up to 2 additional antihypertensive medications</li> <li>o Grade 3 pyrexia that does not result in study discontinuation</li> </ul> </li> </ul>
Cardiac	<ul style="list-style-type: none"> <li>• Ejection fraction <math>&lt;</math> lower limit of normal (LLN) with an absolute decrease of <math>&gt;10\%</math> from baseline with confirmation within 14 days</li> </ul>
Other	<ul style="list-style-type: none"> <li>• Inability to receive <math>\geq 75\%</math> of assigned doses in treatment period due to toxicity</li> <li>• Treatment delay of <math>&gt; 7</math> days due to study treatment-related toxicity</li> <li>• Grade 2 or higher toxicity that occurs beyond 28 days which in the judgment of the investigator is considered to be a DLT</li> </ul>

*Abbreviations: DLT, dose-limiting toxicity; AST, aspartate aminotransferase; ALT alanine aminotransferase; ULN, upper limit of normal; CTCAE, Common Terminology Criteria for Adverse Events' LLN, lower limit of normal.*





6.2

Figure S1. Representative immunohistochemistry sections of pERK (A) and pS6 (B) staining in paired tumor biopsies.



# Chapter 7

## Clinical pharmacology of targeted therapy combined with chemotherapy



### 7.1

#### **Phase I study evaluating WEE1 inhibitor AZD1775 (MK-1775) as monotherapy and in combination with gemcitabine, cisplatin or carboplatin in adult patients with advanced solid tumors**

*Journal of Clinical Oncology 2016, in press*

*Suzanne Leijen, Robin M.J.M. van Geel, Anna C. Pavlick, Raoul Tibes, Lee Rosen, Albiruni R Abdul Razak, Raymond Lam, Tim Demuth, Shelonitda Rose, Mark A. Lee, Tomoko Freshwater, Stuart Shumway, Li Wen Liang, Amit M. Oza, Jan H.M. Schellens, Geoffrey I. Shapiro*

## ABSTRACT

### Purpose

AZD1775 is a WEE1-kinase inhibitor targeting the G2 checkpoint control, preferentially sensitizing TP53-deficient tumor cells to DNA damage. This phase I study evaluated safety, tolerability, pharmacokinetics and pharmacodynamics of oral AZD1775 as monotherapy or in combination with chemotherapy in patients with refractory solid tumors.

### Patients and Methods

In part 1, patients received a single dose of AZD1775 followed by 14 days of observation. In part 2, patients received cycles AZD1775 as a single dose (part 2A) or as 5 twice-daily doses or 2 once-daily doses (Part 2B) in combination with chemotherapy: gemcitabine (1000 mg/m<sup>2</sup>), cisplatin (75 mg/m<sup>2</sup>) or carboplatin (AUC 5 mg/ml·min). Skin biopsies were collected for pharmacodynamic assessments. *TP53* status was determined retrospectively in archival tumor tissue.

### Results

In total, 202 patients were enrolled; 9 in part 1, 43 in part 2A (including 8 roll-over patients from part 1), and 158 in part 2B. Monotherapy AZD1775 given as single dose was well tolerated and the maximum tolerated dose (MTD) was not reached. In the combination regimens, the most common adverse events consisted of fatigue, nausea/vomiting, diarrhea, and hematological toxicity. The MTDs and biologically effective doses were established for AZD1775 combined with each combination. Target engagement, as a predefined 50% pCDK1 reduction in surrogate tissue, was observed in combination with cisplatin and carboplatin. Of 176 patients evaluable for efficacy, 94 (53%) had stable disease as best response, and 17 patients (10%) achieved a partial response. The response rate in *TP53* mutated patients ( $n = 19$ ) was 21% compared to 12% in *TP53* wild-type patients ( $n = 33$ ).

### Conclusion

AZD1775 was safe and tolerable as a single agent and in combination with chemotherapy at doses associated with target engagement.

## Introduction

DNA damage-induced checkpoint control is essential for the maintenance of genomic stability. One of the key proteins regulating the G2 checkpoint is the tyrosine kinase WEE1,<sup>1,2,3</sup> which inhibits the action of its direct substrate cyclin-dependent kinase (CDK1) by phosphorylation of the Tyr15 residue,<sup>3,6</sup> resulting in cell cycle arrest, allowing time for DNA repair. After DNA damage, TP53-mediated induction of p21<sup>Waf1/Cip1</sup> also contributes to cell cycle arrest by activating the G1 checkpoint and strengthening the G2 checkpoint. Mutations in *TP53* occur commonly in cancer causing defective and weakened G1 and G2 checkpoints, respectively, rendering cells highly dependent on activated WEE1 to achieve cell cycle arrest in response to DNA damage. Consequently, WEE1 inhibition abrogates the G2 checkpoint and selectively sensitizes TP53-deficient cells to DNA damaging chemotherapy<sup>7</sup> via premature mitotic entry and mitotic catastrophe<sup>8,9</sup>.

In addition to these events at the G2/M boundary, WEE1 also phosphorylates and inhibits the activity of CDK2 during S phase, allowing regulation of DNA synthesis and maintenance of replication forks<sup>9,10</sup>. WEE1 inhibition may therefore result in increased DNA synthesis and nucleotide insufficiency that reduces replication fork speed, leading to replication fork stalling and double-strand breaks<sup>11</sup>. Such events may be lethal to cancer cells with baseline replicative stress or compromised DNA repair proficiency, or may exacerbate the effects of DNA damaging agents irrespective of TP53 status.

The small molecule inhibitor AZD1775 (formerly MK-1775), a pyrazolo-pyrimidine derivative, is a potent and specific inhibitor of WEE1.<sup>14,19</sup> Preclinically, AZD1775 induced cell death in combination with chemotherapy and preferentially sensitized TP53-deficient tumor cell lines to various anticancer agents, including gemcitabine, cisplatin, carboplatin and radiation.<sup>12-16</sup> The enhancement of antitumor activity by AZD1775 correlated with inhibition of CDK1 Y15 phosphorylation in tumor tissue and skin hair follicles in a dose-dependent manner, suggesting pCDK1 to be a useful pharmacodynamic biomarker.<sup>12</sup> Additionally, in WiDR colorectal xenografts treated with gemcitabine plus AZD1775, reduced pCDK1 in tumor correlated with expression changes in genes associated with the G2 checkpoint comprising a 'WEE1 signature'.<sup>13</sup> This gene signature was also observed in animal skin samples, suggesting that pharmacodynamic markers can also be quantitatively assessed in surrogate tissues.

Other studies have demonstrated that AZD1775-mediated potentiation of antimetabolite chemotherapeutics can occur independent of TP53 status in both hematologic and solid tumor models<sup>17</sup>. Additionally, AZD1775 has demonstrated single-agent activity in subsets of cell lines with either wild type or mutant *TP53*. Sensitivity has been correlated with induction of DNA damage, assayed by phosphorylated histone H2AX ( $\gamma$ H2AX), without evidence of premature mitosis, assayed by phosphorylated histone H3<sup>18,19</sup>, and may occur in cells under oncogene-addicted<sup>20</sup> or epigenetically-mediated replication stress<sup>21</sup>, or in cells with homologous recombination (HR) repair deficiency<sup>22</sup>.

The objectives of this Phase 1 study were to (1) determine the maximum tolerated doses (MTDs), dose limiting toxicities (DLTs) and the biologically effective dose, as well as to characterize (2) safety and tolerability, (3) the pharmacokinetic and pharmacodynamic profile, (4) biomarkers of biological activity and (5) the preliminary anti-tumor activity of oral AZD1775 as monotherapy and in combination with either gemcitabine, cisplatin or carboplatin. Based on the variety of mechanisms by which AZD1775 may induce cytotoxicity, patients with tumors harboring both mutant and wild type TP53 were enrolled.

## Patients and Methods

### *Patient Selection*

Patients were  $\geq 18$  years old, with locally advanced or metastatic solid tumors, for whom no standard therapy was available. All patients had an Eastern Cooperative Oncology Group performance status (ECOG-PS) of  $\leq 1$ , adequate organ function, and evaluable and/or measurable disease according to Response Evaluation Criteria In Solid Tumors (RECIST, version 1.0).<sup>23</sup> (See Appendix for additional inclusion/exclusion criteria)

### *Study Design and Drug Treatment*

This phase 1, open-label, non-randomized three-arm dose-escalation study was conducted in 8 centers in America, Canada and Europe (ClinicalTrials.gov identifier: NCT00648648).

Cohorts of patients were treated at sequentially increasing dose levels of oral AZD1775 (Figure 1). Dose escalation in combination with chemotherapy was performed according to a modified Toxicity Probability Interval scheme that utilized a 30% DLT rate. AZD1775 was titrated using a modified Fibonacci design allowing for 50%, 40% and 30% dose increments in subsequent dose levels<sup>24</sup> (Appendix). The MTD of AZD1775 was evaluated for each of the 3 chemotherapy treatment arms separately. AZD1775 monotherapy consisted of a single dose followed by 14 days of observation (Part 1), after which patients moved to part 2A, in which a single dose of AZD1775 was given 24h after standard chemotherapy with gemcitabine (1000 mg/m<sup>2</sup>), cisplatin (75 mg/m<sup>2</sup>) or carboplatin (AUC 5 mg/ml·min). Part 2B consisted of a multiple-dose regimen of AZD1775 (2.5 days twice-daily doses [BID]) starting concomitantly with chemotherapy. Patients were assigned to a chemotherapy arm according to the judgment of the investigator.

Alternate schedules of AZD1775 in combination with gemcitabine were explored: 1) 50/25mg: 50 mg AZD1775 BID on day 1, 25 mg BID on day 2 and 25 mg QD on day 3, and 2) a QD dose of AZD1775 (varying from 100-200 mg) for two days, the first dose given simultaneously with administration of gemcitabine.

### *Safety and Assessments*

Demographic data and medical history were collected during screening. Physical examination, vital signs and other safety assessments (ECOG-PS, 12-lead ECG, hematology/biochemistry and relevant tumor markers) were performed pre-dose and throughout treatment.

Toxicities were graded according to the National Cancer Institute Common Terminology Criteria for Adverse Events (NCI-CTCAE) version 3.0.<sup>25</sup> DLTs were defined as any grade 4-5 hematological toxicity (with the exception of grade 4 anemia and leucopenia, grade 4 neutropenia lasting for  $<7$  days and grade 4 thrombocytopenia lasting for  $<4$  days [except if a platelet transfusion was required]), and any grade 3, 4, or 5 non-hematologic toxicity (with specific exceptions: Appendix) during the first cycle. Tumor assessments were performed at screening, every two cycles and whenever there was suspicion of disease progression.

Part 1 – 'AZD1775 monotherapy' (n = 9)	AZD1775 dose	Patient number, <i>n</i>
Day 1: 1 Single dose of AZD1775 – a single 14 day cycle	325 mg	3
	650 mg	3
	1300 mg	3
↓ <span style="border: 1px solid black; padding: 2px;">8 of 9 patients from Part 1 proceeded to Part 2A</span>		
Part 2A – 'AZD1775 single dose' (n = 43)	AZD1775 dose	Patient number, <i>n</i>
Day 1: Chemotherapy (one of three arms)		
1. Gemcitabine 1000 mg/m <sup>2</sup> Day 1, 8, 15 (28-day cycle)	100 mg (Day 2, 9, 16)	6
	<b>200 mg</b> (Day 2, 9, 16)	8
2. Cisplatin 75 mg/m <sup>2</sup> Day 1 (21-day cycle)	100 mg	3
	<b>200 mg</b>	10
3. Carboplatin AUC 5 Day 1 (21-day cycle)	100 mg	3
	200 mg	4
	<b>325 mg</b>	9
Day 2: One single dose of AZD1775		
Part 2B – 'AZD1775 multiple dose' (n = 158)	AZD1775 dose	Patient number, <i>n</i>
Day 1: Chemotherapy (one of three arms) + AZD1775 BID		
1. Gemcitabine 1000 mg/m <sup>2</sup> Day 1, 8, 15 (28-day cycle)	25 mg <sup>†</sup>	6
	50 mg <sup>†</sup>	6
	50/25 mg *	13
2. Cisplatin 75 mg/m <sup>2</sup> Day 1 (21-day cycle)	50 mg	4
	100 mg	7
	125 mg	6
	150 mg	10
	<b>200 mg</b>	14
	250 mg	4
3. Carboplatin AUC 5 Day 1 (21-day cycle)	75 mg	4
	150 mg	4
	<b>225 mg</b>	26
	325 mg	12
Day 2: AZD1775 BID, Day 3: AZD1775 QD		
Alternative 'AZD1775 multiple-dose gemcitabine' schedule:		
Day 1: Gemcitabine + AZD1775 QD		
Gemcitabine 1000 mg/m <sup>2</sup> Day 1, 8, 15 – 28-day cycle	100 mg	5
	125 mg	4
	150 mg	11
	<b>175 mg</b>	16
	200 mg	6
Day 2: AZD1775 QD		

Figure 1. Study Setup.

MTDs given in bold. <sup>†</sup>AZD1775 administration on day 1-3, 8-10 and 15-17. \* 50 mg of AZD1775 BID Day 1, 8 and 15; 25 mg BID Day 2, 9, 16; 25 mg QD Day 3, 10, 16. Abbreviations: BID, bidaily; QD, once daily; MTD, maximum tolerated dose.

Table 1. Patient Demographics and Clinical Characteristics							
	P2A Gemcitabine n = 14	P2A Cisplatin n = 13	P2A Carboplatin n = 16	P2B Gemcitabine n = 67	P2B Cisplatin n = 45	P2B Carboplatin n = 46	Total n = 201
<b>Gender, n (%)</b>							
Male	4 (29)	7 (54)	9 (56)	28 (42)	19 (42)	21 (46)	88 (44)
Female	10 (71)	6 (46)	7 (44)	39 (58)	26 (58)	25 (54)	98 (56)
<b>Age (years), n (%)</b>							
<55	7 (50)	3 (23)	7 (44)	18 (27)	23 (51)	14 (30)	72 (36)
55–64	3 (21)	4 (31)	4 (25)	24 (36)	18 (40)	18 (39)	71 (35)
65–74	3 (21)	6 (46)	2 (13)	21 (31)	3 (7)	11 (24)	46 (23)
≥ 75	1 (7)	0 (0)	3 (19)	4 (6)	1 (2)	3 (7)	12 (6)
mean	56.4	60.5	57.4	60.1	53.7	58.1	57.7
SD	14.8	9.7	13.4	11.3	10.3	12.2	12.0
Range	30–83	41–70	35–79	23–79	28–76	27–78	31–78
<b>Ethnicity, n (%)</b>							
Hispanic	0 (0)	0 (0)	1 (6)	4 (7)	1 (2)	1 (2)	7 (4)
Not Hispanic	14 (100)	13 (100)	15 (94)	63 (93)	44 (98)	45 (98)	194 (97)
<b>Tumor type, n (%)</b>							
Melanoma	2 (14)	5 (39)	6 (38)	2 (3)	7 (16)	20 (44)	42 (21)
Ovarian cancer	2 (14)	2 (15)	2 (13)	8 (12)	9 (20)	2 (4)	25 (12)
Lung cancer	3 (21)	0 (0)	0 (0)	13 (19)	1 (2)	1 (2)	18 (9)
Breast cancer	0 (0)	1 (8)	1 (6)	6 (9)	7 (16)	1 (2)	16 (8)
Colorectal cancer	0 (0)	1 (8)	4 (25)	1 (2)	5 (11)	4 (9)	15 (7)
Other	7 (50)	4 (31)	3 (19)	37 (55)	16 (36)	18 (39)	85 (42)
<b>Prior treatments, n (%)</b>							
1	7 (50)	9 (70)	5 (31)	31 (46)	26 (58)	30 (65)	108 (54)
2	5 (36)	3 (23)	6 (38)	15 (22)	12 (27)	10 (22)	51 (25)
3	1 (7)	1 (8)	2 (13)	10 (15)	6 (13)	4 (9)	24 (12)
≥ 4	1 (7)	0 (0)	3 (19)	11 (16)	1 (2)	2 (4)	18 (9)
<b>ECOG PS, n (%)</b>							
0	5 (36)	8 (62)	7 (44)	11 (16)	18 (40)	24 (52)	73 (36)
1	9 (64)	5 (39)	9 (56)	56 (84)	27 (60)	22 (48)	128 (64)

Abbreviations: P2A, part 2A; P2B, part 2B; ECOG, Eastern Cooperative Oncology Group performance status



### ***Exploratory Biomarker and Pharmacodynamic Assessments***

Baseline tumor samples were collected to correlate *TP53* mutation with pharmacodynamic and clinical response. Analysis of *TP53* status was performed by PCR/sequencing of exons 4-9.

Target inhibition of AZD1775 was assessed as a decrease of pCDK1 (Tyr15) relative to total CDK1 measured in skin biopsies using quantitative multiplex immunohistochemistry (IHC). Based on pre-clinical data linking this pharmacodynamic marker with *in vitro* and *in vivo* efficacy,<sup>12</sup> a 50% decrease of pCDK1 post-AZD1775 relative to post-chemotherapy and pre-AZD1775, with a one sided p-value <0.05, was defined as evidence of target engagement. Hair follicles were analyzed by qPCR for the 'WEE1 signature',<sup>13</sup> a gene expression-based pharmacodynamic biomarker that consists of a composite score calculated from the average fold change of up- and down regulated genes relative to pre-dose. Gene expression was measured at pre- and post-dose time-points for 8 genes identified as potential candidates by microarray: *CLSPN*, *FBXO5*, *MCM10*, *CCNE1* and *CCNE2*, *EGR1*, *HIST12BD*, and *MYB*. These genes are closely associated with the G2 checkpoint and commonly modulated by AZD1775 in both *TP53*-mutant and wild type cell lines, as well as in skin samples derived from subcutaneous xenograft tumors in rats treated with gemcitabine and AZD1775.<sup>13</sup>

### ***Statistical Analyses***

Safety assessments, tumor response, pharmacokinetic parameters and pharmacodynamic biomarkers were analyzed by descriptive statistics. An ANOVA was conducted for each quantitative polymerase chain reaction (qPCR) gene on the log fold-change (post-dose to pre-dose) scale. The various treatment and dose combinations were included as distinct categorical factors so that all observations were used to estimate a common residual variance; hence, tests were not dependent on variance estimates derived from only a few patients. A Hochberg multiplicity adjustment was applied over the 3 monotherapy doses tested (adjusting for multiple tests within the gene).

## **Results**

### ***Patient Characteristics***

In total, 202 patients were treated, of whom 176 were evaluable for response (Table 1). Eight out of 9 patients completed part 1 of the study and continued in part 2A. The most common tumor types were melanoma ( $n = 4$ , 44%) and lung cancer ( $n = 2$ , 22%) in part 1, and melanoma ( $n = 42$ , 21%), ovarian cancer ( $n = 25$ , 12%), breast cancer ( $n = 17$ , 8%), colorectal cancer (CRC) ( $n = 16$ , 8%) and lung cancer ( $n = 15$ , 7%) in part 2.

### ***Safety and Tolerability***

Five (56%) out of 9 patients treated in part 1 with a single dose of AZD1775 experienced a drug-related adverse event (AE), with the most frequently reported events being diarrhea (22%) and fatigue (22%). In part 2, 38 (19%) patients had a serious treatment-related AE. The most common treatment-related AEs were gastrointestinal disorders [nausea (67%), vomiting (35%) and diarrhea (41%)], fatigue (58%) and hematological toxicity [thrombocytopenia (44%), neutropenia (32%) and anemia (32%)] (Table 2). DLT criteria were not observed with AZD1775 monotherapy so that the MTD was not formally defined.

**Table 2. Drug-Related Adverse Events (≥10% Incidence)**

Adverse event, n (%)	AZD1775 single dose				AZD1775 multiple dose				Total n = 201
	Gemcitabine n = 14	Cisplatin n = 13	Carboplatin n = 16	Gemcitabine n = 67	Cisplatin n = 45	Carboplatin n = 46	Total n = 201		
<b>Any adverse events</b>	13 (93)	13 (100)	13 (81)	67 (100)	45 (100)	46 (100)	197 (98)		
Grade ≥ 3	7 (50)	4 (31)	2 (13)	45 (67)	21 (47)	31 (67)	110 (55)		
<b>Blood and lymphatic system disorders</b>									
Grade ≥ 3	8 (57)	4 (31)	8 (50)	51 (76)	24 (53)	35 (76)	130 (65)		
Anaemia	6 (43)	2 (15)	1 (6)	37 (55)	13 (29)	26 (57)	85 (42)		
Leukocytopenia	5 (36)	2 (15)	4 (25)	26 (39)	10 (22)	18 (39)	65 (32)		
Grade ≥ 3	0	1 (8)	0	12 (18)	2 (4)	9 (20)	24 (12)		
Neutropenia	4 (29)	1 (8)	1 (6)	11 (16)	5 (11)	6 (13)	28 (14)		
Grade ≥ 3	4 (29)	1 (8)	1 (6)	7 (10)	4 (9)	4 (9)	21 (10)		
Thrombocytopenia	3 (21)	1 (8)	0	28 (42)	12 (27)	16 (35)	64 (32)		
Grade ≥ 3	2 (14)	0	5 (31)	24 (36)	6 (13)	11 (24)	45 (22)		
Tinnitus	2 (14)	0	0	40 (60)	15 (33)	27 (59)	89 (44)		
Grade ≥ 3	2 (14)	0	0	21 (31)	5 (11)	19 (41)	47 (23)		
<b>Ear and labyrinth disorders</b>									
Tinnitus	0	3 (23)	0	0	10 (22)	2 (4)	15 (8)		
<b>Gastrointestinal disorders</b>									
Abdominal pain	0	2 (15)	0	0	7 (16)	1 (2)	10 (5)		
Constipation	9 (64)	11 (85)	8 (50)	52 (78)	43 (96)	40 (87)	163 (81)		
Diarrhoea	0	3 (23)	0	4 (6)	6 (13)	8 (17)	20 (12)		
Grade ≥ 3	0	0	1 (6)	7 (10)	3 (7)	2 (4)	13 (7)		
Nausea	1 (7)	1 (8)	1 (6)	11 (16)	10 (22)	10 (22)	34 (17)		
Stomatitis	2 (14)	5 (39)	3 (19)	21 (31)	20 (44)	31 (67)	82 (41)		
Vomiting	0	2 (15)	0 (0)	1 (2)	1 (2)	7 (15)	11 (7)		
Grade ≥ 3	0	1 (8)	1 (6)	1 (2)	5 (11)	7 (15)	15 (8)		
Dyspepsia	8 (57)	9 (69)	6 (38)	39 (58)	41 (91)	31 (67)	134 (67)		
Nausea	2 (14)	0	0	8 (12)	4 (9)	8 (17)	22 (11)		
Stomatitis	3 (21)	6 (46)	2 (13)	15 (22)	24 (53)	20 (44)	70 (35)		
Vomiting	2 (14)	0	1 (6)	2 (3)	0	1 (2)	6 (3)		
<b>Hepatobiliary disorders</b>									
Hepatotoxicity	2 (14)	0	0	0	0	0	2 (1)		
<b>Musculoskeletal and connective tissue disorders</b>									
Myalgia	2 (14)	2 (15)	1 (6)	16 (24)	3 (7)	4 (9)	28 (14)		
Grade ≥ 3	1 (7)	1 (8)	0	9 (13)	0	3 (7)	14 (7)		

Table 2. Drug-Related Adverse Events ( $\geq 10\%$  Incidence) (continued)

Adverse event, n (%)	AZD1775 single dose					AZD1775 multiple dose					Total n = 201
	Gemcitabine n = 14	Cisplatin n = 13	Carboplatin n = 16	Gemcitabine n = 67	Cisplatin n = 45	Carboplatin n = 46	Total n = 201				
<b>General disorders / administration site conditions</b>											
Fatigue	12 (86)	9 (69)	9 (56)	50 (75)	36 (80)	30 (65)	146 (73)				
Influenza like illness	9 (64)	8 (62)	6 (38)	39 (58)	28 (62)	27 (59)	117 (58)				
Malaise	1 (7)	0	1 (6)	7 (10)	0	0	9 (5)				
Pyrexia	3 (21)	0	0	7 (10)	1 (2)	8 (17)	19 (10)				
	5 (36)	2 (15)	1 (6)	21 (31)	4 (9)	4 (9)	37 (18)				
<b>Investigations</b>											
Grade $\geq 3$	4 (29)	1 (8)	1 (6)	20 (30)	15 (33)	6 (13)	47 (23)				
Alanine aminotransferase increased	0 (0)	0	0	5 (8)	5 (11)	1 (2)	11 (6)				
Aspartate aminotransferase increased	3 (21)	0	0	15 (22)	3 (7)	0	21 (10)				
Blood creatinine increased	3 (21)	0	0	9 (13)	1 (2)	0	13 (7)				
Neutrophil count decreased	0	1 (8)	0	1 (2)	7 (16)	1 (2)	10 (5)				
	0	0	0	5 (8)	5 (11)	2 (4)	12 (6)				
<b>Metabolism and nutrition disorders</b>											
Decreased appetite	5 (36)	3 (23)	4 (25)	24 (36)	21 (47)	11 (24)	68 (34)				
Dehydration	4 (29)	2 (15)	2 (13)	18 (27)	12 (27)	3 (7)	41 (20)				
	0	2 (15)	2 (13)	3 (5)	7 (16)	1 (2)	15 (8)				
<b>Nervous system disorders</b>											
Dizziness	2 (14)	2 (15)	1 (6)	21 (31)	13 (29)	18 (39)	57 (28)				
Headache	1 (7)	1 (8)	1 (6)	0	6 (13)	4 (9)	13 (7)				
Neuropathy peripheral	0	0	0	12 (18)	3 (7)	3 (7)	18 (9)				
	1 (7)	1 (8)	0	5 (8)	4 (9)	10 (22)	21 (10)				
<b>Respiratory, thoracic mediastinal disorders</b>											
Dyspnoea	1 (7)	2 (15)	0	13 (19)	5 (11)	13 (28)	34 (17)				
Hiccups	0	0	0	7 (10)	2 (4)	4 (9)	13 (7)				
	0	1 (8)	0	3 (5)	2 (4)	5 (11)	11 (6)				
<b>Skin and subcutaneous tissue disorders</b>											
Alopecia	6 (43)	1 (8)	1 (6)	31 (46)	5 (11)	12 (26)	56 (28)				
Hyperhidrosis	2 (14)	1 (8)	1 (6)	13 (19)	1 (2)	3 (7)	21 (10)				
Rash	2 (14)	0	0	0	0	0	2 (1)				
	3 (21)	0	1 (6)	15 (22)	1 (2)	3 (7)	23 (11)				

Note: Every subject is counted a single time for each adverse event. A subject with multiple adverse events within a system organ class is counted a single time for that organ class.

**Table 3. Number of DLTs, target engagement and antitumor activity per treatment regimen**

	N	DLTs, n	Target engagement	Partial response, n (%)*	Stable disease, n (%)*
<b>Part 1</b>					
Monotherapy	9	-	-	-	-
<b>Part 2A</b>					
Gemcitabine	14	3	No	1 (8%)	8 (67%)
Cisplatin	13	2	No	2 (17%)	7 (58%)
Carboplatin	16	2	No	2 (13%)	3 (20%)
<b>Part 2B</b>					
Gemcitabine	67	8	No	3 (5%)	35 (64%)
Cisplatin	45	7	Yes	7 (18%)	16 (42%)
Carboplatin	46	13	Yes	2 (5%)	25 (57%)

\* Percentages are calculated using the number of patients evaluable for response per treatment arm as denominator. Partial responses include both confirmed and unconfirmed partial responses. Abbreviations: DLT, dose-limiting toxicity.

MTDs were defined in all treatment arms and consisted of AZD1775 225 mg BID x 2.5 days every 21 days, 200 mg BID x 2.5 days every 21 days and 175 mg QD x 2 days weekly for 3 consecutive weeks out of every 4-week cycle, combined with carboplatin (AUC 5), cisplatin (75 mg/m<sup>2</sup>) and gemcitabine (1000 mg/m<sup>2</sup> weekly for 3 consecutive weeks out of every 4-week cycle), respectively, for the multiple dosing regimens (Figure 1).

#### Anti-tumor Activity

Seventeen (10%) of 176 evaluable patients achieved a partial response (PR) (of which 7 [4%] had confirmed PR), and 94 patients (53%) had stable disease (SD) lasting at least 6 weeks as best overall response (Table 3). Responses have been observed in patients with ovarian cancer ( $n = 7$ ), melanoma ( $n = 3$ ) breast cancer ( $n = 2$ ), head and neck cancer ( $n = 3$ ), colorectal cancer ( $n = 1$ ) and squamous cell carcinoma of the skin ( $n = 1$ ). Baseline tumor samples were evaluable from 52 patients. Among 19 patients with tumors harboring a *TP53* mutation, 4 (21%) achieved a PR. Thirty-three patients had *TP53* wild type tumors, of which 4 (12%) achieved a PR.

#### Pharmacokinetics

Plasma exposure increased approximately dose-proportionally in both monotherapy and combination arms with moderate to high variability (Figure 2 & Tables S1-4). Accumulation ratios (geometric mean ratio = day 3/day 1) for the area under the plasma concentration-time curve from time 0 to 8 hours post-dose ( $AUC_{0-8hr}$ ),  $C_{max}$ , and plasma drug concentration observed at 8 hours post-dose ( $C_{8hr}$ ) for twice-daily dosing averaged 0.991-3.82, 0.928-3.32, and 1.01-2.98, respectively, across tested AZD1775 doses in combination with chemotherapy. The pharmacokinetic target of  $C_{8hr} = 240$  nM, which was associated with maximal efficacy in rat tumor xenograft studies, was achieved at 100 mg AZD1775 in combination with cisplatin and 150 mg AZD1775 in combination with carboplatin on day 3 of the multiple AZD1775 dosing regimen (BID for 2.5 days), but not at the MTD of AZD1775 in the multiple-dose regimen in combination with gemcitabine. The alternate dosing regimen of AZD1775 125 mg

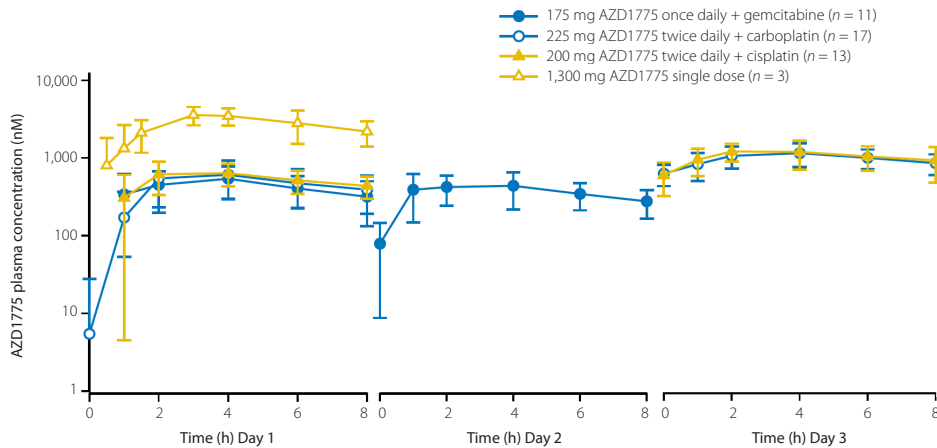


Figure 2. Mean concentration time profiles for single dose/multiple doses of AZD1775 alone and in combination with gemcitabine, carboplatin or cisplatin (semi log plot).

QD dosing for 2 days in combination with gemcitabine achieved the pharmacokinetic target on day 2. Pharmacokinetic parameters of AZD1775 were not significantly different between the three chemotherapy groups.

The anti-emetic aprepitant is a substrate and a weak to moderate inhibitor of CYP3A4. Although the use of strong CYP3A4 inhibitors was prohibited, administration of aprepitant was permitted as supportive care according to institutional guidelines. Comparing the pharmacokinetic parameters of AZD1775 in patients with and without concomitant administration of aprepitant showed an approximate 40% increase in exposure ( $P < 0.0001$  for  $AUC_{0-8hr}$  on day 1 and day 3).

#### Exploratory Biomarker and Pharmacodynamic Analyses

pCDK1 levels relative to total CDK1 were assessed by IHC in pre- and post-dose hair follicles in skin biopsies taken behind the ear. In the combination arms, the pre-dose biopsy was taken following chemotherapy but prior to AZD1775. Target engagement was demonstrated in the multi-dose regimen in combination with cisplatin or carboplatin (Table 4). With the gemcitabine multiple-dose regimen, target engagement was not achieved at the MTD of 25 mg AZD1775 (BID for 2.5 days) or with a regimen of 50 mg AZD1775 BID on day 1, 25 mg BID on day 2 and 25 mg QD on day 3. In an alternate schedule, the MTD of 175 mg AZD1775 QD for 2 days surpassed the dose needed to achieve target engagement in the other arms, but skin biopsies of patients treated at this dose-level were not available for pCDK1 analysis.

**Table 4. Measurement of pCDK1 (direct substrate of WEE1) in epidermis tissue with hair follicles**

	MTD AZD1775 (mg)	AZD1775 dosing schedule	Geometric mean ratio (post/pre)	1-sided p value
<b>Part 1</b>				
AZD1775 monotherapy	1,300*	single dose	0.57	0.064
<b>Part 2A<sup>†</sup></b>				
Gemcitabine	200	single dose	0.88	0.293
Cisplatin	200	single dose	0.77	0.114
Carboplatin	325	single dose	0.76	0.12
<b>Part 2B<sup>‡</sup></b>				
Gemcitabine	175	once daily, 2 days	ND	ND
Cisplatin	200	twice daily, 2.5 days	0.24	< 0.001
Carboplatin	225	twice daily, 2.5 days	0.49	< 0.001

\* MTD criteria were not reached; 1300 mg AZD1775 was the highest tested dose

<sup>†</sup> Post-dose biopsies were taken 8 hours post AZD1775 administration

<sup>‡</sup> Post-dose biopsies were taken 48 hours after the first AZD1775 administration

Gene expression measurements ("WEE1 signature"<sup>13</sup>) demonstrated that 4 (*CCNE2*, *EGR1*, *CLSPN* and *HIST1H2BD*) of the 8 selected genes showed significant changes in expression after monotherapy, consistent with preclinical expectations ( $p < 0.05$ , unadjusted for multiplicity). Most notable were the effects on expression of *EGR1* and *CCNE2* ( $p < 0.003$  and  $p = 0.005$ , respectively, after adjustment for multiplicity) at the highest dose levels, suggesting a dose-response correlation. A composite score derived from the 4 genes that showed expression changes in the direction consistent with that expected based on pre-clinical data (specifically *CCNE2*, *CLSPN*, and *MCM10* as down-regulated set, and *HIST1H2BD* as up-regulated gene) showed a consistent trend indicating target engagement at all monotherapy doses, although a strong dose-response trend is not evident employing the limited data available (Appendix).

## Discussion

In this study, we explored the tolerability, safety and anti-tumor activity of the WEE1 inhibitor AZD1775 in combination with cisplatin, carboplatin and gemcitabine, based on the potentiation by AZD1775 of their antitumor activity *in vitro* and *in vivo*.<sup>12</sup> In general, AZD1775 was well tolerated. In combination with chemotherapy, toxicities observed in the AZD1775 single-dose regimen were consistent with those expected for the individual chemotherapeutic agents. However, in the AZD1775 multiple-dose regimen, toxicities likely related to AZD1775 were observed, including bone marrow suppression, nausea, vomiting, diarrhea, fatigue and hiccups. Episodes of nausea, vomiting and diarrhea occurred primarily at days 2-3, suggesting a correlation with exposure.

The pharmacokinetic parameters of AZD1775 were approximately linear and increased in a dose-proportional manner, and were not significantly changed in combination with chemotherapy (Tables S1-4). However, we found a significant difference in AZD1775 exposure between patients treated with and without aprepitant, likely the result of CYP3A4 inhibition by aprepitant. *In vitro* data suggested that the major pathway of AZD1775 metabolism in humans involves CYP3A4, although FMO3 and FMO5 may be involved as well. Given the 40% increase in AZD1775 exposure upon concomitant use of

aprepitant, this drug-drug interaction (DDI) was considered clinically relevant and the use of aprepitant has been prohibited in subsequent studies until further crossover-DDI studies are conducted.

Since early *in vitro* experiments examining the sequence of gemcitabine and AZD1775 administration demonstrated greatest anti-tumor activity when AZD1775 was given approximately 24 hours following exposure to DNA damaging agents,<sup>12</sup> patients in part 2A received the chemotherapy infusion on day 1 and one dose of AZD1775 24h ( $\pm$ 2) after chemotherapy on day 2. The relatively short half-life of AZD1775 *in vivo*, as well as preclinical data that emerged while the study was ongoing, suggested that multiple doses of AZD1775 administered with chemotherapy would increase the combinatorial efficacy without affecting tolerability.<sup>16</sup> In order to maximize checkpoint escape in cancer cells that transition through S-phase during the time of treatment with chemotherapy, the protocol was amended and AZD1775 was given twice-daily for 5 doses in all three treatment arms, comprising Part 2B of the study. However, this schedule did not allow us to achieve doses in combination with gemcitabine that met predicted pharmacokinetic levels for efficacy or the minimum threshold required for target engagement, prompting us to investigate an attenuated once-daily schedule allowing administration of AZD1775 doses that met these endpoints. After this adjustment, doses in combination with gemcitabine were achieved consistent with proof-of-mechanism that was demonstrated in the other arms, with reduced pCDK1 relative to total CDK1 in post-treatment compared to post-chemotherapy and pre-AZD1775 skin biopsies. Together with changes in gene expression in hair follicles observed after monotherapy that reflected a previously defined WEE1 signature, evidence of WEE1 inhibition in surrogate tissue was established in this study.

Using the defined doses and schedules, further confirmatory pharmacodynamic assessments in optimally timed tumor biopsies post-chemotherapy and post-chemotherapy/AZD1775 will be required to confirm proof-of-mechanism in tumor tissue. Although the patient population was heavily pre-treated, partial responses and instances of prolonged stable disease were achieved. Mechanistically, tumors harboring *TP53* mutation or p53 pathway alterations are expected to benefit most from the addition of AZD1775 to cytotoxic chemotherapy. Indeed, our data suggested that tumors from responding patients were mildly enriched for *TP53* mutations, given the response rates of 21% and 12%, in *TP53* mutated and *TP53* wild type patients, respectively. However, larger patient sample sizes, better knowledge of the underlying biology, and a more detailed characterization of p53 pathway components in resistant and sensitive tumors will be necessary to optimize the identification of patients most likely to derive benefit from chemotherapy/AZD1775 combinations. Notably, AZD1775 is being actively developed in high-grade serous ovarian cancer, a tumor type where *TP53* mutation is ubiquitous, in combination with carboplatin (NCT01164995, NCT01357161) or gemcitabine (NCT02101775). Preliminary results have demonstrated promising anti-tumor activity with AZD1775 plus carboplatin in patients with platinum-resistant *TP53* mutated ovarian cancer<sup>27</sup>, as well as a significant increase in progression-free survival with AZD1775 added to paclitaxel and carboplatin when compared with paclitaxel plus carboplatin alone in patients with platinum-sensitive ovarian cancer.<sup>28</sup>

Further development of AZD1775 may also occur in combination with radiation therapy, particularly in glioblastoma (GBM), where WEE1 is overexpressed and radiosensitizing effects have been demonstrated in preclinical models.<sup>29-33</sup> Additionally, preclinical synergism has been observed with CHK1 inhibitors<sup>34-37</sup>; combined WEE1/CHK1 inhibition, if tolerable, may achieve even more potent G2

checkpoint abrogation in concert with DNA damaging agents. Interestingly, the activation of CDK1 afforded by WEE1 inhibition may also predispose to immunotherapy responses in tumors that have undergone epithelial-mesenchymal transition, prompting interest in combinations with immune checkpoint blockade.<sup>38</sup>

Based on the multiple-dose regimen (BID x 2.5 days) established in this study, a monotherapy study was launched with a similar schedule administered for up to 2 weeks/21-day cycle. The MTD was 225 mg, with biopsies after the 5<sup>th</sup> dose demonstrating reduced CDK1 Y15 phosphorylation and induction of  $\gamma$ H2AX. Responses were observed among patients carrying *BRCA* mutations.<sup>39</sup> Such work may also inform the optimal populations to study in combination trials.

In summary, we have established tolerable doses of oral AZD1775 in combination with cisplatin, carboplatin and gemcitabine that exceed threshold pharmacokinetic levels for efficacy and preliminary pharmacodynamic evidence of WEE1 inhibition in concert with these DNA damaging agents. Our results lay the groundwork for follow-up studies that will be required for proof-of-principle in order to definitively assess the contribution of AZD1775 to the anti-tumor activity of these combinations.



## References

1. Coleman TR, Dunphy WG. Cdc2 regulatory factors. *Curr Opin Cell Biol* 1994;6:877-82.
2. Morgan DO. Cyclin-dependent kinases: engines, clocks, and microprocessors. *Annu Rev Cell Dev Biol* 1997;13:261-91.
3. Parker LL, Piwnica-Worms H. Inactivation of the p34cdc2-cyclin B complex by the human WEE1 tyrosine kinase. *Science* 1992;257:1955-7.
4. Featherstone C, Russell P. Fission yeast p107wee1 mitotic inhibitor is a tyrosine/serine kinase. *Nature* 1991;349:808-11.
5. Lundgren K, Walworth N, Booher R, et al. mik1 and wee1 cooperate in the inhibitory tyrosine phosphorylation of cdc2. *Cell* 1991;64:1111-22.
6. Rowley R, Hudson J, Young PG. The wee1 protein kinase is required for radiation-induced mitotic delay. *Nature* 1992;356:353-5.
7. Leijen S, Beijnen JH, Schellens JH. Abrogation of the G2 checkpoint by inhibition of Wee-1 kinase results in sensitization of p53-deficient tumor cells to DNA-damaging agents. *Curr Clin Pharmacol* 2010;5(3):186-91.
8. Aarts M, Sharpe R, Garcia-Murillas I, et al. Forced mitotic entry of S-phase cells as a therapeutic strategy induced by inhibition of WEE1. *Cancer Discov* 2012;2(6):524-39.
9. Do K, Doroshow JH, Kummar S. Wee1 kinase as a target for cancer therapy. *Cell Cycle* 2013;12(19):3159-64.
10. Vriend LE, De Witt Hamer PC, Van Noorden CJ. WEE1 inhibition and genomic instability in cancer. *Biochim Biophys Acta* 2013;1836(2):227-35.
11. Beck H, Nähse-Kumpf V, Larsen MS, et al. Cyclin-dependent kinase suppression by WEE1 kinase protects the genome through control of replication initiation and nucleotide consumption. *Mol cell boil* 32(20):4226-4236, 2012.
12. Hirai H, Iwasawa Y, Okada M, et al. Small-molecule inhibition of Wee1 kinase by MK-1775 selectively sensitizes p53-deficient tumor cells to DNA-damaging agents. *Mol Cancer Ther* 2009;8:2992-3000.
13. Mizuarai S, Yamanaka K, Itadani H, et al. Discovery of gene expression-based pharmacodynamic biomarker for a p53 context-specific anti-tumor drug Wee1 inhibitor. *Mol Cancer* 2009;8:34.
14. Bridges KA, Hirai H, Buser CA, et al. MK-1775, a novel Wee1 kinase inhibitor, radiosensitizes p53-defective human tumor cells. *Clin Cancer Res* 2011;17:5638-48.
15. Kawabe T. G2 checkpoint abrogators as anticancer drugs. *Mol Cancer Ther* 2004;3:513-9.
16. Hirai H, Arai T, Okada M, et al. MK-1775, a small molecule Wee1 inhibitor, enhances anti-tumor efficacy of various DNA-damaging agents, including 5-fluorouracil. *Cancer Biol Ther* 2010;9:514-22.
17. Van Linden AA, Baturin D, Ford JB, et al. Inhibition of Wee1 sensitizes cancer cells to antimetabolite chemotherapeutics in vitro and in vivo, independent of p53 functionality. *Mol Cancer Ther* 2013;12(12):2675-84.
18. Guertin AD, Li J, Liu Y, Hurd MS, et al. Preclinical evaluation of the WEE1 inhibitor MK-1775 as single-agent anticancer therapy. *Mol Cancer Ther* 2013;12(8):1442-52.
19. Krahling JM, Gemmer JY, Reed D, et al. MK1775, a selective Wee1 inhibitor, shows single-agent antitumor activity against sarcoma cells. *Mol Cancer Ther* 2012;11(1):174-82.

20. Weisberg E, Nonami A, Chen Z et al. Identification of Wee1 as a novel therapeutic target for mutant RAS-driven acute leukemia and other malignancies. *Leukemia* 2015;29(1):27-37.
21. Pfister SX, Markkanen E, Jiang Y, et al. Inhibiting WEE1 Selectively Kills Histone H3K36me3-Deficient Cancers by dNTP Starvation. *Cancer Cell* 2015;28(5):557-68.
22. Aarts M, Bajrami I, Herrera-Abreu MT, et al. Functional Genetic Screen Identifies Increased Sensitivity to WEE1 Inhibition in Cells with Defects in Fanconi Anemia and HR Pathways. *Mol Cancer Ther* 2015;14(4):865-76
23. Therasse P, Arbutck SG, Eisenhauer EA, et al: New guidelines to evaluate the response to treatment in solid tumors. European Organization for Research and Treatment of Cancer, National Cancer Institute of the United States, National Cancer Institute of Canada. *J Natl Cancer Inst* 92:205-216, 2000.
24. Ji Y, Li Y, Nebiyu Bekele B. Dose-finding in phase I clinical trials based on toxicity probability intervals. *Clin Trials* 2007;4:235-44.
25. National Cancer Institute Cancer Therapy Evaluation Program Common Terminology Criteria for Adverse Events, version 3.0.09 August 2006 [http://ctep.cancer.gov/protocolDevelopment/electronic\\_applications/docs/ctcaev3.pdf](http://ctep.cancer.gov/protocolDevelopment/electronic_applications/docs/ctcaev3.pdf).
26. Xu Y, Fang W, Zeng W, et al. Woolf E. Evaluation of dried blot spot (DBS) technology versus plasma analysis for determination of MK-1775 by HILIC-MS/MS in support of clinical studies. *Anal Bioanal Chem* 2012;404:3037-48.
27. Leijen S, Van Geel RMJM, Sonke GS, et al. Phase II study with Wee1 inhibitor AZD1775 plus carboplatin in patients with p53 mutated ovarian cancer refractory or resistant (<3 months) to standard first line therapy. *J Clin Oncol* 2015;33, (suppl;abstr 2507).
28. Oza AM, Weberpals JI, Provencher DM, et al. An international, biomarker-directed, randomized, phase II trial of AZD1775 plus paclitaxel and carboplatin (P/C) for the treatment of women with platinum-sensitive, TP53-mutant ovarian cancer. *J Clin Oncol* 2015;33, (suppl;abstr 5507).
29. Bao S, Wu Q, McLendon RE, et al. Glioma stem cells promote radioresistance by preferential activation of the DNA damage response. *Nature* 2006;444:756-60.
30. Mir SE, Witt Hamer PC, Krawczyk PM, et al. In silico analysis of kinase expression identifies WEE1 as a gatekeeper against mitotic catastrophe in glioblastoma. *Cancer Cell* 2010;18:244-57.
31. Sarcar B, Kahali S, Prabhu AH, et al. Targeting radiation-induced G2/M checkpoint activation with the Wee-1 inhibitor MK-1775 in glioblastoma cell lines. *Mol Cancer Ther* 2011;10:2405-14.
32. PosthumaDeBoer J, Wurdinger T, Graat HC, et al. WEE1 inhibition sensitizes osteosarcoma to radiotherapy. *BMC Cancer* 2011;11:156.
33. Witt Hamer PC, Mir SE, Noske D, et al. WEE1 kinase targeting combined with DNA-damaging cancer therapy catalyzes mitotic catastrophe. *Clin Cancer Res* 2011;17:4200-7.
34. Davies KD, Cable PL, Garrus JE, et al. Chk1 inhibition and Wee1 inhibition combine synergistically to impede cellular proliferation. *Cancer Biol Ther* 2011;12:788-96.
35. Carrassa L, Chila R, Lupi M, et al. Combined inhibition of Chk1 and Wee1: In vitro synergistic effect translates to tumor growth inhibition in vivo. *Cell Cycle* 2012;11:2507-17.
36. Guertin AD, Martin MM, Roberts B, et al. Unique functions of CHK1 and WEE1 underlie synergistic anti-tumor activity upon pharmacologic inhibition. *Cancer Cell Int* 2012;12:45.

37. Chaudhuri L, Vincelette ND, Koh BD, et al: CHK1 and WEE1 inhibition combine synergistically to enhance therapeutic efficacy in acute myeloid leukemia ex vivo. *Haematologica* 2014;99(4):688-96.
38. Hamilton DH, Huang B, Fernando RI, et al. WEE1 inhibition alleviates resistance to immune attack of tumor cells undergoing epithelial-mesenchymal transition. *Cancer Res* 2014;74(9):2510-9.
39. Do K, Wilsker D, Ji J, et al. Phase I study of single-agent AZD1775 (MK-1775), a Wee1 kinase inhibitor, in patients with refractory solid tumors. *J Clin Oncol* 2015;33:3409-15.

## APPENDIX

### Supplementary Methods

#### *Patient inclusion/exclusion criteria*

Eligible patients had adequate bone marrow (absolute neutrophil count  $\geq 1,500/\text{mm}^3$ ; platelet count  $100,000/\text{mm}^3$ ; hemoglobin  $\geq 9 \text{ g/dL}$ ), liver function (serum total bilirubin  $\leq 1.5\times$  upper limit of normal [ULN] or direct bilirubin ULN for patients with serum total bilirubin  $> 1.5 \text{ ULN}$ ; ALT and AST  $\leq 2.5\times \text{ ULN}$  or  $\leq 5 \times \text{ ULN}$  for patients with liver metastases, alkaline phosphatase if  $\geq 2.5\times \text{ ULN}$ , the liver fraction had to be  $\leq 2.5\times \text{ ULN}$ ); renal function (serum creatinine  $\leq 1.5\times \text{ ULN}$  or  $\geq 60 \text{ mL/min}$  for patients with creatinine levels  $> 1.5\times \text{ ULN}$ ), and adequate coagulation status (International Normalized Ratio [INR] or Prothrombin Time [PT]  $\leq 1.5\times \text{ ULN}$ ; Activated Partial Thromboplastin Time [aPTT]  $\leq 1.5\times \text{ ULN}$ ). Previous anti-cancer treatment had to be completed at least 4 weeks prior to study entry. Up to 4 prior cytotoxic chemotherapy regimens were permitted. Drugs or other products known to be metabolized by CYP3A4, or to inhibit or induce CYP3A4 were not allowed. Patients with Central Nervous System (CNS) metastases were also excluded unless they were clinically stable for 1 month prior to study entry (*i.e.* no evidence of new enlarging CNS metastasis and off steroids or on a stable dose of steroids for  $\geq 2$  weeks). Other exclusion criteria included ongoing systemic infections, symptomatic ascites or pleural effusion, pregnancy, and hypersensitivity to the chemotherapy.

#### *Study Design and Treatment*

Part 1 of the study (one single dose of AZD1775) used a dose escalation scheme with 100% dose increments and dose level 1 of 325 mg AZD1775. DL1 was calculated based on a dose of 180 mg/m<sup>2</sup> (average Body Surface Area [BSA] of 1.8 m<sup>2</sup>) and rounded to the closest multiple of 25. The dose of 180 mg/m<sup>2</sup> AZD1775 was established as the maximum no-effect level in a single dose oral toxicity study in dogs. Combination therapy with AZD1775 and chemotherapy (Parts 2A and 2B) used a modified Fibonacci scheme. The modified Fibonacci scheme used 50%, 40% and 30% dose increments in subsequent dose levels. The TPI targets a DLT rate of 30% and allows escalation or de-escalation based on the number of DLT's observed at a given dose level. Upon definition of a preliminary MTD in 6 patients, a cohort expansion for a total of 13 evaluable patients is triggered. During cohort expansion, dose assignment actions continue based on continuous assessment of tolerability information. In case of DLT or toxicity after cycle 1 dose modification to a lower dose level was permitted in individual patients.

#### *Safety assessments*

Demographic data and medical history were collected during screening. Physical examination, vital signs and other safety assessments (ECOG-PS, 12-lead ECG, hematology/biochemistry and relevant tumor markers) were performed pre-dose and throughout treatment. DLTs were defined as any grade 4-5 hematological toxicity (with the exception of grade 4 anemia and leucopenia, grade 4 neutropenia lasting for  $<7$  days and grade 4 thrombocytopenia lasting for  $<4$  days [except if a platelet transfusion was required]), and any grade 3, 4, or 5 non-hematologic toxicity (with specific exception (with the specific exception of grade 3 nausea, vomiting, diarrhea, or dehydration occurring in the setting of

inadequate compliance with supportive care measures and lasting for less than 48 hours, alopecia [of any grade] and inadequately treated hypersensitivity reactions).

#### **Pharmacokinetic assessments**

Whole blood samples of 4 mL each, for determination of AZD1775 plasma concentrations, were collected at the following time points: Part 1 (monotherapy): pre-dose (0), and then 0.5, 1, 1.5, 3, 4, 6, 8, 24, and 48 hrs after the administration of AZD1775; Part 2A (AZD1775 single dose combination therapy): cycle 1 day 1: pre-dose (0), and then 0.5, 1, 1.5, 3, 4, 6, 8, 24, and 48 hrs after the administration of AZD1775; Parts 2B and 3 (AZD1775 multiple-dose combination therapy) cycle 1 day 1, and day 3: pre-dose, 1, 2, 4, 6, and 8 hrs after the first administration of AZD1775 (+ chemotherapy on day 1), cycle 1 day 2: pre-dose (prior to the third administration of AZD1775). Twenty four and 48 hrs after the fifth administration of AZD1775 were optional time points for blood sample collection. In the gemcitabine + QDx2 AZD1775 dosing regimen the time points for plasma collection of day 1 and 2 were similar to day 1 and 3 of the AZD1775 multiple-dose schedule (part 2B). For pharmacokinetic parameters see Supplementary Tables 1-4.

#### **Pharmacodynamic assessments**

##### *pCDK1*

Preclinical data indicated that the hair bulb is the preferable tissue for pCDK1 analysis. However, this study demonstrated that bulbs are only present in a minority of patient specimens. Therefore epidermis of the scalp behind the ears (containing hair follicles) was used for pCDK1 analysis, since it is also an actively proliferating tissue and present in all punch biopsies.

AZD1775, by inhibition of WEE1, reduces pCDK1 levels relative to total CDK1. Phosphorylation of CDK1 is induced by chemotherapy, especially gemcitabine. Correction for the chemotherapy effect was therefore applied in the analysis of the post-dose skin biopsy samples.

##### *WEE1 signature*

Plucked hair follicles were obtained pre-dose and post-dose (8 hrs [ $\pm$ 2 hrs] after [last] oral administration of AZD1775 in cycle 1). Skin biopsies were obtained pre-dose and post-dose (Part 1 and 2A: 8 hrs [ $\pm$ 2 hrs] and part 2B within 2 hrs after last oral administration of AZD1775 in cycle 1).

qPCR assays were performed for all clinical hair follicle samples from the single-dose regimen to analyze gene expression of a selected group of genes, also referred to as the 'WEE1 signature'. A signature responsive to AZD1775 was derived from preclinical experiments<sup>13</sup> and assessed in hair follicles collected at baseline and 8 hrs post dose from patients participating in the monotherapy part of this study. Briefly, a composite score was calculated as the average fold change of genes down regulated relative to pre-dose levels subtracted from the average fold change of genes up-regulated relative to pre-dose levels. The initial 8-gene signature (*HIST1H2BD*, *EGR1*, *CCNE1/2*, *CLSPN*, *MCM10*, *FBOX5*, *MYB*) was refined based on an interim analysis that pooled all the treatment groups (not just monotherapy) and determined which genes showed significant effects in a direction consistent with pre-clinical experiments. This led to a reduced 4-gene signature (up-regulated: *HISTH1HSBD*; and down-regulated *CCNE2*, *CLSPN*, *MCM10*).

Individual measurements that fell below the limit of quantification established via an assay validation process ( $C_t > 34.06$ ) were not used in the analysis. Fold-change (post-dose versus pre-dose) values were calculated using the Comparative Ct Method ( $\Delta\Delta C_t$ ). Statistical tests leading to p-values were conducted using the log (base 2) of fold change. As a QC check, trends in fold-change versus RNA yield were checked and in general there did not appear to be any strong trends for the genes examined. An analysis of the pre/post changes in the house keeping genes was conducted to confirm that effects on those genes were not driving significant results.

An ANOVA was conducted for each gene to estimate the mean fold-change at each of the combinations of treatment and dose level. All treatments and dose levels were included in a single ANOVA model for each gene as distinct categorical factors so that all observations were used to estimate a common residual variance. However, findings conducted in a separate study of standard of care therapies suggested that the natural course of gene expression changes over the time period of interest (24 to 32 hrs) after receipt of standard of care is a confounding factor in interpreting the effects of AZD1775 in the combination setting. Hence, statistical inference was restricted to just the monotherapy results. The Hochberg step-up procedure was used to report p-values adjusted for the multiple tests (for different monotherapy dose combinations) within each gene. (See Supplementary Figures 1 and 2, and Supplementary Tables 5 and 6)

Supplementary Table 1. Pharmacokinetic parameters of AZD1775 (part 2A)

Therapy	Dose (mg)	N	C <sub>max</sub> <sup>*</sup> (nM)	T <sub>max</sub> <sup>†</sup> (hr)	AUC <sub>0-8</sub> <sup>*</sup> (nM·hr)	AUC <sub>0-∞</sub> <sup>*</sup> (nM·hr)	t <sub>1/2</sub> <sup>*</sup> (hr)	C <sub>8</sub> <sup>*</sup> (nM)	AUC <sub>0-24</sub> <sup>*</sup> (nM·hr)
AZD1775 Monotherapy	325	3	806 (44.1)	4.00 (3.00-6.00)	4530 (43.9)	12100 (29.0)	9.02 (15.4)	585 (44.8)	9950 (34.1)
AZD1775 Monotherapy	650	3	2340 (13.4)	3.00 (3.00-3.00)	13100 (9.1)	29100 (12.6)	9.15 (27.2)	1130 (6.5)	24100 (6.7)
AZD1775 Monotherapy	1,300	3	3720 (27.6)	3.00 (3.00-3.00)	20600 (34.9)	61800 (56.6)	12.3 (27.1)	2190 (36.1)	43800 (45.3)
AZD1775 + Cisplatin	100	3	207 (56.7)	3.07 (2.95-4.30)	1140 (59.1)	2610 (44.7)	11.5 (36.1)	108 (57.9)	2110 (54.7)
AZD1775 + Cisplatin	200	9	207 (56.7)	4.00 (1.50-8.17)	2520 (36.0)	6820 <sup>*</sup> (74.0)	9.12 <sup>*</sup> (29.7)	310 <sup>*</sup> (54.1)	5560 (49.0)
AZD1775 + Gemcitabine	100	6	313 (61.5)	1.54 (0.97-6.02)	1460 (50.3)	2870 (39.1)	7.85 (26.6)	129 (36.0)	2510 (41.1)
AZD1775 + Gemcitabine	200	7	478 (49.7)	3.00 (1.50-6.00)	2330 (52.4)	5960 (45.9)	11.8 (60.2)	235 (57.7)	4510 (49.1)
AZD1775 + Carboplatin	100	3	323 (47.2)	1.52 (1.00-6.00)	1440 (46.9)	3100 (28.5)	9.31 (19.4)	119 (0.6)	2600 <sup>b</sup> (32.0)
AZD1775 + Carboplatin	200	4	463 (22.5)	3.03 (3.00-3.90)	2410 (14.5)	5800 (23.2)	11.2 (13.2)	262 (19.9)	4540 (23.2)
AZD1775 + Carboplatin	325	8	914 (45.1)	3.04 (1.00-8.00)	4680 (49.7)	10700 <sup>*</sup> (34.7)	8.43 <sup>*</sup> (20.7)	425 (44.8)	8490 (43.1)

\* median (SD); † Median (Range);<sup>a</sup>n = 7; <sup>a</sup>, n = 8; <sup>b</sup>, n = 2.

**Table S2. Pharmacokinetic parameters of AZD1775 following administration of multiple doses of AZD1775 (twice daily for 2.5 days) in combination with cisplatin (part 2B)**

AZD1775 dose	Day	N	C <sub>max</sub> <sup>*</sup> (nM)	T <sub>max</sub> <sup>†</sup> (hr)	AUC <sub>0-8</sub> <sup>*</sup> (nM·hr)	C <sub>8</sub> <sup>*</sup> (nM)	t <sub>1/2</sub> <sup>*</sup> (hr)
50 mg	1	4	155 (23.1)	2.01 (1.02-4.30)	742 (23.4)	66.3 (35.9)	NA
	3	4	226 (28.5)	3.00 (0.98-4.22)	1080 <sup>c</sup> (17.4)	113 (86.3)	11.9 <sup>b</sup> (10.1)
	GMR		1.45		1.52 <sup>c</sup>	1.34	
100 mg	1	7	227 (44.4)	4.00 (1.98-5.92)	1210 <sup>f</sup> (44.2)	139 <sup>f</sup> (53.4)	NA
	3	7	562 (24.5)	2.05 (2.00-6.17)	3640 (28.1)	388 (38.4)	13.7 <sup>e</sup> (34.8)
	GMR		2.64		3.08 <sup>f</sup>	2.85 <sup>f</sup>	
125 mg	1	6	596 (56.0)	3.29 (1.00-8.00)	3230 (53.6)	367 (64.4)	NA
	3	5	1350 (18.7)	2.03 (1.17-6.00)	8590 (19.2)	748 (31.3)	7.78 <sup>d</sup> (48.0)
	GMR		3.32 <sup>e</sup>		3.82 <sup>e</sup>	2.89 <sup>e</sup>	
150 mg	1	8	753 (41.6)	2.00 (0.98-4.05)	3630 (38.2)	341 (40.6)	NA
	3	7	1390 (41.1)	2.00 (1.00-6.03)	8730 (41.5)	920 (47.7)	13.0 (37.2)
	GMR		1.69 <sup>g</sup>		2.17 <sup>g</sup>	2.39 <sup>g</sup>	
200 mg	1	13	754 (29.7)	3.00 (1.98-5.98)	3850 <sup>i</sup> (29.9)	436 <sup>i</sup> (31.3)	NA
	3	11	1570 (36.0)	2.13 (1.00-7.92)	9310 <sup>i</sup> (36.6)	1070 <sup>j</sup> (49.4)	8.60 <sup>h</sup> (39.6)
	GMR		2.03 <sup>k</sup>		2.30 <sup>h</sup>	2.45 <sup>i</sup>	
250 mg	1	3	1050 (49.3)	4.25 (2.00-6.00)	6020 (55.6)	724 (38.8)	NA
	3	3	2520 (22.4)	4.00 (3.25-4.02)	19800 <sup>a</sup> (NC)	2010 (28.9)	NA
	GMR		2.58		3.08 <sup>a</sup>	2.86	

\* Median (SD); † Median (Range); a, n = 1; b, n = 2; c, n = 3; d, n = 4; e, n = 5; f, n = 6; g, n = 7; h, n = 8; i, n = 9; j, n = 10; k, n = 11; l, n = 12; GMR, Geometric Mean Ratio; NA, Not applicable; NC, Not calculated.



**Table S3. Pharmacokinetic parameters of AZD1775 following administration of multiple doses of AZD1775 (twice daily for 2.5 days) in combination with carboplatin (part 2B)**

AZD1775 dose	Day	N	C <sub>max</sub> <sup>*</sup> (nM)	T <sub>max</sub> <sup>†</sup> (hr)	AUC <sub>0-8</sub> <sup>*</sup> (nM·hr)	C <sub>8</sub> <sup>*</sup> (nM)	t <sub>1/2</sub> <sup>*</sup> (hr)
75 mg	1	4	223 (41.2)	1.02 (0.98-1.98)	1100 (34.8)	83.4 (39.3)	NA
	3	4	300 (65.5)	3.07 (2.05-8.00)	1750 (79.8)	184 (55.0)	10.4 <sup>a</sup> (51.7)
	GMR		1.20		1.21	2.12	
150 mg	1	4	355 (81.5)	2.99 (1.97-4.00)	1710 (71.7)	133 (56.5)	NA
	3	4	646 (56.5)	1.98 (0.98-4.00)	3600 (59.8)	295 (54.5)	9.68 <sup>a</sup> (6.2)
	GMR		2.16		2.32	2.26	
225 mg	1	17	663 (52.2)	4.00 (2.00-5.25)	3510 <sup>b</sup> (54.1)	390 <sup>b</sup> (51.1)	NA
	3	15	1410 (32.0)	4.00 (1.00-6.00)	9050 <sup>a</sup> (30.1)	985 <sup>f</sup> (30.6)	11.7 <sup>b</sup> (29.7)
	GMR		2.62 <sup>h</sup>		3.08 <sup>e</sup>	2.98 <sup>d</sup>	
225 mg	1	9	987 (51.0)	2.03 (1.98-6.00)	5120 (39.2)	535 (42.5)	NA
	3	9	1850 (46.3)	4.00 (2.02-4.13)	11800 (44.1)	1340 (45.7)	13.2 (41.3)
	GMR		1.90		2.27	2.47	
325 mg	1	12	1380 (41.4)	3.95 (1.90-6.08)	7220 (42.7)	773 (42.7)	NA
	3	11	2630 (36.2)	3.98 (1.00-6.83)	17100 (37.4)	1960 (33.3)	16.9 <sup>c</sup> (48.2)
	GMR		1.84 <sup>d</sup>		2.31 <sup>d</sup>	2.57 <sup>d</sup>	

\* Median (SD); † Median (Range); <sup>a</sup>, n = 3; <sup>b</sup>, n = 6; <sup>c</sup>, n = 8; <sup>d</sup>, n = 11; <sup>e</sup>, n = 12; <sup>f</sup>, n = 13; <sup>g</sup>, n = 14; <sup>h</sup>, n = 15; GMR, Geometric Mean Ratio; NA, Not applicable.

**Table S4. Pharmacokinetic parameters of AZD1775 following administration of multiple doses of AZD1775 (twice daily for 2.5 days) in combination with gemcitabine (part 2B)**

AZD1775 dose	Day	N	C <sub>max</sub> <sup>*</sup> (nM)	T <sub>max</sub> <sup>†</sup> (hr)	AUC <sub>0-8</sub> <sup>*</sup> (nM·hr)	AUC <sub>0-24</sub> <sup>*</sup> (nM·hr)	C <sub>8</sub> <sup>*</sup> (nM)	t <sub>1/2</sub> <sup>*</sup> (hr)
25 mg	1	6	42.6 (56.4)	3.13 (1.98-6.08)	200 (50.3)	NA	19.8 (53.5)	NA
	3	6	92.7 (40.4)	2.13 (1.00-4.00)	501 (40.2)	NA	41.7 (39.0)	7.23 <sup>a</sup> (11.9)
	GMR		2.29		2.59		2.25	
50 mg	1	6	134 (13.0)	3.08 (1.00-6.18)	658 <sup>b</sup> (15.2)	NA	78.5 <sup>b</sup> (29.7)	NA
	3	6	247 (23.8)	1.99 (0.63-6.00)	1360 <sup>a</sup> (22.1)	NA	138 <sup>b</sup> (28.2)	11.5 <sup>a</sup> (61.1)
	GMR		1.80		2.11 <sup>d</sup>		1.87 <sup>d</sup>	
50/25 mg <sup>‡</sup>	1	13	162 (55.8)	2.00 (0.98-4.02)	791 (49.8)	NA	63.0 (36.8)	NA
	3	13	139 (37.4)	1.98 (1.00-4.00)	751 (37.8)	NA	65.4 (39.9)	8.58 <sup>d</sup> (35.6)
	GMR		0.928		0.991		1.01	
100 mg	1	4	387 (40.9)	2.00 (1.98-3.98)	1820 (38.1)	3300 (31.1)	169 (25.5)	NA
	3	4	315 (16.6)	3.01 (2.00-3.98)	1790 (14.9)	NA	188 (25.4)	8.47 (38.5)
	GMR		0.849		1.02		1.11	
125 mg <sup>‡</sup>	1	3	463 (50.0)	2.02 (2.00-2.03)	2550 (43.4)	4510 (33.9)	228 (30.2)	NA
	3	3	532 (60.7)	2.00 (0.98-8.00)	2460 (53.4)	NA	241 (38.3)	8.23 <sup>f</sup> (20.9)
	GMR		1.05		0.910		1.04	
150 mg <sup>‡</sup>	1	11	491 (61.2)	3.98 (1.00-6.00)	2510 (57.2)	4520 <sup>e</sup> (54.6)	282 (64.1)	NA
	3	11	564 (71.7)	2.17 (0.95-7.42)	3240 (78.5)	NA	355 (64.7)	9.84 <sup>b</sup> (63.9)
	GMR		1.15		1.23		1.28	
175 mg <sup>‡</sup>	1	11	623 (37.3)	2.00 (0.97-4.10)	3190 <sup>a</sup> (40.0)	6090 (51.5)	317 (58.1)	NA
	3	11	666 (44.5)	2.02 (1.00-6.02)	3790 <sup>a</sup> (40.9)	NA	346 (41.5)	9.79 <sup>h</sup> (17.5)
	GMR		1.04		1.11		1.14	
200 mg <sup>‡</sup>	1	6	690 (35.2)	2.01 (1.98-4.17)	3500 (36.4)	6020 (40.7)	276 (42.5)	NA
	3	6	782 (48.2)	2.15 (0.98-4.17)	4080 <sup>b</sup> (53.0)	NA	407 (45.0)	8.48 <sup>a</sup> (29.0)
	GMR		1.10		1.10 <sup>b</sup>			

\* Median (SD); <sup>†</sup> Median (Range); <sup>‡</sup> 50 mg twice daily on Day 1, 25 mg twice daily on Day 2, 25 mg once daily on Day 3; <sup>§</sup> Once-daily dosing. All other groups were dosed twice daily; <sup>a</sup>, n = 4; <sup>b</sup>, n = 5; <sup>d</sup>, n = 12; <sup>e</sup>, n = 2; <sup>f</sup>, n = 9; GMR, Geometric Mean Ratio; NA, Not applicable.

<b>Table S5. Gene expression measurements ('WEE1 signature'): unadjusted p-values testing for a non-zero mean log fold-change based on ANOVA</b>								
Treatment group	CCNE1	CCNE2	CLSPN	EGR1	FBXO5	HIST1	MCM10	MYB
Mono dose level 1 (325 mg)	0.576 (n = 3)	0.816 (n = 3)	0.793 (n = 3)	0.963 (n = 3)	0.067 (n = 3)	0.719 (n = 3)	0.127 (n = 2)	0.530 (n = 3)
Mono dose level 2 (650 mg)	0.628 (n = 2)	0.106 (n = 2)	0.657 (n = 3)	0.205 (n = 3)	0.398 (n = 2)	0.050 (n = 3)	0.767 (n = 2)	0.951 (n = 3)
Mono dose level 3 (1300 mg)	0.410 (n = 3)	0.002 (n = 3)	0.020 (n = 3)	<0.001 (n = 3)	0.865 (n = 3)	0.136 (n = 3)	0.550 (n = 2)	0.212 (n = 3)

<b>Table S6. Gene Signature: adjusted p-values testing for a non-zero mean log fold-change based on ANOVA (Hochberg adjustment applied to all tests within a given gene)</b>								
Treatment group	CCNE1	CCNE2	CLSPN	EGR1	FBXO5	HIST1	MCM10	MYB
Mono dose level 1 (325 mg)	0.628 (n = 3)	0.816 (n = 3)	0.793 (n = 3)	0.963 (n = 3)	0.201 (n = 3)	0.719 (n = 3)	0.381 (n = 2)	0.951 (n = 3)
Mono dose level 2 (650 mg)	0.628 (n = 2)	0.1212 (n = 2)	0.793 (n = 3)	0.410 (n = 3)	0.796 (n = 2)	0.150 (n = 3)	0.767 (n = 2)	0.951 (n = 3)
Mono dose level 3 (1300 mg)	0.628 (n = 3)	0.006 (n = 3)	0.060 (n = 3)	0.003 (n = 3)	0.865 (n = 3)	0.272 (n = 3)	0.767 (n = 2)	0.636 (n = 3)



# Chapter 7

## Clinical pharmacology of targeted therapy combined with chemotherapy



### 7.2

#### Phase II study of WEE1 inhibitor AZD1775 plus carboplatin in patients with *TP53* mutated ovarian cancer refractory or resistant (< 3 Months) to first-line therapy

*Journal of Clinical Oncology* 2016, in press

Suzanne Leijen\*, Robin M.J.M. van Geel\*, Gabe S. Sonke, Daphne de Jong, Efraim H. Rosenberg, Serena Marchetti, Dick Pluim, Erik van Werkhoven, Shelonitda Rose, Mark A. Lee, Tomoko Freshwater, Jos H. Beijnen, Jan H.M. Schellens

*\* Authors contributed equally*

## ABSTRACT

### Purpose

AZD1775 is a first-in-class, potent and selective inhibitor of WEE1 with proof of chemopotential in p53 deficient tumors in preclinical models. In a phase 1 study the maximum tolerated dose of AZD1775 in combination with carboplatin demonstrated target engagement. We conducted a proof of principle, phase 2 study in patients with p53 tumor suppressor gene (*TP53*) mutated ovarian cancer refractory or resistant (<3 months) to first-line platinum-based therapy, to determine overall response rate (ORR), progression-free and overall survival (PFS, OS), pharmacokinetics, and modulation of pCDK1 in skin biopsies.

### Patients and Methods

Patients were treated with carboplatin (AUC 5 mg/mL·min) combined with 225 mg AZD1775 orally twice daily over 2.5 days every 21-day cycle until disease progression. Paired skin biopsies were obtained at baseline and after the fifth dose to determine pCDK1 modulation.

### Results

AZD1775 plus carboplatin demonstrated manageable toxicity with fatigue (87%) nausea (78%), thrombocytopenia (70%), diarrhea (70%) and vomiting (48%) as most common adverse events. Most frequent grade 3/4 adverse events were thrombocytopenia (48%) and neutropenia (37%). Out of 24 patients enrolled, 21 patients were evaluable for efficacy endpoints. The ORR was 43% (95%-confidence interval (CI), 22%-66%), including 1 patient (5%) with a prolonged complete response. Median PFS and OS were 5.3 months (95%-CI, 2.3–9.0 months) and 12.6 months (95% CI 4.9–19.7), respectively, with 2 patients on study for over 31 and 42 months at data cut off.

### Conclusion

This is the first report providing clinical proof that AZD1775 enhances carboplatin efficacy in *TP53* mutated tumors. The encouraging anti-tumor activity observed in patients with *TP53* mutated ovarian cancer who were refractory or resistant (<3 months) to first-line therapy warrants further development.

## Introduction

WEE1 is a tyrosine kinase that regulates cell cycle progression by governing the G2 checkpoint.<sup>1-3</sup> Binding of cyclin B to CDK1 can trigger mitosis, while inhibition of the CDK1/cyclin B complex by WEE1 induced phosphorylation of CDK1 at tyrosine 15 (Y15) will result in cell cycle arrest and allows for DNA repair. Pharmacological inhibition of WEE1 is a strategy to abrogate G2 cell cycle arrest, and to exploit G1 checkpoint deficiency of p53 deficient tumor cells, thereby enhancing their apoptotic response to DNA damage.<sup>4</sup>

AZD1775 (formerly MK-1775) is a potent and selective inhibitor of WEE1 ( $IC_{50} = 5,18$  nM in kinase screens) which demonstrated preclinical proof of principle in *in vitro* and *in vivo* models.<sup>5-7</sup> A previous phase 1 study of AZD1775 in combination with either carboplatin, cisplatin or gemcitabine in patients with different kinds of advanced solid tumors demonstrated an acceptable toxicity profile, linear pharmacokinetics and target engagement, as defined by reduced phosphorylated CDK1 (pCDK1) in surrogate tissue (skin biopsies), at tolerable dose levels.<sup>8</sup>

Despite initial therapy consisting of cytoreductive surgery and platinum-based chemotherapy, the majority of epithelial ovarian cancer patients will relapse at some point in time. About 25% of these patients are platinum resistant, with disease recurrence within 6 months after finishing first-line therapy. Refractory patients are those progressive during first-line therapy. Both refractory and resistant ovarian cancer patients have a very poor prognosis.<sup>9</sup>

We conducted a proof of principle phase 2 study with AZD1775 combined with carboplatin in ovarian cancer patients refractory or early resistant (< 3 months) after first-line platinum-based therapy because: 1) there is an unmet medical need for better treatment options for platinum refractory/resistant ovarian cancer patients;<sup>9-12</sup> 2) reintroduction of carboplatin in combination with WEE1 inhibitor AZD1775 provides a setting in which patients serve as their own control; 3) mutations in the p53 pathway are frequently observed in platinum resistant and platinum refractory ovarian cancer.<sup>13-17</sup> The primary objective of this study was to determine the overall response rate (ORR) of AZD1775 plus carboplatin. Secondary objectives included determination of progression-free survival (PFS) and overall survival (OS), assessment of the safety and tolerability of AZD1775 plus carboplatin, and to explore pharmacokinetic and pharmacodynamic parameters of AZD1775 and carboplatin when given together.

## Patients and Methods

### *Patient Selection*

Patients were  $\geq 18$  years of age with confirmed histological diagnosis of epithelial ovarian cancer and *TP53* mutation determined by polymerase chain reaction (PCR) sequencing of exons 2-10. All patients previously received first-line platinum plus paclitaxel-based therapy only and showed evidence of disease recurrence during or within 3 months after the end of this treatment according to Response Evaluation Criteria In Solid Tumors (RECIST, version 1.0)<sup>18</sup> or elevated Cancer Antigen (CA)-125 levels that could be monitored according to GCIg criteria.<sup>19</sup> All patients underwent either primary or interval debulking surgery. All patients had an Eastern Cooperative Oncology Group performance status (ECOG-PS) of  $\leq 2$ , adequate organ function and evaluable or measurable disease according to RECIST, version 1.0.<sup>18</sup>

### ***Study Design and Drug Treatment***

This investigator initiated, phase 2, open label, non-randomized, proof of concept study was conducted at the Netherlands Cancer Institute in Amsterdam, the Netherlands. The study (ClinicalTrials.gov identifier: NCT01164995) received approval of the institutional medical ethical review board and was conducted in accordance with the Declaration of Helsinki and Good Clinical Practice. All patients gave written informed consent prior to inclusion in the study.

Patients received carboplatin intravenously at a dose resulting in a target platinum AUC of 5 mg/mL·min in a 30-minute infusion, combined with 225 mg oral AZD1775 BID for 2.5 days in 21-day cycles. Study treatment was continued until disease progression. Carboplatin doses were calculated using the modified Calvert formula, in which glomerular filtration rate was estimated using the Cockcroft-Gault equation. AZD1775 was administered with 12-hour dose intervals and the first dose started concomitantly with the start of carboplatin infusion.

### ***Safety and Assessments***

Demographic data and medical history were collected during screening. Physical examination, vital signs and other safety assessments (ECOG-PS, registration of concomitant medication, hematology/biochemistry, urine analysis) were performed at baseline and hematology/biochemistry throughout treatment. Radiological disease assessments were performed by computer tomography (CT) scan or magnetic resonance imaging (MRI) at baseline and every 2 cycles. Tumor response was evaluated using RECIST v1.0<sup>18</sup>. Serum CA-125 was investigated as a secondary endpoint for efficacy and was defined as a 50% reduction during treatment with confirmation after 4 weeks according to the GCIg criteria.<sup>19</sup> Adverse events (AEs) were graded according to the National Cancer Institute Common Terminology Criteria (CTC) version 4.0.<sup>20</sup>

### ***Statistical Analyses***

The primary endpoint of the study was the overall response rate (ORR) of AZD1775 225 mg (BID for 2.5 days) in combination with carboplatin (AUC 5) in *TP53* mutated epithelial ovarian cancer patients not responding to first-line therapy. According to A'Herns single stage phase 2 design, a sample size of 21 evaluable patients provides a 61% power and a 5% level of significance to demonstrate whether the proportion of patients with a response is  $\leq 13\%$  or  $\geq 30\%$ . Accordingly, an ORR of at least 30% was required to declare efficacy, whereas an ORR of 13% or less would indicate no efficacy of interest.

### ***Pharmacokinetic and Pharmacodynamic Assessments***

To determine the pharmacokinetic parameters of AZD1775, blood samples were collected pre-dose on day 1, pre-dose on day 3, and 3 and 8 hours after the last AZD1775 dose of the first cycle. For platinum pharmacokinetic analysis 4 mL venous blood was collected in lithium-heparin tubes pre-dose on day 1, at end of infusion (EOI), EOI + 1 hour, EOI + 5 hour, and 24 hours after infusion start.

Skin biopsies from the hairy part behind the ear were collected pre-dose and on day 3 within 2 hours after the fifth dose of AZD1775 to measure phosphorylated CDK1 (pCDK1). pCDK1 levels relative to CDK1 were assessed by immunohistochemistry (IHC). Subsequently, the fold change between pre- and post-dose pCDK1/CDK1 ratio was calculated. Target engagement was defined as 50% reduction.<sup>21</sup>



<b>Table 1. Baseline patient characteristics</b>	
	<b>Patients (n = 23)</b>
Age, median (range), years	58 (25–74)
Stage of cancer, n (%)	
IIB	1 (4%)
IIIA	1 (4%)
IIIC	12 (52%)
IVA	9 (40%)
Histological subtype, n (%)	
Serous	16 (70%)
Clear cell	3 (13%)
Mucinous	2 (9%)
Mixed epithelial	1 (4%)
Unknown	1 (4%)
Number of prior lines of therapy, n (%)	
1	23 (100%)
Previous chemotherapy regimen, n (%)	
Carboplatin plus paclitaxel	20 (87%)
Carboplatin plus paclitaxel plus tamoxifen	2 (9%)
Carboplatin plus paclitaxel plus bevacizumab	1 (4%)
Number of first-line treatment cycles, n (%)	
< 6	3 (13%)
≥ 6	20 (87%)
Refractory to first-line therapy, n (%)	9 (39%)
Resistant (≤ 3 months) to first-line therapy, n (%)	14 (61%)
Prior debulking surgery, n (%)	
Yes	23 (100%)
TP53 mutation (PCR, exon 2–10)*, n (%)	
Missense	19 (83%)
Frameshift	3 (13%)
Nonsense	1 (4%)
Deletion	1 (4%)
No mutation	1 (4%)
BRACA1 mutation, n (%)	
Yes	2 (9%)
No	21 (91%)

Note: Twenty-four patients were enrolled. One patient never started study treatment because of rapid disease progression. In one patient TP53 mutation could not be confirmed by sequencing analysis and therefore did not meet the inclusion criteria. One patient went off-study due to clinical deterioration during cycle 1. She did not receive at least two cycles of study treatment and did not reach the first CT evaluation after 2 cycles. Therefore, these two patients were excluded from the response evaluation, but included in the toxicity evaluation. \*3 patients had multiple types of TP53 mutations. Therefore, percentages do not add up to 100%. Abbreviations: PCR, polymerase chain reaction.

### *p53 Status and Exploratory Genetic Analysis*

*TP53* mutation status was analyzed in archival tumor tissue, mostly obtained during debulking surgery. Standard IHC and mutation analysis by Sanger sequencing as routinely performed in our laboratory were performed prior to inclusion. All samples were analyzed by the AmpliChip p53 test for verification.<sup>22</sup> (See Appendix) Targeted next-generation sequencing (NGS) of cancer-related genes was performed to explore potential biomarkers predictive for response.

## Results

### *Patient Population*

A total of 24 patients were enrolled in the study and twenty-three patients started study treatment (Table 1). One patient never started study treatment because of early progression in the period between registration and study start. Median age of the patients was 58 years (range 25–74), the majority of patients (56%) were diagnosed with stage III ovarian cancer according to the International Federation of Obstetricians and Gynecologists Staging System for Ovarian Cancer (FIGO), and most patients (70%) had WHO performance status 0. These findings are in line with what can be expected from this particular patient group.

Twenty-three patients were evaluable for toxicity (*i.e.* received at least one cycle). Within 3 months after first-line therapy, 19 patients had recurrent disease according to RECIST 1.0 criteria and 4 patients according to GCIg criteria for CA-125. All patients showed radiological measurable or evaluable disease prior to study start.

### *Safety*

The main treatment related and clinically significant adverse events per patient are presented in Table 2. Bone marrow toxicity, fatigue, diarrhea, nausea and vomiting were the most common adverse events. Thrombocytopenia grade 4 and/or neutropenia grade 2-4 resulted in dose reductions 11 times (in 11 patients).

Adverse event, <i>n</i> (%)	Grade 1	Grade 2	Grade 3	Grade 4	Total
<b>Bone marrow toxicity</b>					
Thrombocytopenia	2 (9%)	3 (13%)	0 -	11 (48%)	16 (70%)
Neutropenia	0 -	1 (4%)	4 (17%)	5 (22%)	10 (43%)
Anemia	0 -	12 (52%)	2 (9%)	0 -	14 (61%)
<b>Gastrointestinal toxicity</b>					
Nausea	14 (61%)	3 (13%)	1 (4%)	0 -	18 (78%)
Diarrhea	9 (39%)	6 (26%)	1 (4%)	0 -	16 (70%)
Vomiting	8 (35%)	3 (13%)	0 -	0 -	11 (48%)
Pyrosis	2 (9%)	2 (9%)	0 -	0 -	4 (17%)
<b>Other</b>					
Fatigue	10 (43%)	9 (39%)	1 (4%)	0 -	20 (87%)
Hypomagnesemia	7 (30%)	2 (9%)	2 (9%)	0 -	11 (48%)
Peripheral sensory neuropathy	2 (9%)	3 (13%)	0 -	0 -	5 (22%)

### **Anti-Tumor Activity**

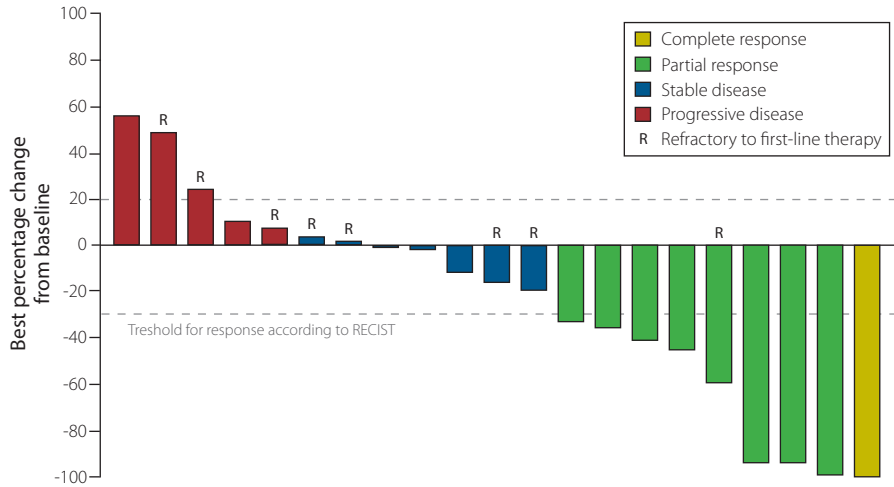
Out of 23 patients who started study treatment, one patient did not meet all inclusion criteria, as *TP53* mutation could not be confirmed by sequencing analysis. Therefore, the intention to treat (ITT) population consisted of 22 patients, of which 21 were considered evaluable for efficacy evaluation. One patient did not receive at least 2 cycles of study treatment and did not reach the first response evaluation after 6 weeks of treatment due to clinical deterioration. Of these 21 patients, 5 patients (24%) showed progressive disease (PD) on the first evaluation after 2 cycles. Seven patients (33%) experienced stable disease (SD) as best response. Eight patients (38%) showed a partial response (PR) as best response, and one patient (5%) had a complete response (CR) resulting in a 43% (95% Confidence Interval (CI), 22–66%) ORR (Figures 1 and S1) (41% in the ITT population). Two patients with a PR discontinued study treatment because of maximum benefit obtained according to their treating physician. Out of the 15 patients with serous ovarian cancer 7 (47%) achieved a response, including 1 CR, and the ORR among the 5 patients with non-serous subtypes was 20%. One patient with an unknown histological subtype had a PR. Out of 18 patients with *TP53* missense mutations, 1 (6%) achieved a CR and 6 patients (33%) had a PR, and 2 (67%) out of 3 patients with non-missense *TP53* mutations achieved a response. All patients with a CA-125 marker response also demonstrated a PR according to RECIST criteria and 2 patients had a PR while CA-125 levels did not reach the threshold of PR according to GCIG criteria. Eight patients (38%) were refractory to first-line therapy, of which 3 patients (38%) had PD as best response, 4 patients (50%) SD, and 1 patient (12%) PR. The median PFS was 5.3 months (95% CI, 2.3–9.0 months) with 2 patients (1 PR and 1 CR) still on study for over 31 and 42 months respectively at data cut off (Figure 2 and 3A). Median OS was 12.6 months (95% CI 4.9–19.7) (Figure 3B).

### **Pharmacokinetics and Pharmacodynamics**

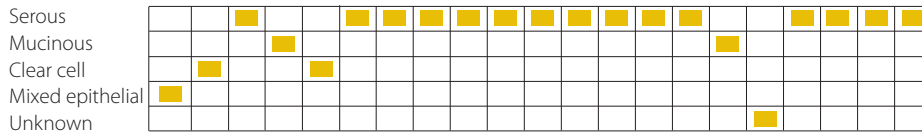
Blood samples for the measurement of total and free platinum and AZD1775 were obtained in all patients. AZD1775 mean plasma concentration 8 hours post-dose ( $C_{8h}$ ), maximum plasma concentration ( $C_{max}$ ) and AUC from time 0 to 8 hours post-dose ( $AUC_{0-8h}$ ) on day 3 were 834 nM, 1380 nM, and 8590 nM\*h, respectively. Pharmacokinetic parameters  $C_{8h}$ ,  $C_{max}$  and  $AUC_{0-8h}$  were consistent with data obtained in the previous phase 1 study with moderate variation on day 3 with a coefficient of variation in geometric mean  $C_{max}$  and AUC of 37% and 40%, respectively (Figure S2).

Mean free platinum  $C_{max}$  and  $AUC_{0-\infty}$  were 18.31  $\mu\text{g/mL}$  (%CV, 23.8) and 5.08 mg/mL\*min (%CV 26.4) respectively (Figure S3).

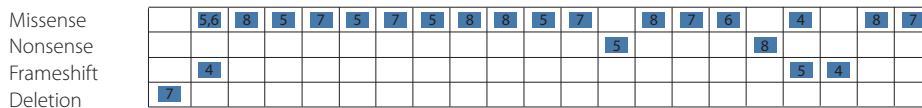
Skin biopsies were collected in all patients on day 1 (pre-dose) and day 3 (post-dose). Only samples containing more than 50 CDK1 positive cells were scored ( $n = 20$ ). The geometric mean pCDK1/CDK1 ratio modulation in skin tissue was -58% (range, +56% to -85%) upon 3 days of treatment, which was similar to the phase 1 data of AZD1775 plus carboplatin. Target engagement (*i.e.* > 50% pCDK1/CDK1 reduction) was achieved in 13 (65%) out of 20 patients who met evaluability criteria (Figure S3).



**Histological subtype**



**TP53 mutation**



**Mutations in WEE1 related genes**

**HRD genes**



**Oncogene induced replication stress**



**Other cell cycle related genes**

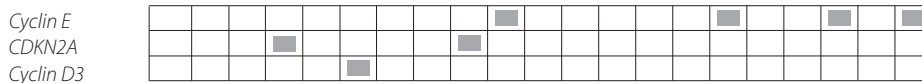


Figure 1. Waterfall plot of best percentage change in tumor size from baseline by best response and correlation with molecular characterization. Numbers in the blue squares represent mutated TP53 exons. Abbreviations: HRD, homologous recombination deficiency.

### *p53* Status and Exploratory Genetic Analysis

Results from the *p53* status analysis by IHC, direct sequencing and AmpliChip *p53* array are presented in table S1. In two patients with negative IHC staining for *p53*, a mutation and a deletion, respectively, were found with PCR/direct sequencing and AmpliChip *p53* array. The majority of *TP53* mutations found were in exons 5-8, which is in line with results published in the literature (IARC *TP53* database) (Table S1).

Targeted NGS revealed mutations in several *WEE1* related genes, including DNA damage response genes such as *BRCA1* ( $n = 2$ ), oncogene induced stress genes such as *KRAS* ( $n = 2$ ) and *MYC* ( $n = 4$ ), and other genes involved in the cell cycle like *Cyclin E* ( $n = 4$ ). The 2 patients with prolonged responses of over 31 and 42 months had mutations in *Cyclin E* and in *BRCA1*, *MYC* and *Cyclin E*, respectively (figure 1).

## Discussion

We report the results of an investigator initiated, proof of principle phase 2 study with first-in-class *WEE1* inhibitor AZD1775. AZD1775 in combination with carboplatin was generally well tolerated and demonstrated manageable toxicity. The toxicity profile of the AZD1775-carboplatin combination, with nausea/vomiting, diarrhea, fatigue and bone marrow suppression as major adverse events, is consistent with the toxicity profile observed in the phase 1 study with AZD1775 and carboplatin (or cisplatin or gemcitabine) in patients with advanced solid tumors.<sup>8</sup> Grade 4 thrombocytopenia and neutropenia events were manageable and did not lead to complications or treatment discontinuation.

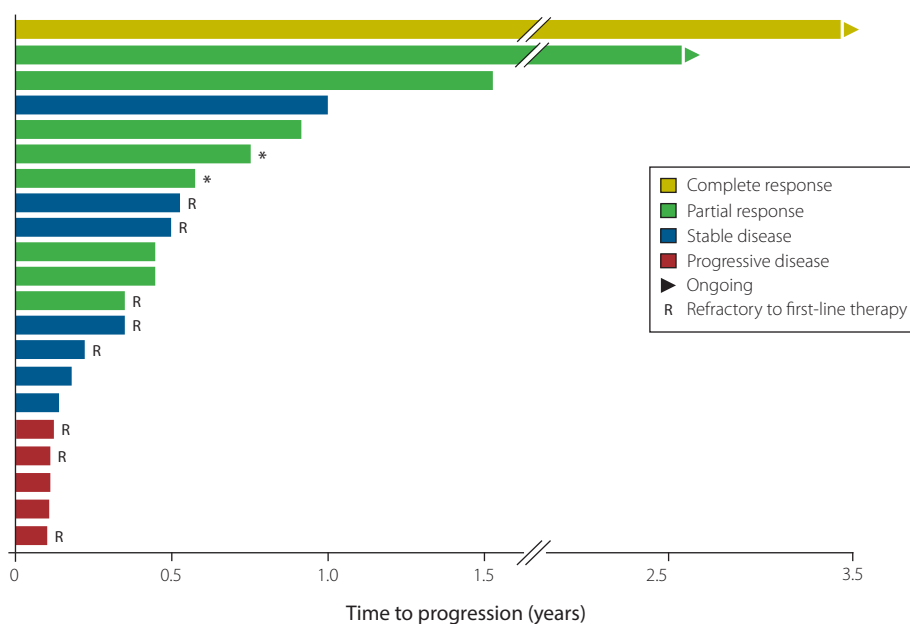


**Figure 2. Swimmer plot of progression-free survival by best response**

Two patients ongoing at data cut off (indicated by arrows). \* Patients who discontinued study treatment because of maximum benefit obtained according to their treating physicians.

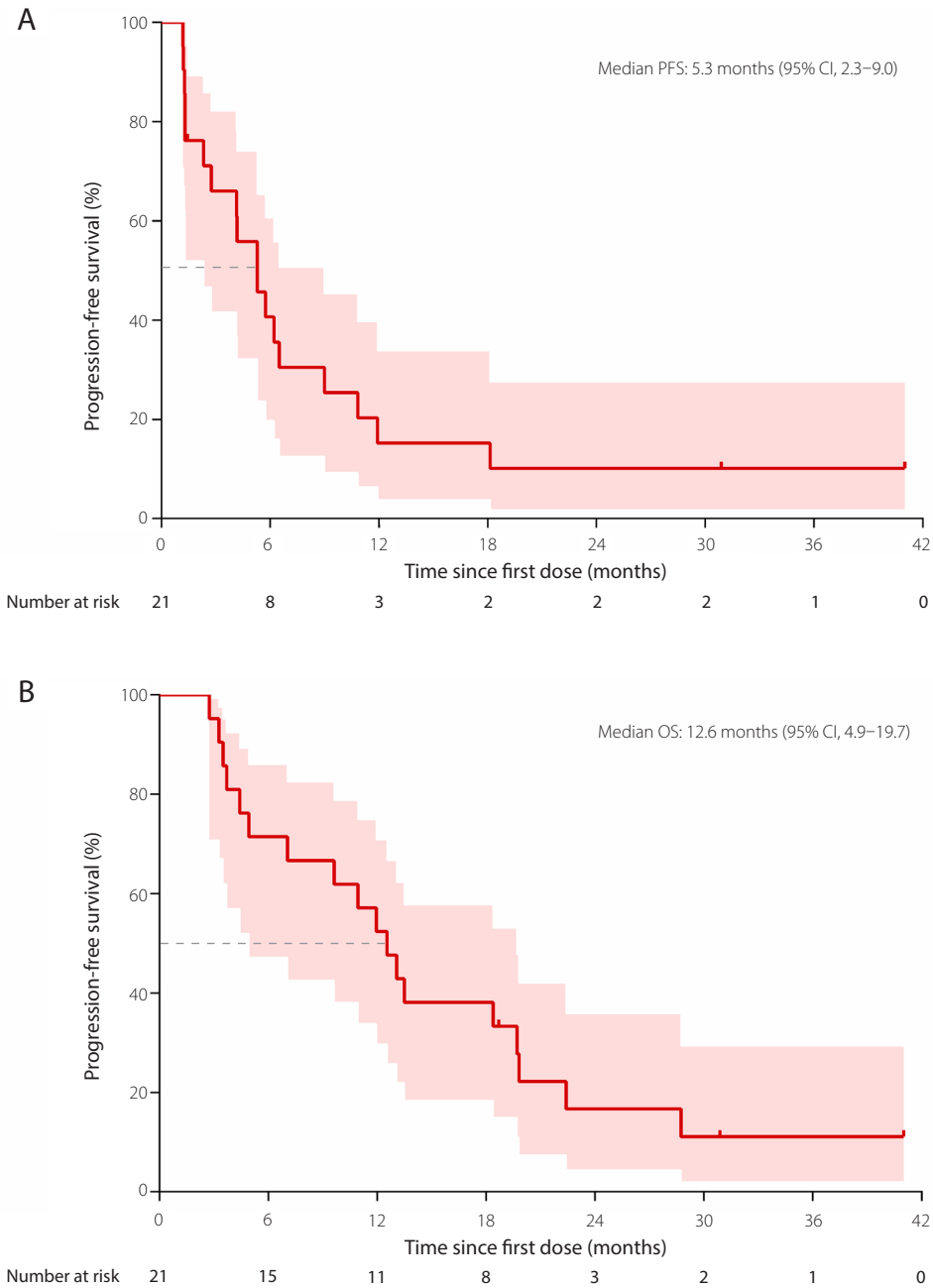


**Figure 3. Kaplan-Meier plots of overall survival and progression-free survival**

(A) Progression-free survival; 2 patients were censored who both remained in follow-up for progression-free survival. (B) Overall survival; 3 patients were censored who all remained in follow-up for overall survival. Colored areas represent the pointwise 95% confidence bands and thick marks indicate censored patients.

The results of p53 analysis were in line with data reported in the literature, and mainly encountered mutations in exon 5-8 of *TP53* which are known to cause loss-of-function according to the IARC *TP53* database.

We tested the hypothesis of chemosensitization by abrogation of the G2 checkpoint using WEE1 inhibitor AZD1775 in patients with *TP53* mutated ovarian cancer refractory or resistant (< 3 months) to first-line platinum-based therapy. These patients are known for their poor prognosis and effective treatment options are currently lacking. Patients served as their own control as they were re-exposed to carboplatin, in combination with orally administered WEE1 inhibitor AZD1775. Whereas first-line treatment consists of a predefined number of 6 carboplatin treatment cycles, in this study we continued carboplatin plus AZD1775 until disease progression. Encouraging anti-tumor activity was observed. The ORR was 43% including 1 (5%) complete response and 8 (38%) partial responses. This response rate exceeds the effect that could be expected with second-line single agent treatment options, including paclitaxel, pegylated liposomal doxorubicin, bevacizumab and topotecan, which reported response rates of 11% to 21%.<sup>24-26</sup> Three studies investigating combination strategies in ovarian cancer patients pretreated with platinum-based therapy demonstrated clinical activity in the range of our study. The randomized phase III AURELIA study reported a 52% ORR with bevacizumab plus weekly paclitaxel in patients with platinum-resistant ovarian cancer.<sup>27</sup> Two small studies published by Sharma et al. and Van den Burg et al. reported ORRs of 60% and 46% with weekly dose-dense paclitaxel/carboplatin and weekly cisplatin plus daily etoposide, respectively, in pre-treated platinum-resistant patients.<sup>28,29</sup> However, patients treated in AURELIA and in the study reported by Sharma et al. were platinum-resistant within a 6-month time period and the majority of patients had a platinum-free interval of  $\geq 3$  months. Moreover, in these studies, as well as in the study published by van den Burg et al., platinum-refractory patients were excluded and a large portion of the patients treated by Van den Burg et al. (82%) were not pre-treated with a paclitaxel-containing regimen. In contrast, our study solely enrolled patients who developed platinum-resistant disease within 3 months including platinum-refractory-patients (40%), which indicates the particularly aggressive disease present in our patients, and all patients were pre-treated with the highly active carboplatin/paclitaxel combination therapy. Therefore, our results suggest that AZD1775 plus carboplatin may improve first-line carboplatin/paclitaxel chemotherapy in resistant ovarian cancer patients, in terms of progression-free survival, warranting further clinical evaluation in patients with *TP53* mutated ovarian cancer. Phase II/III studies are needed to confirm the observed anti-tumor activity and to give a definite answer whether or not the carboplatin plus AZD1775 combination is synergistic, or AZD1775 monotherapy is equally effective.

Pharmacokinetic parameters of AZD1775 in our study were consistent with data obtained in the phase 1 study. Mean plasma concentration of AZD1775 at 8 hours post-dose well exceeded the preclinical target of 240 nM and target engagement, defined as a 50% reduction of pCDK1 in surrogate skin tissue, was observed in 65% of the patients. However a clear correlation between pCDK1 reduction and efficacy was not observed.

Genetic alterations in three gene groups were hypothesized to benefit from WEE1 inhibition: 1) cell cycle dependent genes (like *TP53* and *RB1*); 2) homologous recombination deficiency (HRD) genes (like *BRCA1*); 3) oncogene induced replication stress genes (like *KRAS* and *MYC*). Although the sample size is too small to draw conclusions, alterations in *BRCA1*, *Cyclin E* and *MYC* may, in addition to *TP53* mutations, enrich for response to WEE1 inhibition combined with carboplatin.

Two patients discontinued study treatment because of maximum benefit obtained according to their treating physician. However, two months after discontinuation an increase of CA-125 levels was observed in both patients, followed by disease progression on CT-scan. Therefore, given the long-lasting (*i.e.* more than 1 year) disease control and manageable toxicity observed in 4 patients enrolled in this study, treatment continuation beyond maximum benefit needs to be considered in future studies.

Initial preclinical data primarily supported combination therapy of AZD1775 with DNA damaging agents based on the rationale that cells defective in the G1 checkpoint due to loss of function of p53 are more dependent on the G2 checkpoint for DNA repair. However, recent preclinical and clinical research demonstrated AZD1775 single agent activity based on the role of WEE1 in the stabilization of replication forks and homologous recombination (HR) repair.<sup>30,31</sup> Do et al. demonstrated that some patients obtained benefit from AZD1775 monotherapy for a prolonged period of time.<sup>31</sup> However, responses were merely seen in patients with *BRCA1/2* mutations and not in patients with *TP53* mutations or patients with concurrent *BRCA1/2* and *TP53* mutations. Nevertheless, a possible role for maintenance therapy with AZD1775 as single agent following combined carboplatin plus AZD1775 is worth exploring in the *TP53* mutated ovarian cancer patient population, particularly since AZD1775 is orally administered and will be less onerous than the combination with additional intravenous chemotherapy.

Another attractive option for future studies is to explore simultaneous inhibition of multiple DNA repair mechanisms, for instance 1) dual inhibition of WEE1 and poly (ADP ribose) polymerase (PARP), in combination with DNA damaging anticancer agents, in patients with tumors harboring aberrations in DNA repair mechanisms, like *BRCA* mutations(23); or 2) the combination of AZD1775 with a Chk1 inhibitor, another key player with a coordinating role in the cell cycle and DNA damage response.<sup>32</sup>

Finally, the activity of AZD1775 might not be limited to solid tumors, but could potentially be extended to hematologic malignancies based on promising preclinical results in mantle cell lymphoma.<sup>33</sup> A complete overview of ongoing and future clinical studies is available at: [www.clinicaltrials.gov](http://www.clinicaltrials.gov).

In conclusion, our study provides clinical evidence that AZD1775 enhances anti-tumor efficacy of carboplatin in *TP53* mutated ovarian cancer patients resistant to first-line therapy and suggests that AZD1775 plus carboplatin may outperform first-line platinum-based chemotherapy in these patients. Based on these encouraging results, further development, starting with a randomized phase II or III study is warranted in this particular patient group and in other p53 deficient tumors to substantiate the true value of AZD1775.



## References

1. Watanabe N, Broome M, Hunter T. Regulation of the human WEE1Hu CDK tyrosine 15-kinase during the cell cycle. *Embo J* 1995;14:1878–91.
2. McGowan CH, Russell P. Human Wee1 kinase inhibits cell division by phosphorylating p34cdc2 exclusively on Tyr15. *EMBO J* 1993;12:75–85.
3. Squire CJ, Dickson JM, Ivanovic I, Baker EN. Structure and Inhibition of the Human Cell Cycle Checkpoint Kinase, Wee1A Kinase: An Atypical Tyrosine Kinase with a Key Role in CDK1 Regulation. *Structure* 2005;13:541–50.
4. Wang Y, Decker SJ, Sebolt-Leopold J. Knockdown of Chk1, Wee1 and Myt1 by RNA interference abrogates G2 checkpoint and induces apoptosis. *Cancer Biol Ther* 2004;3:305–13.
5. Hirai H, Arai T, Okada M, et al. MK-1775, a small molecule Wee1 inhibitor, enhances antitumor efficacy of various DNA-damaging agents, including 5-fluorouracil. *Cancer Biol Ther* 2010;9:514–22.
6. Rajeshkumar N V, De Oliveira E, Ottenhof N, et al. MK-1775, a potent Wee1 inhibitor, synergizes with gemcitabine to achieve tumor regressions, selectively in p53-deficient pancreatic cancer xenografts. *Clin Cancer Res* 2011;17:2799–806.
7. Hirai H, Iwasawa Y, Okada M, et al. Small-molecule inhibition of Wee1 kinase by MK-1775 selectively sensitizes p53-deficient tumor cells to DNA-damaging agents. *Mol Cancer Ther* 2009;8:2992–3000.
8. Schellens JHM, Shapiro G, Pavlick AC, et al. Update on a phase I pharmacologic and pharmacodynamic study of MK-1775, a Wee1 tyrosine kinase inhibitor, in monotherapy and combination with gemcitabine, cisplatin or carboplatin in patients with advanced solid tumors. *J Clin Oncol* 2011;29 (suppl;abstr 3068).
9. Fung-Kee-Fung M, Oliver T, Elit L, et al. Optimal chemotherapy treatment for women with recurrent ovarian cancer. *Curr Oncol* 2007;14:195–208.
10. Thigpen T. A Rational Approach to the Management of Recurrent or Persistent Ovarian Carcinoma. *Clin Obstet Gynecol* 2012;55:114–30.
11. Monk BJ, Coleman RL: Changing the paradigm in the treatment of platinum-sensitive recurrent ovarian cancer. from platinum doublets to nonplatinum doublets and adding antiangiogenesis compounds. *Int J Gynecol Cancer* 2009;19 Suppl 2:S63–7.
12. Pectasides D, Psyrri A, Pectasides M, et al. Optimal therapy for platinum-resistant recurrent ovarian cancer: doxorubicin, gemcitabine or topotecan? *Expert Opin Pharmacother* 2006;7:975–87.
13. Bernardini MQ, Baba T, Lee PS, et al. Expression signatures of TP53 mutations in serous ovarian cancers. *BMC Cancer* 2010;10:237.
14. Leitao MM, Soslow RA, Baergen RN, et al. Mutation and expression of the TP53 gene in early stage epithelial ovarian carcinoma. *Gynecol Oncol* 2004;93:301–6.
15. Olivier M, Hollstein M, Hainaut P. TP53 mutations in human cancers: origins, consequences, and clinical use. *Cold Spring Harb Perspect Biol* 2010;2:1–17.
16. Berchuck A, Iversen ES, Lancaster JM, et al. Patterns of gene expression that characterize long-term survival in advanced stage serous ovarian cancers. *Clin Cancer Res* 2005;11:3686–96.
17. Hagopian GS, Mills GB, Khokhar AR, et al. Expression of p53 in cisplatin-resistant ovarian cancer cell lines: modulation with the novel platinum analogue (1R, 2R-diaminocyclohexane)(trans-diacetato)(dichloro)-platinum(IV). *Clin Cancer Res* 1999;5:655–63.

18. Therasse P, Arbuck SG, Eisenhauer EA, et al. New guidelines to evaluate the response to treatment in solid tumors. European Organization for Research and Treatment of Cancer, National Cancer Institute of the United States, National Cancer Institute of Canada. *J Natl Cancer Inst* 2000;92:205–16.
19. Rustin GJS, Vergote I, Eisenhauer E, et al. Definitions for response and progression in ovarian cancer clinical trials Incorporating RECIST 1.1 and CA 125 agreed by the gynecological cancer intergroup. *Int J Gynecol Cancer* 2011;21:419–23.
20. National Cancer Institute: Common Terminology Criteria for Adverse Events v4.0. NCI, NIH, DHHS, 2009. [http://evs.nci.nih.gov/ftp1/CTCAE/CTCAE\\_4.03\\_2010-06-14\\_QuickReference\\_5x7.pdf](http://evs.nci.nih.gov/ftp1/CTCAE/CTCAE_4.03_2010-06-14_QuickReference_5x7.pdf).
21. Rose S, Cheng JD, Viscusi J, et al. Pharmacodynamic evaluation of pCDC2 as target engagement biomarker to assess activity of MK-1775 a Wee1 tyrosine kinase inhibitor. *J Clin Oncol* 2012;30 (suppl;abstr e13598).
22. Marton MJ, McNamara AR, Nikoloff DM, et al. Analytical Validation of AmpliChip p53 Research Test for Archival Human Ovarian FFPE Sections. *PLoS One* 2015;10:e0131497.
23. Gaidano G, Ballerini P, Gong JZ, et al. p53 mutations in human lymphoid malignancies: association with Burkitt lymphoma and chronic lymphocytic leukemia. *Proc Natl Acad Sci U S A* 1991;88:5413–7.
24. Markman M, Blessing J, Rubin SC, et al. Phase II trial of weekly paclitaxel (80 mg/m<sup>2</sup>) in platinum and paclitaxel-resistant ovarian and primary peritoneal cancers: A Gynecologic Oncology Group study. *Gynecol Oncol* 2006;101:436–40.
25. Gordon AN, Tonda M, Sun S, et al. Long-term survival advantage for women treated with pegylated liposomal doxorubicin compared with topotecan in a phase 3 randomized study of recurrent and refractory epithelial ovarian cancer. *Gynecol Oncol* 2004;95:1–8.
26. Burger RA, Sill MW, Monk BJ, et al. Phase II trial of bevacizumab in persistent or recurrent epithelial ovarian cancer or primary peritoneal cancer: A Gynecologic Oncology Group study. *J Clin Oncol* 2007;25:5165–71.
27. Poveda AM, Selle F, Hilpert F, et al. Bevacizumab combined with weekly paclitaxel, pegylated liposomal doxorubicin, or topotecan in platinum-resistant recurrent ovarian cancer: analysis by chemotherapy cohort of the randomized phase III AURELIA trial. *J Clin Oncol* 2015;33(32): 3836-38.
28. Sharma R, Graham J, Mitchell H, et al. Extended weekly dose-dense paclitaxel/carboplatin is feasible and active in heavily pre-treated platinum-resistant recurrent ovarian cancer. *Br J Cancer* 2009;100:707-12.
29. Van den Burg MEL, de Wit R, van Putten WLJ, et al. Weekly cisplatin and daily oral etoposide is highly effective in platinum pretreated ovarian cancer. *Br J Cancer* 2002;86:19-25.
30. Do K, Doroshow JH, Kummur S. Wee1 kinase as a target for cancer therapy. *Cell Cycle* 2013;12:3159–64.
31. Do K, Wilsker D, Ji J, et al. Phase I Study of Single-Agent AZD1775 (MK-1775), a Wee1 Kinase Inhibitor, in Patients With Refractory Solid Tumors. *J Clin Oncol* 2015;33(30):3409-15.
32. Guertin AD, Martin MM, Roberts B, et al. Unique functions of CHK1 and WEE1 underlie synergistic anti-tumor activity upon pharmacologic inhibition. *Cancer Cell Int* 2012;12:45.
33. Chilà R, Basana A, Lupi M, et al. Combined inhibition of Chk1 and Wee1 as a new therapeutic strategy for mantle cell lymphoma. *Oncotarget* 2014;6(5):3394-408.

## APPENDIX

### Supplementary Methods

#### *Patient Inclusion and Exclusion Criteria*

Eligible patients had a life expectancy of  $\geq 16$  weeks, adequate bone marrow function defined as absolute neutrophil count (ANC)  $\geq 1500/\text{mm}^3$  (or  $\geq 1.5 \times 10^9/\text{L}$ ), platelet count  $\geq 100,000/\text{mm}^3$  (or  $100 \times 10^9/\text{L}$ ), hemoglobin (Hgb)  $\geq 9.0 \text{ g/dL}$  (or  $5.6 \text{ mmol/L}$ ), adequate hepatic function defined as alanine transaminase (ALT) and aspartate aminotransferase (AST)  $\leq 2.5$  upper limit of normal (ULN) ( $\leq 5$  times ULN in case of liver metastases), adequate renal function defined by serum creatinine  $\leq 1.5$  times ULN or creatinine clearance (estimated using the formula of Cockcroft and Gault)  $\geq 60 \text{ mL/min}$  for patients with creatinine levels  $> 1.5$  times ULN. Exclusion criteria included cerebral or leptomeningeal metastases, radio- or chemotherapy within the last 4 weeks prior to study entry (limited palliative radiation for pain reduction was allowed), concurrent medication or other products known to be metabolized by, to inhibit or induce CYP3A4, and the use of aprepitant as an anti-emetic treatment.

#### *Study Design*

Oral intake was not allowed 2 h before and up to 1 h after intake of AZD1775. In case of toxicity, treatment was postponed for 1 week until recovery to CTC grade  $\leq 1$ . Readministration of study treatment occurred at a reduced dose level; in case of nausea and vomiting during optimal anti-emetic treatment AZD1775 was reduced to 175 mg (both BID for 2.5 days); in case of hematologic toxicity (*i.e.* decreased platelet count grade 4 ( $< 25,000/\text{mm}^3$  or  $< 25 \times 10^9/\text{L}$ ) or decreased neutrophil count grade 4 ( $< 500/\text{mm}^3$  or  $0.5 \times 10^9/\text{L}$ )) carboplatin was reduced to AUC 4 mg/mL·min; if recurrent hematologic toxicity was encountered, AZD1775 dose was reduced to 175 or 125 mg (BID for 2.5 days). Prophylactic anti-emetic treatment was applied as follows: day 1, granisetron 1 mg BID intravenously (IV) and dexamethasone 10 mg once daily (QD) IV; days 2 and 3, granisetron 1 mg BID orally (PO) and dexamethasone 3 mg BID PO, days 4 and 5, dexamethasone 1.5 mg QD PO and metoclopramide 10 mg QID (4 times daily) PO or 20 mg 3 times daily as suppository on indication.

#### *Pharmacokinetic analysis*

Plasma for AZD1775 pharmacokinetic (PK) analysis was obtained by immediate centrifugation (10 minutes;  $4^\circ\text{C}$   $1,500 \times g$ ) of whole blood. Samples were stored in 3.6 mL internally-threaded NUNC cryotubes at  $-20^\circ\text{C}$  until analysis. Analysis was performed through hydrophilic interaction liquid chromatography (HILIC) coupled with tandem mass spectrometry (LC-MS/MS).<sup>1</sup> Plasma for carboplatin PK analysis was obtained by immediate centrifugation (10 minutes;  $4^\circ\text{C}$   $2000 \times g$ ). Plasma was transferred directly to a Centrifree® UF device with an Ultracel YM-T membrane filter (Millipore® Ireland Ltd, Co.Cork, Ireland) and centrifuged at  $1500 \times g$  for 35 minutes at room temperature (RT). The resulting plasma ultrafiltrate, representing the free non-protein bound platinum fraction, was stored at  $-80^\circ\text{C}$  until analysis. Total platinum and free platinum concentrations were measured using a validated inductively coupled plasma mass spectrometry (ICP-MS) method.<sup>2</sup> A previously described population pharmacokinetic model was used to determine the AUC of free platinum.<sup>3</sup>

### ***p53 Status Analysis***

For p53 IHC staining the standard antibody DO-7 (DAKO M7001) was used and a minimum tumor cell percentage of 50% was necessary for evaluation. Strong staining of at least 50% of cells was required for a positive p53 scoring. Co-scoring by a central pathologist was performed to support scoring consistency.

For Sanger sequencing analysis, *TP53* exons 2-10 were amplified by PCR from genomic DNA, as previously described.<sup>23</sup> Subsequently, electrophoresis in 2% agarose gels with 0.5X Gelred (Biotium®) was used to assess PCR products. Sequencing was performed using the automatic ABI PRISM 3730 DNA genetic analyzer (Applied Biosystems®). Sequence data were compared with wild type (WT) sequences with Mutation Surveyor software (Softgenetics®).

The AmpliChip p53 test is a micro-array based sequencing test that allows sequencing of the entire coding region of *TP53*, including the flanking splicing regions of exons 2-11, and detection of single nucleotide substitutions and one base pair deletions.

The micro-array based AmpliChip p53 test performs comparative analysis of the hybridization pattern of a series of probes to sample, and wildtype (WT) reference DNA. Each probe contains multiple copies of a specific nucleotide sequence, and a total of 1,300 nucleotide positions of coding regions are tiled on the AmpliChip array. Another advantage would be the ability to identify p53 mutations in samples that contain a mixture of normal and tumor cells, without the need for microdissection. Main steps of AmpliChip TP53 array consist of extraction of genomic DNA extraction, PCR amplification of purified DNA, fragmentation and labeling of PCR products, followed by hybridization to the microarray, staining, scanning and determination of the sequence of the p53 gene.<sup>4-6</sup>

Clinical implications of encountered missense mutations and deletions with both methods were compared with results on the IARC TP53 database (<http://www.p53.iarc.fr/index.html>). Functional classification of the missense mutations in the IARC TP53 database has been based on the overall transcriptional activity on 8 different promoters. For each mutant the median of the 8 promoter-specific activities (expressed as the percentage of wild-type protein) has been calculated. Missense mutations are classified as 'non-functional' if the median is < 20%, partially functional' if the median is >20% and ≤ 75%, while 'functional' if the median is >75%. In case of missense mutations dominant-negative effect (DNE) has been established according to the results of Kato et al.<sup>7</sup> DNE over wild-type p53 was established as 'yes' in case of DNE on both WAF1 and RGC promoters, or on all promoters in a large study (by Dearth et al.<sup>8</sup>), 'moderate' in case of DNE on some promoters and not others, and 'no' in case of no DNE. Protein p21, encoded by the gene named WAF1, localized on chromosome 6 (6p21.2), is a potential mediator of p53 suppression.<sup>9</sup> Heterogeneity in transcriptional activity is observed between WT and mutant p53 in different target sequences, one of them is named ribosomal gene cluster (RGC).<sup>10</sup>

## **Supplementary Results**

### ***Pharmacokinetic Analysis***

Geometric means of AZD1775  $AUC_{0-8hr}$ ,  $C_{max}$  and  $C_{8hr}$  were 8590 nM·hr, 1380 nM, and 834 nM on Day 3, respectively, which were similar to those observed at the same dose level in the previous phase 1 study (8560 nM·hr, 1330 nM and 928 nM). See Figures S2-4 for AZD1775 and carboplatin pharmacokinetics. Although CYP3A4 modulating drugs were not allowed per protocol, an exception was made for

aprepitant as part of anti-emetic treatment. The first 3 patients received aprepitant and these PK results, together with the PK results of patients treated in the phase 1 study that received aprepitant, showed significant increased AZD1775 plasma concentrations. Based on (unpublished) preclinical data it was anticipated that CYP3A4 modulating drugs could influence uptake of AZD1775 and result in different plasma concentrations. After these results the protocol was amended and, like other CYP3A4 modulating drugs, the use of aprepitant was prohibited.

### ***p53 Status Analysis***

AmpliChip p53 and direct sequencing found similar aberrations, except for 3 patients. These discrepancies may be explained by technical difference between the two techniques (*e.g.* sensitivity and mutation types that can be detected) or by tumor heterogeneity. AmpliChip p53 array identified in two patients one and two additional mutations in the TP53 gene, respectively. The first patient (patient number 7) had been included based on a missense mutation in exon 6 (c.643A>G;p.Ser215Gly) known to result in a non-functional protein. With AmpliChip p53 analysis one additional missense mutation in exon 5 (c.523C>T;p.Arg175Cys, known to result in a partially functioning protein) and one frameshift mutation in exon 4 (c.293delC;p.Pro98fs) were identified. In the second patient (patient number 12) two missense mutations were identified: one missense mutation in exon 6 (c.587G>A;p.Arg196Gln - known to result in a partially functioning protein) and a missense mutation in exon 8 (c.817C>T;p.Arg273Cys - known to result in a non-functional protein). With AmpliChip TP53 analysis an additional missense mutation in exon 8 (c.799C>T;p.Arg267Trp - also known to result in a non-functional protein) was identified. In the third patient (patient number 15) Sanger sequencing and AmpliChip TP53 analysis both identified a different mutation. Sanger identified a frameshift mutation in exon 5 (c.469\_473delGTCCG;p.Val157fs), while AmpliChip TP 53 array identified a missense mutation in exon 4 (c.313G>T;p.Gly105Cys - known to result in a non-functional protein). This is one of the patients with negative p53 IHC results. See Table S1.

## References - Appendix

1. Xu Y, Fang W, Zeng W, et al. Evaluation of dried blot spot (DBS) technology versus plasma analysis for determination of MK-1775 by HILIC-MS/MS in support of clinical studies. *Anal Bioanal Chem* 2012;404:3037-3047.
2. Brouwers EE, Tibben MM, Rosing H, et al. Sensitive inductively coupled plasma mass spectrometry assay for the determination of platinum originating from cisplatin, carboplatin, and oxaliplatin in human plasma ultrafiltrate. *J Mass Spectrom* 2006;41(9):1186-1194.
3. Ekhart C, de Jonge ME, Huitema ADR, et al. Flat dosing of carboplatin is justified in adult patients with normal renal function. *Clin Cancer Res* 2006;12:6502-6508.
4. Chiaretti S, Tavaloro S, Marinelli M, et al. Evaluation of TP53 mutations with the AmpliChip p53 research test in chronic lymphocytic leukemia: correlation with clinical outcome and gene expression profiling. *Genes Chromosomes Cancer* 2011;50:263-274.
5. Li X, Quigg RJ, Zhou J, et al. Clinical utility of microarrays: current status, existing challenges and future outlook. *Curr Genomics* 2008;9:466-474.
6. Grollman AP, Shibutani S, Moriya M, et al. Aristolochic acid and the etiology of endemic (Balkan) nephropathy. *Proc Natl Acad Sci U S A* 2007;104:12129-12134.
7. Kato S, Han SY, Liu W, et al. Understanding the function-structure and function-mutation relationships of p53 tumor suppressor protein by high-resolution missense mutation analysis. *Proc Natl Acad Sci U S A* 2003;100(14):8424-8429.
8. Dearth LR, Qian H, Wang T, et al. Inactive full-length p53 mutants lacking dominant wild-type p53 inhibition highlight loss of heterozygosity as an important aspect of p53 status in human cancers. *Carcinogenesis* 2007; 28: 289-298.
9. el-Deiry WS, Tokino T, Velculescu VE, et al. WAF1, a potential mediator of p53 tumor suppression. *Cell* 1993; 75: 817-825.
10. Chen JY, Funk WD, Wright WE, et al. Heterogeneity of transcriptional activity of mutant p53 proteins and p53 DNA target sequences. *Oncogene* 1993;8:2159-2166.

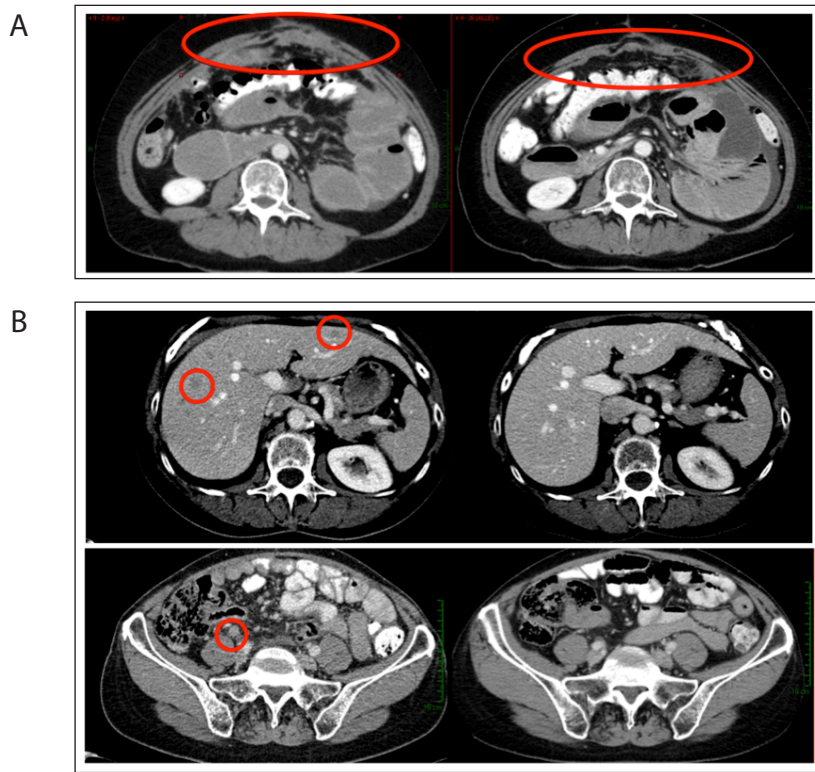


Figure S1. Computed tomography (CT) scan images of two patients. Patient case I (A): peritoneal lesions growing into the abdominal wall decreased to residual lesions after 2 cycles of study treatment. Patient case II (B): liver lesions and a pathological lymph node prior to start, which have disappeared after 5 cycles of study treatment.

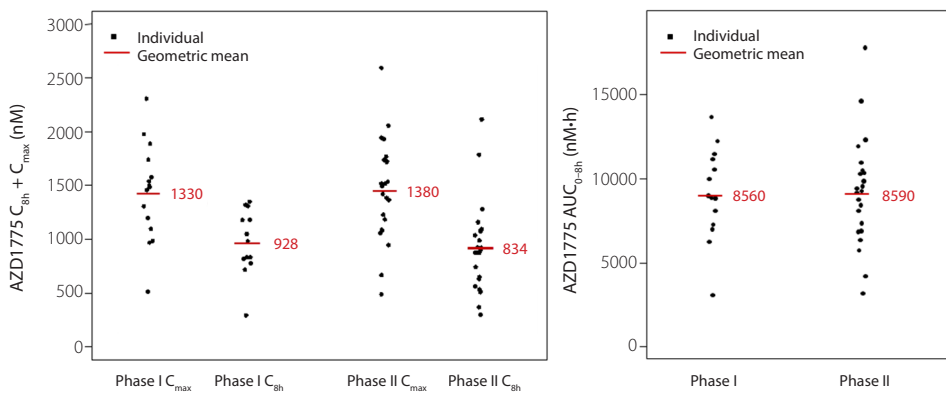


Figure S2. Comparison of AZD1775 pharmacokinetic parameters. Data from our phase 2 ovarian study versus data from previous phase I study. Comparison of  $C_{0-8h}$  (nM) and  $C_{max}$  (nM) (A), and  $AUC$  (nM·h) (B) on day 3 (after the last intake of 225 mg AZD1775).

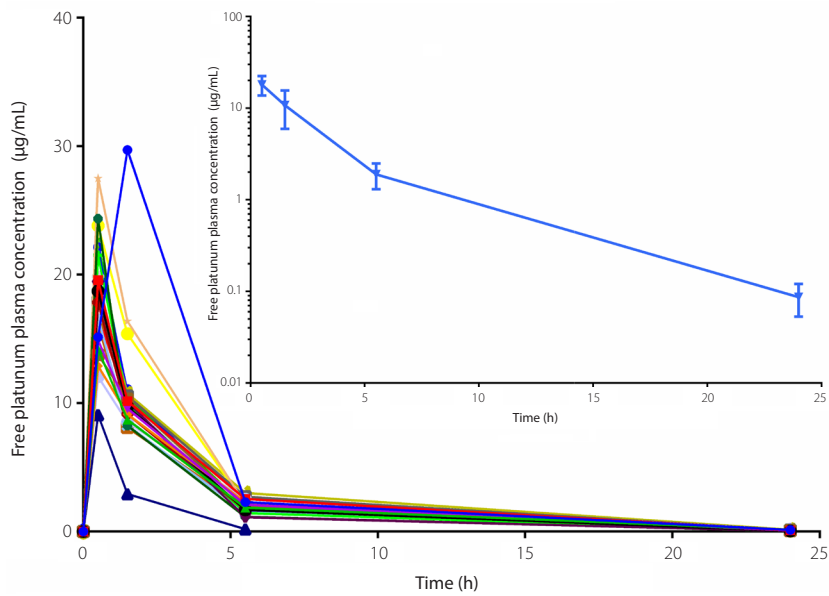


Figure S3. Pharmacokinetic profiles of free platinum.

Plasma concentration-time curve of free platinum measured in ultrafiltrates ( $n = 23$ ), demonstrating platinum decay in a biphasic manner after a 30-minute intravenous infusion. Insert: mean free platinum concentration-time curve on logarithmic scale (error bars represent standard deviations).

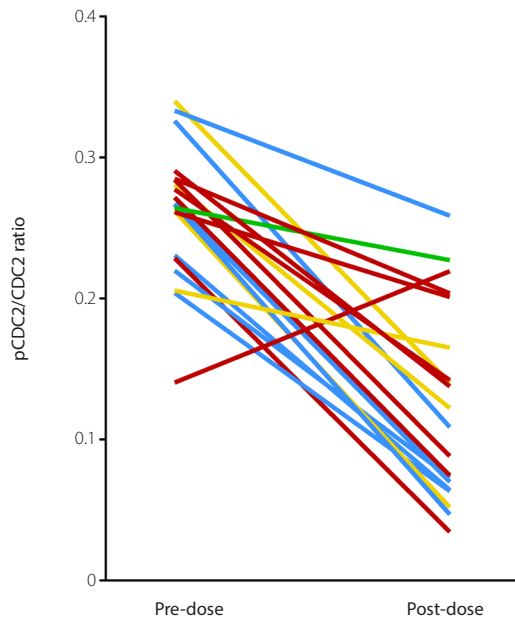


Figure S3. pCDC1/CDK1 ratio reduction in surrogate skin tissue by RECIST response. Progressive disease (red), stable disease (yellow), partial response (blue), complete response (green).



Table S1. p53 analysis results									
Patient	IHC positive	Sanger Sequencing	AmpliChip p53 array	Exon	Codon	Mutation	Mutation type	Transactivation class (IARC TP53 database)	Dominant negative effect
1	30–40%	Negative	Negative	NA	NA	NA	NA	NA	NA
2	100%	Positive	Positive	5	175	c.524G>A;p.Arg175His	Missense	Non-functional	Yes
3	100%	Positive	Positive	7	238	c.713G>T;p.Cys238Phe	Missense	Non-functional	Yes
5	70%	Positive	Positive	5	164	c.490A>G;p.Lys164Glu	Missense	Non-functional	NA
6	90%	Positive	Positive	8	275	c.824G>A;p.Cys275Tyr	Missense	Non-functional	NA
7	70%	Positive	Positive	6	215	c.643A>G;p.Ser215Gly	Missense	Non-functional	NA
				5	175	c.523C>T;p.Arg175Cys	Missense	Partially functional	NA
				4	98	c.293delC;p.Pro98fs	Frameshift	NA	-
8	100%	Positive	Positive	7	248	c.742C>T;p.Arg248Trp	Missense	Non-functional	Yes
9	100%	Positive	Positive	5	179	c.535C>G;p.His179Asp	Missense	Partially functional	NA
10	0%	Positive	Negative	8	298	c.892G>T;p.Glu298*	Nonsense	NA	-
11	100%	Positive	Positive	8	273	c.818G>T;p.Arg273Leu	Missense	Non-functional	Yes
12	100%	Positive	Positive	6	196	c.587G>A;p.Arg196Gln	Missense	Partially functional	NA
				8	273	c.817C>T;p.Arg273Cys	Missense	Non-functional	Yes
				8	267	c.799C>T;p.Arg267Trp	Missense	Non-functional	Moderate
13	50–60%	Positive	Negative	7	255	c.764_766delTCA;p.Ile255del	Deletion	NA	-
14	70–80%	Positive	Positive	8	282	c.844C>T;Arg282Trp	Missense	Non-functional	No
15	0%	Positive	Positive	5	157	c.469_473delGTCCG;p.Val157fs	Frameshift	NA	-
				4	105	c.313G>T;p.Gly105Cys	Missense	Non-functional	NA
16	0%	Positive	Negative	4	114	c.341dupT;p.Leu114fs	Frameshift	NA	NA
17	95%	Positive	Positive	7	248	c.743G>A;p.Arg248Gln	Missense	Non-functional	Yes
18	70–80%	Positive	Positive	5	155	c.464C>A;p.Thr155Asn	Missense	Non-functional	Moderate
19	0%	Positive	Positive	5	163	c.489C>G;p.Tyr163*	Nonsense	NA	NA
20	90%	Positive	Positive	8	273	c.818G>A;p.Arg273His	Missense	Non-functional	Yes
21	90%	Positive	Positive	7	245	c.734G>A;p.Gly245Asp	Missense	Non-functional	Yes
22	100%	Positive	Positive	7	242	c.725G>T;p.Cys242Phe	Missense	Non-functional	Yes
23	100%	Positive	Positive	8	282	c.844C>T;p.Arg282Trp	Missense	Non-functional	Moderate
24	90%	Positive	Positive	6	193	c.577C>T;p.His193Tyr	Missense	Non-functional	No

Analysis was performed by immunohistochemistry (IHC), polymerase chain reaction (Sanger sequencing and AmpliChip p53 array). Patient 4 never started study treatment due to early PD. IARC TP53 Mutation Database <http://www.p53.iarc.fr/index.html>; IHC = immunohistochemistry; NA, not applicable.



# Chapter 8

## Conclusions and perspectives



### CONCLUSIONS AND PERSPECTIVES

In the past two decades, a major paradigm shift has taken place in the field of cancer therapy. From non-specific cytotoxic chemotherapy that damages both tumor and normal cells, to more specific targeted agents directed against specific mechanisms that tumor cells rely on for their uncontrollable expansion. The rapidly growing armamentarium of targeted therapeutic agents can be subdivided according to their respective effects on one or more hallmark capabilities of cancer, as described by Hanahan and Weinberg.<sup>1</sup> These hallmarks include sustaining proliferative signaling, evading growth suppressors, resisting cell death, enabling replicative immortality, inducing angiogenesis, activating invasion and metastasis, deregulating cellular energetics, tumor-promoting inflammation, avoiding immune destruction and genome instability and mutation.<sup>1</sup>

The research described in this thesis mainly focused on novel agents and combination strategies targeting the sustained proliferative signaling, arguably the most fundamental trait of cancer cells. Molecular evaluation of cancer cells using high-throughput DNA sequencing revealed the presence of somatic mutations that predict constitutive proliferative signaling. As the most common affected pathways, the mitogen-activated (MAPK) and phosphoinositide 3-kinase (PI3K) cascades attracted most attention. However, even though patients are selected based on genetic alterations and receive matched targeted therapy, the overall response rate remains low.<sup>2</sup> This emphasizes a major complication of targeted therapy and raises a number of questions that remain to be answered.

For example, are we really targeting the main drivers? Or are tumor cells intrinsically resistant against single-target inhibition, and if so, through which mechanisms? Because the majority of tumors harbor multiple oncogenic mutations, they may be less dependent on a single driver, making single target inhibition insufficient for clinical efficacy. In addition, as many molecular signaling cascades are interconnected, the inhibition of one pathway component may activate the other.<sup>3</sup> Therefore, elucidating the main underlying mechanisms of unresponsiveness to single agent targeted therapy holds promise to overcome this problem. In this regard, we made great progress for patients with *BRAF* mutated (*BRAF*<sub>m</sub>) colorectal cancer (CRC), as described in **chapter 5**.

Following the preclinical finding that *BRAF* inhibitors synergize with EGFR inhibition in *BRAF*<sub>m</sub> CRC,<sup>4</sup> we obtained clinical proof of this concept by achieving promising response rates with *BRAF* plus EGFR inhibitor-based combinations. In two separate phase I studies, combinations of encorafenib plus cetuximab with or without alpelisib and dabrafenib plus panitumumab with or without trametinib were investigated. The doublet combinations encorafenib plus cetuximab and dabrafenib plus panitumumab were safe and tolerable at full single agent doses. Remarkably, the incidence of dermatologic adverse events with these two combinations was much lower compared to each individual single agent. The apparent protective effect that *BRAF* inhibitors and anti-EGFR-directed antibodies have on each other's effects on normal skin tissue may be explained by the paradoxical activation of the MAPK pathway upon *BRAF* inhibition in normal *BRAF* wild type cells.<sup>5,6</sup> Whereas anti-EGFR antibodies cause cutaneous adverse events by inhibiting MAPK signaling in both tumor and normal cells, skin-related toxicity with *BRAF* inhibitors emerges from paradoxical MAPK pathway activation in normal skin tissue. Therefore, these agents have contrary effects in *BRAF* wild type cells of the skin, but synergize in *BRAF*<sub>m</sub> tumor cells. Although similar in concept, the clinical efficacy of encorafenib plus cetuximab compared favorably to that of dabrafenib plus panitumumab, as indicated by the overall response rate of 23% versus 10%. This difference may be caused by differences in patient populations, but a meaningful difference in *BRAF* inhibitor characteristics should not be ruled out. Encorafenib demonstrated greater potency compared to dabrafenib in preclinical models,<sup>7</sup> potentially due to its significantly longer *BRAF* dissociation half-life and its lower half maximal inhibitory concentration ( $IC_{50}$ ) for CRAF. In agreement with this, the addition of trametinib increased the degree of pERK modulation measured in paired tumor biopsies, and resulted in improved anti-tumor activity. Interestingly, in the phase I study with encorafenib, cetuximab and alpelisib, the presence of concurrent *PIK3CA* alterations did not correlate with a lack of response to encorafenib plus cetuximab, suggesting that PI3K pathway activation does not play a major role in this setting. In addition, patients who received dual treatment appeared to have similar responses to patients who received triple treatment with alpelisib included. Nevertheless, in the randomized phase II study (**chapter 5.2**), the triple combination resulted in a longer median progression-free survival and overall survival compared to the dual encorafenib-cetuximab combination, albeit not statistically significant in the interim analysis. Although escalation of the encorafenib dose in the phase I study (**chapter 5.1**) did not seem to improve antitumor activity, a potential effect of the observed pharmacokinetic drug-drug interaction between encorafenib and alpelisib should not be ignored. As the encorafenib exposure at 200 mg increased approximately two-fold in the presence of 300 mg alpelisib, this may have caused overestimation of the added value, if any, of alpelisib. Given the excellent safety profile of encorafenib at doses beyond 200 mg, further evaluation

of the encorafenib plus cetuximab combination using a higher encorafenib dose is warranted in a pivotal phase III study. Taken together, the clinical efficacy of encorafenib plus cetuximab with or without alpelisib, and dabrafenib plus panitumumab plus trametinib compared favorable to historical data on standard of care chemotherapy with or without anti-EGFR-directed agents in the second-line treatment of patients with advanced *BRAF*m CRC. Therefore, these combination regimens are likely to replace the currently available standard treatment options and improve the clinical outcome of the particularly difficult to treat patient population with *BRAF*m CRC. Despite these promising findings, the development of resistance remains inevitable. Strikingly, in each patient with evaluable tumor material at progression, a different molecular mechanism of resistance was identified, including *KRAS* mutation, *KRAS* amplification, *BRAF* amplification, and *MEK1* mutation.<sup>8</sup> However, as all of these mechanisms rely on the reactivation of the MAPK pathway, ERK inhibitors may provide valuable additions to the investigated combination regimens. Indeed, as preclinical research demonstrated that ERK inhibitors retained the ability to suppress MAPK signaling in *BRAF*m cells that had become resistant to BRAF plus EGFR inhibition, this strategy should be considered in future clinical studies. The emergence of *KRAS* mutations was surprising as mutations in *KRAS* and *BRAF* were thought to be mutually exclusive. However, an exploratory analysis by Kopetz et al. revealed the presence of rare low-frequency *KRAS* mutant (*KRAS*m) clones in 68% of the patients with *BRAF*m CRC that were previously classified as *KRAS* wild type based on standard clinical sequencing with a sensitivity of 10%.<sup>9</sup> Follow-up studies in which *BRAF*m CRC cells with low-frequency *KRAS*m clones were xenografted into mice showed that upon an initial response, these tumors became resistant within 8 weeks. Sequencing of the resistant tumors confirmed the persistent presence of the *BRAF* mutation, with *KRAS* mutations present at allele frequencies greater than 40%,<sup>9</sup> resembling our observations in patients. By successfully treating the *BRAF*m cell population, subclones containing *KRAS* mutations get the chance to expand and progress. These findings emphasize the major challenge for successful implementation of genotype-directed therapy. Inter- and intratumor heterogeneity can lead to underestimation of the tumor genomics landscape obtained from single tumor-biopsy samples<sup>10</sup> and may thereby limit the clinical activity of a matched targeted treatment strategy.

In addition, given the finding that *KRAS* mutations seem to be present at a much higher frequency than previously thought, this also highlights the major role of *KRAS* in cancer and the need for effective therapy options against *KRAS*m tumors. Whilst to date, efforts to target *KRAS* directly have been unsuccessful, novel combination strategies using targeted agents have emerged from synthetic lethality screens.<sup>11,12</sup> We investigated one of these strategies in two phase I studies evaluating the concept of combined inhibition of MEK and multiple upstream tyrosine kinase receptors, including EGFR and the human epidermal growth factor receptor 2 (HER2). In these studies (**chapters 6.1** and **6.2**) we demonstrated that PD-0325901 plus dacomitinib, and trametinib plus lapatinib could be combined safely, albeit not at full single agent doses, in patients with *KRAS*m CRC, non-small cell lung cancer (NSCLC) and pancreatic cancer. Additionally, the absence of clinically significant pharmacokinetic drug-drug interaction between these compounds was demonstrated, we showed pharmacodynamic responses in tumor tissue in the majority of patients, and preliminary anti-tumor activity was reported. However, whereas the pharmacodynamic effects, *i.e.* downstream pERK modulation, seemed strong, the clinical activity was mostly limited to relatively short-lived disease stabilizations. Because toxicity restricted further

dose-escalation, the preclinical plasma concentration target of trametinib was exceeded during less than 50% of the 24-hour dosing interval. As all on-treatment tumor biopsies were taken within 4 hours of study drug administration, *i.e.* at the highest drug exposure, the pharmacodynamic effect may be much less upon decreasing drug exposure later in the dosing interval, explaining the discrepancy between strong pERK modulation and modest clinical activity. Additional explanations for the limited preliminary antitumor activity include the extensive inter-pathway connections of the KRAS protein that may cause intrinsic resistance against the combination, and reactivation of the MAPK pathway due to insufficient high doses of EGFR/HER2 inhibitor. Therefore, we continue to explore intermittent dosing schedules in an effort to optimize the antitumor activity without compromising tolerability. Interestingly, in both studies patients with NSCLC responded better than patients with CRC in terms of target lesion regression and time to progression. As this suggests a difference in sensitivity, elucidating the underlying mechanism may help to identify better predictive biomarkers.

Besides combinations of targeted agents, rational combinations with chemotherapy may also provide synergistic activity by boosting the cytotoxic effects. Given the critical role of the WEE1 tyrosine kinase in maintaining genomic stability upon DNA damage, inhibition of WEE1 combined with DNA-damaging chemotherapy has become a promising strategy for the treatment of cancer.<sup>13,14</sup> Because cells that lack a functional p53 protein rely on WEE1 function for DNA repair, p53-deficient tumors are particularly sensitive to WEE1 inhibition combined with chemotherapy.<sup>15,16</sup> In **chapter 7** we described the results of two studies investigating the combined use of AZD1775, a novel targeted agent against WEE1, and chemotherapy. After establishing the recommended phase II dose of AZD1775 when combined with chemotherapy, we selected the combination of AZD1775 plus carboplatin for further investigation in patients with p53-deficient platinum-resistant ovarian cancer. Because all patients were only pretreated with carboplatin plus paclitaxel they served as their own control as they were re-exposed to carboplatin, but in combination with AZD1775 as a chemosensitizer. The data collected in this study demonstrated encouraging efficacy as AZD1775 plus carboplatin compared favorably to first-line and second-line treatment options in this patient population. Therefore AZD1775 combined with carboplatin could improve clinical outcome in a patient population that has shown poor prognosis and very limited response to currently available treatment options.

In conclusion, the research described in this thesis provides evidence of effective genotype-directed combination strategies with targeted therapy and chemotherapy. However, it also emphasizes the challenges that remain to be overcome in order to further improve the individualization of cancer therapy. Despite the genotype-directed nature of the described studies, patients still respond remarkably differently due to extensive molecular heterogeneity beyond the level of one single driver mutation (**chapter 4**). In addition, genetic analysis of tumor biopsy samples may miss critical aberrations present in other sections of the biopsied lesion or other metastatic sites, thereby affecting the efficacy of genotype-directed therapy. Novel technologies such as liquid biopsies using circulating tumor DNA for treatment decision-making, may become valuable in this regard. Now more than ever, we are beginning to understand the heterogeneity of cancer, how signaling pathways are interconnected, how tumor cells evolve upon treatment, and how we could interfere with these signaling networks in the most effective way. Further refinement in our understanding of the underlying molecular

characteristics of tumors should lead to better prediction of which patients benefit most from treatment, whether that may be chemotherapy, targeted therapy, immunotherapy or a combination strategy using multiple modalities.

## References

1. Hanahan D, Weinberg RA. Hallmarks of cancer: The next generation. *Cell* 2011;144:646–74.
2. Dienstmann R, Serpico D, Rodon J, et al. Molecular profiling of patients with colorectal cancer and matched targeted therapy in phase I clinical trials. *Mol Cancer Ther* 2012;11:2062–71.
3. Bernards R. A missing link in genotype-directed cancer therapy. *Cell* 2012;151:465–8.
4. Prahallad A, Sun C, Huang S, et al. Unresponsiveness of colon cancer to BRAF(V600E) inhibition through feedback activation of EGFR. *Nature* 2012;483:100–3.
5. Holderfield M, Nagel TE, Stuart DD. Mechanism and consequences of RAF kinase activation by small-molecule inhibitors. *Br J Cancer* 2014;111:640–5.
6. Holderfield M, Merritt H, Chan J, et al. RAF inhibitors activate the MAPK pathway by relieving inhibitory autophosphorylation. *Cancer Cell* 2013;23:594–602.
7. Stuart D, Li N, Poon DJ, et al. Preclinical profile of LGX818: A potent and selective RAF kinase inhibitor. *Cancer Res* 2012;72(8 Suppl):Abstract nr 3790.
8. Ahronian LG, Sennott EM, Van Allen EM, et al. Clinical acquired resistance to RAF inhibitor combinations in BRAF-mutant colorectal cancer through MAPK pathway alterations. *Cancer Discov* 2015;5:358–67.
9. Kopets S, Desai J, Chan E, et al. Phase II pilot study of vemurafenib in patients with metastatic BRAF-mutated colorectal cancer. *J Clin Oncol* 2015;33:4032–4038 (2015).
10. Gerlinger M, Roawn AJ, Horswell S, et al. Intratumor heterogeneity and branched evolution revealed by multiregion sequencing. *N Engl J Med* 2012;366:883–92.
11. Sun C, Hobor S, Bertotti A, et al. Intrinsic resistance to MEK inhibition in kras mutant lung and colon cancer through transcriptional induction of ERBB3. *Cell Rep* 2014;7:86–93.
12. Corcoran RB, Cheng KA, Hata AN, et al. Synthetic Lethal Interaction of Combined BCL-XL and MEK Inhibition Promotes Tumor Regressions in KRAS Mutant Cancer Models. *Cancer Cell* 2013;23:121–8.
13. Kawabe T. G2 checkpoint abrogators as anticancer drugs. *Mol Cancer Ther* 2004;3:513–9.
14. Bucher N, Britten CD. G2 checkpoint abrogation and checkpoint kinase-1 targeting in the treatment of cancer. *Br J Cancer* 2008;98:523–8.
15. Hirai H, Iwasawa Y, Okada M, et al. Small-molecule inhibition of Wee1 kinase by MK-1775 selectively sensitizes p53-deficient tumor cells to DNA-damaging agents. *Mol Cancer Ther* 2009;8:2992–3000.
16. Leijen S, Beijnen JH, Schellens JHM. Abrogation of the G2 checkpoint by inhibition of Wee-1 kinase results in sensitization of p53-deficient tumor cells to DNA-damaging agents. *Curr Clin Pharmacol* 2010;5:186–91.







# Appendix

Summary

Summary in Dutch

Acknowledgements

Curriculum Vitae

List of publications



## SUMMARY

In the past decade, a large number of novel targeted anticancer agents have been developed and investigated in clinical studies. In **chapter 2.1**, the pharmacological characteristics of two such agents, pazopanib and axitinib, have been reviewed. These ATP-competitive inhibitors of the vascular endothelial growth factor receptor have shown to be effective and tolerable treatment options for metastatic renal cell cancer. After publication of our concise drug review, two large randomized phase III trials were published; reporting favorable outcomes for pazopanib compared with sunitinib in the first line setting and for axitinib compared with sorafenib in the second line setting for patients with metastatic renal carcinoma.<sup>1,2</sup>

In contrast to chemotherapy, which attacks all dividing cells, targeted anticancer agents are directed against specific proteins that stimulate tumor cells to survive and proliferate. As such, targeted therapy was expected to cause less and less severe adverse effects compared to conventional chemotherapy. Nevertheless, clinical investigation provided insight in the toxicity profiles of each novel compound, revealing on- and off-target adverse events, which in some cases have life-threatening consequences. In **chapter 2.2** we described an example of a rare but severe case of off-target toxicity, caused by crizotinib, a small-molecule inhibitor of the anaplastic lymphoma kinase protein. A 62-year old female with non-small cell lung cancer, presented with acute liver failure after 24 days of treatment with crizotinib. Despite crizotinib discontinuation and intensive supportive therapy, the patient died due to massive liver cell necrosis.

With the emergence of numerous targeted anticancer agents in recent years, the risk of new drug-drug interactions (DDIs) with concurrently used medication continues to increase. **Chapter 3** provides an update on pharmacokinetic and pharmacodynamic DDIs in oncology. DDIs are a major safety concern in oncology and account for a large portion of adverse drug reactions. Detrimental DDIs can occur at all levels of pharmacokinetics and pharmacodynamics, but mainly concern pharmacokinetic mechanisms at metabolizing enzymes and drug transporters. On the other hand, DDIs are increasingly deployed to enhance the efficacy of anti-cancer therapy; pharmacokinetic DDIs to improve the bioavailability of cytotoxic drugs, and pharmacodynamic DDIs to exploit their synergistic effect on anti-tumour activity. Noteworthy examples of potential beneficial pharmacodynamic DDIs have been investigated in the studies described in chapters 5, 6 and 7 of this thesis.

Upon the recognition that clinical responses of multiple targeted agents were restricted to patients with tumors containing genetic alterations within the targeted protein, early phase clinical studies started to implement a more genotype-directed strategy. Relying on the principle that cancer cells become dependent on the effect of oncogenic driver mutations, selecting patients based on genetic characteristics and subsequently treat them with a matching targeted agent was the next step forwards. However, although successes have been achieved with this strategy, its major limitation lays in the extensive heterogeneity within tumors. Most tumors harbor multiple oncogenic mutations, making them less dependent on a single driver, acquired resistance may emerge through new mutations, and as many molecular signaling pathways are interconnected, inhibiting one may activate the other. In **chapter 4**, we discussed this issue specifically for colorectal cancer (CRC). With the exception of the combination therapies described in chapter 5.1–5.3, effective single gene guided treatment strategies for patients with metastatic CRC have not yet been reported. Furthermore, patients with the same genetic driver mutation still respond very differently to therapy. Emerging molecularly defined CRC subtypes based on gene expression patterns highlight the heterogeneity beyond genetic mutations and the lack of unique driver mutations in each of these subtypes indicates distinct differences within the *KRAS* mutant (*KRASm*) and *BRAF* mutant (*BRAFm*) populations. Clearly, genetic aberrations are often not accurately defining a colorectal tumor's phenotype and are highly insufficient to guide treatment decisions in most cases. Therefore, validation of gene expression signatures, or equivalent simpler marker systems, and implementing these in the stratification of patients receiving pharmacological therapy may help defining the patients most likely to benefit from a given (experimental) therapy.

The impact of inter-pathway cross talk became particularly evident when *BRAF* inhibitors were investigated in patients with *BRAF* mutated (*BRAFm*) CRC. Whereas in patients with *BRAFm* melanoma, pharmacological inhibition of *BRAF* resulted in dramatic responses and a significant survival benefit compared to standard chemotherapy, the antitumor activity of *BRAF* inhibitors in patients with *BRAFm* CRC was disappointing. Preclinical work demonstrated the presence of a negative feedback activation loop that activates the epidermal growth factor receptor (EGFR) and thereby reactivates the MAPK- and phosphoinositide 3-kinase (PI3K) signaling pathways upon *BRAF* inhibition in *BRAF* mutated CRC cells, explaining their resistance against single-agent *BRAF* inhibitor. A *BRAF* inhibitor combined synergistically with inhibitors of EGFR in *BRAFm* CRC cells and xenografts, resulting in the complete inhibition of tumor growth. These findings formed the basis of the studies described in chapter 5. The

primary objective of the phase I study described in **chapter 5.1** was to determine the recommended phase II dose (RP2D) of BRAF inhibitor encorafenib plus the anti-EGFR antibody cetuximab (dual) with or without the PI3K inhibitor alpelisib (triple). In total, 54 patients with metastatic *BRAF*<sub>V600E</sub> CRC were enrolled in the dual ( $n = 26$ ) or triple combination ( $n = 28$ ) group. Dose-limiting toxicities were reported in three patients receiving dual (grade 3 arthralgia, vomiting, and QT interval prolongation) and two patients receiving triple treatment (grade 4 increased creatinine, grade 3 bilateral interstitial pneumonitis). The RP2D was established as 200 mg encorafenib (both groups) and 300 mg alpelisib, combined with standard cetuximab. Overall response rates (ORR) of 23% in the dual- and 32% in the triple-combination therapy group were achieved. This study showed that combinations of encorafenib, cetuximab and alpelisib are tolerable and provide promising antitumor activity in the difficult-to-treat patient population with metastatic *BRAF*<sub>V600E</sub> CRC.

Following these encouraging results, we developed a randomized phase II study, described in **chapter 5.2**, to investigate and directly compare the efficacy and safety of the dual and triple combination therapy. In this study we randomly assigned patients with advanced *BRAF*<sub>V600E</sub> CRC who failed at least one prior standard therapy to receive dual or triple combination therapy. Progression-free survival was the primary endpoint and secondary endpoints included ORR and overall survival. Patients were treated with the recommended phase II doses as established in the previous described phase I study. Out of the 102 patients, 52 were randomized to receive the triple combination and 50 to receive the dual combination. A planned progression-free survival analysis comparing the triple to the dual combination after 77 events showed a hazard ratio (HR; 95% confidence interval [CI]) of 0.8 (0.5–1.2;  $P = 0.14$ ), with median progression-free survival (95% CI) of 5.4 (4.1–7.2) and 4.2 (3.4–5.4) months, respectively. The confirmed ORR (95% CI) was 27% (16%–41%) with the triple and 22% (12%–36%) with the dual combination therapy. Grade 3/4 adverse events, regardless of causality, occurred in 79% (triple) and 58% (dual) of patients, and consisted mainly of anemia (17% vs 6%), hyperglycemia (13% vs 2%), and increased lipase (8% vs 18%) for the triple and dual arm, respectively. With this study we confirmed that combined targeted therapy with encorafenib and cetuximab with or without alpelisib was safe and tolerable. Relative to historical data, encorafenib plus cetuximab with or without alpelisib showed promising antitumor activity in patients with *BRAF*<sub>V600E</sub> CRC. The addition of alpelisib may provide a slight PFS benefit at the expense of additional toxicity.

In **chapter 5.3** we described a phase I study with combinations of dabrafenib (BRAF inhibitor), panitumumab (anti-EGFR antibody) and trametinib (MEK inhibitor) in patients with metastatic *BRAF*<sub>V600E</sub> CRC. In this dose-escalation study, followed by a cohort expansion part, the primary objective was to determine the safety and tolerability of these combinations. Secondary objectives included assessing the pharmacodynamic response in tumor tissue and the clinical antitumor activity following combination therapy. A total of 74 patients were enrolled across the dabrafenib plus panitumumab doublet ( $n = 20$ ), the dabrafenib-panitumumab-trametinib triplet ( $n = 35$ ), and the trametinib plus panitumumab doublet ( $n = 19$ ). One patient experienced dose-limiting grade 3 acneiform rash in the trametinib plus panitumumab arm. The most common adverse events were dermatitis acneiform (60%) and fatigue (45%) for dabrafenib plus panitumumab, diarrhea (86%) and dermatitis acneiform (66%) for the triplet, and dermatitis acneiform (63%) and diarrhea (52%) for trametinib plus panitumumab.

Pharmacodynamic response, as measured by pERK modulation in tumor biopsies taken at baseline and after 15 days of treatment, was seen with all regimens. Confirmed response rates were 10% and 26% for the dabrafenib plus panitumumab doublet and the triplet, respectively. With the trametinib-panitumumab combination, no responses were achieved. We demonstrated that combinations of dabrafenib plus panitumumab and dabrafenib plus panitumumab plus trametinib have manageable toxicity profiles at their full monotherapy doses, and that the triplet combination provides promising clinical activity, warranting further exploration in patients with *BRAF*<sup>m</sup> CRC.

In our effort to find an effective combination therapy for patients with *KRAS*<sup>m</sup> tumors we developed two phase I studies, of which the interim analyses were discussed in **chapter 6.1** and **6.2**. Mutations in the *KRAS* gene are common in several cancer types and result in a constitutively activated MAPK pathway. Until now, the development of effective agents acting directly against the KRAS protein has been challenging. Preclinical work showed that *KRAS*<sup>m</sup> cancer cells are intrinsically resistant against MEK inhibition due to feedback activation of upstream tyrosine kinase receptors, providing rationale to investigate combined MEK and upstream receptor inhibition. In two different studies we investigated the combinations of dacomitinib (pan-human epidermal growth factor receptor [HER] inhibitor) plus PD-0325901 (MEK inhibitor) and lapatinib (dual EGFR/HER2 inhibitor) plus trametinib (MEK inhibitor).

In the dacomitinib/PD-0325901 study, 33 patients were enrolled, of whom 25 had CRC, five NSCLC, and three patients had pancreatic cancer. The most common treatment-related adverse events were acneiform rash (94%), diarrhea (85%), and nausea (54%). The maximum tolerated dose with continuous dacomitinib dosing was established and intermittent dosing schedules are currently being explored. Signs of significant pharmacokinetic drug-drug interactions were not observed. Clinical activity was seen in six patients, of whom five had NSCLC and 1 pancreatic cancer. With this study we demonstrated that the combination of dacomitinib plus PD-0325901 is tolerable albeit only at doses lower than the recommended single agent doses. Given the modest clinical activity observed so far, potentially due to toxicity that prevented high continuous dosing of dacomitinib, the ongoing study will focus on confirming the signs of activity in more patients and on finding a dose-level with optimal efficacy and tolerability.

In the lapatinib/trametinib study, 22 patients were enrolled across 4 different dose-levels; 16 patients with CRC, three with NSCLC, and three patients with pancreatic cancer. At all doses, inhibition of the MAPK pathway was confirmed in on-treatment biopsies. Among 16 evaluable patients, 1 partial response was achieved and 8 had stable disease. This trial confirms that inhibition of MEK together with EGFR and HER2, by trametinib and lapatinib, reduces MAPK signaling in *KRAS*<sup>m</sup> tumors. Nevertheless, clinical efficacy is limited so far and dose-escalation is hindered by toxicity. Therefore, intermittent regimens were initiated to optimize efficacy and tolerability.

In **chapter 7**, we described two studies investigating the concept of chemosensitization using AZD1775, a targeted small molecule inhibitor of the WEE1 tyrosine kinase. WEE1 is one of the key proteins regulating the G2 checkpoint, by inhibiting its direct substrate CDK1. As cell cycle checkpoints are critical in response to DNA damage, WEE1 inhibition was hypothesized to sensitize tumor cells to the cytotoxic effects of chemotherapy. The phase I study described in **chapter 7.1** was developed to

determine the maximum tolerated dose (MTD) of AZD1775 when combined with cisplatin, carboplatin or gemcitabine. In total, 202 patients were enrolled and the MTD was established for each combination regimen. AZD1775 combined with chemotherapy had acceptable toxicity, with hematologic toxicity, nausea, vomiting and fatigue being the most frequently observed adverse events. Target engagement, as a predefined 50% pCDK1 reduction in surrogate tissue, was observed in combination with cisplatin and carboplatin. This study demonstrated that AZD1775 could be combined safely with chemotherapy, warranting further investigation of these combinations in specific patient populations.

Based on their increased G2 checkpoint dependency for DNA repair, p53-deficient tumor cells were hypothesized to be especially sensitive to WEE1 inhibition in combination with DNA damaging chemotherapy. To test this hypothesis we conducted a proof of concept phase II study with AZD1775 plus carboplatin in ovarian cancer patients refractory or resistant (within 3 months) after first-line platinum-based therapy (**chapter 7.2**). AZD1775 plus carboplatin demonstrated manageable toxicity with fatigue (87%), nausea (78%), thrombocytopenia (70%), diarrhea (70%) and vomiting (48%) as most common adverse events. In the 21 patients who were evaluable for efficacy endpoints, the ORR was 43% (95% CI, 22%–66%), including one patient with a complete response. Median PFS and OS were 5.3 months (95% CI, 2.3–9.0) and 12.6 months (95% CI 4.9–19.7), respectively, with two patients on study for over 31 and 42 months at data cut off. Therefore, AZD1775 plus carboplatin demonstrated promising antitumor and favorable clinical outcomes compared to historical data with currently available treatment options for patients with platinum-resistant ovarian cancer.



## References

1. Motzer RJ, Escudier B, Tomczak P, et al. Axitinib versus sorafenib as second-line treatment for advanced renal cell carcinoma: overall survival analysis and updated results from a randomized phase 3 trial. *Lancet Oncol* 2013;14(6):552–62.
2. Motzer RJ, Hutson TE, Cella D, et al. Pazopanib versus sunitinib in metastatic renal-cell carcinoma. *N Engl J Med* 2013;369(8):722–31.



## SUMMARY IN DUTCH

In de afgelopen 10 jaar is een groot aantal nieuwe doelgerichte antikanker geneesmiddelen ontwikkeld en onderzocht in klinische studies. **Hoofdstuk 2.1** bevat een review waarin de farmacologische eigenschappen van twee van zulke middelen, pazopanib en axitinib, worden beschreven. Deze ATP-competitieve remmers van de vasculaire endothele groeifactor receptor zijn effectieve en tolerabele behandelopties gebleken voor patiënten met gemetastaseerd niercelcarcinoom. Na publicatie van ons beknopte review zijn de resultaten van twee grote gerandomiseerde fase III trials gepubliceerd, waarin pazopanib en axitinib gunstiger resultaten bereikten vergeleken met respectievelijk sunitinib in de eerstelijns setting en sorafenib in de tweedelijns setting bij patiënten met gemetastaseerd niercelcarcinoom.<sup>1,2</sup>

Doelgerichte geneesmiddelen werken op specifieke eiwitten die de proliferatie en overleving van tumorcellen stimuleren, dit in tegenstelling tot chemotherapie waarbij alle delende cellen beschadigd worden. Daarom werd van doelgerichte therapie verwacht dat het minder, en minder ernstige bijwerkingen veroorzaakt dan conventionele chemotherapie. Desalniettemin, klinisch onderzoek heeft inzicht gegeven in het toxiciteitsprofiel van nieuwe middelen, waarbij zowel on- als off-target bijwerkingen aan het licht kwamen, welke in sommige gevallen levensbedreigende consequenties kunnen hebben. In **hoofdstuk 2.2** van dit proefschrift is een voorbeeld beschreven van zeldzame, maar ernstige toxiciteit, veroorzaakt door crizotinib, een *small molecule inhibitor* van het anaplastisch lymfoom kinase eiwit. Een 62-jarige vrouw met niet-kleincellig longcarcinoom presenteerde zich met acuut leverfalen na 24 dagen crizotinib behandeling. Ondanks staken van crizotinib en intensieve ondersteunende therapie, kwam de patiënt te overlijden als gevolg van massale levercelnecrose.

Met de komst van talrijke doelgerichte antikanker geneesmiddelen in de afgelopen jaren wordt het risico op geneesmiddelinteracties met gelijktijdig gebruikte medicijnen steeds groter. **Hoofdstuk 3** geeft een *update* over farmacokinetische en farmacodynamische geneesmiddelinteracties binnen de oncologie. Geneesmiddelinteracties zijn een belangrijk veiligheidsprobleem bij patiënten met kanker en zijn verantwoordelijk voor een groot gedeelte van geneesmiddel bijwerkingen. Aan de andere kant worden geneesmiddelinteracties ook in toenemende mate toegepast om de effectiviteit van antikanker behandeling te verbeteren; farmacokinetische interacties om de biologische beschikbaarheid van cytotoxische geneesmiddelen te vergroten, en farmacodynamische interacties om een synergistisch effect op de antitumor activiteit te bewerkstelligen. Noemenswaardige voorbeelden van potentieel gunstige farmacodynamische interacties zijn onderzocht in de studies beschreven in hoofdstuk 5, 6 en 7 van dit proefschrift.

Na de ontdekking dat verschillende doelgerichte geneesmiddelen alleen effectief zijn bij patiënten met tumoren die genetische veranderingen bevatten in het eiwit waartegen het middel gericht is, zijn vroege fase klinische studies een meer genotype-gestuurde strategie gaan implementeren. Uitgaande van het principe dat kankercellen afhankelijk worden van het effect van oncogene *driver* mutaties, werden patiënten geselecteerd op basis van de genetische eigenschappen van hun tumor om vervolgens behandeld te worden met een bijpassend doelgericht geneesmiddel. Echter, ook al

zijn er enkele successen behaald met deze strategie, de genetische heterogeniteit binnen tumoren vormt een belangrijke valkuil. De meeste tumoren bevatten meerdere oncogene mutaties waardoor ze minder afhankelijk zijn van een enkele *driver*, verworven resistentie kan zich ontwikkelen door nieuwe mutaties, en doordat veel moleculaire signaaltransductie routes verbonden zijn met elkaar, kan remming van de ene er voor zorgen dat de andere geactiveerd wordt. In **hoofdstuk 4** wordt dit onderwerp specifiek voor colorectaal carcinoom (CRC) besproken in een review. Met uitzondering van de combinatiebehandelingen beschreven in de hoofdstukken 5.1 – 5.3, zijn behandelstrategieën gericht op een enkel gemuteerd gen nog niet effectief gebleken voor patiënten met gemetastaseerd CRC. Bovendien reageren patiënten met dezelfde genetische *driver* mutatie zeer verschillend op standaard- en experimentele behandelingen. De ontdekking dat CRC is onder te verdelen in moleculaire subtypen op basis van gen expressie patronen benadrukt dat de heterogeniteit van tumoren verder gaat dan alleen genetische mutaties, en de afwezigheid van unieke *driver* mutaties in elk subtype geeft aan dat er duidelijke verschillen zijn tussen *KRAS* en *BRAF* gemuteerde tumoren. Het is duidelijk dat genetische afwijkingen vaak geen accuraat beeld geven van het fenotype van een colorectaal tumor en daarom in veel gevallen niet geschikt zijn om behandelbeslissingen op te baseren. Het valideren van gen expressie patronen en het implementeren hiervan bij het stratificeren van patiënten die een farmacologische behandeling ondergaan kan bijdragen aan het vaststellen van welke patiënten de grootste kans maken om baat te hebben bij een bepaalde (experimentele) behandeling.

De impact van *crosstalk* tussen verschillende signaaltransductie routes werd in het bijzonder duidelijk op het moment dat BRAF remmers onderzocht werden bij patiënten met *BRAF* gemuteerd (*BRAFm*) CRC. Waar bij patiënten met *BRAFm* melanoom farmacologische inhibitie van BRAF tot indrukwekkende responsen leidde en een significant verlengde overleving vergeleken met standaard chemotherapie, was de antitumor activiteit van BRAF remmers bij patiënten met *BRAFm* CRC teleurstellend. Preklinisch onderzoek heeft aangetoond dat deze ongevoeligheid voor monotherapie met een BRAF remmer wordt veroorzaakt door de aanwezigheid van een negatief *feedback* mechanisme. Na inhibitie van BRAF wordt hierdoor de epidermale groeifactor receptor (EGFR) geactiveerd met als gevolg dat de MAPK- en fosfoinositide 3-kinase (PI3K) signaaltransductie routes gestimuleerd worden. Echter, wanneer een BRAF remmer gecombineerd werd met middelen die EGFR remmen resulteerde dit in een synergetisch effect in *BRAFm* CRC cellen en *xenograft* modellen, waarbij de tumorgroei volledig werd geremd. Deze bevindingen vormden de basis voor de studies die beschreven zijn in hoofdstuk 5. Het primaire doel van de fase I studie beschreven in **hoofdstuk 5.1** was om de aanbevolen fase II dosering te bepalen van de BRAF remmer encorafenib gecombineerd met het anti-EGFR antilichaam cetuximab (*dual*) met of zonder de PI3K remmer alpelisib (*triple*). In totaal werden 54 patiënten met gemetastaseerd *BRAFm* CRC geïncludeerd in de *dual* ( $n = 26$ ) en *triple* ( $n = 28$ ) groep. Dosis-limiterende toxiciteit werd gezien bij drie patiënten in de *dual* groep (graad 3 artralgie, braken en QT interval verlenging), en bij 2 patiënten die werden behandeld met de *triple* combinatie (graad 4 verhoogd creatinine, graad 3 bilaterale interstitiële pneumonitis). De aanbevolen fase II dosering werd vastgesteld op 200 mg encorafenib (beide combinaties) en 300 mg alpelisib gecombineerd met de standaarddosering cetuximab. De *overall response rate* (ORR) bedroeg 25% in de *dual* groep en 32% in de *triple* groep. Hiermee heeft deze studie aangetoond dat combinaties van encorafenib, cetuximab en alpelisib tolerabel zijn en veelbelovende antitumor activiteit genereren bij moeilijk te behandelen

patiënten met gemetastaseerd *BRAF*m CRC.

In navolging van deze bemoedigende resultaten hebben we een gerandomiseerde fase II studie opgezet (**hoofdstuk 5.2**), om de veiligheid van de *dual* en *triple* combinaties verder te onderzoeken en vergelijken. In deze studie hebben we patiënten met gemetastaseerd *BRAF*m CRC die progressief waren na tenminste één lijn standaardbehandeling willekeurig toegewezen om behandeld te worden met de *dual* of *triple* combinatietherapie. Progressievrije overleving was hierbij het primaire eindpunt en secundaire eindpunten waren onder andere ORR en *overall survival*. Patiënten werden behandeld met de aanbevolen fase II dosering zoals vastgesteld in de eerder beschreven fase I studie. Van de 102 patiënten werden er 52 gerandomiseerd in de *triple* combinatie en 50 in de *dual* combinatie. Een geplande progressievrije overleving analyse waarbij de *triple* combinatie werd vergeleken met de *dual* combinatie na 77 events toonde een *hazard ratio* (HR; 95% betrouwbaarheidsinterval [BI]) van 0,8 (0,5–1,2;  $P = 0,14$ ), met een mediane progressievrije overleving (95% BI) van respectievelijk 5,4 (4,1–7,2) en 4,2 (3,4–5,4) maanden. De bevestigde ORR (95% BI) was 27% (16%–41%) voor de *triple* en 22% (12%–36%) voor de *dual* combinatie behandeling. Graad 3/4 bijwerkingen, ongeacht causaliteit, deden zich voor bij 79% (*triple*) en 58% (*dual*) van de patiënten, en bestonden voornamelijk uit anemie (17% vs. 6%), hyperglykemie (13% vs. 2%), en verhoogd lipase (8% vs. 18%). Met deze studie hebben we bevestigd dat gecombineerde doelgerichte therapie met encorafenib en cetuximab, met of zonder alpelisib veilig en tolerabel is. Vergeleken met historische data vertoonde encorafenib plus cetuximab, met of zonder alpelisib veelbelovende antitumor activiteit bij patiënten met *BRAF*m CRC. Het toevoegen van alpelisib zou kunnen zorgen voor een klein voordeel in progressievrije overleving, maar veroorzaakt ook extra toxiciteit.

In **hoofdstuk 5.3** hebben we een fase I studie beschreven waarin combinaties van dabrafenib (*BRAF* remmer), panitumumab (anti-EGFR antilichaam) en trametinib (MEK remmer) zijn onderzocht bij patiënten met gemetastaseerd *BRAF*m CRC. Het primaire doel van deze dosisescalatie studie was het vaststellen van de veiligheid en verdraagbaarheid van deze combinatiebehandelingen. Secundaire doelstellingen waren onder andere het bepalen van de farmacodynamische respons in tumorweefsel en de klinische antitumor activiteit. Een totaal van 74 patiënten werd geïnccludeerd, verspreid over drie combinaties: dabrafenib-panitumumab ( $n = 20$ ), dabrafenib-panitumumab-trametinib ( $n = 35$ ) en trametinib-panitumumab ( $n = 19$ ). Eén patiënt ervoer dosis-limiterende toxiciteit (graad 3 acneiform rash) in de trametinib plus panitumumab arm. De meest voorkomende bijwerkingen waren dermatitis acneiform (60%) en vermoeidheid (45%) voor dabrafenib plus panitumumab, diarree (86%) en dermatitis acneiform (66%) voor dabrafenib-panitumumab-trametinib, en dermatitis acneiform (63%) en diarree (52%) voor trametinib plus panitumumab. Een farmacodynamische respons, gedefinieerd als pERK modulatie in tumor biopsen genomen voor start en na 15 dagen van studiebehandeling, werd waargenomen bij alle combinatie regimes. De bevestigde *response rates* waren 10% in de dabrafenib-panitumumab arm en 26% in de dabrafenib-panitumumab-trametinib arm. In de trametinib-panitumumab arm werden geen responsen bereikt. Met deze studie hebben we daarom aangetoond dat de combinaties dabrafenib plus panitumumab, met of zonder trametinib beheersbare toxiciteit hebben op de volledige monotherapie doseringen. Bovendien hebben we laten zien dat de dabrafenib-panitumumab-trametinib combinatie veelbelovende antitumor activiteit heeft, waardoor

verder onderzoek van deze combinatie bij patiënten met *BRAF*m CRC gerechtvaardigd is.

In onze poging om ook voor patiënten met *KRAS* gemuteerde (*KRAS*m) tumoren een effectieve behandeling te vinden, hebben we twee fase I studies opgezet, waarvan de interim analyses besproken zijn in **hoofdstuk 6.1** en **6.2**. Mutaties in het *KRAS* gen komen vaak voor bij verschillende tumortypen en resulteren in een continue activatie van de MAPK signaalroute. Tot nu toe is de ontwikkeling van effectieve geneesmiddelen die direct aangrijpen op het *KRAS* eiwit weinig succesvol geweest. Preklinisch onderzoek heeft aangetoond dat *KRAS*m kankercellen intrinsiek resistent zijn tegen MEK remmers dankzij een feedback activatie mechanisme van *upstream* tyrosine kinase receptoren, op het moment dat het MEK eiwit geremd wordt. Deze bevinding gaf ons de rationale om MEK remming te combineren met *upstream* receptor inhibitie. In twee verschillende studies hebben we daarom de combinaties dacomitinib (pan-humane epidermale groeifactor receptor [HER] remmer) plus PD-0325901 (MEK remmer) en lapatinib (EGFR/HER2 remmer) plus trametinib (MEK remmer) onderzocht.

In de dacomitinib/PD-0325901 studie werden 33 patiënten geïncludeerd, waarvan 25 met CRC, vijf met niet-kleincellig long carcinoom en drie met pancreas carcinoom. De meest voorkomende bijwerkingen waren acneiform rash (94%), diarree (85%) en misselijkheid (54%). De maximaal tolereerbare dosis met continu gedoseerd dacomitinib is vastgesteld en intermitterende doseerschema's worden nog onderzocht. Tekenen van significante geneesmiddelinteracties werden niet waargenomen. Klinische activiteit werd gezien bij zes patiënten, waarvan er vijf niet-kleincellig longcarcinoom hadden en één pancreas carcinoom. Met deze studie hebben we gedemonstreerd dat dacomitinib plus PD-0325901 tolerabel is, maar niet in de volledige monotherapie doseringen van beide middelen. Vanwege de matige klinische antitumor activiteit die werd bereikt tot nu toe, mogelijk doordat hogere continue doseringen van dacomitinib niet mogelijk waren vanwege toxiciteit, zal de studie in het vervolg focussen op het bevestigen van de antitumor activiteit in meer patiënten en het vinden van een *dose-level* met optimale effectiviteit en toxiciteit.

In de lapatinib/trametinib studie werden 22 patiënten geïncludeerd verspreid over 4 *dose-levels*: 16 patiënten met CRC, drie met niet-kleincellig longcarcinoom, en drie met pancreas carcinoom. Op alle doseringen werd inhibitie van de MAPK signaaltransductie cascade aangetoond in tumorbiopten. Onder de 16 evalueerbare patiënten bereikte er één een partiële respons en acht patiënten hadden stabiele ziekte als beste resultaat. Deze trial bevestigt dat inhibitie van MEK gecombineerd met remming van EGFR en HER2, door trametinib en lapatinib, de MAPK signalering vermindert in *KRAS*m tumoren. Desalniettemin was de klinische effectiviteit tot nog toe beperkt en werd dosis escalatie beperkt door toxiciteit. Daarom zijn we gestart met het onderzoeken van intermitterende doseerschema's om de verdraagbaarheid en effectiviteit zo veel mogelijk te optimaliseren.

**Hoofdstuk 7** beschrijft twee studies waarin het concept van chemosensitisatie met behulp van AZD1775, een doelgerichte *small molecule inhibitor* gericht tegen het WEE1 tyrosine kinase eiwit, onderzocht wordt. WEE1 speelt door middel van remming van zijn directe substraat, CDK1, een belangrijke rol bij het reguleren van het G2 *checkpoint*. Omdat *checkpoints* in de celcyclus van groot belang zijn voor de respons op DNA schade werd de hypothese gesteld dat remming van WEE1 tumorcellen gevoeliger zouden kunnen maken voor de cytotoxische effecten van chemotherapie. De

fase I studie die beschreven is in **hoofdstuk 7.1** werd opgezet om de maximaal tolereerbare dosering (MTD) van AZD1775 vast te stellen wanneer dit middel gecombineerd wordt met cisplatine, carboplatine of gemcitabine. In totaal werden er 202 patiënten geïnccludeerd en de MTD werd vastgesteld voor elke combinatie. *Target engagement*, gedefinieerd als 50% pCDK1 reductie in surrogaat weefsel, werd waargenomen in de combinaties met cisplatine en carboplatine. Met deze studie is aangetoond dat AZD1775 veilig gecombineerd kan worden met chemotherapie en motiveert daarmee om verder onderzoek te doen met deze combinaties bij specifieke patiëntpopulaties.

Omdat p53 deficiënte tumorcellen in grotere mate afhankelijkheid zijn van het G2 *checkpoint* voor het repareren van DNA schade, ontstond de gedachte dat deze cellen in het bijzonder gevoelig zouden zijn voor WEE1 inhibitie gecombineerd met DNA schade inducerende chemotherapie. Nadat preklinisch onderzoek deze hypothese bevestigde, hebben we een *proof of concept* fase II studie met AZD1775 plus carboplatine opgezet om dit concept te onderzoeken bij patiënten met ovariumcarcinoom die refractair of binnen 3 maanden resistent waren na eerstelijns platina-bevattende chemotherapie (**hoofdstuk 7.2**). In deze studie werd bevestigd dat AZD1775 plus carboplatine hanteerbare toxiciteit heeft, waarbij vermoeidheid (87%), misselijkheid (78%), trombocytopenie (70%), diarree (70%), en braken (48%) de meest voorkomende bijwerkingen zijn. Onder de 21 patiënten die evalueerbaar werden geacht voor effectiviteit eindpunten was de ORR 43% (95% BI, 22%–66%), inclusief één patiënt met een complete respons. De mediane progressievrije overleving en *overall survival* waren respectievelijk 5,3 maanden (95% BI, 2,3–9,0) en 12,6 maanden (95% BI, 4,9–19,7). Dit onderzoek heeft dus laten zien dat AZD1775 plus carboplatine bemoedigende antitumor activiteit heeft en bovendien lijkt deze experimentele behandeling betere resultaten te geven dan de huidige beschikbare standaard behandelopties voor patiënten met platina-resistent ovariumcarcinoom.

## Referenties

1. Motzer RJ, Escudier B, Tomczak P, et al. Axitinib versus sorafenib as second-line treatment for advanced renal cell carcinoma: overall survival analysis and updated results from a randomized phase 3 trial. *Lancet Oncol* 2013; 14(6):552–62.
2. Motzer RJ, Hutson TE, Cella D, et al. Pazopanib versus sunitinib in metastatic renal-cell carcinoma. *N Engl J Med* 2013; 369(8):722-31.



## ACKNOWLEDGEMENTS

Ineens is het zover. Meer dan 4 jaar wetenschappelijk onderzoek moet gebundeld worden tot een proefschrift. Op dat moment ga je pas beseffen wat je in de afgelopen jaren allemaal hebt gedaan en bereikt, maar vooral ook hoe ongelofelijk dankbaar je alle mensen bent die een belangrijke bijdrage hebben geleverd aan het tot stand komen van dit eindresultaat.

Allereerst wil ik mijn bijzondere waardering uitspreken voor alle patiënten die hebben deelgenomen aan de klinische studies. Dankzij deze patiënten, en hun naasten die hen hierbij hebben gesteund, hebben we nieuwe behandelstrategieën kunnen onderzoeken waar vele andere patiënten in de toekomst mogelijk baat bij kunnen gaan hebben. Zij hebben mij enorm geïnspireerd.

Mijn promotoren, prof. dr. Jan Schellens en prof. dr. Jos Beijnen wil ik hartelijk danken voor de uitdaging die zij mij geboden hebben in dit promotietraject en voor de uitstekende begeleiding. Jan, gedurende mijn wetenschappelijke stage was ik al onder de indruk van je arbeidsethos, passie voor onderzoek en immense hoeveelheid kennis, maar je bent me blijven verbazen de afgelopen jaren. Ik heb veel bewondering voor de manier waarop je invulling geeft en hebt gegeven aan je vele functies zowel binnen als buiten het Antoni van Leeuwenhoek (AvL) ziekenhuis. Jos, veel dank voor je kritische blik op mijn manuscripten en voor je positiviteit. Wat me altijd bij zal blijven is dat je me 's avonds op belde om me een hart onder de riem te steken tijdens een lastige periode. Dat motiveerde me enorm.

Het AvL als organisatie en al haar medewerkers wil ik bedanken voor het creëren van een uitstekende werksfeer. De unieke combinatie van basic research, translationeel en klinisch onderzoek, en klinische zorg van het hoogste niveau maken dit ziekenhuis tot een wereldwijd vooraanstaand instituut.

Alle artsen die betrokken zijn geweest bij de studies wil ik bedanken. Uiteraard alle oncologen, maar ook de afdelingen radiologie, pathologie, dermatologie en oogheelkunde hebben onmisbare bijdragen geleverd aan het klinisch onderzoek. Frans, Serena en Neeltje, bedankt ook voor jullie hulp bij onze 'huisstudies'. Neeltje, bedankt voor de prettige begeleiding tijdens mijn opleiding Klinische Farmacologie.

Prof. Bernards, beste René, in het beginstadium van mijn promotietraject nam je de tijd om aan mij persoonlijk toe te lichten wat jullie op B7 hadden ontdekt voor *BRAF* gemuteerd colorectaal kanker. Een paar dagen later mocht ik dit, aangevuld met ons voorstel voor een klinische studie, overbrengen op een zaaltje vol oncologen. Ik vond het een eer om met jullie ontdekking uit het lab verder te gaan in de kliniek en het enthousiasme waarmee je over deze ontdekking vertelde werkte aanstekelijk. Ik wil je heel erg bedanken voor de uiterst prettige samenwerking en vruchtbare discussies over het vertalen van ontdekkingen in het lab naar de patiënt, en het verklaren van onze bevindingen bij patiënten.

I would like to express my sincere thanks to Chong and Anirudh. Thank you for your tremendous enthusiasm and the pleasant collaboration. It was due to your research that we were able to investigate new treatment strategies that already provided clinical benefit for a lot of patients.



Dr. Eskens (ErasmusMC) en dr. Langenberg (UMCU), beste Ferry en Marlies, helaas pakte de M13DAP studie minder positief uit dan we vooraf gehoopt hadden, maar ik wil jullie bedanken voor de uiterst prettige samenwerking en voor jullie kritische input op het manuscript.

I would like to thank Alejandro for helping me out with the population pharmacokinetic model for M13DAP. Thank you for your hard work and dedication to the project.

Alle verpleegkundig specialisten, Annemarie, Anne Miek, Emmy, Jana, Karina, Mariska, Marianne, Saskia en Wendy, veel dank voor jullie hulp en prettige samenwerking bij alle verschillende studies waar we samen voor verantwoordelijk waren. De afdeling farmacologie is inmiddels te groot geworden om iedereen bij naam te noemen, maar ik wil alle verpleegkundigen, de secretaresses, planners en teamleiders op 4C hartelijk danken voor hun tomeloze inzet om alles op het gebied van logistiek en patiëntenzorg in goede banen te leiden.

Alle medewerkers van het trialbureau, de wetenschappelijke administratie, het triallab, de CFMPB, de apotheek en de start-up specialists (Brenda & Pascal), heel erg veel dank voor jullie belangrijke ondersteuning.

Marja, jouw multitasking capaciteiten zijn bewonderenswaardig. Bedankt voor al je hulp bij TC's, contact met studie sponsors en het meedenken bij alle 'brandjes' die geblust moesten worden.

Yvonne, Carla en GerritJan, ook jullie hulp als CRA's van de verschillende huisstudies was van vitaal belang. Bedankt voor jullie kritische blik op alle protocollen, voor jullie ondersteuning bij alle METC indieningen, voor het monitoren van de CRF's en daarmee het waarborgen van de kwaliteit van de studiedata.

Jolanda en Mirna, zonder jullie zou het hele traject een stuk moeizamer verlopen zijn. Bedankt voor al jullie hulp en voor jullie motiverende woorden wanneer ik die nodig had.

Judith, Pia en Ilse, veel dank voor de enorme inhaalslag die jullie gemaakt hebben om de eCRF's van verschillende studies weer up-to-date te brengen.

Uiteraard wil ik mijn directe collega-onderzoekers bedanken voor alle vruchtbare discussies. Bart, Bojana, Didier, Emilie, Geert, Jill, Linda, Marit, Mark, Rik, Ruud, Sanne, Suzanne en Vincent, maar natuurlijk ook alle OiO's uit de keet, enorm bedankt voor jullie gezelligheid tijdens het werk, bij etentjes, het OiO weekend, de OOA retreat en labuitjes.

Een bijzonder woord van dank wil ik richten tot Bart, toch wel de sfeermaker van de 2047-kamer. Ik kijk met heel veel plezier terug op de tijd die we samen hebben doorgebracht in het AvL, maar natuurlijk ook op onze rondjes 34 blank op de Jaap Edenbaan en die Brand Weizen na afloop, als noodzakelijke afleiding van onze dagelijkse bezigheden. Ik ben blij dat je mij, mits Jacobs junior het toelaat, bij zult staan als paranimf bij mijn verdediging.

Suzanne, dankzij jouw hulp en advies maakte ik een vliegende start met alle klinische studies. Bedankt ook voor de fijne samenwerking in het kader van de M07MKC en M10MKO studie. We vulden elkaar goed aan, en dat heeft geleid tot twee top publicaties. Veel succes in je verdere carrière, blijf je dromen najagen!

Artur en Dick, ik wil jullie bedanken voor onze interessante en soms felle discussies over mijn en jullie onderzoek, over de aandelenmarkt, de wereldeconomie en de politiek. Het was leerzaam en een genot om jullie er bij te hebben.

Rutger, als huisgenoten hebben we mooie tijden beleefd. Ik denk met veel plezier terug aan ons 'maximaal-gezond' concept, onze avonden in de sportschool en onze vakinhoudelijke discussies. Ik heb veel respect en bewondering voor je carrière, keep up the good work! Met een man van staal als paranimf aan mijn zijde zie ik mijn verdediging met veel vertrouwen tegemoet.

Joris en Wouter, als overgebleven harde kern na onze middelbare school periode zien we elkaar helaas te weinig. Maar de momenten dat we dan weer eens samen komen zijn altijd onvergetelijk. Bedankt voor jullie ultieme Brabantse gezelligheid en voor jullie initiatieven om samen een biertje te gaan drinken. Is die wintersport 2017 al geboekt?

Lieve Tessy, zonder jou was dit me nooit gelukt. Ik ben je ongelooflijk dankbaar voor je liefde, geduld en steun de afgelopen jaren. Jij maakt me blij en gelukkig. Ik kijk uit naar alle avonturen die we samen nog zullen gaan beleven.

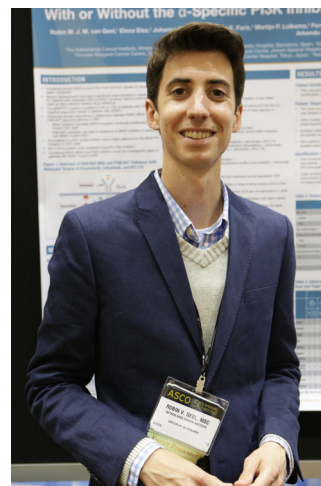
Papa en mama, alle superlatieven schieten te kort om de waardering die ik voor jullie heb te beschrijven. Dankzij jullie heb ik altijd alles kunnen doen wat ik wilde doen en heb ik kunnen bereiken wat ik tot nu toe bereikt heb. Jullie onvoorwaardelijke steun is voor mij van onschatbare waarde.

Bedankt!

Robin

## CURRICULUM VITAE

Robin van Geel was born on September 2, 1987 in Roosendaal, The Netherlands. In 2005, he graduated from high school at the Norbertus College in Roosendaal and started studying pharmaceutical sciences at the University of Utrecht. After receiving his Bachelor of Science degree in 2009, Robin started his master program with a scientific internship at the department of Experimental Therapy of the Netherlands Cancer Institute. Under the supervision of prof. dr. J.H.M. Schellens and dr. M.J. Deenen he developed a rapid and sensitive radio-assay to determine the dihydropyrimidine dehydrogenase enzyme activity in human peripheral blood mononuclear cells. In November 2011, Robin obtained his Master of Science degree in Pharmacy and started with his PhD project at the Netherlands Cancer Institute, supervised by prof. dr. J.H.M. Schellens and prof. dr. J.H. Beijnen. During this PhD project, Robin also followed the clinical pharmacology training program of the Dutch Society of Clinical Pharmacology and Biopharmacy. In October 2016, he will start as a hospital pharmacist in training at the Maastricht University Medical Center.



Robin van Geel is geboren op 2 september 1987, te Roosendaal. In 2005 behaalde hij zijn gymnasium diploma aan het Norbertuscollege in Roosendaal waarna hij begon met de studie Farmacie aan de Universiteit Utrecht. Na het behalen van zijn bachelordiploma in 2009 begon Robin zijn masterfase met een wetenschappelijke stage bij de afdeling Experimentele Therapie van het Nederlands Kanker Instituut – Antoni van Leeuwenhoek ziekenhuis. Onder supervisie van prof. dr. J.H.M. Schellens en dr. M.J. Deenen ontwikkelde hij een snelle en sensitieve assay om met radioactief gelabelde stoffen de enzymactiviteit van dihydropyrimidine dehydrogenase te bepalen in witte bloedcellen. In 2011 ontving Robin zijn masterdiploma en begon hij aan het onderzoek dat beschreven staat in dit proefschrift. Het onderzoek werd uitgevoerd in het Nederlands Kanker Instituut – Antoni van Leeuwenhoek ziekenhuis, onder supervisie van prof. dr. J.H.M. Schellens en prof. dr. J.H. Beijnen. Tijdens dit promotieonderzoek volgde Robin tevens de opleiding tot klinisch farmacoloog van de Nederlandse Vereniging voor Klinische Farmacologie & Biofarmacie. In oktober 2016 start hij als ziekenhuisapotheker in opleiding bij het Maastricht Universitair Medisch Centrum.

## LIST OF PUBLICATIONS

### Articles

**van Geel RMJM**, Tabernero J, Elez E, Bendell JC, Spreafico A, Schuler M, Yoshino T, Delord J-P, Yamada Y, Lolkema MP, Faris JE, Eskens FALM, Sharma S, Yaeger R, Lenz H-J, Wainberg ZA, Avsar E, Chatterjee A, Jaeger S, Tan E, Demuth T, Schellens JHM. **A Phase 1b Dose-Escalation Study of Encorafenib (LGX818) and Cetuximab With or Without Alpelisib in Metastatic BRAF-Mutant Colorectal Cancer.** *Submitted for publication*

**van Geel RMJM**, Beijnen JH, Schellens, JHM. **Drug-Drug Interactions in Oncology: Bogey or Godsend?** *Submitted for publication*

**van Geel RMJM**, Hendriks JJMA, Vahl JE, Van Leerdam ME, Van den Broek D, Huitema ADR, Beijnen JH, Schellens JHM, Burgers SA. **Crizotinib-Induced Fatal Fulminant Liver Failure.** *Lung Cancer* 2016;93:17-19

**van Geel RMJM**, Beijnen JH, Bernards R, Schellens JHM. **Treatment Individualization in Colorectal Cancer.** *Curr Colorectal Cancer Rep* 2015;11:335-344

**van Geel RMJM**, Bernards R, Voest EE, Lolkema MPJK, Cats A, Sleijfer S, Eskens FALM, Schellens JHM **Innovatieve combinatie van doelgerichte middelen voor de behandeling van gemetastaseerd BRAF-gemuteerd colorectaal carcinoom.** *Ned Tijdschr Oncol* 2014;11:69-72

Leijen S, **van Geel RMJM**, Pavlick AC, Tibes R, Rosen L, Abdul Razak AR, Lam R, Demuth T, Rose S, Lee MA, Freshwater T, Shumway S, Liang LW, Oza AM, Schellens JHM, Shapiro GI. **Phase I Study Evaluating WEE 1 Inhibitor AZD1775 (MK-1775) as Monotherapy and in Combination with Gemcitabine, Cisplatin, or Carboplatin in Patients with Advanced Solid Tumors.** *J Clin Oncol.* 2016, *in press*

Leijen S\*, **van Geel RMJM\***, Sonke GS, De Jong D, Rosenberg EH, Marchetti S, Pluim D, Van Werkhoven E, Rose S, Lee MA, Freshwater T, Beijnen JH, Schellens JHM. **Phase II Study of WEE1 Inhibitor AZD1775 plus Carboplatin in Patients with TP53 Mutated Ovarian Cancer Refractory or Resistant (< 3 Months) to First-Line Therapy.** *J Clin Oncol.* 2016, *in press*

Oddo D, Sennott EM, Barault L, Valtorta E, Arena S, Cassingena A, Filiciotto G, Marzolla G, Elez E, **van Geel RMJM**, Bartolini A, Crisafulli G, Boscaro V, Godfrey JT, Buscarino M, Cancelliere C, Linnebacher M, Corti G, Truini M, Siravegna G, Grasselli J, Gallicchio M, Bernards R, Schellens JHM, Tabernero J, Engelman JA, Sartore-Bianchi A, Bardelli A, Siena S, Corcoran RB, Di Nicolantonio F. **Molecular Landscape of Acquired Resistance to Targeted Therapy Combinations in BRAF-Mutant Colorectal Cancer.** *Cancer Res.* 2016;76(15):1-12

Jacobs BAW, Deenen MJ, Pluim D, van Hasselt JG, Krähenbühl MD, **van Geel RMJM**, de Vries N, Rosing H, Meulendijks D, Burylo AM, Cats A, Beijnen JH, Huitema ADR, Schellens JHM. **Pronounced between-subject and circadian variability in thymidylate synthase and dihydropyrimidine dehydrogenase enzyme activity in human volunteers.** *Br J Clin Pharmacol.* 2016;82(3):706–16

Pluim D, Jacobs BAW, Deenen MJ, Ruijter AE, **van Geel RMJM**, Burylo AM, Meulendijks D, Beijnen JH, Schellens JHM. **Improved pharmacodynamic assay for dihydropyrimidine dehydrogenase activity in peripheral blood mononuclear cells.** *Bioanalysis.* 2015;7(5):519-29

### *Abstracts and presentations*

**van Geel RMJM**, Prahallad A, Sun C, Huang S, Eskens FALM, Lolkema MP, Langenberg M, Bernards R, Schellens JHM. **Combined targeted therapy for the treatment of BRAF and KRAS mutant colorectal cancer.** *CancerGenomics.nl Annual Scientific Meeting, January 8, 2016*

**van Geel RMJM**, Tabernero J, Elez E, Bendell JC, Spreafico A, Schuler M, Yoshino T, Delord JP, Yamada Y, Lolkema MP, Faris JE, Eskens FALM, Sharma S, Yaeger R, Lenz HJ, Wainberg Z, Avsar E, Chatterjee A, Jaeger S, Tan E, Demuth T, Schellens JHM. **Combined targeted therapy for the treatment of advanced BRAF<sup>V600</sup> mutated colorectal cancer.** *Dutch Society for Clinical Pharmacology and Biopharmacy Meeting, March 20, 2015*

**van Geel RMJM**, Prahallad A, Sun C, Huang S, Eskens FALM, Lolkema MP, Langenberg M, Bernards R, Schellens JHM. **Combined targeted therapy for the treatment of BRAF and KRAS mutant colorectal cancer.** *CancerGenomics.nl Annual Scientific Meeting, January 9, 2015*

**van Geel RMJM**, Elez E, Bendell JC, Faris JE, Lolkema MP, Eskens FALM, Spreafico A, Kavan P, Delord JP, Schuler M, Wainberg Z, Yamada Y, Yoshino T, Demuth T, Avsar E, Chatterjee A, Zhu P, Bernards R, Tabernero J, Schellens JHM. **Phase I Study of the Selective BRAF<sup>V600</sup> Inhibitor Encorafenib (LGX818) Combined with Cetuximab and the  $\alpha$ -Specific PI3K inhibitor BYL719 in Patients with Advanced BRAF-Mutant Colorectal Cancer.** *J Clin Oncol.* 2014;32:5s (suppl; abstr 3514)

Tabernero J, **van Geel RMJM**, Guren TK, Yaeger RD, Spreafico A, Faris JE, Yoshino T, Yamada Y, Kim TW, Bendell JC, Schuler MH, Lenz H-J, Eskens F, Desai J, Hochster HS, Avsar E, Demuth T, Sandor V, Elez E, Schellens JHM. **Phase 2 results: Encorafenib (ENCO) and cetuximab (CETUX) with or without alpelisib (ALP) in patients with advanced BRAF-mutant colorectal cancer (BRAFM CRC).** *J Clin Oncol* 34, 2016 (suppl; abstr 3544)

Schuler MH, Berardi R, Lim W-T, **van Geel RMJM**, De Jonge MJ, Bauer TM, Azaro A, Gottfried M, Han J-Y, Lee DH, Wollner M, Hong DS, Vogel A, Delmonte A, Krohn A, Zhang Y, Squires M, Giovannini M, Akimov M, Bang Y-J. **Phase I study of the safety and efficacy of the cMET inhibitor capmatinib (INC280) in patients with advanced cMET+ non-small cell lung cancer.** *J Clin Oncol.* 2016;34 (suppl; abstr 9067)

Leijen S, **van Geel RMJM**, Sonke GS, De Jong D, Rosenberg EH, Marchetti S, Pluim D, Van Werkhoven ED, Rose S, Lee MA, Beijnen JH, Schellens JHM. **Phase II study with WEE1 inhibitor AZD1775 plus carboplatin in patients with p53 mutated ovarian cancer refractory or resistant (<3 months) to standard first line therapy.** *J Clin Oncol.* 2015;33 (suppl; abstr 2507)

Schellens JHM, **van Geel RMJM**, Bendell JC, Spreafico A, Schuler M, Yoshino T, Delord J-P, Yamada Y, Lolkema MP, Faris JE, Eskens FALM, Sharma S, Yaeger R, Lenz H-J, Wainberg ZA, Avsar E, Chatterjee A, Jaeger S, Tan E, Demuth T, Tabernero J. **Final biomarker analysis of the phase I study of the selective BRAF V600 inhibitor encorafenib (LGX818) combined with cetuximab with or without the  $\alpha$ -specific PI3K inhibitor alpelisib (BYL719) in patients with advanced BRAF-mutant colorectal cancer.** *Cancer Res.* 2015;75(15 Suppl):Abstract nr CT136

Atreya CE, Van Cutsem E, Bendell JC, Andre T, Schellens JHM, Gordon MS, McRee AJ, O'Dwyer PJ, Muro K, Tabernero J, **van Geel RMJM**, Sidhu R, Greger JG, Rangwala FA, Motwani M, Wu Y, Orford KW, Corcoran RB. **Updated efficacy of the MEK inhibitor trametinib, BRAF inhibitor dabrafenib, and anti-EGFR antibody panitumumab in patients with BRAF V600E mutated metastatic colorectal cancer.** *J Clin Oncol.* 2015;33 (suppl; abstr 103)

Elez E, Schellens JHM, **van Geel RMJM**, Bendell JC, Spreafico A, Schuler M, Yoshino T, Delord JP, Yamada Y, Lolkema MP, Faris JE, Eskens FALM, Sharma S, Yaeger R, Lenz HJ, Wainberg ZA, Avsar E, Chatterjee A, Jaeger S, Demuth T, Tabernero J. **Phase 1b/2 Study of the Selective BRAF V600 Inhibitor Encorafenib (LGX818) Combined with Cetuximab and with or without the  $\alpha$ -specific PI3K inhibitor alpelisib (BYL719) in Patients with Advanced BRAF-mutant Colorectal Cancer.** *Ann Oncol.* 2015;26 (suppl 4):117-122

Van Cutsem E, Atreya CE, André T, Bendell JC, Schellens JHM, Gordon MS, McRee A, Yoshino T, Muro K, O'Dwyer PJ, Tabernero J, Middleton G, Ducreux M, **van Geel RMJM**, Sidhu R, Greger JG, Rangwala F, Liu Y, Wu Y, Mookerjee B, Corcoran RB. **Updated Results of the MEK inhibitor trametinib (T), BRAF inhibitor dabrafenib (D), and anti-EGFR antibody panitumumab (P) in patients (pts) with BRAF V600E mutated (BRAFM) metastatic colorectal cancer (mCRC).** *Ann Oncol.* 2015;26 (suppl 4):iv119

Tabernero J, **van Geel RMJM**, Bendell JC, Spreafico A, Schuler M, Yoshino T, Delord JP, Yamada Y, Lolkema MP, Faris JE, Eskens FALM, Sharma S, Yaeger R, Lenz HJ, Wainberg ZA, Avsar E, Chatterjee A, Jaeger S, Demuth T, Schellens JHM. **Phase 1 Study of the Selective BRAF V600 Inhibitor Encorafenib (LGX818) Combined with Cetuximab and with or without the  $\alpha$ -specific PI3K inhibitor alpelisib (BYL719) in Patients with Advanced BRAF-mutant Colorectal Cancer.** EORTC-NCI-AACR Symposium on Molecular Targets and Cancer Therapeutics November 18-21, 2014

Gonzalez-Angulo AM, Juric D, Argilés G, Schellens JHM, Burris HA, Berlin J, Middleton MR, Schuler M, **van Geel RMJM**, Bootle D, Boehm M, Goggin T, Demanse D, Quadt C, Baselga J. **Safety, pharmacokinetics and preliminary activity of the  $\alpha$ -specific PI3K inhibitor BYL719: Results from the first-in-human study.** *ASCO Annual Meeting, May 31 – June, 2013*

Jacobs BAW, Pluim D, Krähenbühl MD, Deenen MJ, **van Geel RMJM**, Cats A, Beijnen JH, Schellens JHM.  
**Circadian rhythm of DPD and TS enzyme activity in PBMCs from healthy volunteers.** *FIGON Dutch  
Medicine Days, October 1 – 3, 2012*



